NMR studies of silicate & aluminosilicate solutions

Seyed Naser Azizi

NMR STUDIES OF SILICATE & ALUMINOSILICATE SOLUTIONS

By

Seyed Naser Azizi

A thesis submitted in partial fulfilment of the requirements for the degree of Doctor of Philosophy at the University of Durham.

Department of Chemistry
University of Durham
September 2001

Abstract

The work described in this thesis deals with the use of ^{29}Si and ^{27}Al NMR to obtain information about the chemical structure of aqueous silicate and aluminosilicate solutions. This has extended the knowledge gained in previous studies. A wide range of alkaline and tetraalkylammonium hydroxide silicate and aluminosilicate solutions (mostly also containing sodium) has been examined. Such solutions are shown to contain a large range of anions. The first highly-resolved ^{27}Al NMR spectra of alkaline aluminosilicate solutions are presented and discussed. The linewidths and number of resolved lines are shown to depend critically on several factors, especially the pH and Si:Al ratio, as well as the concentration of various components. At least thirteen separate peaks or bands are observed at the optimum conditions of pH ~10.35 and Si:Al = 1. Tentative assignments of some bands are presented, based on ^{27}Al and ^{29}Si shift comparability, ^{27}Al linewidths and ^{27}Al spin-lattice relaxation measurements. Relative intensities of the various ^{27}Al signals are given for the pH ~10.35 solution. A correlation of ^{27}Al and ^{29}Si chemical shifts has been established. Dilution effects and dynamic equilibria are considered for the aluminosilicate solutions.

Trends in the spectra with changing concentrations of the various components have been identified. Under certain conditions, additional peaks are observed. Two of these are tentatively assigned to aluminium nuclei in "three-membered" rings. Moreover, a few very sharp lines (i.e. with very low electric field gradients), currently of unknown origin, are observed in several spectra. At certain concentrations chemical exchange can be shown to take place.

The effects of tetraalkylammonium (TAA) and alkali metal cations on the equilibrium distribution of aluminosilicate oligomers in aqueous alkaline aluminosilicate solutions have been investigated using evolution with time of Al-27 NMR spectra. The results indicate that there are no observable differences in the initial distribution of aluminosilicate species (i.e. immediately following solution mixing) involving a mixture of TAA and Na cations and those involving alkali metal cations alone. However, in the latter case, this distribution, in contrast to those for TAA/Na solutions, is not stable, the species quickly re-equilibrating, giving broad signals of q^3 and perhaps q^4 type.

The effect of Al and Si concentration on the formation of gel in aluminosilicate solutions is also investigated with ^{27}Al NMR spectra. It is shown that the gel time strongly depends on the Al concentration and the temperature. A graph of Al and Si concentrations with gel time has been established.

Silicon-29 NMR spectra have been obtained for more than 20 aqueous alkaline silicate solutions containing methanol. A signal assigned to $CH_3OSi(OH)_3$ or one of its deprotonated congeners is studied in detail for the first time for the solution conditions involved. Its appearance has been monitored as a function of the solution composition. The equilibrium constant for its formation is of the order of 0.65. The effects of alcohol, silicate and TAAOH concentration and of the nature of the alkylammonium base on this reaction have been investigated.

Memorandum

The research presented in this thesis has been carried out in the Department of Chemistry, University of Durham, and in the Department of Chemistry, University of Mazandaran, between October 1997 and October 2001. It is the original work of the author unless stated otherwise. None of the work has been submitted for any other degree or qualification of the University of Durham or of any other university or other institute of learning.

Acknowledgements

It is with pleasure that I would like to thank the following:

Prof. Robin K. Harris, my supervisor, from whom I have learnt an immense amount over the past four years. I am indebted to him for the patience and kindness he has shown me over the past four years. I am sure that without all of his assistance, comments, great help with interpreting spectra, and explanation of theoretical concepts of the NMR experiment, patient advice and encouragement during the course of my studies I would not have continued the struggle with many of the aspects of science pertaining to this thesis.

Dr Abdolraouf Samadi-Maybodi, my Iranian supervisor, for his help, advice and fruitful discussions. I am sure that without all of his assistance, comments, I would not have continued with the research involved in this thesis.

The people I have worked alongside,especially Dr Alan M. Kenwright for his helpful lectures and all his advice, and Ian H. McKeag for his patient help in the operation of the various NMR experiments. The members of the NMR research group for countless enjoyable discussions on a wide range of topics.

My family, for all their love and encouragement, without which I would not be writing this thesis.

Finally I am grateful to the Iranian Ministry of Science, Researches and Technology for a student-ship

Date: September 2001 Seyed Naser Azizi

Preface

Symbols and abbreviations

Hz	Hertz
MHz	Megahertz
kHz	kilohertz
ppm	parts per million
ms	millisecond
s & μs	second and microsecond
NMR	Nnuclear Magnetic Resonance
S/N	Signal-to-Noise ratio
FID	Free Induction Decay
T_1	spin-lattice relaxation time
T_2	spin-spin relaxation time
TMS	Tetramethylsilane
FT	Fourier Transform
EFG	Electric Field Gradient
ml	millilitre
P	angular momentum
T	temperature °K
Δn	Population difference between nuclear states (Δn_0 at Boltzmann equilibrium)
LP	Linear Prediction
mol. wt.	molecular weight
δ	Chemical shift
σ	Shielding constant
B_0	the external magnetic field
B	Effective magnetic field
J	scalar coupling constant

J & kJ	Joule and kiloJoule
h	Planck's constant
λ	Wavelength
ν	frequency of the electromagnetic radiation
ΔE	energy difference between the energy levels
IR	Infrared
UV	Ultraviolet
I	Spin quantum number
γ	Magnetogyric ratio
m_I	Azimuthal nuclear spin quantum number
TMAOH	Tetramethylammonium hydroxide
TEAOH	Tetraethylammonium hydroxide
TPAOH	Tetrapropylammonium hydroxide
TBAOH	Tetrabutylammonium hydroxide
$HM(OH)_2$	Hexamethonium hydroxide $(CH_3)_3N^+$-$(CH_2)_6$-$N^+(CH_3)_3.2OH^-$
TAAOH	Tetraalkylammonium hydroxide
HMBTP	2,3,4,5,6,7,8,9-octahydro-2,2,5,5,8,8-hexamethyl-2H-benzo(1,2-c:3,4-c':5,6-c") tripyrrolium cation, $C_6[CH_2N(CH_3)_2(OH)CH_2-)]_3$
o.d.	Outside diameter
T_C	Coalescence Temperature

Contents **Page**

Chapter One

The study of aqueous silicate and aluminosilicate solutions by ^{27}Al and ^{29}Si NMR spectroscopy: Introductory notes

1.1. Introduction

The nature of the species present in aqueous silicate and aluminosilicate solutions has been the subject of debate for many years and many studies using various methods have been devoted to this subject, which is still of considerable current interest. Whereas it was concluded from the early work on aqueous sodium metasilicate solutions that the silicate species is entirely monomeric,[1] evidence for the existence of polysilicate ions has come from, e.g., Raman spectroscopy,[2] paper chromatography,[3] trimethylsilylation [4] and reaction with molybdic acid [5]. It is generally accepted now that a dynamic equilibrium exists in silicate and aluminosilicate solutions between a range of silicate and aluminosilicate anions of varying degrees of condensation and molecular weight, which cannot be chemically separated owing to their rapid exchange rates.

The equilibria depend sensitively on silica concentration, alumina concentration, pH, cation content, temperature and possibly solution history. Therefore, all the methods involving chemical treatment of the solutions, as in trimethylsilylation, silicomolybdate formation and paper chromatography, have to be used with caution, and in some cases their results have been a matter of controversy.[6,7] Nevertheless, valuable information on the complex nature of silicate and aluminate solutions has been obtained by these methods, especially after some modifications of the experimental procedures had been introduced taking into account the above-mentioned complications. However, ^{29}Si and ^{27}Al NMR spectroscopy, like other spectroscopic methods, can be used to study the original solutions without any pre-treatment and should give detailed information on the structural entities in silicate solutions in a similar manner to that for polyorganosiloxanes.[8]

On the other hand, several experimental difficulties, mainly connected with the low sensitivity of the ^{29}Si NMR method, strongly restricted its early applications to silicate solutions. It was only the introduction of the pulse Fourier transform NMR technique that opened the way to the routine use of ^{29}Si NMR as a powerful tool in silicate chemistry. The first ^{29}Si NMR spectrum of a sodium silicate solution was published in 1973,[9] followed by three independent papers on this topic in 1974.[10-12] These studies clearly demonstrated that ^{29}Si NMR might contribute greatly to the knowledge of the complex nature of aqueous silicate solutions, owing to two fundamental features of the spectra: (i). Characteristic and mostly well-separated signals for the SiO_4 groups in different structural surroundings may be observed in the ^{29}Si NMR spectra (i.e. the exchange rate between the species is slow on the NMR timescale), and (ii). From the signal intensities, the relative concentrations of the different structural entities can be estimated. Therefore, detailed information on the structure and the quantitative distribution of the various building groups and silicate species present in the solutions may be obtained from ^{29}Si NMR spectra.

The nucleation of zeolite formation and crystal growth occurs through the polymerisation of aluminate and silicate ions present in the aqueous phase of the synthesis mixture. Identification of the structure and composition of silicate and aluminosilicate ions has become, therefore, a subject of considerable interest, pursued through the application of various techniques. NMR (^{27}Al as well as ^{29}Si) spectroscopy is particularly well suited for such studies; accordingly, a number of reports have appeared addressing the structure of silicate ions present in various alkaline silicate and aluminosilicate solutions. To date, ^{27}Al NMR has been less used than ^{29}Si NMR for this purpose because the quadrupolar nature of the former

causes line broadening, leading to lower resolution in the spectra. The present work demonstrates the application of NMR (especially ^{27}Al) spectroscopy to define the effects of silicate ratio, R=SiO_2/TMAOH, and silica to alumina ratio on the connectivity of aluminosilicate anions in aluminosilicate solutions pertinent to zeolite synthesis.

By means of ^{27}Al chemical shifts, one can readily distinguish between tetrahedrally and octahedrally co-ordinated aluminium atoms. The wide range of chemical shifts for four co-ordinated aluminium from about 50 ppm up to 80 ppm from the reference $Al(H_2O)_6^{3+}$ ion indicates that, in addition to the direct-neighbour oxygen atoms, the nuclei of the second co-ordination sphere (e.g. Al or Si) contribute to the shielding of the aluminium.

1.2. Introductory notes to silicate solutions

Although silica (SiO_2) constitutes by far the major component of the earth's crust, our knowledge of its chemistry is disproportionately small, (see Fig. 1.1). By far the most abundant elements in the earth's crust are oxygen, silicon, and aluminium (62.6, 21.2, and 6.5 atom % respectively).

In particular, there is a great deal still to be learnt about the behaviour of silica in aqueous solution, and it is the nature of the silica-water system that is investigated in this work.

The term silica denotes the compound silicon dioxide, SiO_2.[13] In technological usage, this designation includes various, primarily amorphous, forms of the parent compound which are hydrated or hydroxylated to a greater or lesser degree, e.g. types of colloidal silica and silica gel. Silicon dioxide is the most common binary compound of silicon and oxygen. This oxide shows acidic properties by its reaction with a large number of basic oxides to form silicates. The effects of impurities have complicated reliable determination of the solubility of silica in water, and of surface layers that

may affect attainment of equilibrium. Reported values [13] for the solubility of quartz at room temperature are in the range 6-11 ppm (as SiO_2). The concentration found in seawater [14] is 5 ppm. Typical values for massive amorphous silica at room temperature are around 70 ppm and for other forms of amorphous silica in the range 100-130 ppm. Solubility increases with temperature (see below). It appears to be at a minimum at ca. pH 7 and increases substantially above pH = 9.[13]

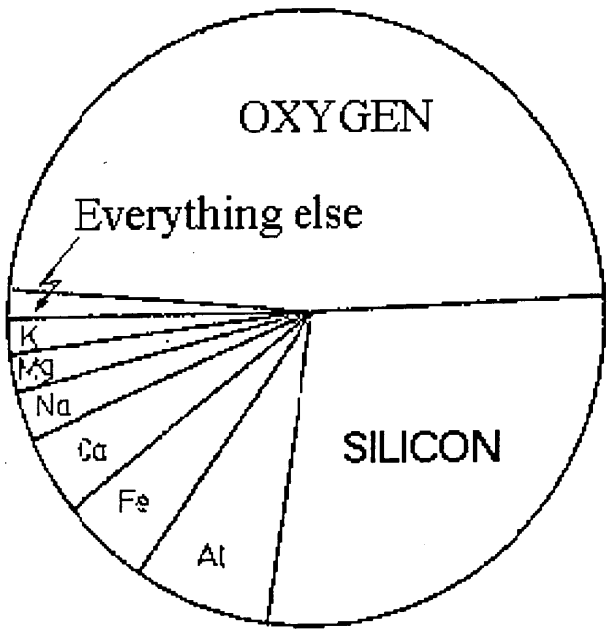

Figure 1.1 Composition of the earth's crust, shown as weight percent of elements [13,14,15]

At ordinary temperatures and neutral pH the solution in equilibrium with amorphous silica contains monomeric monosilicic acid, $Si(OH)_4$. Solutions of monosilicic acid may be obtained by careful acidification of alkali silicate solutions. By operating under carefully controlled conditions at low temperature and pH, solutions may be obtained that remain supersaturated with respect to amorphous silica for hours at temperatures of ca. 0 °C. Eventually, however, polymerisation reactions involving the

formation of siloxane linkages occur, leading ultimately to the formation of colloidal particles and further aggregation or gel formation. A general polymerisation scheme is shown in figure 1.2. Thus, when a solution of $Si(OH)_4$ is formed (as by acidification of a solution of a soluble silicate) at a concentration greater than the solubility of amorphous silica (100-200 ppm), the monomer polymerises to form dimers and higher molecular weight species. The polymerisation occurs in such a way as to maximise formation of siloxane linkages (Si-O-Si), forming particles with internal siloxane linkages and external SiOH groups. Above pH 7, stabilised particles (sols) grow to radii of ca 100 nm.[13]

At lower pH, or if salts are present to neutralise the charge on the growing particles, aggregation of particles occurs, with the formation of chains and, ultimately, three-dimensional gel networks. Control of this process by adjustment of pH and addition of coagulants is the basis of the technology for formation of amorphous silica.[13]

Silica dissolves in water at high temperatures and pressures. For amorphous silica up to 200 °C, the solubility in liquid water (under suitable pressure) is given:

$$c=0.382(13.6+t)\times 10^{-3}$$

where c is the concentration of dissolved silica in wt % and t is the temperature in °C.

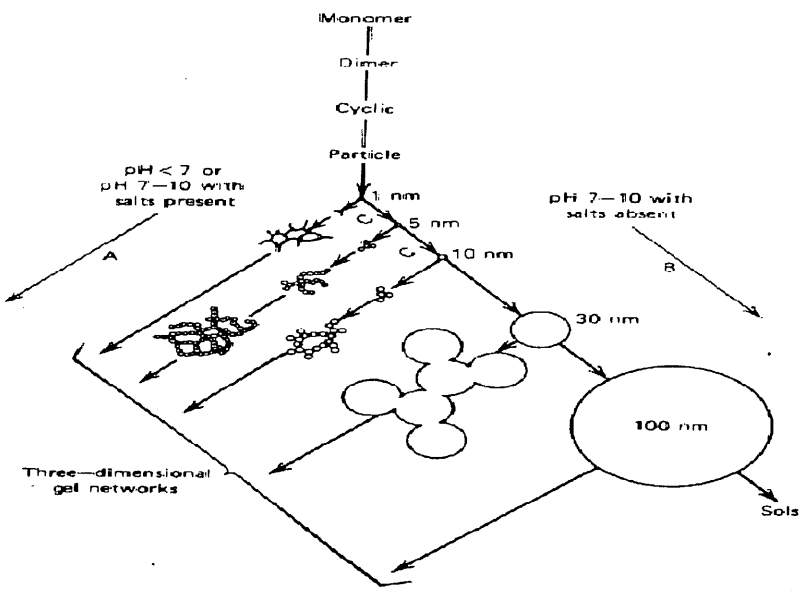

Figure 1.2 Schematic representation of the polymerisation of monosilicic acid.[13] On polymerisation of silica in basic solution (B), particles in the sol grow in size with decrease in numbers; in acid solution or in the presence of flocculating salts (A), particles aggregate into three-dimensional networks and form gels.[13]

1.3. The Nature of Dissolution

Silica does not merely dissolve in water, but is solubilised via a chemical reaction, namely hydrolysis, in excess water, i.e. amorphous silica dissolves (or de-polymerises) in water according to following equation:

$$SiO_{2(s)} + 2H_2O \rightarrow H_4SiO_{4(aq)}$$

Orthosilicic acid, monosilicic acid

$H_4SiO_{4(aq)}$ can also be expressed as $Si(OH)_{4(aq)}$ or $H_2SiO_{3(aq)}$. Small amounts of impurities (especially aluminium or iron) in solid silica cause a decrease in solubility. Below pH 9 the solubility of amorphous silica is independent of pH; above pH 9 the solubility increases because of increased ionisation of silicic acid (silica hydrate).[13] Silicic acid is a very weak acid. The acid is dibasic, dissociating in two steps [13]

$Si(OH)_4+H_2O \rightarrow SiO(OH)_3^-+H_3O^+$ $pK_1= 9.8$ (20 °C)

$SiO(OH)_3^-+H_2O \rightarrow SiO_2(OH)_2^{2-}+H_3O^+$ $pK_2= 11.8$ (20 °C)

At pH 7, only 0.2 % of the dissolved silica occurs as silicate ion; at pH>9, the dimers $Si_2O_6(OH)^{5-}$ and $Si_2O_3(OH)_4^{2-}$ also become important species in addition to $H_3SiO_4^-$, whilst above pH 11, $H_2SiO_4^{2-}$ and $Si_2O_4(OH)_3^{3-}$ exist. At pH 10, undissociated silicic acid is less than 10 % .[13]

Thus, stable solutions containing significant amounts of silica exist only at high pH. Figure 1.3 summarises silicate solutions in terms of pH and concentration.[16] The boundaries between the regions have been shaded where they are not well determined. Solutions in the instability region sooner or later precipitate solids. For the silicate solutions there are two types of equilibria governing the species found, an acid-base equilibrium, such as:

$$(HO)_3Si\text{-}OH + OH^- \rightleftharpoons (HO)_3Si\text{-}O^- + H_2O \qquad (1)$$

and a polymerisation-depolymerisation equilibrium, such as:

$$(HO)_3Si\text{-}OH + HO\text{-}Si(OH)_3 \rightleftharpoons (HO)_3Si\text{-}O\text{-}Si(OH)_3 + H_2O \qquad (2)$$

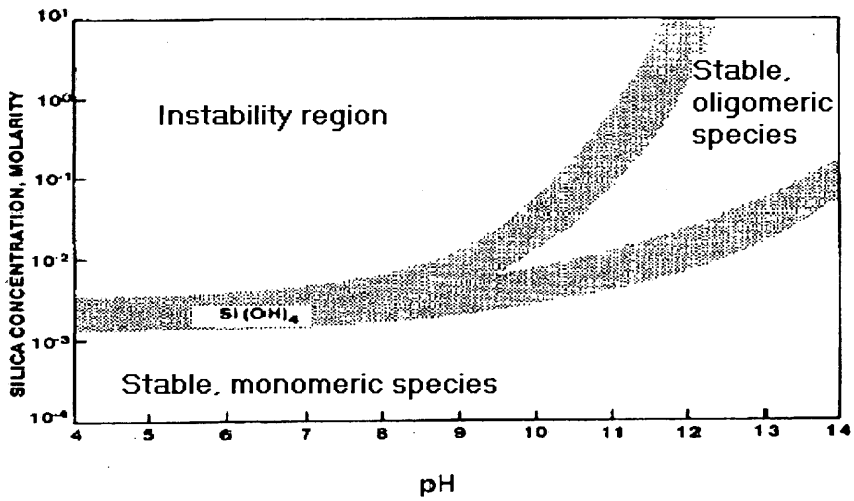

Figure 1.3. Silicate solutions summarised in terms of pH and concentration,[16] showing regions in the silicate equilibrium.

The term "polymerisation" here is defined as the mutual condensation of SiOH fragments to give molecularly coherent units of increasing size. No distinction is made as to whether these species contain rings of increasing diameter or branched chains of an increasing number of silicate units. Acidity is coupled with polymerisation, as it is known that the greater the number of siloxane linkages and the fewer the OH groups on a silicon atom, the stronger the acidity:

$$Si(OH)_4 < \text{-Si-O-Si(OH)}_3 < (\text{-Si-O})_2Si(OH)_2 < (\text{-Si-O})_3Si(OH)$$

least acidic most acidic

In this way polymerisation-depolymerisation and the base-acid properties of these silicate species are tied together. In general, decreasing concentration and increasing pH both favour the formation of less condensed species.

Aluminosilicates are the most abundant minerals in the earth's crust and have received corresponding attention from mineralogists and petrologists. Their structure may be derived by isomorphous substitution of AlO_4^- for SiO_4 tetrahedra in the framework of the various silicate structural types, with embedding of cations (which compensate the extra negative charge) in the interstices of the framework.

1.4. Why study silicate and aluminosilicate solutions?

A wealth of literature has accumulated concerning the behaviour of 'silicic acid', since Thomas Graham [17] first made an intensive study of aqueous silicate solutions. This is in part due to the industrial applications of soluble silicates.

The glass and ceramics industries have been in existence for thousands of years, and there is evidence that soluble silicate glasses were known to the Phoenicians.[14] In the nineteenth century, Von Fuch [18] proposed

their use for adhesives, cements and fire-proof paints. Industrial production started around 1840 in Europe and 1860 in America. Consequently sodium silicate was one of the first chemicals to be produced on a large scale. Today the silicate industry is one of the largest chemical enterprises, producing an estimated three million tonnes of glass per annum.[14] Soluble silicates are now used in detergent and soap powders, and in the brewing, dairying, food and metal industries (for cleaning purposes). Silica and silicates are also used as deflocculants in the cement industry, and for sand cores and moulds in the foundry industry.[19] Soluble silicate derivatives are also widely used. The dissolution, transport and deposition of silica occur in nature on a massive scale. Livingstone [20] (1963) estimated that the movement of silica from the landmass to the world ocean is of the order of 10^8 tonnes/year, and that the dissolution of opaline silica adds another 10^{12} tonnes/year. This is extraordinary in view of the low solubility of opaline silica, and should be compared to the figure of 10^{10} tonnes/year, estimated [14] as the amount of carbon incorporation in the biosphere. The actual percentage of silica contained in vegetation varies widely from species to species, but an average value of 0.15% by weight of elemental silicon has been quoted.[14] (This may be compared to the value of 0.3% by weight for elemental nitrogen and potassium). Although not indispensable to vegetative growth, the presence of silica often has secondary effects. For example, it has been held responsible for the reduction of the toxic effect of metals in plants.[21] Increased resistance to disease and fungal attack has been attributed to silica,[22] and there is evidence that silica is involved in mechanically strengthening plant tissue.[23]

Silica is present in trace amounts in higher animals, and seems to have some definite function, particularly in bone development and in the tissue ageing process.[14]

A good deal of work has been centred upon the toxicological effects of silica. The most common manner of ingestion of particulate silica in human beings is via the lungs. This is the direct cause of silicosis. Greater probability of tuberculosis also results, and susceptibility to lung cancer is increased (although silica itself is not carcinogenic). It is pertinent to note that asbestosis is not directly related to the chemistry of silica; rather it is the result of mechanical damage by the needle-like fibres found in asbestos. Non-siliceous particles may also induce asbestosis.[24]

Silicate solutions were for many years believed to be either a reasonably homogenous mixture of monosilicic acid and/or unspecified oligomers, or else they were presumed to contain highly condensed polymers of colloidal dimensions. In fact, aqueous silicate solutions are generally composed of many low molecular weight polymers in dynamic equilibrium, the exact constitution of any given solution being dependent upon a number of variables. Much confusion exists in the old literature because this situation has only recently been fully appreciated. Possibly the most telling reason for the extensive study of aqueous silicate solutions, however, must lie in the intractable nature of the solutions themselves. The study of these solutions is fraught with difficulties. They offer no easy 'handle' for investigation, and it is only with the recent advent of sophisticated spectroscopic techniques that their true nature has begun to be demonstrated.

Aluminium has vast silicate chemistry, since a high proportion of the world's silicate minerals, which together with silica constitute the bulk of

the earth's crust, contain aluminium. The enormous variety of aluminium silicate structural types arises in part from the variety of stoichiometries and structures possible for silicate anions, each of which is capable of accommodating Al^{3+} ions, either exclusively or accompanied by other metal ions, in the lattice. The situation is, however, made far more complex since varying proportions of the silicon atoms of such anions, and indeed of silica itself, are capable of replacement by aluminium atoms with the formation of aluminosilicate anions which are structurally analogous to the silicate parent but bearing an extra negative charge for each silicon atom replaced by aluminium. For example, the amphiboles, which contain $(Si_4O_{11})^{6-}$ as the repeating unit in their polymeric anions, have as their counterparts aluminosilicates containing the repeating unit $(AlSi_3O_{11})^{7-}$. These, moreover, merely represent limiting species; actually minerals based on such anions may have Al:Si ratios intermediate between the limiting values of 0 and 1/3.

A well-known class of alkali aluminosilicates found in nature is that of zeolites. The AlO_4 and SiO_4 tetrahedra of zeolites are stacked in a manner which leaves cavities large enough to take up water, gases like CO_2 or NH_3, alcohol, and mercury with relative ease. They function as cation-exchangers, and sodium-containing zeolites (permutites) have long been used for water softening, exchanging their sodium ions for the more strongly coordinating calcium ions of the water. It is proposed that nucleation for zeolite formation and crystal growth occurs through the co-polymerisation of aluminates and silicate ions in a solution mixture.

Therefore, aqueous aluminosilicate solutions are receiving increasing attention, due to their role in zeolite synthesis, which makes them industrially important. Tetraalkylammonium (TAA) cations may exert substantial structure-forming effects on the silicate anions present in aqueous

TAA silicate solutions. The nature of the aluminosilicate ions formed and of their reactions in solution is of considerable current interest. One central problem has been the nature of the aluminium co-ordination in aluminosilicate solutions.

Over 50 topologically distinct zeolites have been produced from silicon, aluminium, and oxygen simply by varying the ratio of SiO_2 to Al_2O_3 in the synthesis mixture, the alkalinity of the mixture, and the composition of the base.[25] Theoretical studies, on the other hand, have shown that there are also many other types of structures which ought to be stable but have not as yet been synthesized.[25] These observations have stimulated a desire to understand the chemistry of zeolite formation at a molecular level so that this knowledge can be used to guide the synthesis of new materials. With this objective in mind, numerous investigations have been carried out to identify the species present in synthesis mixtures and the extent to which these species contribute to the formation of zeolites.

The aim of the work presented in this thesis is to understand of the structure and chemistry of soluble silicate and aluminosilicate anions. Particular attention is given to examining the effects of pH, cation and addition of methanol on the distribution and reactivity of these species.

1.5. Experimental techniques used in the study of silicate and aluminosilicate solutions

In attempts to elucidate the chemical structure of the species present in silicate solutions, and in investigations into the polymerisation of silicic acid many techniques, both chemical and physical, have been employed. For the purposes of this work, it is convenient to divide these techniques into three classes: physical, chemical and spectroscopic.

Physical techniques were, as a rule, the earliest to be used, and rely on the observation of a characteristic property of the solution. Such methods include:

- Turbidity measurements [26-28]
- Viscosity measurements [28,29]
- Gel time comparisons [27,29]
- Depression of freezing point [29]
- Conductivity [30,19]
- Ultra centrifugation [27]
- pH measurements [30,19]

Chemical methods of analysis have been extensively applied, the most important being:

- Reactions with molybdic acid [31,14]
- Paper and gel chromatography [3]
- Trimethylsilylation followed by chromatographic separation [6,32]

More recently, spectroscopic methods of investigation have been evoked, principally:

- Infrared spectroscopy [33,34]
- Raman spectroscopy [35]
- Nuclear magnetic resonance spectroscopy (NMR) [7,9,51,36,37]

It is the chemical techniques that have yielded the most information about the structure of silicate solutions in the past. Physical techniques, by their nature, tend to be limited to the classification of solutions, rather than their structural characterisation. Details of the various methods of the chemical analysis are given in chapter two of reference 14, but it should be noted at this point that they all involve the chemical modification, by acidification, of the original solution. It has been held that silicate anions do

not undergo substantial rearrangement during the (brief) period of acidification, and consequently that the modified solutions accurately reflect the chemical distribution of the anions originally present. This premise has been the subject of some debate in the literature,[6] but has been nevertheless widely accepted in the past. It arises from the results of early measurements of conductivities, viscosities and pH, which suggested that silicate solutions required long intervals, of the order of days, to regain equilibrium after the system had been disturbed by, for instance, dilution or a change in the pH. Lagerstrom [30] (1959) showed this to be correct only for solutions whose compositions placed them within an 'instability range' governed by specific pH and concentration limits [16] (see fig. 1.3). Solutions outside this range equilibrate very rapidly. The results obtained[38, 39] from spectroscopic techniques (which do not interfere with the solutions) demonstrate that considerable rearrangement of the silicate anions occurs when the conditions are changed for solutions outside the instability range. This must be taken into account when interpreting the results of the chemical techniques.

The signals obtained from IR. and Raman spectroscopy of aqueous silicate solutions arise from vibrations of the Si-OH bond, the $Si-O^-$ bond and the siloxane linkage. Thus, IR. and Raman spectroscopy may provide information about the degree of protonation of simple silicate anions; for example, they will be of some (rather limited) value in the determination of Si-O-Si or Si-O-Al framework structures.

Structural variation in the siloxane skeleton will have a marked influence upon the chemical environment of the silicon nuclei in the structure, and this will be reflected in the NMR spectrum. Engelhardt and Michel [40] reviewed the NMR literature on aqueous aluminosilicates up to 1987, at which time the existence of aluminosilicate species in alkali metal

hydroxide solutions had not been proven because of the low solubility in typical preparation conditions at the time; two Raman studies, for example, had led to opposite conclusions.[14,40] Experience with the ^{29}Si NMR of solid aluminosilicates, however, enabled the authors [40] to predict the likely chemical shift ranges of Si atoms in a $Q^x(yAl)$ environment (where x is the total connectivity through oxygen to Si and Al atoms, and y is the number of those atoms that are Al), which reflect a parameter which may be visualised as the effective electron density around the silicon nucleus.

Nowadays, however, with the routine availability of Fourier transform multinuclear magnetic resonance spectroscopy at magnetics field 4.7 T and higher, structural, thermodynamic and kinetic information specific to ^{29}Si, ^{27}Al, and even ^{17}O can be obtained 'non-invasively, i.e., without perturbing the solution chemically. Furthermore, NMR spectra (chemical shifts) of species in solution can be compared with those of relevant solids of known structure.[40] Therefore, among the spectroscopic methods given above, NMR appears most suited to the study of silicate and aluminosilicate solutions. This becomes evident when considering the physical phenomena on which each technique relies.

1.6. NMR

Nuclear magnetic resonance (NMR) was first demonstrated in condensed matter in 1946 by two groups of American physicists independently. It arises because isotopes of most elements possess a property referred to as nuclear spin, which confers a magnetic moment on the nucleus. NMR spectroscopy is based on transitions (stimulated by radiofrequency radiation) between the quantised nuclear spin energy levels of suitable isotopes in compounds placed in a strong homogeneous magnetic field. Soon after the initial discovery of NMR, it was realised that the

magnetic field acting on a nucleus is less than the applied field because of electronic shielding, which shifts the resonance to lower frequency. The extent of shielding is found to vary with the electronic environment of the nucleus, which correlates with the chemical activity of the atom concerned. Thus the resonance for a given nucleus varies with its chemical site, giving a so-called "chemical shift" to the signal. The discovery of such an effect sparked a rapid development of NMR for the determination of chemical structure and it is now the supreme technique for such purposes for molecules in the solution state.

The principles of NMR are now well-known and are covered by many text-books.[41-46] The NMR methods used for the work described in this thesis are mostly straightforward and it is, therefore, not appropriate to describe them in detail here. However, a few remarks are in order:-

(a) The population difference between relevant energy levels is extremely small, so NMR is basically an insensitive technique.

(b) Following excitation of nuclear spins to higher energy levels, the bulk magnetization of the sample will relax to its equilibrium state in two distinct ways:

(i) The z component will revert to the equilibrium value by spin-lattice (longitudinal) relaxation, which may take of the order of 10^{-2} to 10^{2} seconds for solutions.

(ii) The x and y components decay to zero by spin-spin (transverse) relaxation, which (for liquids and solutions) takes a similar time to spin-lattice relaxation. This "free induction decay" (FID) gives the observed NMR signal.

(c) Modern spectrometers operate in a pulsed mode, and the resulting FID is Fourier transformed to give the spectrum. Many such transients

may be needed to get an acceptable signal-to-noise ratio. Various pulse sequences are tailored to give specific items of information.

Each isotope has a characteristic magnetic moment, expressed by its magnetogyric ratio, γ, and this determines its gross NMR frequency (modified by shielding). The frequency ranges of different isotopes do not generally overlap. The only nuclei examined in the research carried out for this thesis were ^{29}Si and ^{27}Al. Their properties are as follows:

Isotope	**Spin**	**Natural abundance (%)**	**Magnetic moment (μ/μ_N)**	**Mgnetogyric ratio γ (10^7 rad T^{-1} S^{-1})**	**NMR frequency[a] Ξ (MHz)**
^{29}Si	1/2	4.70	-0.96174	-5.3188	19.867184
^{27}Al	5/2	100	4.3084	6.9760	26.077

a. In a field such that the protons in TMS resonate at exactly 100 MHz

The NMR spectroscopies of these two isotopes are fundamentally different in two ways:

(a) The ^{27}Al nucleus is much more receptive (gives better signal intensity) than ^{29}Si, largely because of its greater natural abundance.

(b) The ^{27}Al nucleus is quadrupolar because its spin quantum number is $\rangle 1/2$. This means it can interact with an electric field gradient and consequently relaxes much more quickly than ^{29}Si. This in turn has two consequences. Firstly, pulses can be repeated rapidly, giving a further intensity advantage, and, secondly, the transitions lines are likely to be broadened significantly, especially when the Al is in a site of low symmetry. The latter effect reduces the resolution of the spectrum.

1.7.a. Advantages and difficulties of silicon-29 NMR spectroscopy of silicate solutions

Although ^{29}Si NMR is a valuable tool for the study of aqueous silicate solutions there are several difficulties, namely:

- The *low sensitivity* of the method due to the rare-spin character (4.7% natural abundance) of ^{29}Si, which restricted its early application to silicate solutions.
- Silicate solutions contain a large number of species, even when differences in protonation are ignored, giving rise to complicated ^{29}Si spectra. *Spectral overlap* is therefore a considerable problem.
- Because ^{29}Si is a 'rare spin', each chemically distinguishable silicon site gives rise to a single resonance, no (Si, Si) *spin-coupling* effects being visible.
- Proton exchange is rapid on the NMR time-scale, so that no (Si, H), *multiplet structure* is observed in the spectra.

Thus there is no obvious method of even demonstrating which resonances belong to the same ionic species. The assignment of individual resonances to definite chemical sites has therefore required special techniques: [14]

i) Use of the highest feasible applied magnetic field to achieve maximum dispersion and improvement of resolution or prevention of spectral overlap.

ii) Use of samples enriched in ^{29}Si. This not only improves the signal-to-noise ratio, S/N, but also introduces splittings in the spectra for many silicon environments due to (Si, Si) spin-spin coupling.

iii) Selective homonuclear Si-{Si} decoupling that enables bands due to nuclei in the same chemical species to be located for ^{29}Si-enriched samples.

Although the advent of pulsed (FT) NMR made the study of aqueous silicate solutions by ^{29}Si NMR an attractive proposition, little structural information was deduced until ca. 1982, at which time only two of the many resonance signals observed in such spectra had been unambiguously assigned to definite silicate structures.[36,47] Most notably, ^{29}Si NMR studies of solutions isotopically enriched in ^{29}Si with special emphasis on homonuclear spin-spin couplings of ^{29}Si nuclei has been done by Harris and co-workers.[7,47-51] A typical ^{29}Si spectrum is shown in figure 1.4 (extracted from the reference 57, with the quoted numbers referring to the structures in figure 1.5.

Sample purity may limit the range of solutions that can be studied.[14] Because of the spectral line broadening caused by low concentrations of paramagnetic species, it is often difficult to observe individual resonances for samples not prepared under laboratory conditions. Such samples include most industrial liquors and solutions.[24]

Moreover, because ^{29}Si NMR is a relatively insensitive technique, there are difficulties in examining solutions with concentrations much below ca. 0.5 M in silica, even under pH conditions where few species are present. Consequently, NMR investigations into biological systems, for example, where the silica concentration is measured in ppm, are not feasible. When examining relatively dilute solutions, or solutions in which many species are present, an inordinate amount of spectrometer time is required. For example, the first 19.8 MHz spectrum of a silicate solution to appear in the literature required 83.3 hours to accumulate.[10]

1.7.b. Advantages and difficulties of high-resolution ^{27}Al NMR of aluminosilicate solutions

Aluminium-27 NMR can provide structural information about the environment of Al nuclei for aluminosilicate solutions through use of both chemical shifts and intensities of the signals. The striking range of chemical shifts for tetrahedral AlO_4^- from ca. 50 ppm up to ca. 80 ppm suggests that there are, beyond the immediate Al co-ordination with oxygen atoms, more subtle structural influences on the Al shielding. In particular, in addition to the directly-bonded oxygen atoms, the nuclei of the second co-ordination sphere (i.e. Si in the case discussed herein) contribute to the shielding of the aluminium. Corresponding ^{29}Si NMR investigations of silicates and aluminosilicates [52-54] have shown that possible influences are: cation effects, bond distances and angles, and the degree of condensation of the tetrahedral groups under consideration. In solutions involving reaction between silicate and aluminate with excess of the former, ^{27}Al NMR spectra confirm that little or no free $Al(OH)_4^-$ is present and that a major fraction of the bound Al is connected to more than one SiO_4 unit.

For ^{27}Al chemical shifts, a few of these structural influences have been investigated.[55-57] In contrast to the well-known dependence of ^{29}Si chemical shifts on the degree of condensation of SiO_4 tetrahedra in silicates, knowledge of the behaviour of ^{27}Al chemical shifts for corresponding condensed aluminate anions is as yet lacking because only a small number of such species seem to exist, in conformity to Loewenstein's rule,* which excludes Al-O-Al bonds. For aluminosilicates the number of AlO_4 environments is also reduced by Loewenstein's rule.[55,57]

---

* Loewenstein [40] 'Whenever two tetrahedra are linked by one oxygen bridge, the centre of only one of them can be occupied by silicon, or another small ion of electrovalence four or more, e.g. phosphorus.

Unlike ^{29}Si, which has a nuclear spin *I=1/2,* ^{27}Al has *I=5/2* and therefore possesses a nuclear quadrupole moment, which gives additional complications at the experimental and theoretical level. Therefore, because of the loss of regular symmetry around the aluminium in most aluminosilicate anions, there is an increased line width. The general lack of resolution in the ^{27}Al NMR spectra suggests that the quadrupole coupling constants for the tetrahedral aluminium sites in aluminosilicate anions are substantial. Consequently, to resolve a separate resonance line for each aluminium site seems to be impossible.[57] Hence there is a requirement for a very high-field spectrometer. However, there are two features which make ^{27}Al a favourable nucleus for NMR investigation: 100% natural abundance and fast relaxation, the latter arising from the quadrupolar nature of the nucleus. Therefore short recycle delays can be applied between pulses, and a ^{27}Al NMR spectrum of good quality with high signal-to-noise can be obtained within comparatively short measurement times. These advantages allow time-evolution experiments to be carried out for aluminosilicates solutions, which is not possible from ^{29}Si experiments.

However, an Al-27 background from NMR probes hinders Al-27 NMR.[58] This background is a very broad, featureless resonance with a chemical shift of about 50 ppm. It is often difficult to distinguish resonances of many aluminium species, which are themselves usually very broad, from the probe background. Such a probe background occurs for the Al-27 experiments described in this thesis. Simeral et al.[58] reported that they found three probe components to contribute the ^{27}Al NMR background: borosilicate glass probe dewars, inserts, and coil mounts; sapphire dielectric materials in probe electronic components; and fibreglass mounts of the electrical circuits in the probe. In addition they found that borosilicate glass

NMR tubes account for about one quarter of the background. In order to eliminate the background resonance, they used three approaches; one approach was to work with very concentrated samples where the background resonance is very small compared with that of the sample itself. As discussed above, there are limitations arising from the low solubility of aluminosilicates. In dilute solution, the background resonance can be as large as, or larger than, that of the sample. The second approach was to obtain a spectrum of the background only, by using a blank (aluminium-free) silicate solution with exactly the same concentrations as for the aluminosilicate solution of interest, and to digitally subtract the background spectrum from the sample spectrum. This approach required that the probe tuning with the sample be exactly matched to that of a solvent blank, and that the baseline be well behaved. These conditions are not easily met, particularly for polar and ionic materials with broad resonances. This approach is the one used at first for the work of this thesis, but results were frequently not ideal. Baseline "roll" and incomplete background subtraction similar to that described in reference [58] were often observed in the present work. Therefore, as described in chapter 2, backward linear prediction was used to process the spectra.

Silicon-29 NMR has also been used to characterize the structure of aluminosilicate anions. This task is complicated by the fact that ^{29}Si peaks from aluminosilicates species are much broader than those for purely silicate species and by the absence of many well-defined aluminosilicate structures on which to base peak assignments. As a consequence, only a fragmentary picture of the interactions of aluminate and silicate anions has been achieved thus far.[25]

1.8. Notation

To simplify writing the various silicate species that can occur in solution, an abbreviated notation has been utilised to describe the structures. The use of "Q-units" was first proposed by Engelhardt et al. [10,36] and they have been used by most investigators in later studies. In this notation, Q represents a silicon atom bonded to four oxygen atoms forming a tetrahedron. The superscript *i* indicates the connectivity, i.e. the number of other Q units attached to the SiO_4 tetrahedron under study. Thus Q^0 denotes the monomeric orthosilicate anion SiO_4^{4-}, Q^1 end-groups of chains, Q^2 middle groups in chains or cycles, Q^3 chain-branching sites and Q^4 three-dimensionally cross-linked groups. Also in this representation the subscript *j* tells you how many Si(Q-units) there are in a given species. With this notation the extent of ionisation is ignored; therefore, the full structure corresponding to a given abbreviated notation may be either completely ionised or entirely as the protonated form, or at any stage in between. Thus the linear trinuclear silicate species would be represented as:

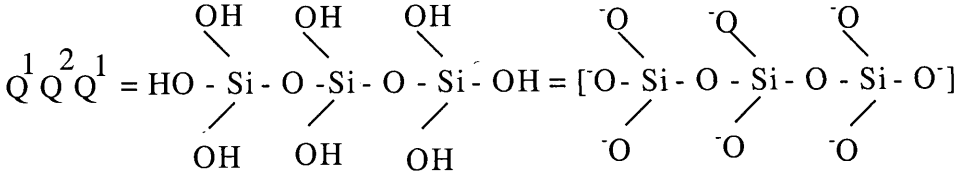

The term 'species' is used to denote a given silicic acid or any ion derived from it, that is, to refer to the Si-O skeleton only. The terms 'n-mer' and 'n-membered' are used in reference to species containing n "Q" sites, as in the linear 'trimer' or the 'three-membered' ring. It must be noted, however, that a ring containing three "Q" sites is in fact a six-atom ring. The

chemical structures of silicate species identified by silicon-29 NMR [7,50,51,59] are provided in figure 1.5.

In considering heavily condensed species and zeolites, some authors[10] define secondary building units (SBU), with two types of structure: single-ring (SR) and double-ring (DR). The former is two-dimensional and the latter has three dimensions. For instance, S4R and S5R mean single four-ring and single five-ring systems respectively. Likewise D4R and D5R are double-four and double-five rings. It should be noticed that D3R, D4R and D5R are contained in the Q^3_6 , Q^3_8 and Q^3_{10} species respectively. The SBU notation will not be used in this thesis.

For aluminosilicate solutions a similar notation can be introduced to deal with species containing aluminium as well as silicon. The notation dealing with the silicate sites is the same as above (i.e. as for silicate solutions). The only difference is in the way the number of aluminium atoms involved in the species in question is indicated. For instance: the prismatic hexamer with one aluminium will be denoted as Q^3_6(1Al), and the cubic octamer with two aluminium sites will be shown as Q^3_8(2Al). For individual silicon sites the number of bridges to aluminium is similarly indicated, e.g. Q^2(1Al), Q^3(2Al) etc.

In the case of individual aluminium sites, the notation is similar to that for silicon. An aluminium site is indicated as "q" (rather than Q for the silicon sites). For such a site, linkage to one siloxane bridge is denoted q^1. In the same way, if it links to 2, 3 and 4 siloxane bridges it is indicated as q^2, q^3 and q^4 respectively. If aluminium has no siloxane bridge, as for the aluminate anion, AlO_4^-, it is represented as q^0. Therefore q^0, q^1, q^2, q^3 and q^4 are Al(0OSi), Al(1OSi), Al(2OSi), Al(3OSi) and Al(4OSi) respectively.

Under Loewenstein's rule, it is unnecessary to introduce a notation for aluminium sites with aluminoxy bridges, since these are forbidden (though they do occur in some minerals, including alumina itself).

The notation Q^n for silicon in silicate solutions, and q^n for aluminium in aluminosilicate solutions, is well established and will therefore be used throughout this thesis. It should be remembered that the ^{29}Si signal for each Q-unit is shifted by ca. 10 ppm to lower frequency when the number of siloxane bridges is increased by one, but in the case of q-units (i.e. aluminium sites) the ^{27}Al resonance is shifted by only ca. 5 ppm to lower frequency, e.g. from q^0 to q^1.

Figure 1.4. 119.2 MHz ^{29}Si NMR spectrum of a Na silicate solution with Si/cation =1 and a concentration of silica of 5.78 wt%. The computer expansion of the $Q^2/Q^3{}_\Delta$ region is shown at the left-hand side of the upper trace and a computer expansion of the cubic octamer region is shown at the right-hand side of the upper trace. Spectral parameters: 50 s recycle delay; 11965.3 Hz total spectral width; 1 s acquisition time and 1000 transients. The spectrum was obtained at ambient probe temperature (ca. 25°C). Assignment of peaks is quoted on the top of each peak. The number refers to the structures presented in figure 1.5. Figure 1.4 is reproduced from reference 57

Figure 1.5. Silicate structures that have been detected by ^{29}Si NMR in alkaline aqueous media. Each line represents a SiOSi linkage.

I:dimer, II:linear trimer, III:linear tetramer, IV:cyclic trimer, V:monosubstituted cyclic trimer, VI:cyclic tetramer, VII: monosubstituted cyclic tetramer, VIII:bridged cyclic tetramer, IX:doubly bridged cyclic tetramer, X:bicyclic pentamer, XI:tricyclic hexamer a, XII:tricyclic hexamer b (transoid), XIII:tricyclic hexamer c (cisoid), XIV:prismatic hexamer, XV:pentacyclic heptamer, XVI:bicyclic octamer, XVII:tricyclic octamer, XVIII:bicyclic hexamer, XIX:cubic octamer, XX:tetracyclic nonamer, XXI:tetracyclic octamer, XXII:hexacyclic octamer, XXIII:prismatic decamer. XXIV:$Q^1{}_4Q^3{}_4Q^4{}_4$

Figure 1.4.

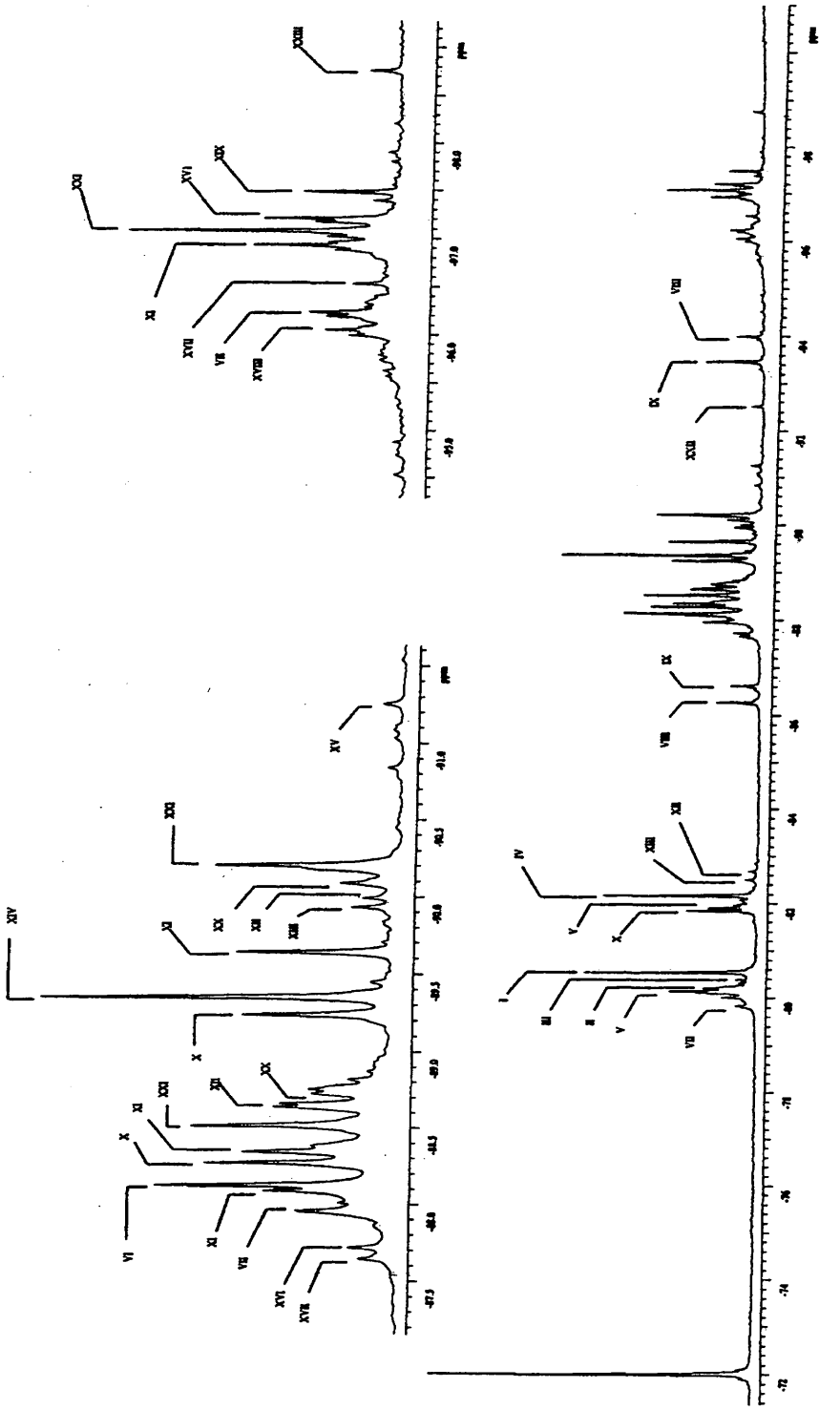

Figure 1.5.

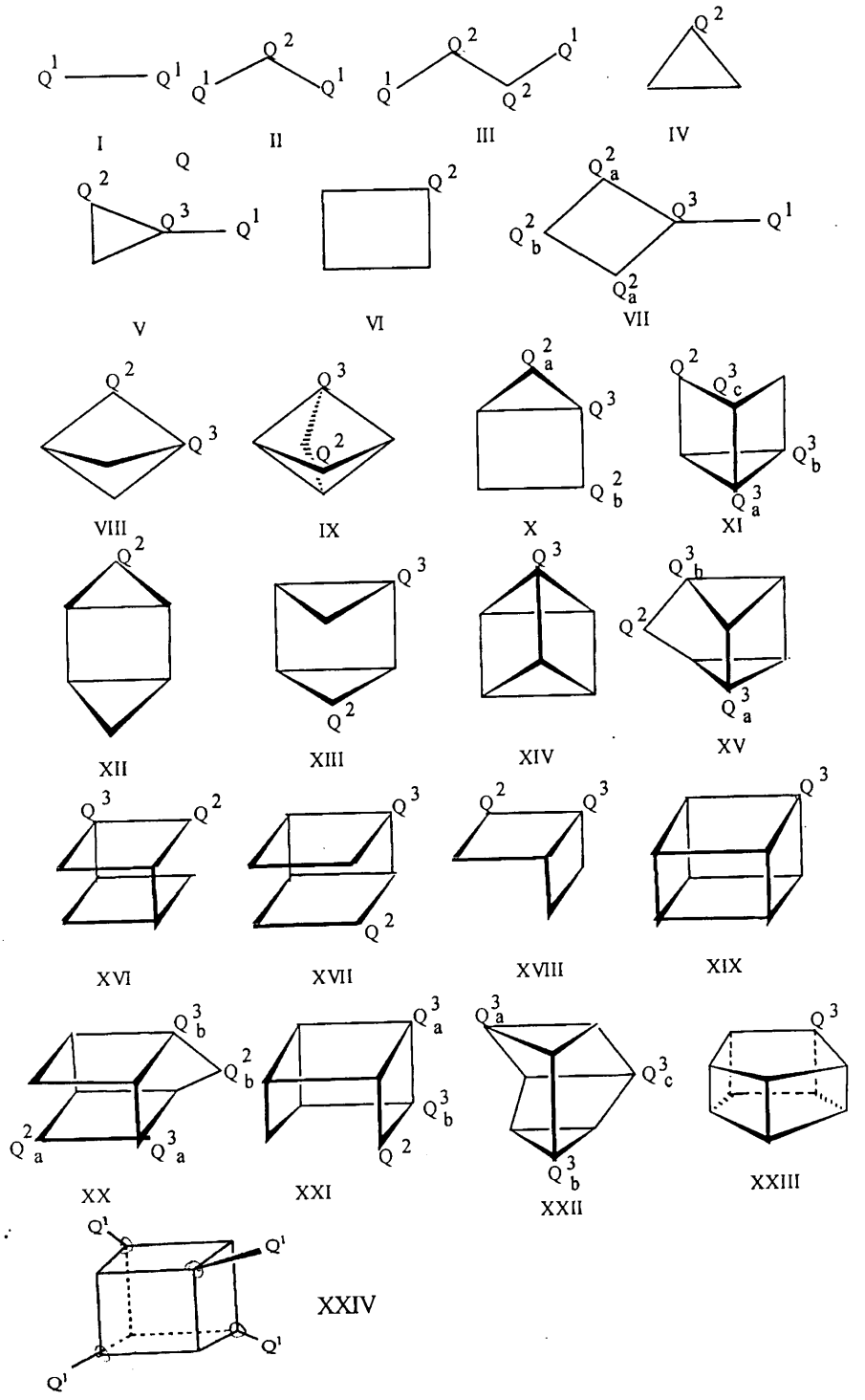
I
II
III
IV
V
VI
VII
VIII
IX
X
XI
XII
XIII
XIV
XV
XVI
XVII
XVIII
XIX
XX
XXI
XXII
XXIII
XXIV

1.9. Assignment of ^{27}Al spectra

The isotropic ^{27}Al chemical shifts of aluminosilicate species are primarily determined by the co-ordination number of the aluminium atoms. The shift ranges observed are about +50 to +80 ppm for AlO_4 (tetrahedral), about -10 to +20 ppm for AlO_6 (octahedral), while about +30 to +40 ppm has been proposed for the relatively rare AlO_5 unit (all from the signal for $Al(H_2O)_6^{3+}$ in an aqueous $Al(NO_3)_3$ solution).[40] In general, these well-separated shift ranges permit the co-ordination number of the AlO_n polyhedra present in the aluminosilicate samples to be determined unambiguously for the ^{27}Al NMR spectra, even from relatively broad lines.

For a broad range of AlO_4 tetrahedral sites present in aluminates, aluminosilicates and aluminophosphates, Muller et al.[15] observed distinct ^{27}Al chemical shift ranges for the AlO_4 units linked to different neighbouring TO_4 tetrahedral (T=Al, Si, P) and AlO_6 octahedral units. However, there is some controversy for the assignment of aluminium sites in aluminosilicates by the various workers. Muller et al.[15] assigned the chemical shifts of 79.5, 74.3, 69.5 and 64.2 ppm (from $Al(H_2O)_6^{3+}$) to q^0, q^1, q^2 and q^3 respectively, using TMA aluminosilicate solutions. Dent Glasser and Harvey,[60] using potassium aluminosilicate solutions, found several bands in the ^{27}Al NMR spectrum lying at shift ranges of 80, 70-72, 66, 61 and 58 ppm and assigned them to q^0, q^1, q^2, q^3 and q^4 respectively. Kinrade and Swaddle [38] observed different signals in ^{27}Al NMR using sodium aluminosilicate solutions. They assigned shifts of 80, 75, 70 and 65 ppm to q^0, q^1, q^2 and q^3 respectively. On the other hand, Mortlock et al.[61,62] using tetraalkyl ammonium aluminosilicate solutions, assigned the signals located at the 74-77, 69-72, 64-67 and 58-61 ppm to q^0, q^1, q^2 and q^3, respectively.

It should be mentioned that in our studies, the ^{27}Al NMR peak assignments of TMAOH aluminosilicate solution species are based on the assignment of similar peaks that appear in TMA aluminosilicate proposed by Muller et al.[63] and Harris et al.[57,64,65] in HMBTP and TMA aluminosilicate solution, i.e. the shift ranges of ca. 80, 75, 70, 65 and 60 ppm are ascribed to the species of q^0, q^1, q^2, q^3 and q^4 respectively.

1.10. References

1. R. K. Iler, "*The colloid chemistry of silica and the silicates*", Cornell University Press, Ithaca, NY (1955).
2. E. Freund, *Bull. Soc. Chim. Fr.,* 2238 (1973); 2244 (1973).
3. W. Weiker, and D. Hoebbel, *Z. Anorg. Allg. Chem.* **366**, 139 (1969).
4. C. W. Lentz, *Inorg. Chem.,* **3**, 574 (1964); B. R. Currell and J. R. Parsonage, *J. Macromol. Sci., Chem.*, **A16**, 141 (1981).
5. E. Thiol, W. Wieker and H. Stade, *Z. Anorg. Allg. Chem.,* **340**, 261 (1965).
6. L. S. Dent-Glasser, and E. E. Lachowski, *J. Chem. Soc. Dalton*, 393 (1980).
7. R. K. Harris and C. T. G. Knight, *J. Chem. Soc., Faraday Trans.* 2, **79**, 1539 (1983).
8. G. Engelhardt, M. Magi and E. Lippmaa, *J. Organomet. Chem.*, **54**, 115 (1973).
9. H. C. Marsmann, *Chem. Zeit.* **97**, 128 (1973).
10. G. Engelhardt, H. Jancke, D. Hoebbel, and W. Wieker, *Z. Chem.*, **14**, 109 (1974).
11. H. C. Marsmann, *Z. Naturforsch. B.,* **29**, 495 (1974).
12. R. O. Gould, B. M. Lowe, and N. A. McGilp, *J. Chem. Soc. Chem. Commun.*, 720 (1974).

13. Kirk-Othmer, *Encyclopedia of Chemical Technology*. Third edition, volume 20 (1982).

14. C. T. G. Knight, *Ph.D. Thesis, University of East Anglia*, and references therein (1982).

15. D. Muller, W. Gessner, A. Samoson, E. Lippmaa, and G. Scheler, *J. Chem. Soc., Dalton Trans.,* 1277 (1986).

16. W. Stumm, H. Huper, and R. I. Champlin, *Enviro. Sci. Technol.* , **1**, 221 (1967).

17. T. Graham, *Ann. Chem.* **121**, 1 (1862), *J. Chem. Soc.* **13**, 335 (1864) and *Ann. Chem.* **135**, 65 (1865).

18. J. Von Fuchs: *J. Dinglers Polytech*, **17**, 465 (1825).

19. J. G. Vail. *'Soluble silicates: their properties and usage'*, Vol. 2. Rheinhold, New York (1952).

20. D. Livingstone, '*U. S. Geol. Survey prof.*' Paper 440, G63 (1963).

21. A. Okuda and E. Takahashi, *Nippon Dojo Hiryogaku Zasshi*, **33**, 1 (1962).

22. G. Izawa and I. Kume, *Hyogo Noka. Daigaku Kenko Hokoku,* **4**, 13 (1959).

23. S. Mitsui and H. Takatoh, *Soil Sci. Plant Nutr. (Tokyo)*, **9**, 49 (1963).

24. J. Jones, *Ph.D. Thesis, University of East Anglia*, (1979).

25. A. V. McCormick and A. T. Bell, *Catal Rev.-Sci. Eng.,* 31 (1&2), 97-127 (1989) and references therein

26. S. A. Greenberg, and D. Sinclair, *J. Phys. Chem.*, **59**, 435 (1955).

27. A. Audsley, and J. Aveston, *J. Chem. Soc.*, 2320 (1962).

28. P. Debye, R. Nauman, *J. Chem. Phys.*, **17**, 664 (1948), and *J. Phys. Chem.*, **55**, 1 (1951).

29. R. K. Iler, *J. Phys. Chem.*, **57**, 604 (1953).

30. G. Lagerstrom, *Acta, Chem. Scand.*, **13**, 722 (1959).

31. G. B. Alexander, *J. Am. Chem. Soc.*, **75**, 2887 (1953), and *J. Am. Chem.*, Soc. **76**, 2094 (1954).

32. C. W. Lentz, *Inorg. Chem.*, **3**, 574 (1964).

33. W. C. Beard, *Adv. Chem. Ser.*, **121**, 162 (1973).

34. O. Bronder, *Z. Physik*, **111**, 1 (1938).

35. E. Frend, *Bull. Soc. Chim. France*, 2238 (1973).

36. G. Engelhardt, D. Ziegan, H. Jancke, D. Hoebbel, and W. Wieker, *Z. Anorg. Allg. Chem.*, 418, 17 (1975).

37. R. K. Harris, and R. H. Newman, *J. Chem. Soc. Faraday*, II, **73**, 1204 (1977).

38. S. D. Kinrade and T. W. Swaddle, *Inorg. Chem.*, **27**. 4253, 4260 (1988).

39. C. T. G. Knight, R. J. Kirkpatrick, and E. Oldfield, *J. Chem. Soc., Chem. Commun.*, **66**, 1986. *J. Magn. Reson.*, **78,** 31 (1988).

40. G. Engelhardt and D. Michel, '*High Resolution Solid-State NMR of Silicates and Zeolites*'., John Wiley & Sons (1987) and references therein.

41. R. K. Harris, *NMR Spectroscopy*, Longman Scientific & Technical (1986).

42. P. J. Hore, *Nuclear Magnetic Resonance*, Oxford University Press (1995).

43. J. K. M. Sanders and B. K. Hunter, *Modern NMR Spectroscopy*, Oxford University Press, second edition (1993).

44. W. Kemp, *NMR in Chemistry*, Macmillan Press Ltd. (1986).

45. J. C. Hoch and A. S. Stern, *NMR Data Processing*, John Wiley & Sons, Inc. (1996).

46. A. E. Derome, *Modern NMR Techniques for Chemistry Reseach*, Pergamon Press (1987).

47. R. K. Harris, J. Jones, C. T. G. Knight, and D. Pawson, *J. Mol. Struct.*, **69**, 95 (1980).

48. R. K. Harris and C. T. G. Knight, and W. E. Hull, *ACS Symp. Ser.*, No. 194, 79 (1982).

49. R. K. Harris and C. T. G. Knight, and W. E. Hull, *J. Am. Chem. Soc.*, **103**, 1577 (1981).

50. R. K. Harris and M. J. O'Connor, E. H. Curzon and O. W. Howarth, *J. Magn. Reson.*, **57**, 115 (1984).

51 R. K. Harris and C. T. G. Knight, *J. Chem. Soc. , Faraday Trans.*, 2, **79**, 1525 (1983).

52. E. Lippmaa, M. Mägi, A. Samoson, G. Engelhardt, and A-R. Grimmer, *J. Am. Chem. Soc.,* **102**, 4889 (1980).

53. M. Mägi, E. Lippmaa, A. Samoson, G. Engelhardt, and A-R. Grimmer, *J. Phys. Chem.,* **88**, 1518 (1984).

54. K. A. Smith, R. J. Kirkpatrick, E. Oldfield, and D. M. Henderson, *Am. Mineral.,* **68**, 1206 (1983).

55. D. Müller, W. Gessner, and G. Scheler, *Polyhedron*, **2**, 1195 (1983).

56 W. Loewenstein, *Am. Mineral.*, **39**, 92 (1954).

57. A. Samadi-Maybodi, *Ph.D. Thesis, University of Durham,* and references therein (1982).

58. L. S. Simeral, T. Zens, and J. Finnegan, *J. App. Spec.*, 47, No. 11, 1954, (1993), and references therein.

59. R. K. Harris, J. Parkinson and A. Samadi-Maybodi, *J. Chem. Soc., Dalton Trans.,* 2533 (1997).

60. L. S. Dent Glasser, and G. Harvey, *Proceeding of the Sixth International Zeolite Conference,*; D. Olson, and A. Bision, Eds. Butterworths: London, 925 (1984).

61. R. F. Mortlock, A. T. Bell, and C. J. Radke, *J. Phys. Chem.*, **95**, 7847 (1991), and references therein

62. R. F. Mortlock, A.T. Bell, and C.J. Radke, *J. Phys. Chem.*, **95**, 372 (1991).

63. D. Müller, D. Hoebbel, and W. Gessner, *Chem. Phys. Lett.*, **84**, 25 (1981).

64. R. K. Harris, J. Parkinson, A. Samadi-Maybodi and W. Smith, *J. Chem. Soc., Chem. Commun.*, 593 (1996)

65. A. Samadi-Maybodi, S. N. Azizi, H. Naderi-Manesh, H. Bijanzadeh, I. H. McKeag and R. K. Harris, *J. Chem. Soc., Dalton Trans.*, 633 (2001).

Chapter Two

Experimental and instrumental considerations

2.1. Instrumentation

To achieve better resolution and signal-to-noise, especially for ^{27}Al, the majority of liquid-state NMR spectroscopy was performed with two main instruments in this study: A Varian VXR 600 spectrometer at the department of chemistry, University of Edinburgh (Ultra High Field NMR Service), operating at 14.1 T (i.e. 156.3 MHz for ^{27}Al NMR); and Varian Inova 500 and Bruker DRS 500 Avance spectrometers at the University of Durham in the UK and Tarbiet Modarres University in Iran respectively, both operating at 11.7 T (i.e. 130.2 MHz for ^{27}Al and 99.3 MHz for ^{29}Si).

The solid-state NMR spectroscopy was performed with the Varian Unity Plus 300 spectrometer at the University of Durham Industrial Laboratories.

2.2. Spectra conditions

Aluminum-27 NMR spectra were obtained by applying 90° pulses (34 μs pulse duration), the time elapsing between pulses being sufficient to allow complete return of the magnetisation to equilibrium, i.e. the recycle delay was 0.2 s. The samples contained 15% D_2O, the D_2O signal served as a field-frequency lock. The probe gives rise to a broad background signal which overlaps with the q^3 and q^4 regions. Two ways of compensating for this signal were tried:

a) The method of background subtraction. In order to give maximum accuracy for the baseline subtraction, a blank (sample tube with a silicate solution containing TMAOH with the same silicate to amine ratio as for the aluminosilicate spectrum) was run with every aluminosilicate sample, and its FID was subtracted from the FID of the relevant aluminosilicate solution.

b) The other method, which was eventually used throughout this work, is backward linear prediction (BLP), which is discussed in detail in section 2.3.5. When this method was first used, in order to find the best number of points for BLP, several experiments using the blank solution with differing numbers of points were carried out to completely eliminate the background (i.e. to get a similar result to the subtraction method). It was found that backward linear prediction for the first 12 points of the FID usually gives spectra of good apparent quality. Therefore mostly this number of points was used in BLP to obtain the spectra of figure 4.1 as well as the other spectra, making many aspects of interpretation easier. However, it probably does result in uncertainties regarding the extent of the true q^4 signal from the aluminosilicate solutions. Moreover, phasing the spectra was not easy because the background signal invariably had a different phase from those of the peaks arising from the solution. There are further complications, because, to obtain spectra of good apparent quality in some cases, the number of points used in BLP ranged from 10 to 20. However, the BLP method is the easiest way to obtain good apparent spectra, but it requires special accuracy.

Silicon-29 NMR spectra were obtained at ca. 22°C. Typically, 90° pulses of duration 10.4 μs were used, with acquisition times of 1.454 s, the time elapsing between pulses being sufficient (typically 20 or 50 s) to allow complete return of the magnetisation to equilibrium. Silicon-29 chemical shifts are referenced to an external (replacement) solution of TMS in $CDCl_3$. A large spectral width was employed to avoid fold back of the background glass peak (see below). Each NMR spectrum was obtained in absolute intensity mode when quantitative comparisons were required. The probe

used for these experiments contained silicate glass. Therefore a broad background signal centred at $\delta_{Si} \cong -120$ ppm (the same region as the Q^4 peak) could be observed. There are several ways of compensating for this signal. In principle, unwanted complications of this type can be avoided by using tubes and inserts manufactured from silica-free material. Alternatively, subtraction of the ^{29}Si signal for an empty NMR tube can overcome this problem, but at the cost of an increase in the spectrometer time used and a deterioration of $\sqrt{2}$ in the S/N ratio. For practical expediency, in this work a backward linear prediction was applied for the first 12 points of the FID in the same way as discussed for aluminium-27 NMR. This gave spectra of good apparent quality, making many aspects of interpretation easier, although it did result in uncertainties regarding the extent of the true Q^4 signal from the silicate solution.

2.3. Data processing [1, 2]

2.3.1. Introduction

NMR instruments have to fulfil two tasks:

1) Acquisition of the spectral data.

2) Processing of the acquired data to get the final spectrum.

Without the NMR instrument, the first task cannot be performed. But the second one can be carried out with any computer running the appropriate software. The advantages of using the spectrometer exclusively for acquiring data and an external computer to process the data are obvious to any researcher in a large institution: a great deal more spectrometer time becomes available for running spectra, and thus a large number of samples can be measured.

A number of NMR data processing systems have been developed (in order to implement this division of labour). The so-called *off-line* processing

has become very popular. Using a personal computer, a chemist can process his/her own spectra, analysing the data for as long as he/she wants, and meanwhile the spectrometer can be used for its main purpose, the acquisition of new spectra. MestRe-C has been developed for the *off-line* processing of NMR spectra in a compatible pc running windows software.

The aim of this text is not to explain the theoretical aspects of NMR, which can be found in a number of books, or to explain all the aspects of processing the data being imported from the different Bruker or Varian or the other spectrometers, since these can be found in the booklets or tutorials enclosed with the software. It will be explained here, briefly, how to process an NMR spectrum to the print-out stage.

2.3.2. Importing data

NMR signals are waves, with frequencies that lie in the radiowave part of the electromagnetic spectrum. When a spectrum is acquired, it is necessary to convert those waves, as analogue, continuous functions, into binary data, digital, discrete functions. The spectrometer is equipped with an A/D (Analog-to-Digital) converter, which performs this task. The analogue numbers will be converted into binary numbers. Such numbers are then stored in the spectrometer's computer. The software knows how to read and process these binary data to convert them into the spectral trace that might be recorded by the printer. This last part is the one for which the spectrometer is not needed; it can be performed on another computer if it has the appropriate software to read and process (binary) data. NMR data are stored on the spectrometer's hard disk. There are two main formats: binary and text. Binary data are only readable by the machine, and they are stored as the machine processes them. This means binary data are numbers. Unlike binary data, text data are readable also by humans. The software used runs

under an Operating System (OS). In the case of MestRe-c, this is Windows 98. The data are imported directly by File Transfer Protocol (FTP).

The Varian Inova spectrometer uses two files for each FID/Spectrum: FID and PROCPAR. The FID file contains the acquired data and the PROCPAR file the parameters. To import the data, the user selects the FID file and MestRe-C retrieves the parameters from the PROCPAR file. To start processing the data with MestRe-c, it is necessary to import the FID file into the program.

2.3.3. Baseline correction

Part of the spectrum is formed by baseline, which does not contain peaks. The baseline of the spectrum must be flat. The baseline can be distorted by many things. There are three sources of baseline distortions [3] which must be removed. Improper phase correction will lead to twists in the baseline near the signals, which in turn distort the integral. The second type of baseline error arises from the finite time taken for the electronics to recover from the effects of the radio frequency pulse. This effect is caused by corruption (or overflowing) of the first few points of the FID, and sometimes it can be corrected by a judicious shift of the FID data points. The third type arises from a frequency-dependent phase change in the audio filters used to exclude high-frequency noise. This distortion can be removed by overriding the preselected filter width with a much larger value. This tactic will, however, introduce more noise into the spectrum. The latter two problems cause a rolling baseline when the whole spectrum is observed with the gain turned up. Fortunately, the manufactures have built baseline flattening routines into their software. These matters are also commented upon in section 2.3.4-5. There are some other facts, which might affect the spectrum, for example: Truncation of the FID before the signal reaches zero

(or noise) level. By the use of an apodization function (see the next section) the truncation effect can be suppressed.

For modelling the baseline, another simple method is to select an equally distributed set of points from the baseline. This set of points is a very schematic model of the baseline. Subtracting the selected points from the baseline usually gives a good correction. The larger the number of points selected, the better the correction is.

2.3.4. Phase correction

NMR signals are waves, and like any other waves they can be in phase or out of phase. This means that all the waves in spectrum can start simultaneously (at the effective zero time) or not. The second is the most usual case, so phase corrections are necessary.

There are actually two phase corrections: the zero-order correction, and the first-order correction. The former is a constant, affecting all the frequencies in the spectrum in the same way, but the latter is frequency-dependent. These phase corrections are applied to all points of the FID, and they may be between 0 and 180°. A phase correction of more than 180° is equal to a negative one. Large phase adjustments may lead to a spectrum corrected in phase, but with the peaks inverted.

The zero-order correction is applied by setting the tallest peak of the spectrum as a pivot point. The peak should appear symmetric when properly phased. Sometimes the zero-order correction is enough to produce an acceptably phased spectrum, but this is not usually the case. In most instances, once the zero-order correction has been applied, it will be necessary to apply a first-order correction. This correction has a less marked effect on the spectrum, and mainly affects peaks which are far from the pivot point.

In some cases, phase correction can be difficult to apply; a careful shift of the pivot point can help to get the best phase correction.

2.3.5. Linear Prediction (LP)

Among the various processing options available to improve the quality of FIDs and the corresponding spectra, linear prediction (LP) is probably the most exciting and powerful, even though it is not widely used.[4]

Raw time-domain data acquired during a pulsed NMR experiment can have two flaws:[5]

- Parts of an FID or early points in the FID may be distorted (see fig. 1) either due to either mis-set acquisition parameters or introduced by some spectrometer perturbation or a host of hardware characteristics, such as preamplifier saturation, probe ringing, and filter non-linearity. Even on a perfect spectrometer, these distortions cannot always be avoided.

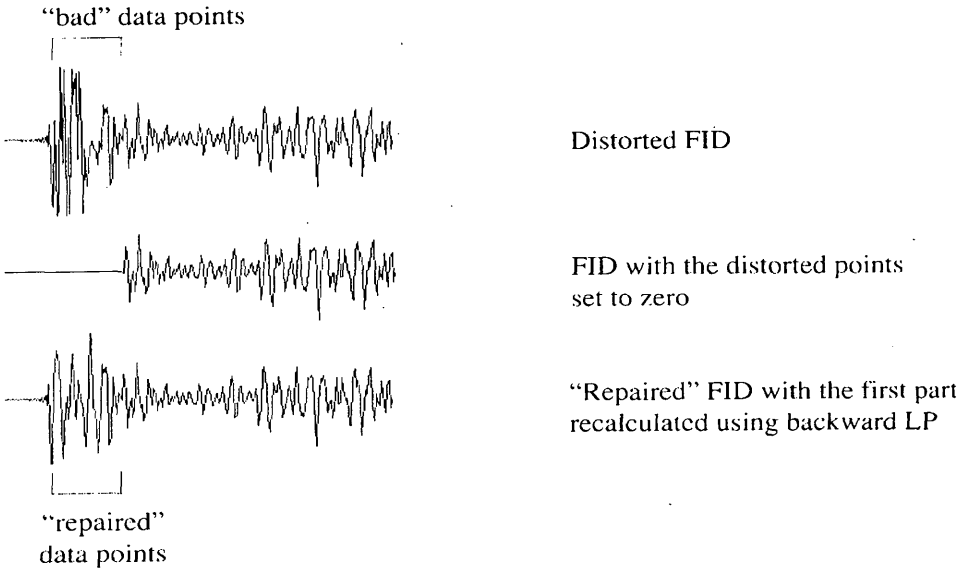

Figure 1. Backward Linear Prediction (reproduced from reference 4).

• The acquisition time of each FID may have been too short to allow for full decay of the signal (see figure 2), leading to distortion in the Fourier transform spectrum.

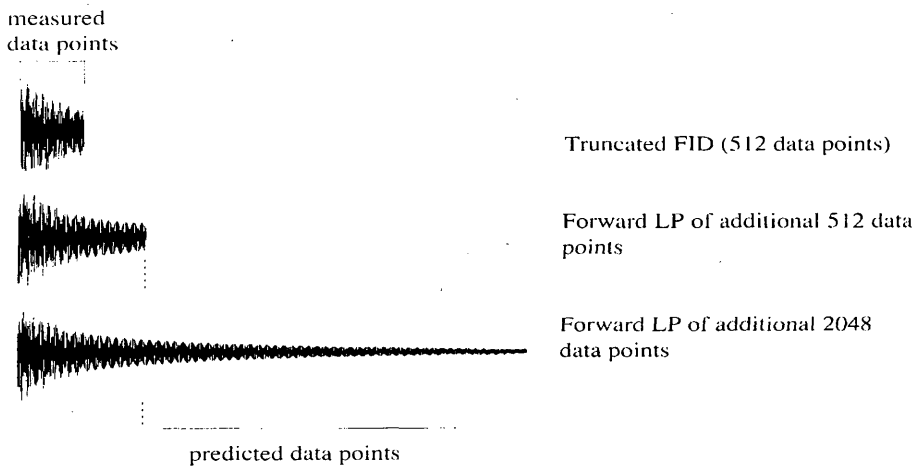

Figure 2. Forward Linear Prediction (reproduced from reference 4).

These unwanted effects are removed from the corresponding spectra using LP by firstly analysing the non-truncated part of the FID and then predicting and reconstructing the truncated part of the FID.[4] Zeroing the first points of a distorted FID or adding additional zeros at the end of an FID (Zero Filling), as outlined below, represents the most primitive approach to LP, since zeros are "predicted" for the FID region to be "repaired" and for the FID region to be extended respectively.

As discussed above, LP methods are applied for different purposes, such as Backward Linear prediction (BLP), which is used throughout this work and Forward Linear Prediction (FLP). In other words, LP uses the "good" part of the FID to analyse for the frequencies that are present in the signal, and then extrapolates that information to extend the FID, either in a reverse direction (to "fix" the first few "bad" points) or in a forward

direction (to eliminate truncation problems). Following this process, the "new, improved" FID is then Fourier transformed in the usual way.

With broad signals such as ^{27}Al signal, the problem is more serious. The signal decays rapidly, making long acquisition times counterproductive and causing substantial loss of magnetization during the time taken for the spectrometer electronics to recover from the pulse (before data acquisition can begin). If the pre-acquisition delay time is not enough, the extraneous signal introduced by the pulse will dominate the earlier part of the FID and will, when transformed, generate a broad rolling component to the baseline. Since the signal of interest is also decaying rapidly, it may become impossible to distinguish the resonance peaks from the rolling baseline. As a general rule, it is not easy to use a high-resolution spectrometer for lines which are more than about 1000 Hz wide.[3] In such cases, it may be necessary to use a different spectrometer to observe the spectra.

Linear prediction in VNMR is incorporated directly into the Fourier transform routine, so that normally one does not see the " improved" FID, but merely the spectrum, which results from Fourier transforming the linear predicted FID.

Since linear prediction involves solving a series of equations for appropriate coefficients based on the actual FID, it involves quite a number of parameters and can be somewhat tricky to optimise (if not optimised properly, or if the data are not amenable, the analysis may simply fail, just as any least-squares fit process may fail to converge).

The advantages of LP extrapolation and zero filling (see next) are fairly obvious. Assuming the prediction filter is stable, the time series it generates is much more realistic than one in which the signal suddenly stops short and instantaneously decays to zero. The sinc wiggle artefacts so

commonly encountered with zero filling are greatly reduced, without the need to apply a drastic line broadening apodization function. This property is very useful for processing multidimensional experiments, where the number of points in the indirect dimensions may be quite limited.[3] An example is shown in figure 3.

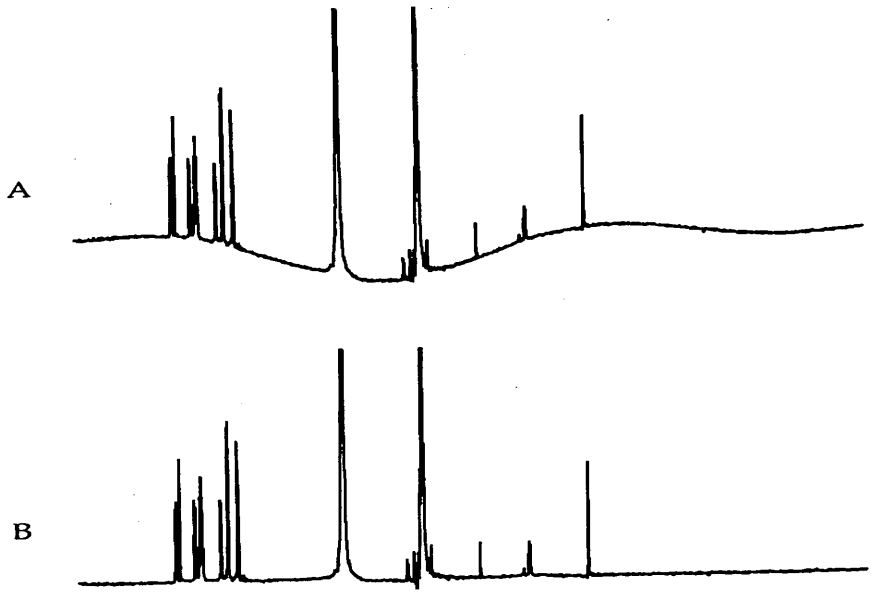

Figure3. Baseline curvature due to corruption of the first few points of the FID (A) can be reduced by using backward-linear prediction to recalculate the values of those points (B). Figure 3 is reproduced from reference 5.

Starting with a time series, such as an FID, the big problem is to find a set of forward or backward LP coefficients for which the time series satisfies the appropriate LP equation.

2.3.6. Sensitivity and resolution enhancement

Once the FID is in the computer, there are several ways in which it may be treated in order to make the spectrum more useful. Either the signal-to-noise or the resolution can be improved by a mathematical treatment known as *apodization*[3, 6] . Because the noise remains constant through the acquisition period, but the signal decays, the early part of the FID contains a

higher proportion of signal. Therefore, if the later part of the FID be suppressed relative to the early part, the apparent signal-to-noise ratio will increase. The most common apodization function for the improvement of signal-to-noise is exponential multiplication, in which the FID is multiplied by an exponential decay. This function contains a term, usually known as line broadening, LB, which is under the control of the operator; the larger the value of LB, the more rapidly the term, and the apodized FID will decay. This more rapid decay leads to a broader line.

Another computer process to improve the signal-to-noise ratio is to add a succession of zeros to the end of the acquired FID before FT, a process known as *zero filling*.[3, 6]

2.4. Preparation of samples

The preparation of samples is explained in detail for each case in the appropriate chapter. The following sections give a general view of the compounds and preparations. The chemical compounds, together with their sources, which were used in this study are presented in table 2.1.

2.4.1. Preparation of pure SiO_2

Pure silica was produced by hydrolysis of silicon tetrachloride (99.8% purity; Janssen Chemical Co.) using doubly distilled water. The precipitate was filtered and washed many times with doubly distilled water to remove all acid. It was then dried at ca. 105°C for 48 hours. The chemical reaction is quite simple:

$$SiCl_4 + 2H_2O \rightarrow SiO_2 + 4HCl \qquad 2.21$$

Regarding this equation from the stoichiometric point of view, much more water was used than is needed.

Table 2.1. Chemical compounds used in this study, together with their sources.

Compounds	**Suppliers**
Deuterium oxide 99.9 atom % D	Aldrich Chemical Co.
Enriched Silicon-29	CIL Cambridge Isotope Laboratories, Inc.
Tetramethylammonium hydroxide, pentahydrate 97% purity	Aldrich Chemical Co.
Tetraethylammonium hydroxide 40% in water	Fluka
Tetrapropylammonium hydroxide	Aldrich
Tetrabutylammonium hydroxide 40% in water	Fluka
Silicon tetrachloride 99.8% purity	Janssen Chemical Co.
Methanol 99.8%	Fluka
Hydrochloric acid 37%	Fluka
Sodium hydroxide	Janssen
Potassium hydroxide	Aldrich
Sodium aluminate technical grade 61.3% Al_2O_3	Fisons plc
Aluminium needles purity ≥ 99%	Fluka
Aluminium chloride hexahydrate 99%	Fisons plc

2.4.2. Making silicate solutions

Aqueous silicate solutions were prepared in a plastic bottle by dissolving an appropriate quantity of silica in doubly distilled water containing ca. 15% v/v of D_2O (Aldrich Chemical Co.) to provide a field/frequency lock for the NMR, and it was then solubilised in an appropriate basic solution. The dissolution of the silica was very slow at room temperature, so it was assisted by heating the sample in an oven at ca. 70°C until the solution became clear. Plastic bottles were employed so as to avoid contamination by paramagnetic ions, which can arise from leaching of glass containers at high pH.

2.4.3. Aluminosilicate solutions

Aqueous sodium aluminate solution was prepared by dissolving $NaAlO_2$ in doubly distilled water. Aluminosilicate solutions were then obtained by mixing the freshly prepared sodium aluminate and alkali silicate solutions in the correct proportions for our investigations (see other chapters for details). After mixing, the solutions were usually allowed to equilibrate for no less than one week at room temperature (ca. 25°C).

2.5. On the choice of suitable reference compounds

Aluminum-27. The sharp resonance of the hexa-aqua Al cation is visible in all aqueous solutions of aluminium salts. Thus, ^{27}Al NMR chemical shifts are referenced with respect to $Al(H_2O)_6^{3+}$. A 1M aqueous aluminium chloride solution was used in the work described here by the tube replacement technique.

For ^{1}H, ^{13}C and ^{29}Si NMR spectroscopy, the use of tetramethylsilane (TMS) as a reference compound is now universally accepted.[7, 8] However, TMS has considerable disadvantages when used in conjunction with aqueous silicate solutions. These are as follows:

(a) TMS is not miscible with water, and must be used in a concentric tube arrangement, i.e. as an external reference, or by tube replacement. A bulk susceptibility correction may be therefore required. There exists a water-soluble salt, 2, 2-dimethyl-2-silapentane-5-sulphonate (DSS), but this was found to be insufficiently soluble to give a strong silicon signal. Furthermore, DSS, being a sodium salt, may interfere with the silicate anion equilibria.

(b) TMS resonates at ca. 70 ppm to high frequency of the highest frequency silicate anion signal, that of the monomer. Since the high-frequency positive convention is adopted in this work, all chemical shifts quoted will be

negative. The large separation between the silicon resonance of TMS and the resonance of the silicate anions usually prevents the inclusion of the reference peak in the spectrum under consideration, it being necessary to run a separate spectrum on a greater spectral width. (By replacing the silicate sample with a TMS sample, it is possible to measure the frequency separation of the TMS and monomer peaks, and reference the spectrum accordingly. This requires running a separate spectrum, and appreciable errors may be introduced, particularly at low frequency).

(c) ^{29}Si-{^{1}H} decoupling techniques are generally required for TMS, but are unnecessary for aqueous silicate solutions since rapid chemical exchange of the protons leaves no multiplet structure to be decoupled.

(d) TMS is volatile, boiling at 26.5 °C,[9] which necessitates specialized handling procedures.

(e) TMS has a long T_1 ^{29}Si (19.8 seconds [6]) relative to that of the silicate anions (ca. 5 seconds).

In view of these considerations, a more practical method of referencing silicate spectra becomes desirable. McFarlane has proposed [10] that chemical shifts be quoted with respect to a magnetic field of strength corresponding to a TMS ^{1}H resonance of exactly 100 MHz (referenced to as the standard field). This procedure, involving the deuterium lock frequency, has been adopted by Harris and Kimber,[6] allowing measurement of chemical shifts 'absolutely but indirectly'. It is, however, susceptible to small errors due to variations in the deuterium lock frequency, induced by temperature and differential solvent and concentration effects.

It has been suggested [11] that the resonance signal of the monomer may be used as a convenient internal reference. However, along with all other peaks observed in the ^{29}Si NMR spectra of silicate solutions, the monomeric

resonance is known [12] to depend upon the pH and concentration of the solution as well as on the methanol concentration, when measured against an external standard (see chapter 3).

An alternative to TMS as a replacement or external standard has been employed in this work. This consists of different concentrations of aqueous and methanolic tetraalkylammonium silicate solution prepared in deuterium oxide and used concentrically in a 5 mm o/d NMR tube. Such a methanolic or concentrated (more than one molar in Si) solution contains a large proportion of the cubic octamer and in some cases prismatic hexamer (see chapter 4). This gives a single, sharp signal and affords several advantages over external TMS. The cubic octamer resonates at ca. –26 ppm from the monomer, to low frequency of all other silicate anion resonances observed in this work. It may consequently be observed directly without recourse to a large spectral width. In common with other silicate anions, no $^{29}Si-\{^{1}H\}$ decoupling is necessary, and its T_1 ^{29}Si is considerably less than that of TMS ($\leq$ 10 seconds). The tetraalkylammonium silicate solution is easily prepared, apparently indefinitely stable, non-volatile and non-toxic. However, apart from the disadvantages inherent in the use of all external or replacement standards, a tetramethylammonium solution displays one other: The concentrated solution tends to crystallize at low temperatures. Tetraalkylammonium aqueous and methanolic silicate solutions are discussed in more detail in chapter 3.

2.6. References

1. A guide of the Mestre-c program (1999).
2. Getting Started: VNMR 6.1, Chapter 8, Advanced Data Processing (1998).
3. J. K. M. Sanders, and B. K. Hunter, *Modern NMR Spectroscopy A Guide for Chemists*; Oxford University Press: Chapters 1, 8 and 9, Oxford, UK, 2nd Edition (1993).
4. P. Bigler, *NMR Spectroscopy: Processing Strategies*, second updated edition,Wiley-VCH, (2000)
5. C. H. Jeffrey and A. S. Stern, *NMR Data Processing*, Chapter 4, Wiley-Liss, Inc. (1996).
6. R. K. Harris and B. J. Kimber, *J. Mag. Res.* 17, 174 (1975).
7. G. C. Levy and J. D. Cargioli, *J. Mag. Res.* 6, 143 (1972).
8. G. C. Levy, J. D. Cargioli. G. E. Maciel, J. J. Natterstad, E. B. Whipple, and E, M. Ruta, *J. Mag. Res.* 11, 352 (1973).
9. C. R. C. *Handbook of Chemistry and Physics*, ed. R. C. Weast, Chemical Rubber Publishing Company, Ohio (1974).
10. W. McFarlane, *Proc. Roy. Soc. Lond.* A306, 185 (1968).
11. R. K. Harris and R. H. Newman, *J. C. S. Faraday Trans.* II, 73, 1204 (1977).
12. J. Jones, *Ph. D. thesis, University of East Anglia* (1979).

Chapter Three

Silicon-29 NMR of methanolic silicate solutions

3.1. Introduction

The compositions of aqueous silicate solutions are of particular practical interest. The presence of individual silicate anions in alkaline solutions of SiO_2 was first established from measurements of pH and through use of trimethylsilylation, chromatography, and the reaction of silicate anions with molybdic acid.[1] Such solutions contain monomeric $[Si(OH)_{4-x}O_x]^{x-}$ anions and a wide range of oligomeric anions that differ in both molecular weight and extent of ionisation.

It is generally accepted now that a dynamic equilibrium exists in silicate solutions between a range of silicate anions of varying degrees of condensation and molecular weights that cannot be chemically separated owing to their rapid exchange rates. The distribution of silicate species in a complex set of equilibria depends on a variety of parameters such as silica concentration, pH, cation content, temperature and probably solution history[2-5], methanol and the presence of other components such as aluminates. Thus under many conditions such solutions contain a large number of species.

The lifetimes of these species are short on the time-scale of normal chemical separation, but long on the NMR time-scale. Therefore, all the methods involving chemical treatment of the solutions, which are mentioned in the introduction of chapter one, have to be used with caution, and in some cases their results have been a matter of controversy [6-7]. Raman spectra of aqueous silicate solutions are not very well defined but suggested that the distribution of silicate species is independent of both the solution history [8] and the alkali-metal cation used [9], statements which are now known to be (at least) only partially correct.

Silicon-29 NMR spectroscopy has been shown to be a very powerful tool for the study of silicate anion species and the structural units present in silicate solutions. Silicon-29 NMR can directly and non-destructively probe such solutions, providing information as to the number, concentration and structures of the constituent species.[10-14] However, it should be noted that proton exchange in silicate anions is rapid on the NMR timescale.

On the basis of the previous studies,[15,16] certain tetraalkylammonium (TAA) cations may exert specific structure-forming effects on the silicate anions present in aqueous silicate solutions. This is clearly demonstrated by the ^{29}Si NMR spectra of tetramethylammonium (TMA) and tetraethylammonium (TEA) aqueous silicate solutions. There is little systematic information on alcoholic TAA silicate solutions. Therefore it seems reasonable to describe some matters about methanolic silicate solutions, since the distribution of silicate species will be related to the influence of methanol. The following sections explain some characteristics of silicate solutions at first, and then attention is paid to a systematic study of the distribution of species in the methanolic silicate solutions. In this work, ^{29}Si NMR spectroscopy was employed to study TMA and TEA methanolic as well as aqueous silicate solutions. Silicon-29 NMR spectra at 99.3 MHz for alcoholic alkaline aqueous silicate solutions show that an esterification reaction occurs. A silicon alkoxide [$(HO)_3Si\text{-}OCH_3$], has been detected. The effects of type and concentration of alcohol, silicate and TAAOH concentration and the nature of the alkylammonium base on this reaction have been investigated.

3.2. Chemistry of dissolved silicate species

The structural characterisation of individual anions and quantitative measurements of aqueous silicate solutions has become possible only within the past three decades through application of ^{29}Si NMR spectroscopy. In an early application of this technique, Marsmann [17] showed that ^{29}Si NMR spectroscopy could distinguish Si atoms with different connectivities, whilst Engelhardt et al.[18] demonstrated that the alkali:silicate ratio has a significant influence on the condensation of the silicate oligomers in solutions used for faujasite synthesis. In an elegant series of studies, Harris et al.[19-21] reported that high-resolution NMR spectroscopy could be used to identify spectral features attributable to individual silicate anions. These authors were able to make peak assignments for 19 anionic structures in potassium silicate solutions prepared with ^{29}Si-enriched SiO_2. Knight,[22] using the technique of two-dimensional homonuclear correlation spectroscopy (COSY), has confirmed the structural assignments proposed by Harris et al.[19-21] and has identified four new silicate species. A typical ^{29}Si spectrum is shown in figure 1.4 (extracted from reference 15), with the quoted numbers referring to the structures in figure 1.5. Throughout this work the assignments are on the basis of these references.[19-21]

3.3. Chemical shifts of species in silicate solutions

In the following discussion the ^{29}Si chemical shifts of tetrahedral environments in silicate solutions are given. The total range of such shifts observed in the ^{29}Si NMR spectra of silicate and silicic acid solutions extends from about -60 to about -120 ppm (TMS reference), i.e. about 60 ppm. Within this range, five reasonably well-separated subdivisions have been found which correspond to the five possible Q^n building units.

The peak of the monomeric silicate anions, Q^0, appears at the high-frequency side of the spectrum (δ = -66 to –73 ppm, depending on pH, concentration and counter-ion) followed in a regular sequence by the Q^1 to Q^4 units shifted by about 10 ppm to low frequency for each newly formed Si-O-Si bond. The relative concentrations of the Q units can be obtained directly from the integrated peak areas and may be used to estimate the mean degree of condensation of the SiO_4 tetrahedra in the solution. A short review on the structural interpretation of the spectra is described in the following:

In the range of about -76 to -83 ppm two groups of signals may be present. The first group, centred at about -76 to -80 ppm, contains the peak of Q^1 units in dimeric silicate anions and the slightly shifted peaks of Q^1 end-groups of chains or Q^1 groups connected with Q^3 or Q^4 units.

The second group of peaks, centred at about -81 to -83 ppm, includes Q^2 groups in trimeric cyclosilicates. The formation of "three-membered" rings apparently causes some deshielding compared to chains or larger rings. A sharp singlet is observed for the cyclotrisilicate anion $Si_3O_9^{6-}$. Nearby signals are of Q^2 groups in mono or di-substituted trimeric rings e.g. $Q^2_2Q^3Q^1$. However, Q^2 groups in four- and higher membered rings and chains give rise to the group of signals in the range of about -86 to -90 ppm.

In contrast with the other Q^3 units, those in trimeric ring structures are shifted by only about 8 ppm relative to the corresponding Q^2 units. Consequently, the peaks of the prismatic hexamer, Q^3_6, and other Q^3 units, located in substituted trimeric rings, appear at the low frequency side of the Q^2 shift range. The signals of other branching Q^3 appear in the shift range of about -95 to -101 ppm. In general, no sharp signals are observed in the Q^4

region (ca. –110 ppm), the only exception being for the species $Q^1{}_4Q^3{}_4Q^4{}_4$ (ca.-108 ppm).[23]

Taking into account not only the number but also the type of the Q^n groups connected directly with a given Q^n site, it can be easily shown that there are only four different types of Q^1, but there are 10 for Q^2, 20 for Q^3 and 35 for Q^4. Therefore the complexity of signals in the various bands is expected to increase from Q^1 to Q^4. Also, second-nearest neighbours and cyclisation effects will affect the chemical shifts. It is clear from these considerations that a wide variety of different structural environments may exist for a certain Q^n unit in silicate solutions, resulting in numerous resonance lines with slight shift differences which often cannot be resolved in the spectrum and hence cause line broadening.

3.4. Silicate anions in the presence of organic amine cations

In the synthesis of zeolites the nature of inorganic alkali and/or amine cations influences the final zeolite structure obtained from crystallisation of aluminosilicate gels. The term "template" has been used on a macroscopic scale to describe their role in directing structure formation. With knowledge of the effect the organic cation has on the components of the reaction mixture, a better understanding might be gained of the "template" mechanism and its effect on product formation in actual zeolite synthesis. Use of different quaternary amine cations in zeolites has led to the discovery of numerous new molecular sieve structures. The way that these species interact with the aluminosilicate ions in solution to cause crystallisation of specific structures has been open to much speculation and conjecture, but only recently to direct examination.

Following the pioneering work of Barre and Denny [24] and Kerr and Kokotailo [25] in the early sixties, organic bases have found wide application

in the synthesis of zeolites. Numerous variations on this theme have resulted in the syntheses of silicon-rich forms of known zeolites and of new, even aluminium-free, frameworks. [26] The cation of the base is considered to play a structure-directing role, an interesting but as yet poorly understood phenomenon. However, the importance of the solution (gel) chemistry for the specific zeolite structure that is being formed has long been recognised.[26,27] Therefore, the question arises whether the organic species already exerts a structure-directing influence in solution *via* the stabilisation of a particular aluminosilicate; such a pre-selected silicate in solution may then act as a building unit for a specific zeolite.

These considerations have given rise to the present study of the influence of some organic ammonium ions with and without methanol on the occurrence of some specific silicate species in solutions from which zeolites may be crystallised. The organic cations used in this study are mostly those derived from TMAOH, TEAOH, and in some cases TPAOH and TBAOH. In section 3.6.1 the Q^0 region of the spectra is discussed in more detail, and a brief consideration of the other regions is presented in section 3.6.2.

3.5. Experimental

All samples were prepared as described in chapter 2. All alcoholic silicate solutions were prepared in an analogous procedure with the appropriate amount of alcohol (volumetric) being added after dissolution of the silica. The samples contained ca. 14% v/v D_2O, the D_2O signal serving to give a field-frequency lock. The volume of the samples was made up to the mark with doubly distilled water to give known molarities of the components. Plastic bottles were employed so as to avoid contamination by paramagnetic ions, which can arise from the leaching of glass containers at high pH. Silicon-29 NMR spectra were obtained as discussed in the

experimental part of chapter 2. Decoupling was employed in the gated mode to avoid the influence of the NOE.

3.6. *Direct Detection by Silicon-29 NMR of a Silicon Alkoxide formed in Methanolic Tetra-alkylammonium Hydroxide Silicate Solutions.*

3.6.1. Studies of the Q^0 region.

3.6.1.1. Introduction

Silicon-29 NMR spectra of solutions of silica ($[SiO_2] \leq 1$ M) in methanolic tetraalkylammonium hydroxide (TAAOH) were investigated. In the region of the expected signal from the monomeric silicate anion (generally designated Q^0) a new band in the range about 0.1-0.4 ppm to low frequency was observed. This signal is designated as $Q^{0'}$. When the present work was started the formation of alkoxysilicic acids under such conditions had not previously been reported. [16,28-35] It is possible to detect, in spectra obtained for aqueous alkaline tetramethylammonium silicate solutions by Knight,[31] two closely-spaced weak peaks in the region associated with monosilicic acid and its anions, but the author did not comment on this fact. Indeed, a peak at this position is shown in Fig. 2B of ref. 31, but is not discussed in the text of the paper at all. A similar situation, but in markedly more favourable circumstances was noticed in spectra obtained for other purposes during the present work, and it was decided to investigate further. Whilst this study was in progress, a short communication appeared[36] reporting the existence of $CH_3OSi(OH)_3$ and a range of other alkylated species in silicate solutions containing tetrabutylammonium hydroxide. However, these authors [36] did not examine the dependence of the concentrations on the various factors involved. Herein the effects of dilution

and of the concentrations of methanol and tetraethylammonium hydroxide on the concentration ratio of methoxysilicic acid to orthosilicic acid are quantitatively reported. *A priori*, the signal may be presumed to belong to $[(HO)_3Si(OCH_3)]$ (a similar comment is made in reference 36) or an anionic form thereof. By observation of this signal it is shown that an esterification reaction has partially occurred between monomeric silicate and methanol. In fact one or two of the terminal OH groups on Si may be replaced by alcohol derived alkoxy-functions.[36] These doubly esterified species are at very low concentration and were not detected in the present work.

It has been found that the extent of the reaction varies greatly with alcohol, silicate and TAA concentration, as well as with the nature of alkylammonium base and the type of alcohol.

3.6.1.2. Results

In the present study, the solutions listed in tables 3.1 to 3.6 were prepared. They were studied by ^{29}Si NMR spectroscopy. Based on the investigations performed, the following results were obtained:

I)- For solutions containing TMAOH and/or TEAOH with different concentrations of Si and cation, but without any methanol, there is only one signal in the monomeric region, as expected (see figure 3.1). However, sample 210, prepared by diluting sample 205 with methanol, and sample 217 (which is similar in compositions to sample 216 except that it contains 45 percent methanol) show about 31 and 46 percent relative intensity of the additional ($Q^{0'}$) signal respectively - see figure 3.2.

It may be noted that the chemical shift of $CH_3OSi(OH)_3$ arising from hydrolysis of $(CH_3O)_4Si$ in acid solution illustrated in figures 1, 4.2, and 8.12 of references 34, 33 and 16 respectively, is at ca. $\Delta\delta$=1 ppm. Because of the different systems and conditions (and, in particular, the fact that

references 16, 33 & 34 relate to low pH), this value of $\Delta\delta$ cannot be compared in detail to the result of the present experiments. In other words the variation in the chemical shift difference between Q^0 and $Q^{0'}$ in acid and alkaline solution is to be expected in view of changes in protonation state. [Note: Unfortunately Table 1 of ref. 34 contains a misprint - the order of the species listed should be reversed, as is clear from figure 1 of the same paper]. Signals other than $Q^{0'}$ that could be assigned to the esterification of condensed silicate species cannot be pinpointed in any of the spectra reported here. However, Kinrade et al.[36] have identified a number of such compounds in silicate solutions containing tetrabutylammonium hydroxide and different alcohols.

Table 3.1. Composition data and relative integrated intensity of $Q^{0'}$ for silicate solutions contain 14 %v/v D_2O.

Sample No.	Molarity Si	Molarity Template TMAOH	TEAOH	MeOH %v/v	Relative intensity % of Q0':Q^0	$\Delta\delta$ * ppm
212	1.00	2.00	0.00	0	0	-
213	2.90	1.30	1.16	0	0	-
216	1.00	0.00	1.00	0	0	-
205	1.00	1.00	0.71	0	0	-
217	1.00	0.00	1.00	45	46	0.23
210	0.50	0.50	0.36	45	31	0.13
290	1.00	0.00	0.71	45**	8	1.00
302=231	0.1	0.2	0.00	76	85	0.42

*$\Delta\delta$) in all the tables means the difference of the chemical shift for Q^0 from that of $Q^{0'}$ i.e. $\Delta\delta=\delta(Q^0)-\delta(Q^{0'})$

** Ethanol in place of methanol

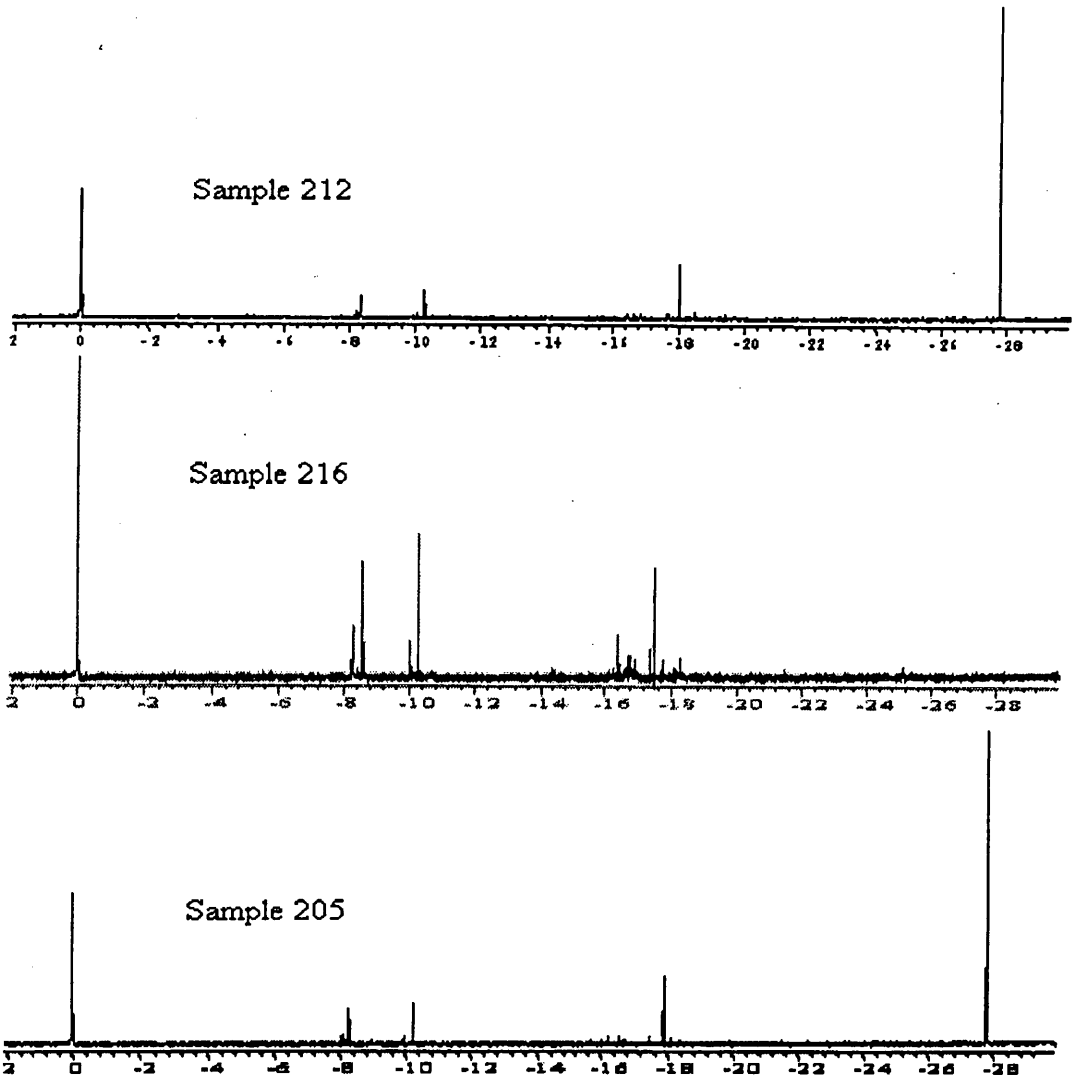

Figure 3.1. 99.23 MHz ^{29}Si Spectra of TAA silicate solutions. (Sample 212) 2 molar TMA, (sample 216) 1 molar TEA, (sample 205) a mixture of 1 molar TMA and 0.7 molar TEA. All samples are 1 molar in Si and contain 14% v/v D_2O. Spectral parameters: 50 s recycle delay; 22008 Hz total spectral width; 65536 data point; 680 repetitions for samples 212 and 205 but 424 transients for sample 216. All spectra were obtained at ambient probe temperature (ca. 22 °C). These spectra are presented referenced to the Q^0 peak at 0 ppm (ca. –72.6 ppm from TMS) using the high frequency is positive convention.

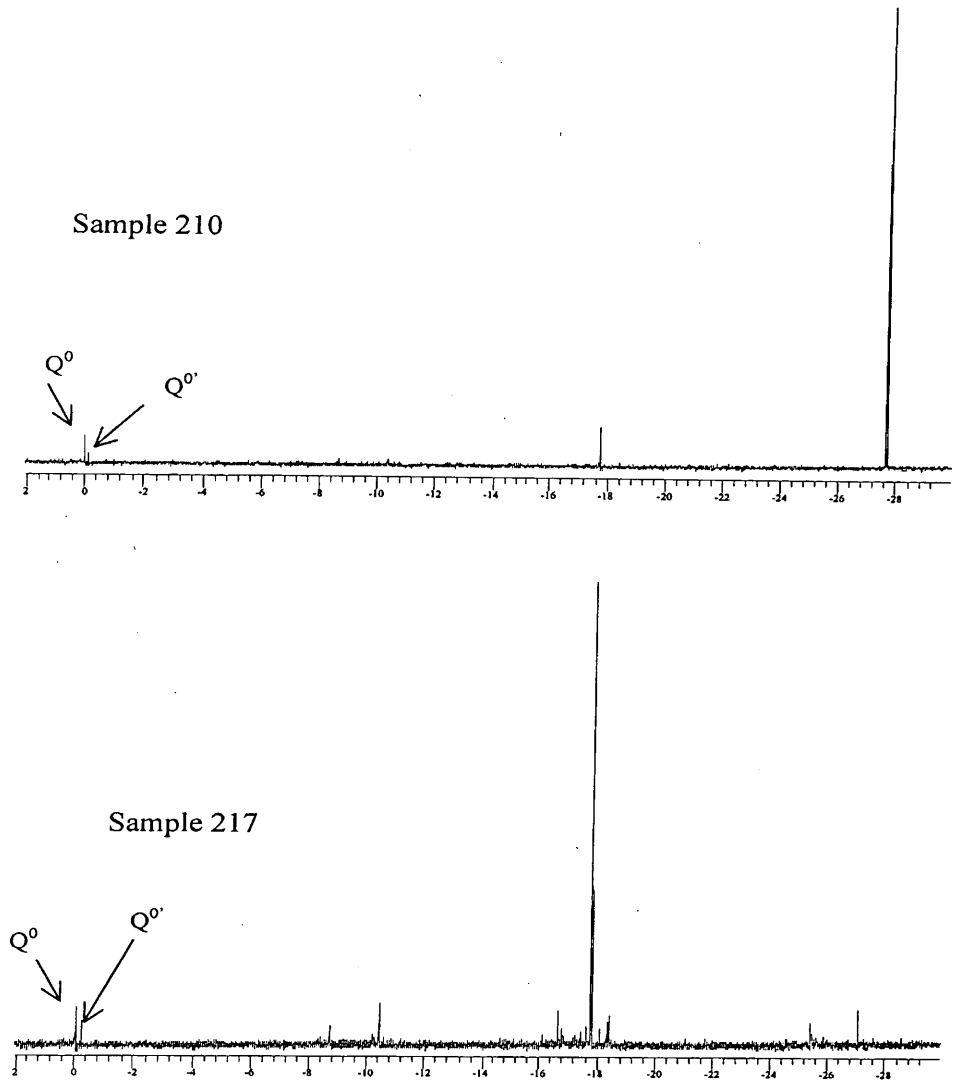

Figure 3.2. The 99.29 MHz ^{29}Si NMR of two spectra obtained from samples 210 and 217 with the compositions given in table 3.1. The upper trace is from sample 210 and the bottom is from sample 217. Both spectra were recorded over a 22008 Hz spectral width with H-decoupling at ambient probe temperature (ca. 22 °C), recycle delay 50 s, 90° (10.7 μs) pulse. Acquisition times of 2.9 and 1.0 s, with 680 and 424 repetitions were used for the spectra of samples 210 and 217 respectively. ^{29}Si chemical shifts are referenced to Q0 signal. These spectra are presented referenced to the Q^0 peak at 0 ppm (ca. –72.6 ppm from TMS) using the high frequency is positive convention.

II)- The ^{29}Si NMR spectrum of sample 206.1*, a methanolic silicate solution, was measured with and without H-decoupling. With H-decoupling the $Q^{0'}$

* Sample 206.1 is a fresh solution with the same composition as sample 206.

signal is shown to be only a singlet. However, by recording ^{29}Si NMR spectra without H-decoupling, the corresponding signal appears as a quartet at δ=-74.76 ppm, with the $|^3J_{Si-H}|$ scalar coupling constant equal to ca. 3.4 Hz, see figure 3.3.

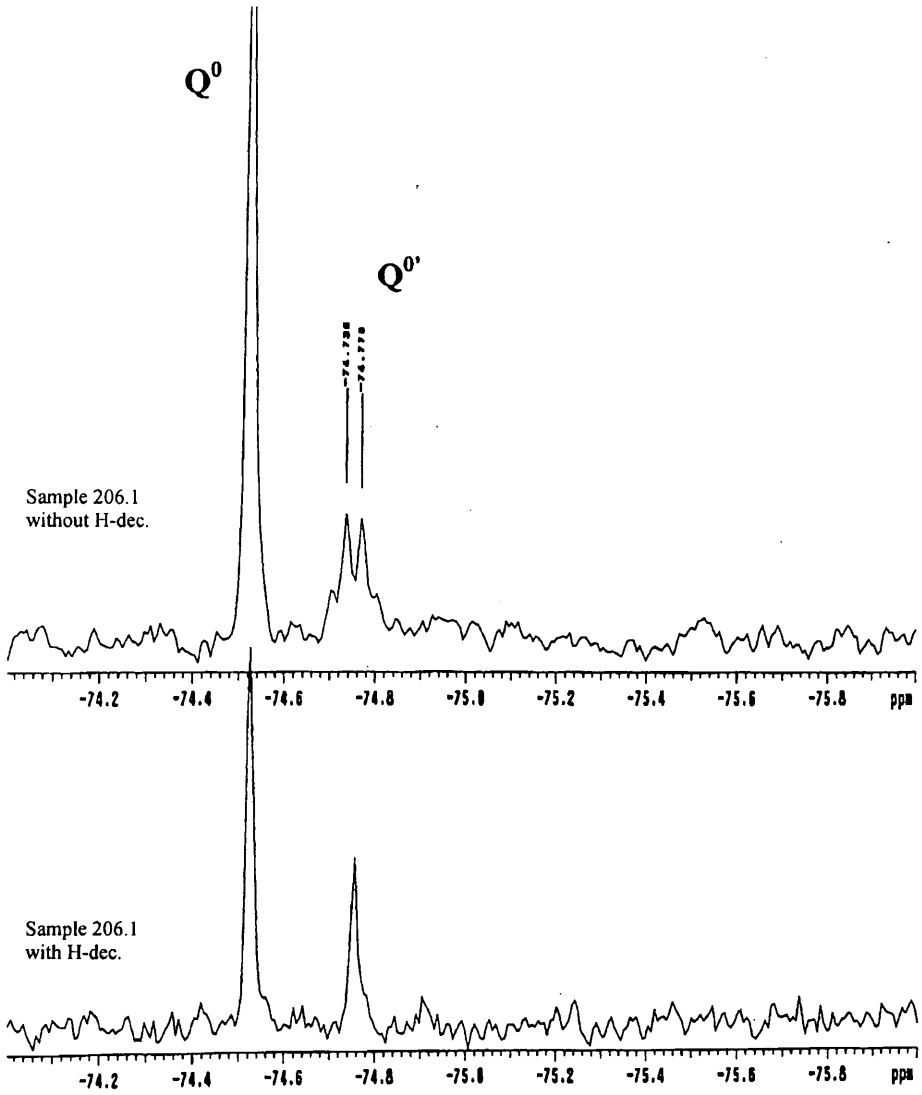

Figure 3.3. Computer expansions of the region lying between –74 and –75 ppm of the high-resolution ^{29}Si NMR spectra obtained with and without H-decoupling at ambient temperature (ca. 22°C) of the sample 206.1, a methanolic tetraethylammonium silicate solution with 45% v/v methanol and the composition listed in table 6. The spectrum was taken one month after preparation. Spectral conditions: Recycle delay 20 s, acquisition time 1.45 s, number of repetitions 2000, spectral width 22008 Hz.

Similar experiments have been carried out for samples 206, 221, and 227, the same results as for sample 206.1 were obtained. The measured magnitude of $^3J_{Si-H}$ is very close to the value reported for $(CH_3O)Si(OH)_3$ in references 34 and 36 and also to what it appears to be in reference 16 (though the author did not quote it). Moreover, the spectrum of a solution containing $[SiO_2]$ = 1 M and [TEAOH] = 0.71 M, prepared with 45% v/v of deuterated methanol (CD_3OH) (sample 303) showed no splitting even in the absence of proton decoupling (see figure 3.13), the value of $^3J_{SiD}$ being too small to resolve. This confirms the formation of $(HO)_3Si(OCH_3)$, i.e. the following reaction has occurred in the alcoholic alkaline environment:

$$Si(OH)_4 + CH_3OH \rightleftharpoons (H_3CO)Si(OH)_3 + H_2O \qquad (1)$$

III)- The NMR spectra may be used to monitor the equilibrium. In this work, it has also been found that the intensity of the $Q^{0'}$ signal varied with the situations explained through sections 3.6.1.3 to 3.6.1.6.

3.6.1.3. ***Dilution effect*****:** Solution sample 215 (one molar Si and TEAOH with 45 %v/v methanol) was diluted to 2, 4 and 10 times its volume with water and methanol to retain the same methanol concentration, forming solution samples 220, 221 and 222 respectively (table 3.2). Measurement of the $Q^{0'}$ intensity indicates a decrease with dilution (see figures 3.4 and 3.5 and table 3.2). Sample 217, prepared separately, duplicates the conditions for 215. As can be seen from Figure 3.4, the result is an approximately linear decrease in the ratio $Q^{0'}/Q^0$ with dilution. A decrease is also seen by comparing the data for samples 230 and 207 (in table 3.6), which have a $[SiO_2]$:[TEAOH] ratio of 0.5. Of course, dilution is also accompanied by some redistribution between the various silicate species, which are in equilibrium. There is also a concomitant change in pH with dilution, so that

quantitative prediction of the effect of dilution on $Q^{0'}$ concentration is not straightforward.

Table 3.2. Composition data and relative intensity of the $Q^{0'}$ signal for silicate solutions with 14 and 45 % v/v D_2O and methanol respectively.

Sample No.	Molarity Si	Molarity TEAOH	Relative intensity % of Q0':Q^0 ca.	Δδ ppm
215	1.00	1.00	46	0.21
220	0.50	0.50	32	0.25
221	0.25	0.25	23	0.24
222	0.10	0.10	18	0.18

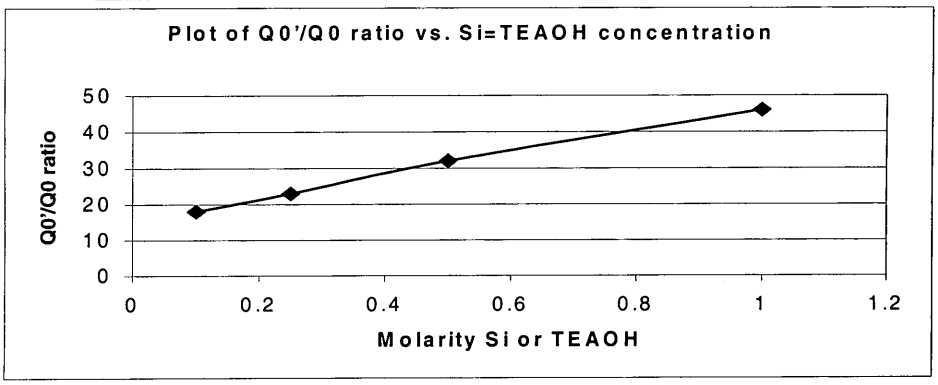

Figure 3.4. Plot of the relative integrated intensity of Q0', ($Q0'/Q^0$), vs. molarity of Si=TEAOH.
N.B. In this and similar plots the line is to guide the eye and has no theoretical significance.

The highest $Q^{0'}/Q^0$ ratio (ca. 80%) was obtained for sample 231. This contains low concentrations of SiO_2 (0.1 M) and TMAOH (not TEAOH) (0.2 M). The dominant signal in the spectrum is for Q^3_8 and the concentrations for Q^0 and $Q^{0'}$ are low, so the measurement of the ratio is not very accurate. Therefore a new sample (302) was prepared with the same composition and the ^{29}Si spectrum obtained with a total accumulation time of 16 hours, which confirmed the high $Q^{0'}/Q^0$ ratio (85%) (see figure 3.6), though still with a significant error in view of the low S/N ratio (~3).

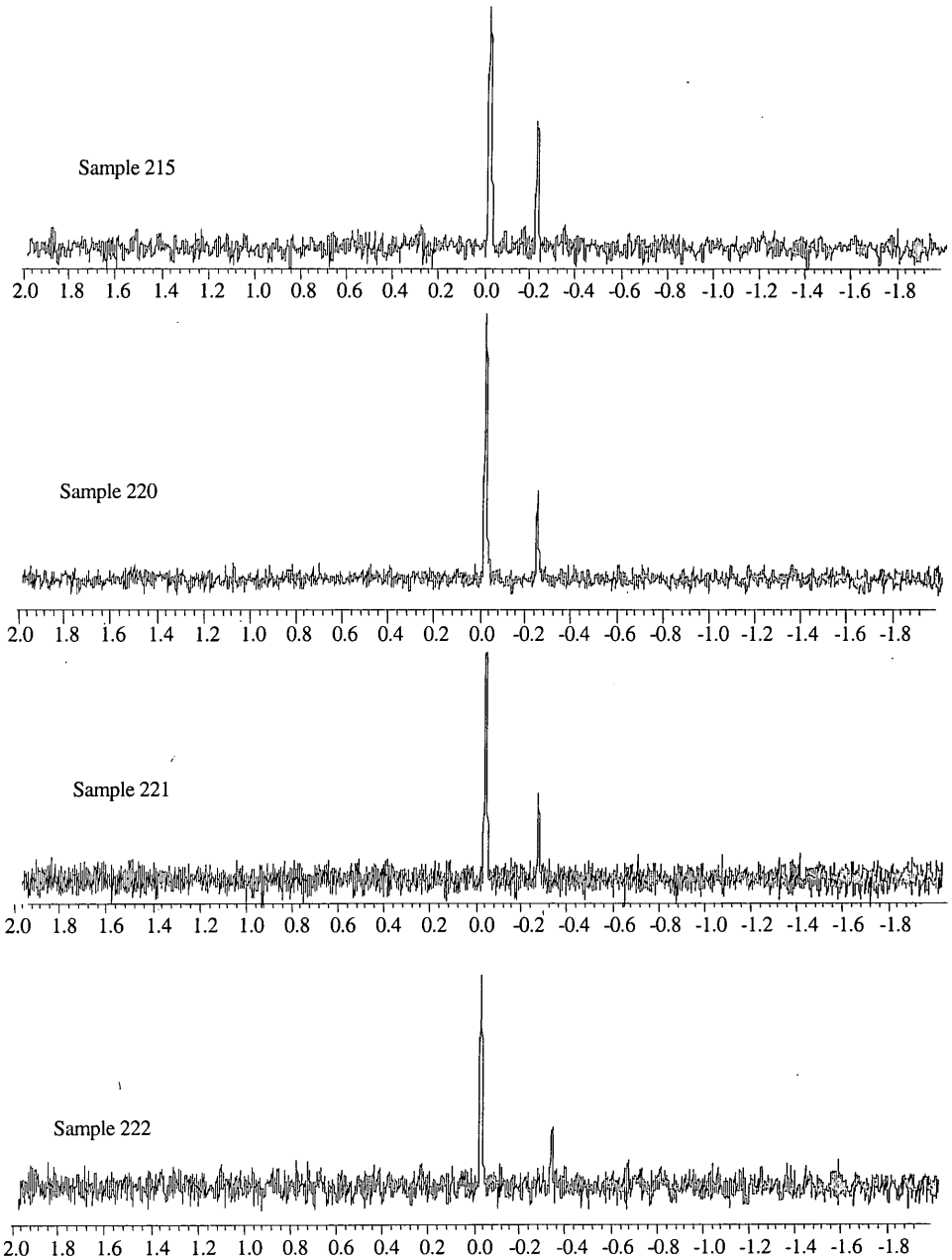

Figure 3.5. Computer expansions of the Q^0 region of the high-resolution ^{29}Si NMR spectra obtained with H-decoupling at ambient temperature (ca. 22°C) of samples 215, 220, 221 and 222 of methanolic tetraethylammonium silicate solutions with 45% v/v methanol and the compositions listed in table 3.2. Spectral conditions: Recycle delay 20 s, acquisition time 1.45 s, spectral width 22008 Hz. No line broadening has been applied. ^{29}Si spectra frequencies are referenced to the monomeric peak (Q^0). These spectra are presented referenced to the Q^0 peak at 0 ppm (ca. –72.6 ppm from TMS) using the high frequency is positive convention.

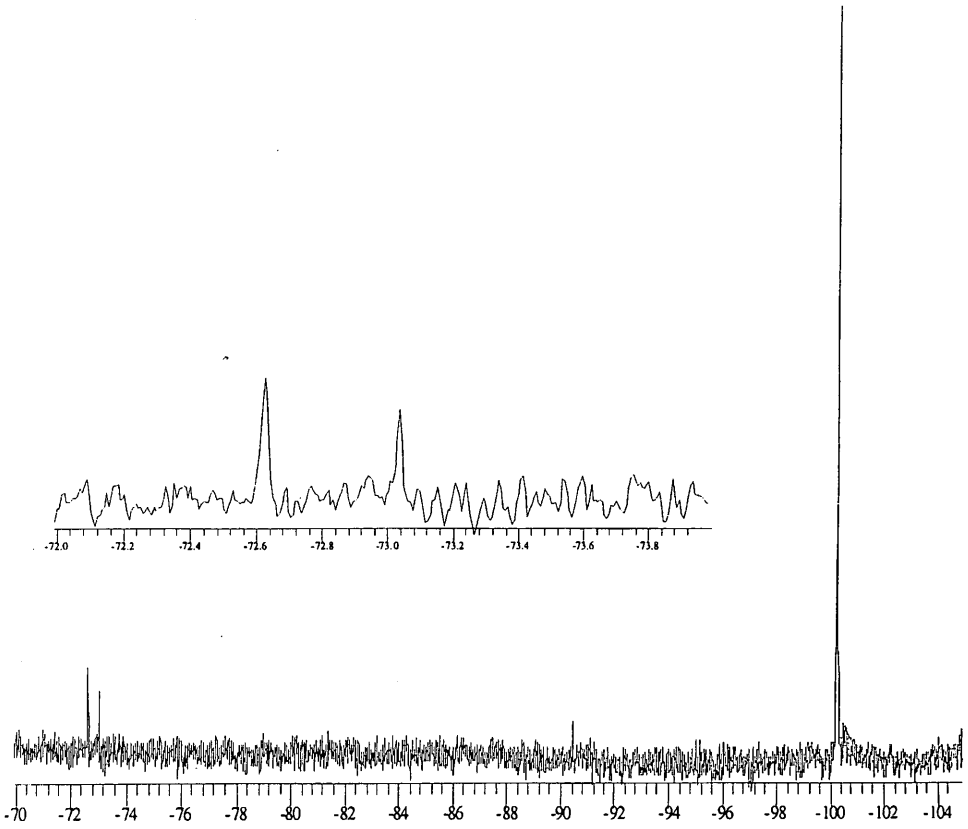

Figure 3.6. High-resolution ^{29}Si NMR spectrum at ambient temperature of a methanolic tetraethylammonium silicate solution with 76% v/v methanol and with Si and TMAOH concentrations equal to 0.1 and 0.2 molar respectively (sample No. 302). The spectrum was taken one week after preparation, with H-decoupling and a total accumulation time of 16 hours. Spectral conditions: Recycle delay: 50 s. Acquisition time: 2.90 s. Spectral width: 22008 Hz. Number of repetitions: 1088. ^{29}Si NMR spectra frequencies are referenced to that of TMS.
The upper trace is a computer expansion of the Q^0 region of the lower spectrum.

3.6.1.4. *The effect of methanol concentration*:

A plot of the ratio $Q^{0'}/Q^0$ as a function of [MeOH] for samples 229, 228, 227 and 309 (which have $[SiO_2]$ = 1 M and [TEAOH] = 0.5 M) shows, as expected, that the ratio $Q^{0'}/Q^0$ increases substantially with concentration of methanol (see figures 3.7 and 3.8, as well as table 3.3). Because of the

lack of solubility of silica in more concentrated methanol in TEA silicate solutions, it is not possible to have the alcohol concentration more than 45% v/v with this concentration of Si.

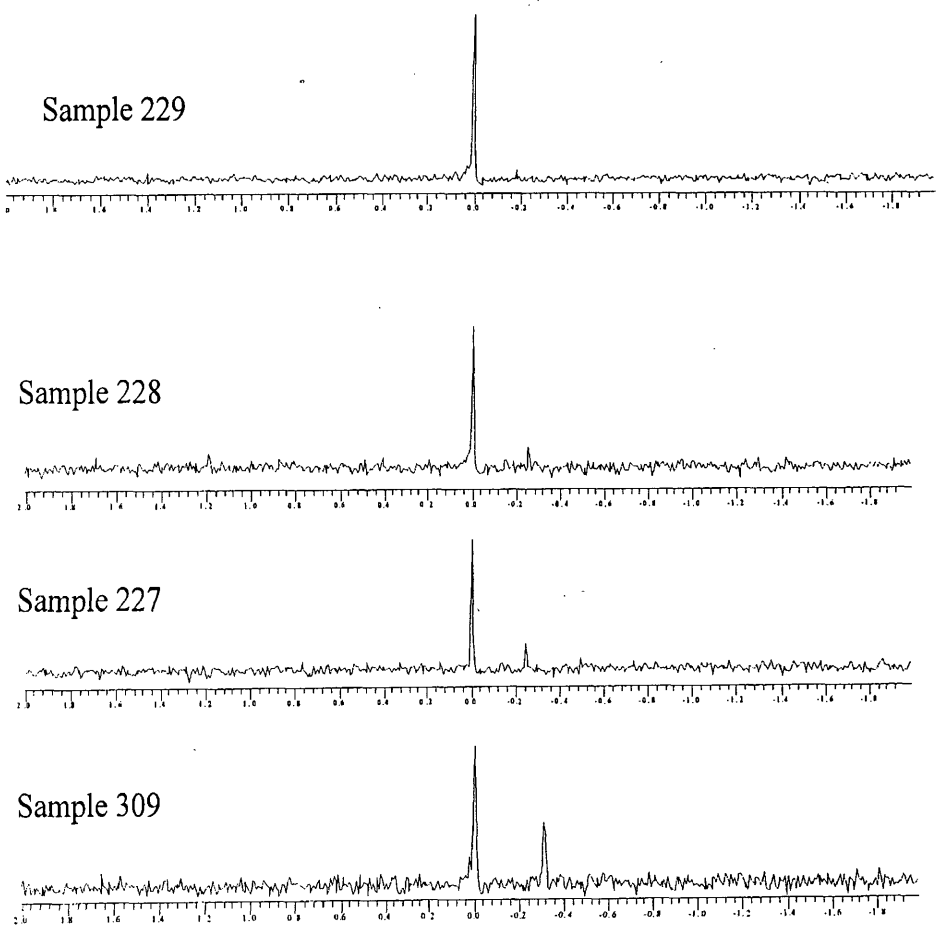

Figure 3.7. Computer expansions of the Q^0 region of ^{29}Si NMR spectra obtained with H-decoupling at ambient temperature (ca. 22°C) of samples 309, 227, 228 and 229 of methanolic tetraethylammonium silicate solutions with 45, 35, 25 and 10 % v/v respectively of methanol and the same concentrations of Si, TEA and D_2O (equal to 1 molar, 0.5 molar and 14% v/v respectively). Spectral conditions: Recycle-delay 50 s, acquisition time 2.90 s, spectral width 22008 Hz, pulse angle 90° (10.4 μs). ^{29}Si NMR spectra frequencies are referenced to the monomeric peak (Q^0). The spectra are scaled to the same Q^0 peak height. These spectra are presented referenced to the Q^0 peak at 0 ppm (ca. –72.6 ppm from TMS) using the high frequency is positive convention.

Table 3.3. Data of relative intensity, $Q^{0'}/Q^{0}$ %, and differences of chemical shifts, $\Delta\delta$, for silicate solutions with Si and TEAOH concentrations equal to 1 and 0.5 molar respectively and with different amounts of alcohol.

Sample No.	MeOH %v/v	Relative intensity Q0':Q^0%	Δδ ppm
309	**45**	33	0.31
227	35	15	0.23
228	25	12	0.26
229	10	5	0.18

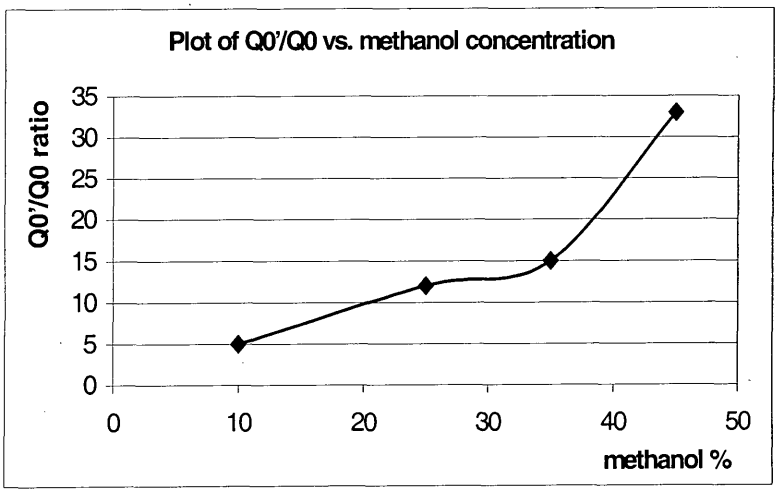

Figure 3.8. Plot of the relative integrated intensity of $Q^{0'}$, ($Q^{0'}/Q^{0}$), vs. methanol concentration.

3.6.1.5. *The effect of TEAOH concentration*:

The relative intensities of the $Q^{0'}$ signals in figure 3.10 (for which the data are listed in table 3.4) are plotted in figure 3.9 as a function of TEAOH concentration for samples 215 (and 217), 308, 206, 309 and 310, all of which have [SiO_2] = 1 M and contain 45% v/v of methanol. This indicates that TEAOH concentration favours the formation of $Q^{0'}$. The change in the $Q^{0} \rightleftharpoons Q^{0'}$ equilibrium may be related to the increase in pH accompanying increasing concentration of TEAOH. Generally speaking, increasing pH will increase the concentration of Q^{0}, though this will not, of itself, increase the $Q^{0'}$:Q^{0} ratio.

Table 3.4. Composition data and relative intensity of $Q^{0'}$ for silicate solutions containing one molar Si, 45 % methanol and 14 % D_2O with different amounts of TEAOH.

Sample No.	Molarity TEAOH	Relative intensity % of $Q^{0'}/Q^0$	Δδ ppm
215	1.00	46	0.21
308	0.80	41	0.23
206	0.71	39	0.24
309	0.50	33	0.31
310	0.30	23	0.31

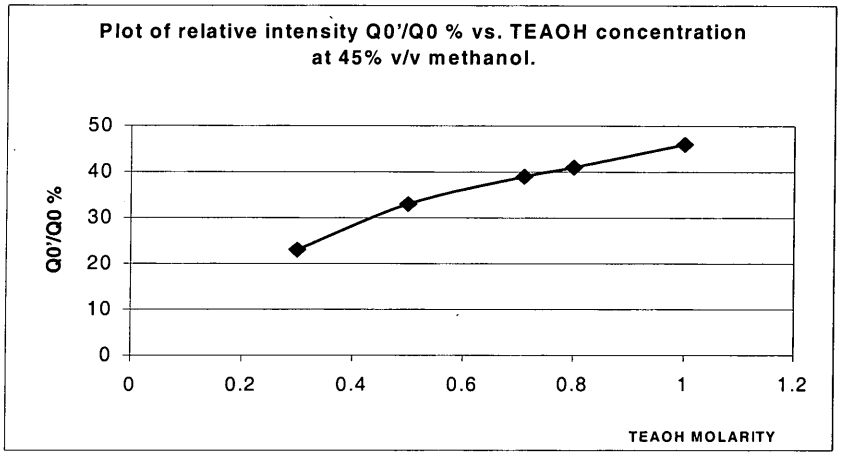

Figure 3.9. Plot of the relative integrated intensity of Q0', ($Q0'/Q^0$), vs. TEAOH concentration.

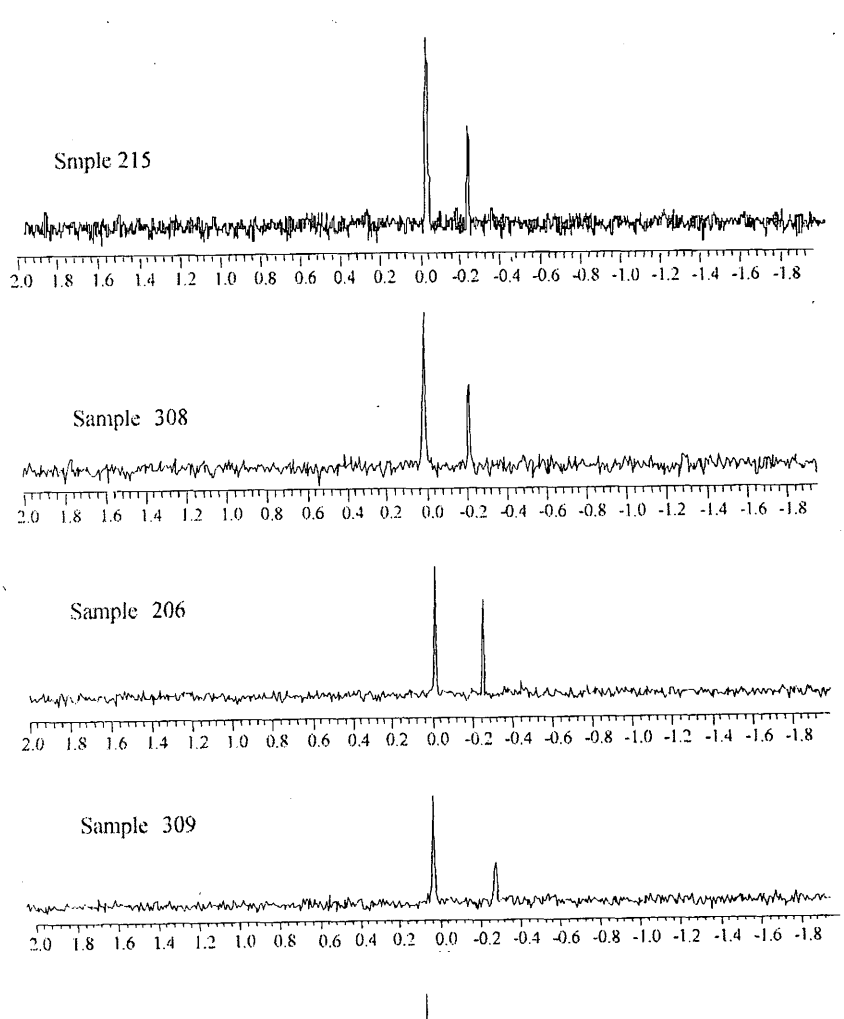

Figure 3.10. Computer expansions of the Q^0 region of the ^{29}Si NMR spectra obtained with H-decoupling at ambient temperature (ca. 22°C) of samples 215, 308, 206, 309 and 310 of 45 % v/v methanolic tetraethyl ammonium silicate solutions with the same concentrations of Si, CH_3OH and D_2O but with different amounts of TEA as listed in table 3.4. Spectral conditions: Recycle delay 50 s. Acquisition time 2.90 s except for sample 215, for which is 1 s. Spectral width 22008 Hz. Pulse angle 90° (10.4 μs). ^{29}Si spectra frequencies are referenced to the monomeric peak. These spectra are presented referenced to the Q^0 peak at 0 ppm (ca. –72.6 ppm from TMS) using the high frequency is positive convention.

3.6.1.6. *The effect of the nature of the tetra-alkylammonium ion.*

Gradual replacement of TEAOH by TMAOH occurs for the sample series 215 → 311 → 312 → 313, all of which contain 1 M SiO_2 and 45% v/v MeOH. This seems to give a small reduction in $Q^{0'}$:Q^0 (see the measured intensity of this signal obtained from these samples, for which the compositions are listed in table 3.5 and the results plotted in figure 3.11). A similar observation may be made by comparing the $Q^{0'}$ signals in figure 3.12 or from the results listed in table 3.5. It may be noted that the change of composition from TEAOH to TMAOH causes a gross variation in the silicate equilibria, since TMAOH stabilises Q^3_8 and Q^3_6 to the virtual exclusion of other species. Additionally, two solutions were prepared with [SiO_2] = 0.5 M, 35% v/v MeOH and half-molar TPAOH and TBAOH respectively. Their ^{29}Si NMR spectra (recorded without proton decoupling) again showed marginally lower $Q^{0'}/Q^0$ ratios compared to the TEAOH solutions. Speculation about the cation effect on the silicate species distribution is discussed in chapter six.

Table 3.5. Composition data and relative intensity of $Q^{0'}$ for silicate solutions with one molar Si containing 45 and 14 % v/v methanol and D_2O respectively and different amounts of TMAOH and TEAOH.

Sample No.	**Molarity of template**		**Relative intensity $Q^{0'}$:Q^0 %**	**Δδ ppm**
	TMA	**TEA**		
215=331	0.00	1.00	46	0.21
311	0.30	0.70	43	0.19
312=312.1	0.70	0.30	35	0.11
313=330	1.00	0.00	34	0.11
206	0.00	0.71	39	0.24
232	0.71	0.00	22	0.19

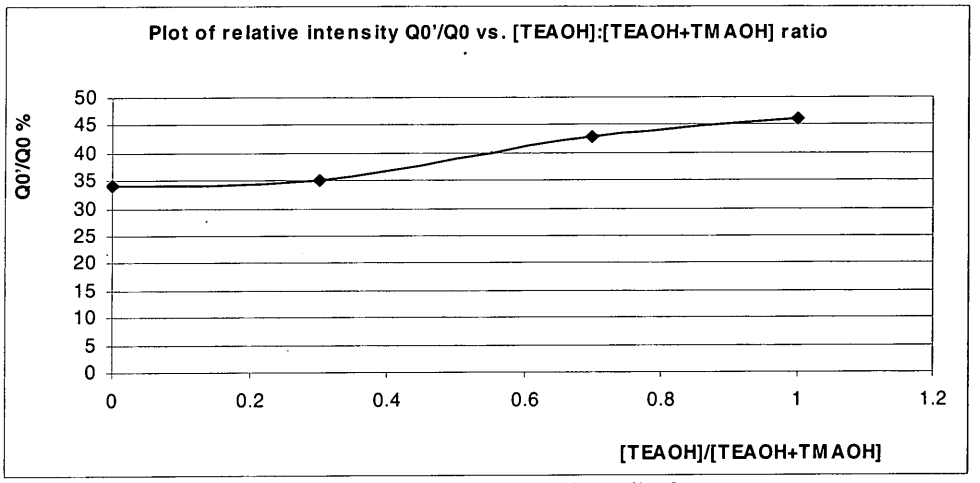

Figure 3.11. Plot of the relative integrated intensity of $Q^{0'}$, ($Q^{0'}/Q^{0}$), vs. mole fraction TEAOH, i.e. [TEAOH]/[TEAOH+TMAOH].

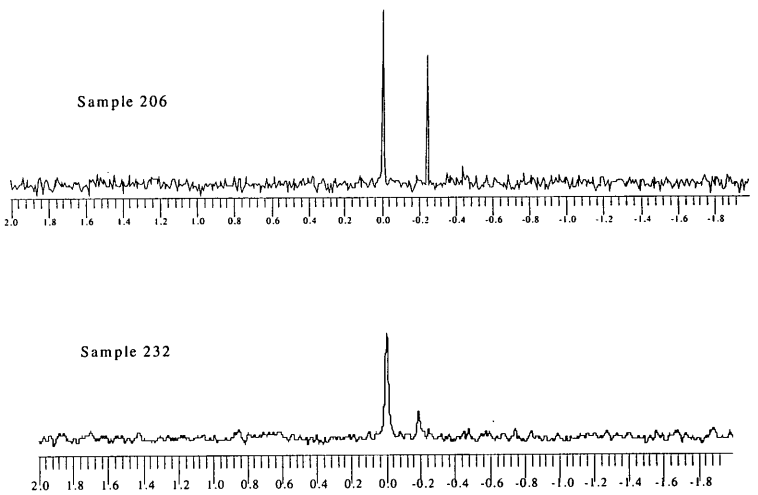

Figure 3.12. Computer expansions of the Q^0 region of the high-resolution ^{29}Si NMR spectra obtained with H-decoupling at ambient temperature (ca. 22°C) of samples 206 and 232 of 45 % v/v methanolic silicate solutions with the same concentrations of Si, template and D_2O, as listed in table 3.5, but with different template type (i.e. sample 206 with TEAOH and sample 213 with TMAOH). Spectral conditions: Recycle delay 50 s. Acquisition time 2.90 s except for sample 232 for which is 1.45 s. Spectral width 22008 Hz. Pulse angle 90° (10.4 μs). These spectra are presented referenced to the Q^0 peak at 0 ppm (ca. –72.6 ppm from TMS) using the high frequency is positive convention.

3.6.1.7. *The effect of alcohol type on the formation of monoalkoxysilanes:*

Solution no. 303 has the same concentration as sample 206 but with methyl-d3 alcohol in place of methanol. Spectra were obtained with and

without H-decoupling. Both spectra show a singlet $Q^{0'}$ signal at ca. $\Delta\delta$=0.12 ppm to low frequency of the Q^0 peak, with a relative intensity $Q^{0'}/Q^0$ of ca. 29 % (see figure 3.13). The integrated $Q^{0'}$ intensity of this solution is apparently decreased with respect to that for solution 206 (methanolic solution) from ca. 39 to ca. 29 %. This might arise from the presence of deuterium of the deuterated methyl near the site of reaction, though this seems to be unlikely, and experimental errors may explain the difference.

Samples 290, 291 and 292 were prepared with the same concentrations as sample 206 but with ethanol, butanol and pentanol, respectively, in place of methanol. In fact, the two last cases were not true solutions, since they appear to be two-phase. The NMR measurement of sample 290 (figure 3.14) shows a similar peak to $Q^{0'}$, but at $\Delta\delta$=1.1 ppm. This presumably arises from $CH_3CH_2OSi(OH)_3$ or one of its deprotonated forms, as is also suggested in reference 36. However this signal is only ca. 8% of that of Q^0. Therefore it can be concluded that the equilibrium of the analogous reaction to (1) when EtOH is used in place of MeOH is relatively unfavourable (compare the two spectra in figure 3.14. Therefore it appears that the presence of bigger alkoxy groups in the alcohol disfavours esterification. Thus the reactivity for esterification in alkaline solution is in the order MeOH>EtOH, which is the same as given in reference 35 for esterification in acidic solution. However, the solubility of the inorganic silicate solution in the organic component for the bigger alkyl groups of the alcohol becomes a problem.

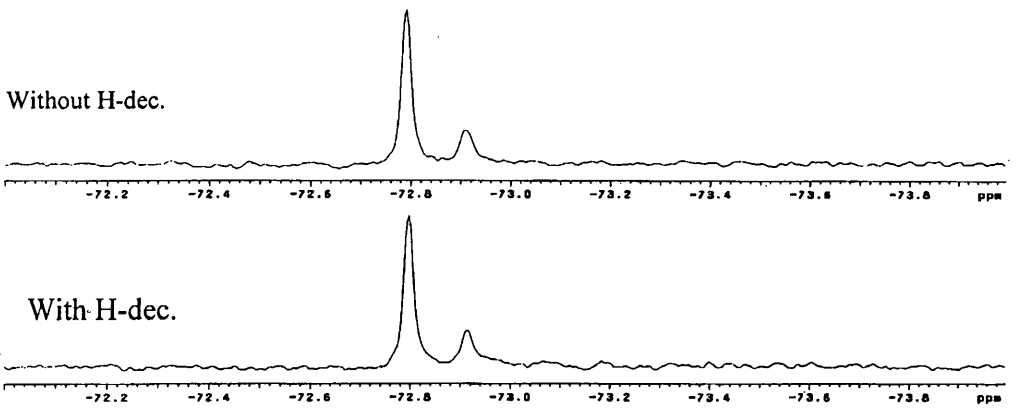

Figure 3.13. Computer expansions of the Q^0 region of the high-resolution ^{29}Si NMR spectra obtained with and without H-decoupling of a deuterated methanolic tetraethyl ammonium silicate solution with 45% v/v methanol-d_3 and with the compositions of Si and TEAOH equal to 1 and 0.71 molar respectively (sample No. 303). The spectra were taken one week after preparation at ambient probe temperature, ca. 22°C. Spectral conditions: Recycle delay: 50 s. Acquisition time: 2.9 s. Spectral width: 22008 Hz. Number of repetitions: 680.

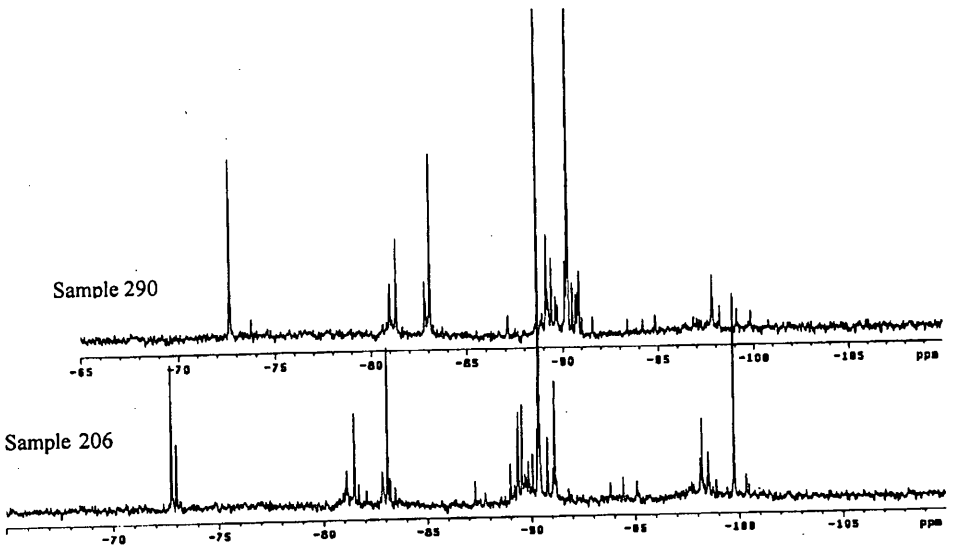

Figure 3.14. The 99.29 MHz ^{29}Si NMR spectra of two equivalent samples (206 and 290) with the same concentrations of Si, TEA, D_2O and alcohol, equal to 1 M, 0.71 M, 14% v/v and 45 % v/v respectively, but containing different types of alcohol (sample 206 contains methanol and 290 contains ethanol). The upper trace is from solution sample 290 and the bottom is obtained from sample 206. Both spectra were recorded over a 22008 Hz spectral width with H-decoupling at ambient probe temperature (ca. 22 °C), recycle delay 50 s, 90° pulse angle (10.4 μs) with an acquisition time of 2.9 s and with 680 repetitions. These two spectra were processed with the absolute intensity mode and in backward linear prediction with the same line broadening and expansion.

3.6.1.8. Calculation of the equilibrium constant for partial esterification of $Si(OH)_4$.

The solutions were allowed to equilibrate for a week before the spectra were obtained, so rate constants could not be estimated. However, the observations reported here can be explained by the establishment of an equilibrium between monosilicic acid and monomethoxysilane, as the first step in the esterification of $Si(OH)_4$. Therefore values of K_{eq} may be calculated for this reaction.

It should be noted that, before the calculation, the information listed in the above tables had to be converted to a suitable form for analysis since the concentrations of the $Q^{0'}$ species have been quoted above as relative integrated intensities of those of Q^0. It is supposed that the esterification is reversible and the approximation of ideal solution behaviour is applied to obtain the equilibrium constant. However, some approximations are used in the calculations for the reaction:

$$\begin{array}{lllll} Si(OH)_4 + CH_3OH & \underset{k_2}{\overset{k_1}{\rightleftharpoons}} & CH_3OSi(OH)_3 + H_2O \\ \text{or} & & \\ Q^0 + CH_3OH & \rightleftharpoons & Q^{0'} + H_2O \end{array} \qquad (1)$$

where k_1 and k_2 are the forward and backward rate constants respectively.

At equilibrium:

$$k_1/k_2=K=([Q^{0'}]/[Q^0])([H_2O]/[CH_3OH]) \qquad (2)$$

$k_1/k_2=K$= equilibrium constant

It is generally assumed here that the water and methanol concentrations at equilibrium may be taken to be the initial values. The approximation is reasonably valid as long as $[Q^0]$ and $[Q^{0'}] << [H_2O]$ and $[CH_3OH]$.

The equilibrium constants were calculated for solution nos. a) 309, 227, 228 and 229, which were made with the same concentrations of Si and TEAOH but contain different amounts of alcohol and water, and also b) for solution samples nos. 215, 220, 221, 222, 206, 230, 207, 232 and 210, which were made with different components and concentrations (listed in table 3.6). The calculated equilibrium constants are also listed in table 3.6.

Table 3.6. Composition data and relative intensity of $Q^{0'}$ for silicate solutions and K_{eq} calculated from NMR data.

Sample No.	Molarity Si	Molarity of template TMAOH	TEAOH	Molarity CH_3OH	Molarity H_2O+D_2O	CH_3OH/H_2O+D_2O ratio	Relative intensity of $Q0'/Q^0$ %	Estimated K values
215=217*	1.00	0.00	1.00	11.11	19.00	0.58	46	0.79
206	1.00	0.00	0.71	11.11	21.30	0.52	39	0.74
220	0.50	0.00	0.50	11.11	24.80	0.45	32	0.71
221	0.25	0.00	0.25	11.11	27.70	0.40	23	0.58
222	0.10	0.00	0.10	11.11	29.40	0.38	18	0.48
309	1.00	0.00	0.50	11.11	23.10	0.48	33	0.69
227	1.00	0.00	0.50	8.64	28.70	0.30	14	0.47
228	1.00	0.00	0.50	6.17	34.20	0.18	13	0.69
229	1.00	0.00	0.50	2.47	42.60	0.06	4	0.68
230	0.50	1.00	0.00	11.11	20.70	0.54	29	0.54
207	0.25	0.50	0.00	11.11	27.10	0.41	24	0.59
232	1.00	0.71	0.00	11.11	23.40	0.48	22	0.46
210	0.50	0.50	0.36	11.11	23.30	0..48	31	0.65
308	1.00	0.00	0.80	11.11	20.60	0.54	41	0.76
310	1.00	0.00	0.25	11.11	24.80	0.45	23	0.52
311	1.00	0.30	0.70	11.11	19.90	0.56	44	0.80
312	1.00	0.70	0.30	11.11	21.00	0.53	35	0.66
313=330	1.00	1.00	0.00	11.11	21.90	0.51	34	0.67

Sample 330 and 331 are fresh solutions with the same compositions as samples 313 and 217 respectively

3.6.1.9. Discussion of the calculation of the equilibrium constant

The derived values of K in table 3.6. show they all lie between 0.46 and 0.80, which is a narrow range given the likely errors (largely unquantifiable), both experimental and in the principles involved. There does appear to be a decrease with dilution, probably because of pH changes,

which may affect protonation states as well as the distribution of condensed silicate species. Other consistent variations are not apparent. It therefore can be concluded that the principal reason for observations in the sections 3.6.1.3-7 above is the change in water and methanol concentrations caused by the variations in sample compositions. However, for the samples whose data are listed in the top 5 rows of table 3.6, for which the alcohol concentration was held constant, it might be concluded that K varies with the Si and TAA concentrations or with the molar ratio of (alcohol/water+D_2O), in spite of the fact that it should be constant. Why is this? Some possible reasons are noted here:

1). For the calculations a simple equation was used, i.e. it is supposed that $Si(OH)_4$, Q^0, undergoes just the change to $Q^{0'}$, but under the conditions employed, in addition of monosilicic acid, other species, involving Q^1, Q^2, Q^3 and Q^4 groups are present in equilibrium. Thus the overall equilibrium situation involves many individual equilibrium constants, and such systems are clearly complicated. The net reaction to form $Q^{0'}$ proceeds from the sum of parallel or successive reactions. Such complications have been ignored here.

2). It seems likely that there are other partially esterified silicate species, but it has not been possible to unambiguously identify signals from such molecules or ions in the ^{29}Si spectra.

3). From previous work it is known that the reactions in silicate solutions also depend on pH. Therefore, if the concentration of the template TAAOH (or, to be more precise, the TAA:Si ratio) changes, the pH of the solution should change and therefore the distribution of all species. However, this effect is not taken into account in the simple equation 1, which is used for the calculation of K.

4). The K values are not very accurate, though errors are difficult to quantify. One reason for errors is that calculations ignore water formation and also the alcohol consumption of esterification. The initial concentrations of water and alcohol are used. Each sample is characterized by the molar ratio of the components to the total volume (water+alcohol+D_2O+...). However, the situation is complicated by the fact that polymerisation of the monomeric species liberates water, which could be used in hydrolysis and so on. Thus it would be difficult to estimate the actual water concentration at equilibrium. Moreover, the methanol concentration will change if there are other esterified species than $Q^{0'}$.

3.6.2. Results and discussion of the spectra other than the Q^0 region.

3.6.2.1. High-field ^{29}Si NMR studies of aqueous and methanolic TAA silicate solutions

In comparison with aqueous TAA silicate solutions, the methanolic solutions may exert specific structure-forming effects on the silicate anions. This is clearly demonstrated by the ^{29}Si NMR spectra of methanolic and non-methanolic silicate solutions (typically TEAOH silicate solutions) shown in figure 3.15 (for samples 216 and 217). Although the silica concentrations and cation-to-silicon ratios of both solutions are equivalent, so that a broad distribution of silicate anions is observed for both silicate solutions, a significantly different distribution is observed in the methanolic solution. In the aqueous TEAOH solution (the bottom trace) the signals attributed to Q^0, Q^1 and$Q^2{}_\Delta$ dominate but in the methanolic case Q^2 and Q^3 signals are more prominent and the $Q^3{}_6$ signal is the most intense. Also, of course a new signal in the Q^0 region appeared, discussed in detail in section 3.6.1. Cage-like species appear to be favoured in the presence of the methanol. This phenomenon was also observed by using

tetramethylammonium cations (TMA) in place of TEA. In the TMA methanolic system, the distribution of silicate species is simpler than that in the aqueous solutions and for the TEAOH methanolic silicate solutions at the same concentrations of components.

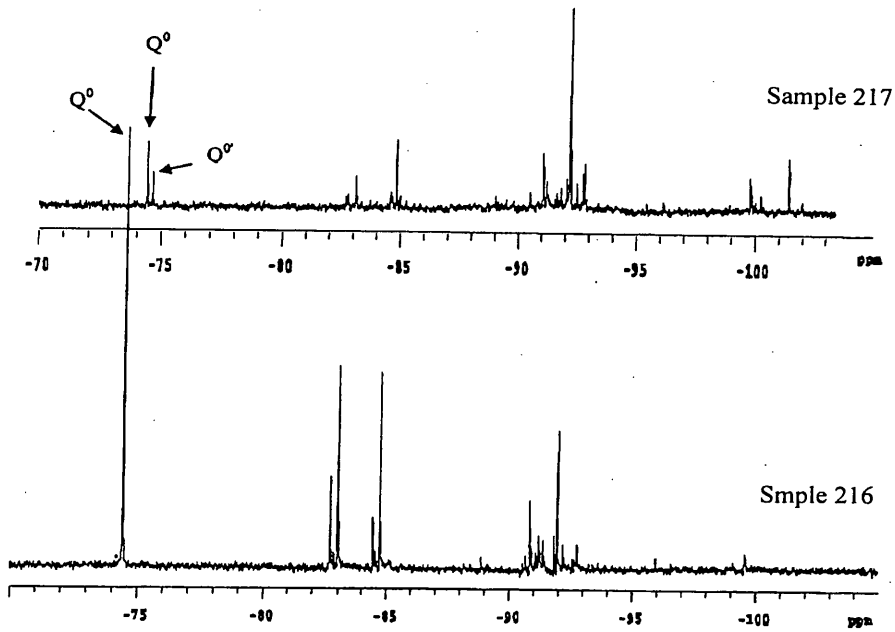

Fig 3.15. The 99.3 MHz ^{29}Si NMR of two tetraethyl ammonium silicate solutions. The bottom trace is that of a solution free from alcohol with the concentrations of Si and TEAOH equal to 1 M (sample No. 216), whilst the upper trace illustrates the spectrum of sample No. 217 (with the same composition as sample 216 but including 45% v/v methanol). In both cases the spectra were recorded one week after preparation and with H-decoupling at ca. 22°C. Spectral conditions: Recycle delay 50 s, spectral width 22008 Hz and line broadening 0.5 Hz. The top trace required 680 repetitions with acquisition time 2.9 s, whilst the lower required 424 repetitions with acquisition time 1 s.

To understand the effects of the amount of methanol and kind of template on the distribution of silicate anions, spectra of samples 330 and 302 can be compared (figure 3.16). These both contain TMAOH, but the concentrations of both TMAOH and Si are lower in sample 302 than 330, whereas [MeOH] is higher in the former. Although the Si concentration and Si/cation ratio would be expected to favour de-polymerisation for 330, the

difference in the distribution of the silicate species for the two solutions would suggest that methanol has an effect of stabilizing the higher molecular weight species. The spectrum of sample 302 shows the system to be almost entirely polymerised to the cubic octamer, Q^3_8, whereas for sample 330 the Q^3_6 and Q^3_8 species appear to be of similar importance. Therefore among the structure-directing species, the amount of alcohol (as well as the cations) occupies an important function.

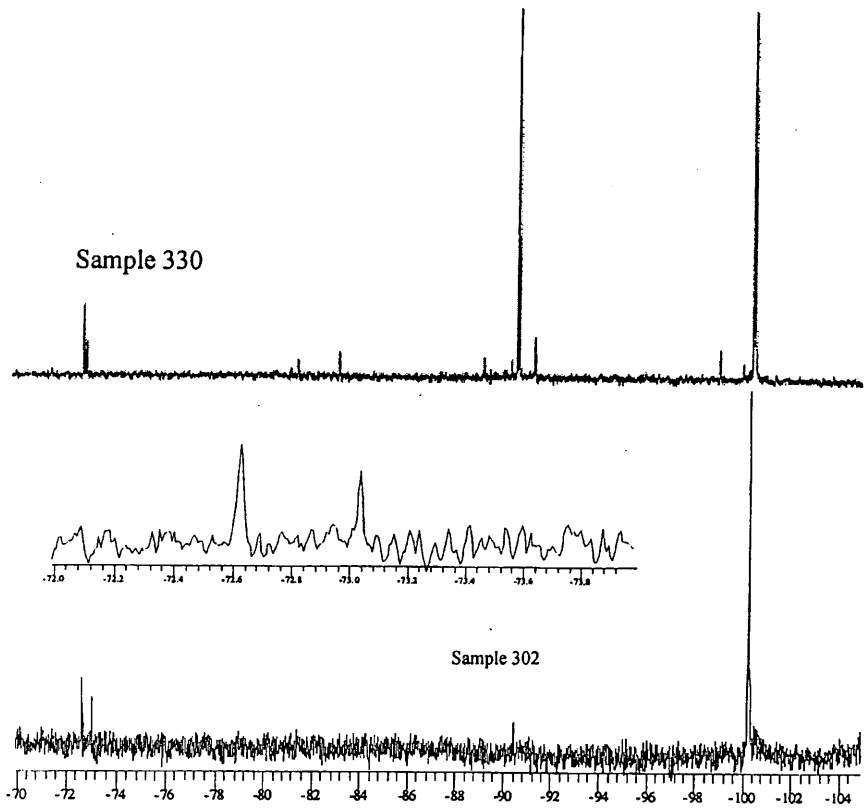

Figure 3.16. For the caption to the bottom trace see figure 3.6. For the top trace see the caption of figure 3.17.

The structure-forming role of the TAA cation in methanolic solutions has been examined. Here are shown (figure 3.17) typically examples of two 45% v/v methanolic TMAOH and TEAOH silicate solutions with the same concentrations of Si, cation and D_2O, equal to 1 M, 1 M and 14% v/v respectively (samples 330 and 331). The spectrum of sample 330 shows

mostly signals from anions in which all the silicon sites are chemically (symmetrically) equivalent. (Such species include the monomer, Q^0, dimer, Q^2, unsubstituted cyclic, e.g. Q^2_Δ or Q^2_4, and regular cage anions, e.g. Q^3_6 or Q^3_8. But although the alcohol and silica concentrations as well as the cation-to-silicon ratios of the two solutions are the same, in the methanolic TEAOH silicate solution a broader distribution of silicate anions is observed. The signal attributed to the prismatic hexamer, Q^3_6, dominates, whereas for the TMAOH case the peak for the cubic octamer, Q^3_8, dominates, while the intensities of other species are decreased or completely diminished (e.g. see the range –93 to –96 ppm).

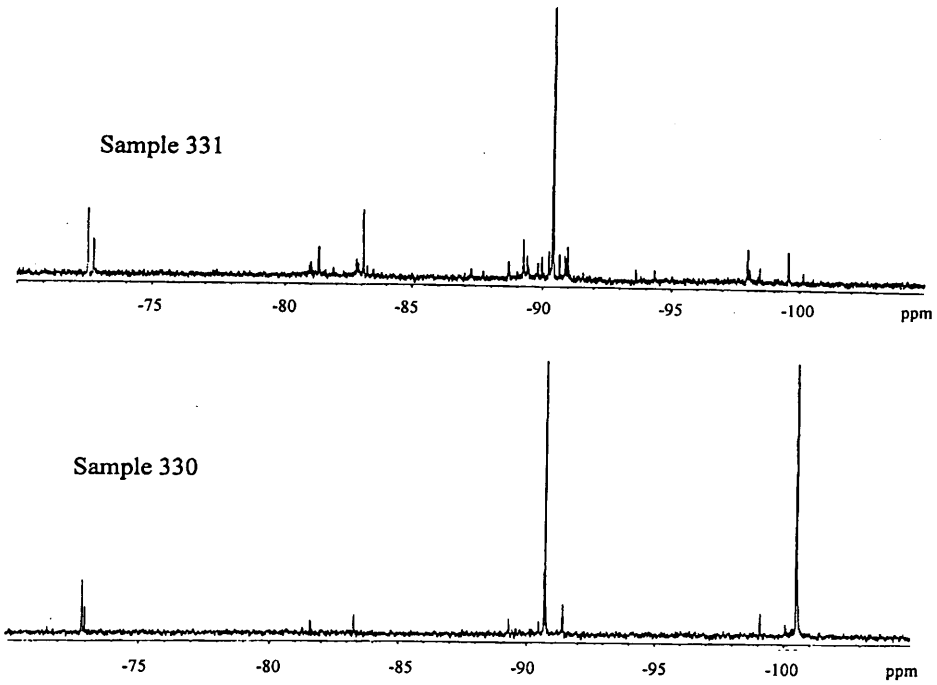

Figure 3.17. The 99.29 MHz ^{29}Si NMR spectra of two equivalent samples (330 and 331) with the same concentrations of Si and cation (equal to one and two molar respectively), with 45 % v/v methanol and 14 % D_2O, but containing different cations (sample 330 contains TMA whereas 331 contains TEA). The upper trace is from solution sample 331 and the bottom is for sample 330. Both spectra were recorded over a 22008 Hz spectral width with H-decoupling at ambient probe temperature (ca. 22 °C), recycle delay 50 s, 90° pulse angle (10.4 μs), an acquisition time of 11.9 s and with 508 repetitions. The two spectra were processed with 0.7 Hz line broadening, absolute intensity mode and backward linear prediction.

Evidence of the effect of the nature of the alcohol on the structure-forming role of the TAA cation has been obtained by a ^{29}Si NMR study of samples 206 and 290, which differ only in that the former contains methanol and the later ethanol (see figure 3.18). There are some differences at the intensities and chemical shifts of many species. It is shown that methanol is more effective than ethanol in stabilising the cubic octamer.

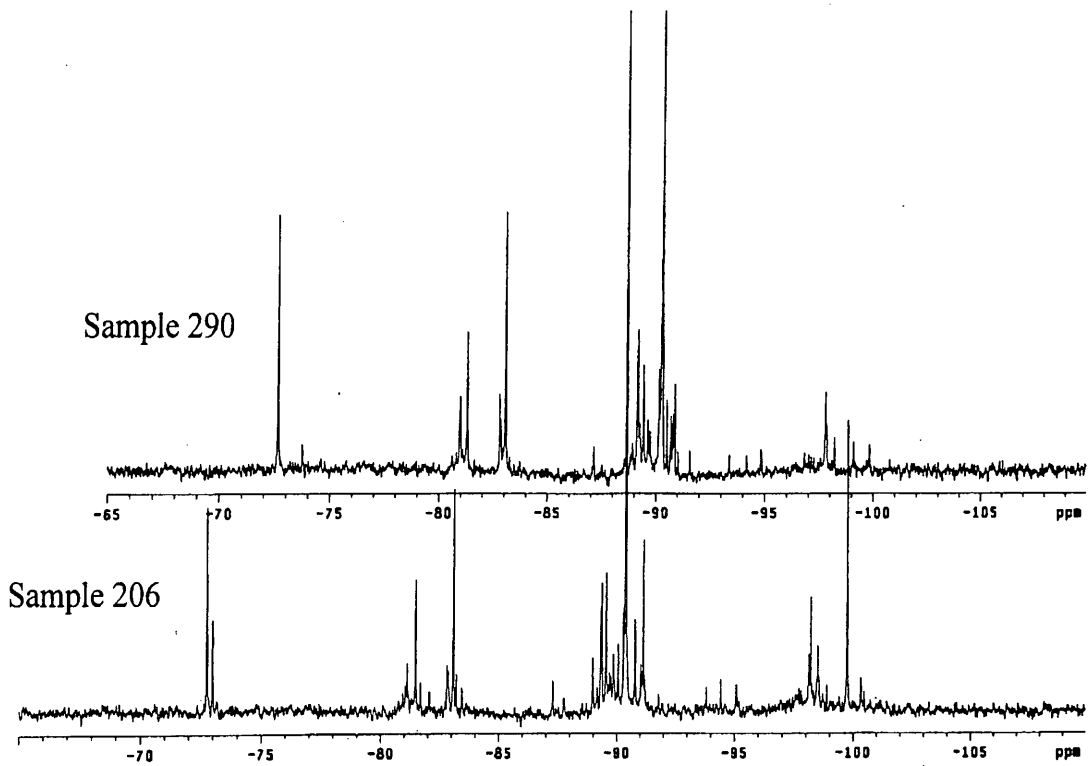

Figure 3.18. The 99.29 MHz ^{29}Si NMR of two equivalent samples (206 and 290) with the same concentrations of Si, TEA, D_2O and alcohol (equal to 1 M, 0.71 M, 14% v/v and 45% v/v respectively), but containing different types of alcohol (sample 206 contains methanol whereas 290 contains ethanol). The upper trace is from sample 290 and the bottom is from sample 206. Both spectra were recorded over a 22008 Hz spectral width, with H-decoupling at ambient probe temperature (ca. 22 °C), recycle delay 50 s, 90° pulse angle (10.4 μs) pulse with an acquisition time of 2.9 s and with 680 repetitions. The two spectra were processed in the absolute intensity mode with backward linear prediction and with the same line broadening and expansion.

3.6.2.2. Study of the relative peak heights of species containing a single silicon site.

Some anionic species in silicate solutions show a single peak in the ^{29}Si NMR spectrum even using isotopic enrichment of silicon-29. The assignment of such species is well defined. Therefore we can attribute the lines denoted to these species unambiguously. The variation of the peak heights relative to that of Q^0, as well as the chemical shifts in methanolic silicate solutions are presented as follows:

Here we consider the signals lying at approximate chemical shifts (relative to the monomer) of ca. 0.3, 9, 11, 16.7, 17.6 and 27.2 ppm, which are assigned to the $Q^{0'}$, Q^1, Q^2_Δ, Q^2_4, Q^3_6 and Q^3_8 species respectively.

a). Effect of differing methanol concentration: Table 3.7 lists the relative peak height measurements for the above species, and figures 3.19a-19d show a schematic representation of the data as a function of methanol concentration (the only variable) for four solutions with the compositions listed in table 3.3.

Table 3.7. Peak heights of the $Q^{0'}$, Q^1, Q^2_Δ, Q^3_6 and Q^3_8 signals relative to that of Q^0, for methanolic silicate solutions (data given as %).

Sample	Q^1/Q^0	Q^2_Δ/Q^0	Q^3_6/Q^0	Q^3_8/Q^0
309	42	92	292	406
227	45	68	114	90
228	50	61	44	40
229	51	60	40	5

Figure 3.20 shows that in methanolic TEAOH silicate solution the prismatic hexamer, Q^3_6, and cubic octamer, Q^3_8, dominate.

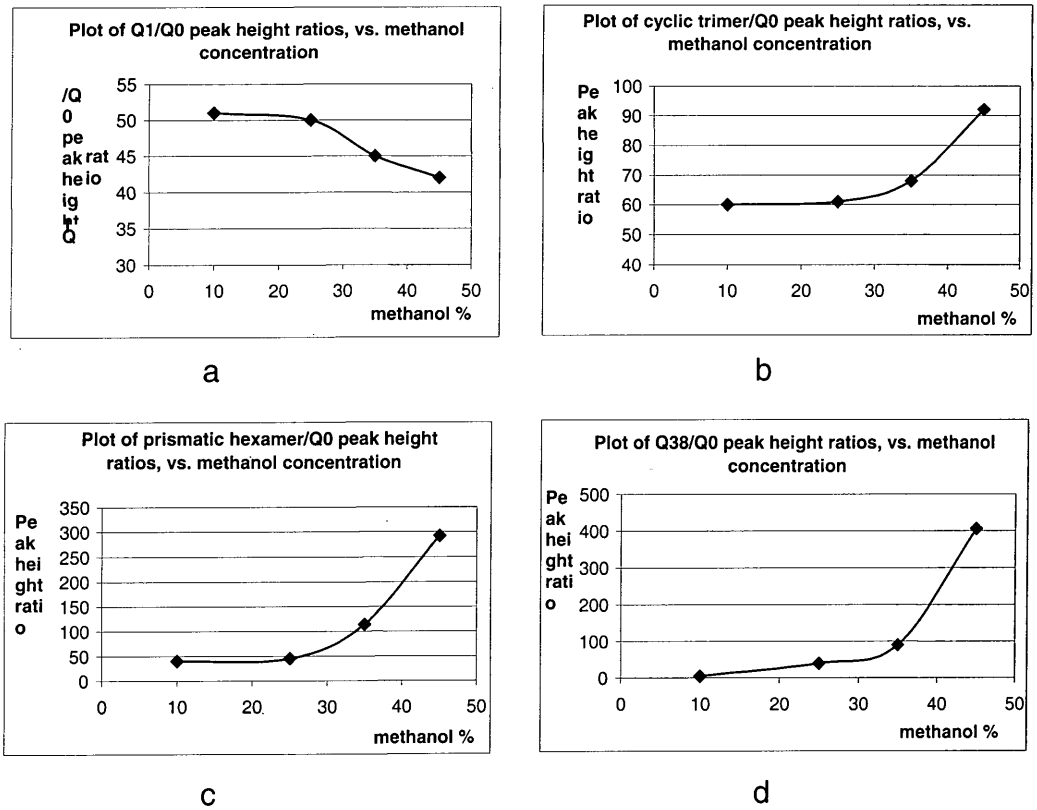

Figure 3.19. Relative peak height dependence of the single silicon sites as a function of methanol concentration. (a) dimer, Q^1_2, (b) cyclic trimer, Q^2_Δ, (c) prismatic hexamer, Q^3_6, and (d) cubic octamer, Q^3_8. Data derived from table 3.7.

Figures 3.19 and 3.20 illustrate the role of the structure-forming methanolic TEA cation very clearly. The peaks assigned to the prismatic hexamer, Q^3_6 and cubic octamer are enhanced with increasing concentration of methanol in the same concentrations of Si and TEA cation. However, when the concentration of methanol is increased, the small silicate anions (especially Q^1) decreases in relative peak height quite significantly - see fig 3.19(a). Therefore in the presence of the methanol the silicate species are polymerised to make the cage-like species such as Q^3_6 or Q^3_8.

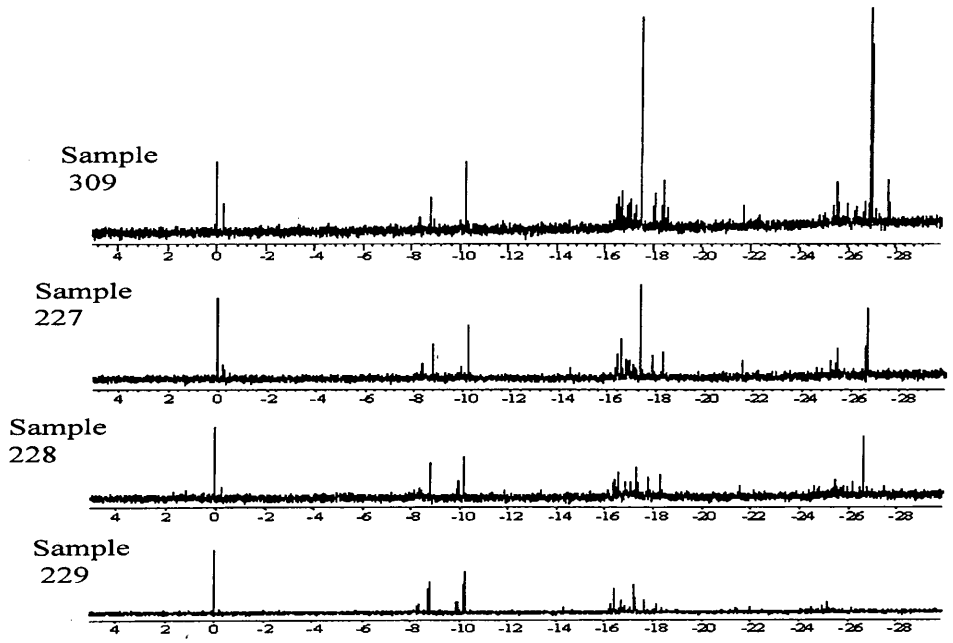

Figure 3.20. High-resolution ^{29}Si NMR spectra obtained with H-decoupling at ambient temperature (ca. 22°C) of samples 309, 227, 228 and 229 of methanolic tetraethyl ammonium silicate solutions with 45, 35, 25 and 10 % v/v methanol respectively and the same concentrations of Si, TEA and D_2O, equal to 1 M, 0.5 M and 14% v/v respectively. Spectral conditions: Recycle delay 50 s. Acquisition time 2.9 s. Spectral width 22008 Hz. Pulse angle 90° (10.4 μs). ^{29}Si frequencies are referenced to the monomeric peak. The spectra are vertically expanded to the same Q^0 peak height, so comparison of intensities between spectra has no significance. These spectra are presented referenced to the Q^0 peak at 0 ppm (ca. –72.6 ppm from TMS) using the high frequency is positive convention.

Whereas this increase in the relative stability of Q^3_6, Q^3_8 in the presence of the methanol has been positively proved by ^{29}Si NMR the conditions of their formation and stability are far from being fully understood. Information of this type is, however, of fundamental interest for a better understanding of mechanisms governing the synthesis of zeolites and other crystalline aluminosilicates. In general, the maximum Q^3_6 and Q^3_8 concentration is found to occur in the 45% v/v methanol in this concentration of TEA silicate solution. Use of more methanol than this is not possible.

b). Effect of changing the Si concentration:

Similar considerations have also been applied to a set of solutions containing 45% methanol but of different Si concentration at constant Si/TEA=1. Table 3.8 gives the peak heights relative to Q^0 derived from the spectra of samples 215 and 220-222. The composition data are listed in table 3.2. Figures 3.21(a)-21(d) show relative peak height variations of the above anions vs. Si concentration. The strong decrease in $Q^1{}_2$, $Q^2{}_{3\Delta}$, $Q^3{}_6$ and $Q^3{}_8$ with dilution is obvious, although the major changes seem to occur at different positions in the plots.

Table 3.8. Peak heights of the Q^1, $Q^2{}_\Delta$, $Q^3{}_6$ and $Q^3{}_8$ signals relative to that of Q^0, for samples 215 and 220-221.

Sample	Q^1/Q^0	$Q^2{}_\Delta/Q^0$	$Q^3{}_6/Q^0$	$Q^3{}_8/Q^0$
215	53	113	1045	67
220	51	66	156	64
221	47	63	84	31
222	17.6	0	0	10

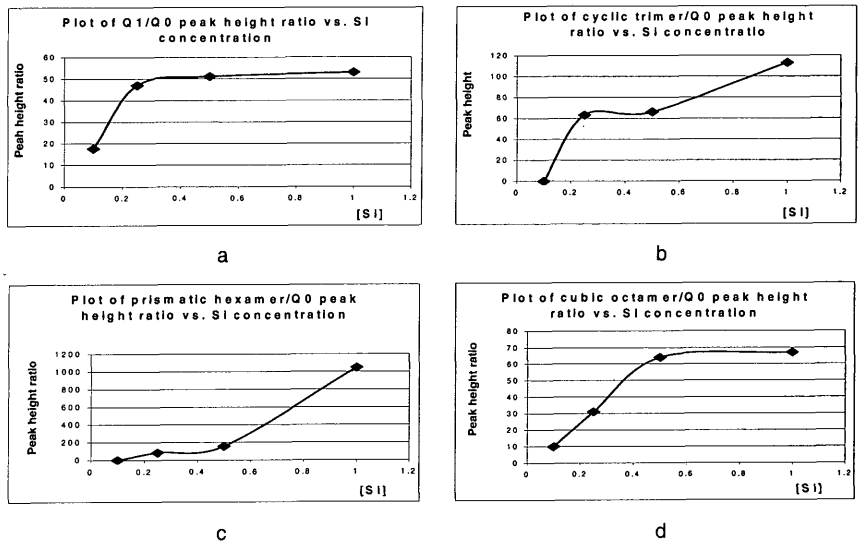

Figure 3.21. Relative peak height dependence of the equivalent silicon sites as a function of Si concentration in Si/TEA=1 methanolic silicate solutions. (a) dimer, $Q^1{}_2$, (b) cyclic trimer, $Q^2{}_\Delta$, (c) prismatic hexamer, $Q^3{}_6$, and (d) cubic octamer, $Q^3{}_8$. Data derived from table 3.8.

3.7. Conclusions

The present study clearly demonstrates that, in alkaline methanolic silicate solutions, an esterification reaction between monomeric silicate and methanol or ethanol occurs. The corresponding signal ($Q^{0'}$) is affected by the Si, methanol and template concentrations and by the types of template and alcohol. The situation for the calculation of the relevant equilibrium constant is very complicated. Values for equilibrium constants, K, estimated from NMR data, for methanolic silicate solutions at ca. 22 °C vary, and it is believed that these may, in part, be real changes. The experimental data show that the concentration of $Q^{0'}$ increases with increasing methanol concentration, i.e. the replacement of water with a methanol molecule in a TAA silicate solution results in an increase in the content of methoxysilicate. The presence of a bigger TAA molecule appears to be less suitable for esterification.

No esterified species other than in the Q^0 region were detected.

3.8. References

1. E. Thio, W. Wieker and H. Stade, *Z. Anorg. Allg. Chem.,* 261, **430** (1965).
2. R. K. Iler, 'The Chemistry of Silica' Wiley, NewYork (1979).
3. L. S. Dent-Gasser and E. E. Lachowki, *J. Chem. Soc. Dalton Trans.*, 399 (1980).
4. K. Shimada and T. Tarutani, *Bull. Chem. Soc. Jpn.* 3488, **53** (1980).
5. T. Shimono, T. Isobe and T. Tarutani, *J. Chromatogr.* 205, **49** (1981).
6. L. S. Dent-Gasser and E. E. Lachowki, *J. Chem. Soc. Dalton Trans.*, 399 (1983).
7. C. W. Lentz, *Inorg. Chem.* 574, **3** (1964).

8. E. Freund, *Bull. Soc. Chim. Fr.* 2238, 2244 (1973).

9. P. K. Dutta, and D.C. Shieh, *Zeolites*, **5**, 135 (1985).

10. E. A. Williams, and J. D. Cargioli, *'Annual Reports on NMR Spectroscopy'*, (Ed. G. A. Webb) Acad. Press (London), **9**, 221 (1979).

11. R. K. Harris, C. T. G. Knight, and W. E. Hull, *J. Am. Chem. Soc.*, **103**, 1577 (1981).

12. R. K. Harris, C. T. G. Knight, and D. N. Smith, *J. Chem. Soc. Chem. Commun.*, 726 (1980).

13. R. K. Harris, J. Jones, C. T. G. Knight, and D. Pawson, *J. Mol. Struct.*, **69**, 95 (1980).

14. R. K. Harris, and R. H. Newman, *J. Chem. Soc. Faraday Trans. 2*, **73**, 1204 (1977).

15. A. Samadi Maybodi, Ph.D. Thesis, "*NMR studies of silicate and aluminosilicate solution as precursors for zeolites*" and references therein, University of Durham (1996).

16. C. T. G. Knight, Ph.D. Thesis, "*Silicon-29 NMR studies of Aqueous silicate solutions*" and references therein, University of East Anglia, (1982).

17. H. C. Marsmann, *Z. Naturforsch. B.*, **29**, 495 (1974).

18. G. Engelhardt, D. Zeigan, H. Jancke, D. Hoebbel, and W. Wieker, *Z. Anorg. Allg. Chem.*, **418**, 17, (1975).

19. R. K. Harris, and C. T. G. Knight, *J. Chem. Soc. Faraday Trans. 2,* **79**, 1525 (1983).

20. R. K. Harris, and C. T. G. Knight, *J. Chem. Soc. Faraday Trans. 2,* **79**, 1539 (1983).

21. R. K. Harris, M.J. O'Connor, E.H. Curzon, and O.W. Howarth, *J. Magn. Reson.* , **57**, 115 (1984).

22. C. T. G. Knight, *J.Chem. Soc., Dalton Trans.*, 1457 (1988).

23. R. K. Harris, J. Parkinson and A. Samadi-Maybodi, *J. Chem. Soc., Dalton Trans.*, 2533 (1997).

24. R. M. Barrer, and P.J. Denny, *J. Chem. Soc.* , 971 (1961).

25. G. T. Kerr, and G. Kokotailo, *J. Am. Chem. Soc.*, **83**, 4675 (1961).

26. B. M. Lok, T.R. Cannan, and C.A. Messina, *Zeolites*, **3**, 282 (1983).

27. R. M. Barrer, *'The hydrothermal chemistry of zeolites'* Academic Press London (1982)

28. R. F. Mortlock, A.T. Bell, and C.J. Radke. *J. Phys. Chem.* 95, 7847-7851 (1991)

29. C. T. G. Knight, R.J. Kirkpatrick, and E. Oldfield. *J. Chem. Soc., Chem. Commun.*, 66 (1986).

30. I. Hasegawa, S. Sakka, Y. Sugahara, K. Kuroda, and C. Kato. *J. Chem. Soc., Chem. Commun.*, 208 (1989).

31. C. T. G. Knight. *Zeolites,* **9**, 448 (1989).

32. J. Sanchoz and A. McCormick. *J.Phys. Chem.*, 96, 8973 (1992).

33. A. J. Haines, Ph.D. Thesis, *'NMR studies of silicates and related compounds both in solution and in the solid state'*, University of East Anglia, (1984)

34. C. T. G. Knight, *J. Non-Cryst. Solids*, **104**, 151 (1988).

35. R. T. Morrison and R. N. Boyd, Organic Chemistry, third edition, chapters 19 & 20 (1973).

36. S.D. Kinrade, K.J. Maa, A.S. Schach, T.A. Sloan, and C.T.G. Knight, *J. Chem. Soc. Dalton*, 3149 (1999).

Chapter Four

Aluminium-27 NMR spectra of aluminosilicate solutions as a function of the Si:Al ratio, the concentrations of Si and Al, and temperature

4.1. Introduction

The synthesis of zeolites normally involves the formation of an aluminosilicate gel. Successful synthesis depends strongly on the gel microstructure, which is determined by the reaction of soluble silicate and aluminate anions.[1] The question of whether dissolved aluminosilicate species are involved as precursors in the hydrothermal formation of natural or synthetic zeolites has been investigated by a number of authors for some years.[2-6] For this reason there is a growing interest in understanding the chemistry of the reactions between soluble aluminate, silicate, and aluminosilicate anions in alkaline solutions.

Much work has been reported on the environment of Al atoms in solid aluminosilicates, while little has been published on the characterization of solutions containing aluminosilicate or aluminate and silicate ions by the ^{27}Al NMR technique.

In contrast to the well-known dependence of ^{29}Si chemical shifts on the degree of condensation of SiO_4 tetrahedra in silicates, a detailed knowledge of the behaviour of ^{27}Al chemical shifts for corresponding condensed aluminate anions is as yet lacking.

Guth *et al.*[7-9] studied changes as aluminate and silicate solutions were mixed using pH, conductivity, and Raman measurements. They showed that aluminosilicate complexes were formed. Other experiments have been used to study the crystallization of zeolites directly from solution.[10-12] McCormick *et al.*[30] observed aluminosilicate species by both ^{27}Al and ^{29}Si NMR spectroscopy in aluminosilicate solutions. ^{27}Al NMR spectra showed broadened and shifted peaks, attributed to aluminium attached to one and two silicate sites. Such complexes have also been observed in tetramethylammonium aluminosilicate solutions, by ^{27}Al NMR.[14-16] Harris *et*

al.[17,18] used octahydrohexamethyl benzotripyrrolium (HMBTP) as a template for studies of aluminosilicate solutions by both one- and two- dimensional ^{27}Al NMR spectroscopy techniques in order to understand the mechanism of the aluminosilicate formation.

For a broad range of AlO_4 tetrahedra present in aluminates, aluminosilicates and aluminophosphates, Muller *et al.*[19] observed distinct ^{27}Al chemical shift ranges for the AlO_4 units linked to different neighbouring TO_4 tetrahedra (T=Al, Si, P) and AlO_6 octahedra. However, there has been some controversy over the assignment of peaks to aluminium sites in aluminosilicates by various workers. Muller et al.[19] assigned the chemical shifts of 79.5, 74.3 69.5 and 64.2 ppm to q^0, q^1, q^2 and q^3 respectively, using TMA aluminosilicate solutions. Dent Glasser and Harvey,[20] using potassium aluminosilicate solutions, found several bands in the ^{27}Al NMR spectrum lying in shift ranges of 72-79, 69-71, 64-66, 60-63 and 57-58 ppm, and assigned them to q^0, q^1, q^2, q^3, and q^4 respectively. Kinrade and Swaddle,[21] observed several signals in ^{27}Al NMR using sodium aluminosilicate solutions. They assigned shifts of 80, 75, 70 and 65 ppm to q^0, q^1, q^2 and q^3 respectively. On the other hand, Mortlock *et al.*[22, 23] using tetraalkyl ammonium aluminosilicate solutions, assigned the signals located at the 74-77, 69-72, 64-67 and 58-61 ppm to q^0, q^1, q^2 and q^3, respectively. Harris *et al.*[17,18,24] using HMBTP and TMAOH aluminosilicate solutions also found four distinct bands in the shift range ca. 80, 75, 70, 65 and 60 ppm and ascribed them to species with q^0, q^1, q^2, q^3 and q^4 sites, respectively.

The nature of the aluminosilicate ions and of their reactions in solution are still of considerable current interest. One central problem has been the nature of the aluminium co-ordination in aluminosilicate solutions. In

principle, NMR spectroscopy is uniquely capable of detecting and characterising ^{27}Al and ^{29}Si centres in aqueous solutions, but its application is hindered by the low solubility of aluminosilicate under many circumstances. In the present study, ^{27}Al NMR has been used to investigate the local structure about the Al in a series of aluminosilicate solutions. This convincingly shows the formation of aluminosilicate anions through the reaction of aluminate and silicate anions. ^{27}Al NMR spectra reveal evidence for Al bound to zero, one, two, three and four Si atoms through oxygen atoms. Also, the effect of temperature on ^{27}Al NMR spectra has been investigated.

As part of this work we carried out a careful study of the effect of varying the Al, Si and template concentration and/or changing the nature of template or lowering the pH and temperature, to obtain highly-resolved spectra with many more resolved lines than previously known. The following sections show some of the results.

4.2. Results and discussion

4.2.1. The effect of aluminium concentration on the ^{27}Al NMR spectra at constant Si and TMAOH concentrations.

In this section results for solutions with [Si] and [TMAOH]=0.875 and 1 molar respectively are reported. [Si/Al] ratios 5, 10, 20, 50 were used. Deconvolutions and resolution enhancements were carried out by using the Lorentz-Gauss transformation.

Aluminium-27 NMR spectra were obtained using the Varian VXR 600 spectrometer at 166.3 MHz (14.1 T) and ca. 25°C. The NMR conditions and the processing data are quoted in the figure captions. The probe used for the experiments involved components containing aluminium, so that a broad

background signal centred at $\delta \approx 60$ ppm (the same region as the q^4 peak) could be observed. In order to give maximum accuracy for the baseline subtraction two ways of compensating for this signal were tried as discussed in detail in chapter 2. It was found that backward linear prediction for the first 12 points of the FID gives spectra of good apparent quality. Therefore these numbers of points were used in BLP to obtain the spectra of figure 4.1 as well the other spectra, making many aspects of interpretation easier. However, it probably results in uncertainties regarding the extent of the true q^4 signal from the aluminosilicate solutions.

Figure 4.1 shows ^{27}Al NMR spectra of four samples of aluminosilicate solutions with constant concentrations of Si and TMAOH equal to 0.875 and 1 M respectively, but with the Al concentration changed to obtain solutions with Si/Al ratios 5, 10, 20 and 50. These spectra were obtained with the same processing parameters (such as BLP number, vertical and horizontal scales, and line broadening (lb)) and used the absolute intensity (ai) mode. The spectra in figure 4.1 illustrate that we have molecular species present which contain aluminium in tetrahedral environments with a variety of structural differences as found earlier in Samadi's work.[25] The spectra are characterised by at least four distinct bands. The bands appearing at 74-77, 68-73, 63-67, and 52-63 ppm are assigned to q^1, q^2, q^3 and q^4 respectively. It is clear from these spectra that the peak assigned to q^4 shows the highest intensity, which indicates that the solutions are dominated by q^4 environments. This phenomenon can be expected since the corresponding TMAOH silicate solution can react with aluminium ions without breaking Si-O-Si bonds in a manner consistent with the observation of Hoebbel et al.[26] on the formation of cubic octamer aluminosilicates in TMA aluminosilicate solutions (see below). Samadi,[25] who worked with similar

concentrations but with a different amine, showed that in that case q^3 had the highest intensity, and concluded that the aluminosilicate solutions are dominated by cage-like species, especially the prismatic hexamer and cubic octamer, as can be seen from the silicon-29 NMR spectra.[21] Although the ^{27}Al spectra exhibit only four major peaks, this does not mean there are only four kinds of anions. Because of the loss of regular symmetry around the aluminium in aluminosilicate anions and the quadrupolar property of Al nuclei, there are increased line widths. The overlap in the ^{27}Al NMR spectra suggests that the quadrupole coupling constants for tetrahedral aluminium sites in aluminosilicate anions are large. Consequently, to resolve a separate resonance line for each aluminium site seems to be impossible, at least in the conditions used for figure 4.1.

As the mole percent of Al increases, the signal-to-noise ratio improves, but the features of the spectra do not change substantially. As a result, the ^{27}Al NMR spectra show that the distribution of Al is not a strong function of the Al concentration. For example, only negligible differences occur between the spectra for Si/Al=5 and Si/Al=50 (figures 4.1 a and d respectively). Therefore the distribution of Al connectivity is not influenced substantially by the concentration of dissolved Al. This result is consistent with previous reports published by Mortlock et al.[22, 23] However, the spectra change significantly with different Si concentrations; details are given in sections 4.2.5a & b.

The intensities of peaks observed in the ^{27}Al NMR spectra are directly related to the number of corresponding aluminium atoms present in the sample being investigated. Therefore, from the relative peak intensities the quantitative proportions of the various Al sites of the sample can be determined directly. Absolute concentrations of Al may be estimated by

comparison with the peak intensities of a standard sample of known composition, which may be mixed in a certain amount with the unknown sample, or may be measured in a separate experiment performed under the same conditions as used for the sample under investigation.[25]

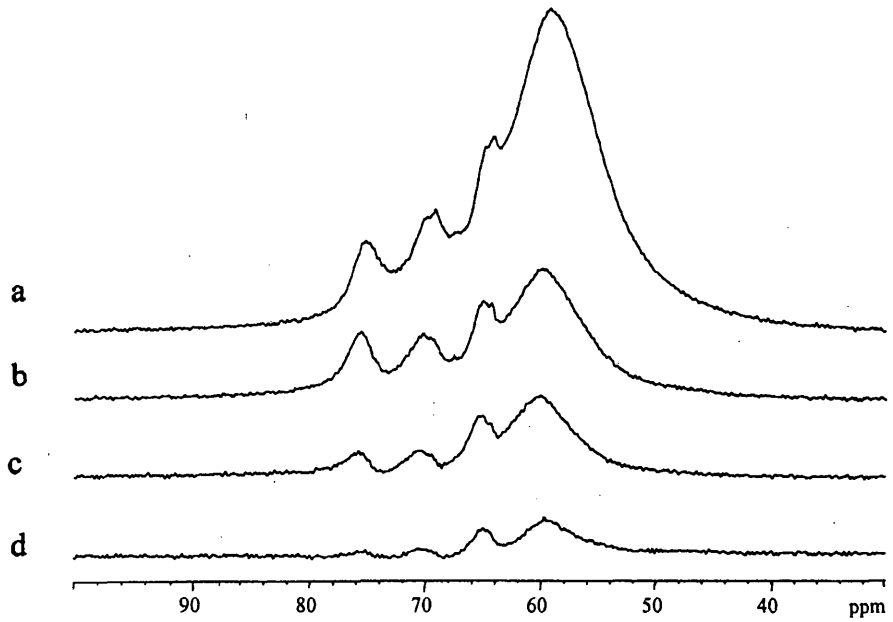

Figure 4.1. High-resolution ^{27}Al NMR spectra at 156.3 MHz of TMAOH aluminosilicate solutions of composition one molar TMAOH, 0.875 molar SiO_2, and Si/Al ratios: a=5, b=10, c=20 and d=50 at 25°C. The spectra were taken two weeks after mixing. Spectrum conditions: Spectral width 29996 Hz. Acquisition time 0.02 s. Recycle delay 0.10 s. Pulse angle 158.8° (34 μs). Number of transients 2048. All were obtained with the same processing. Line broadening not used. BLP 12.

For structural considerations, the relative numbers of Al atoms present in the distinct sites are mostly sufficient. These can be obtained directly from the normalised intensity ratios of the different signals in the spectrum. The intensity of partially overlapping peaks may be separated by deconvolution into individual Gaussian component peaks. A typical deconvolution experiment for spectrum (a) of figure 4.1 is shown in figure 4.2 and the detailed results are shown in table 4.1. For brevity, the other experiments for

the spectra b-c are not shown here and just the calculated values of q^1, q^2, q^3, q^4 are inserted in table 4.2.

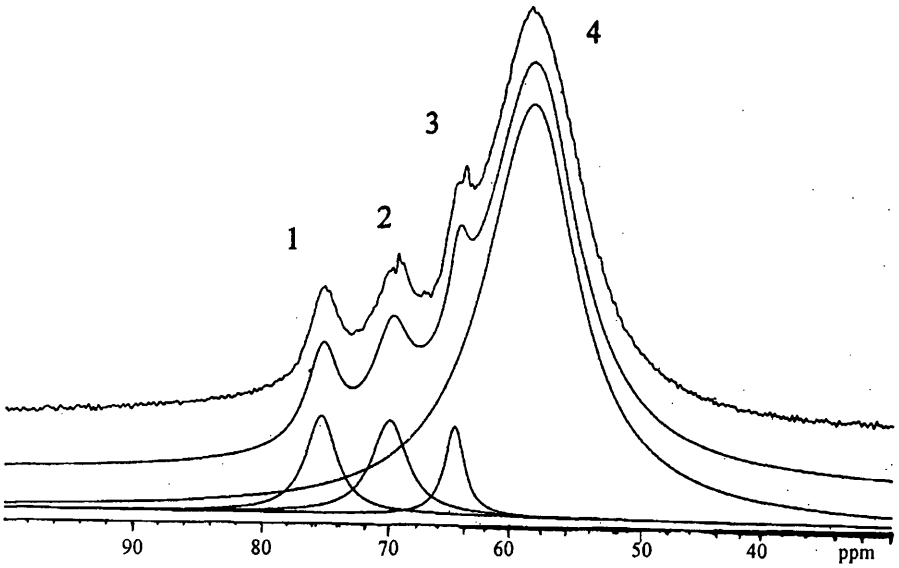

Figure 4.2. Deconvolution experiment. Top: actual spectrum of a sample with 1M TMAOH, 0.875 M Si and Si/Al=5; centre: full fitted spectrum, and bottom: individual component plots. For the caption to the experimental spectrum see the caption of figure 4.1.

Table 4.1. Data obtained from the deconvolution experiment of figure 4.2.

Peak	Chemical shift/ppm	Height	Width/kHz	Integral ratio *
1	75.3	27	0.47	1.00
2	69.9	26	0.53	1.10
3	64.8	24	0.29	0.60
4	59.0	114	1.38	12.7

* Relative to peak 1

However, application of exponential line broadening or a 'window' function to the FID can give rise to substantial errors in the individual line intensities, the correction of which has been discussed by Gladden et al.[27] Further, in order to obtain reliable signal intensities, the pulse repetition time and pulse duration used in the NMR measurement must be carefully selected in order to avoid saturation due to insufficient spin relaxation between the pulses. Fortunately, relaxation times for ^{27}Al are short. However, sometimes

the relaxation times of different Al nuclei in a sample are significantly different. In such cases the pulse conditions must be adjusted with regard to the longest relaxation time, since otherwise the intensity enhancement from pulse repetition may be completely different for Al atoms in different structural sites. However, qualitative or semi-quantitative information on the presence of different AlOH groups may be obtained from comparison of the corresponding intensities observed in the spectra.

The relative concentrations of aluminosilicate species present as q^1, q^2, q^3 and q^4 structural units, which have been estimated from integrated intensities of the corresponding signals of figure 4.1, are listed in table 4.2. It is pertinent to notice that the spectra in figure 4.1 and the data in this table show that the intensity of q^4 (the band at lowest frequency), seems to increase as the Si/Al mole ratio (at constant Si=0.875 and TMAOH=1 M) decreases, i.e. with increasing aluminate concentration. However, the bands become broader as the concentration of Al increases, so that operation of BLP is of variable effect.

Table 4.2. Estimated mole % of aluminosilicate species structural units (q^n)/q for the solutions giving the spectra shown in figure 4.1.

[Si]/[TMAOH]*	[Si]/[Al]	q^1%	q^2%	q^3%	q^4%
0.875	5	6.5	7	4	82
0.875	10	6	2	12	72
0.875	20	7.5	10	12	71
0.875	50	4.5	9.5	23	63.5

*Molarity of TMAOH=1

From the above discussion and study in the section 4.2.3(a), one can expect that cage-like species such as figure 4.15 might be dominant due to the stability of the corresponding silicate anions in TMAOH silicate

solutions. However, this present result is not consistent with the previous reports. [21,25]

There are some other facts that should also be mentioned, such as the use of exponential/Gaussian resolution enhancement. The spectra in figure 4.3 are of a TMAOH aluminosilicate solution with a Si/Al ratio=5 at 0 °C. The upper trace was obtained using a Lorentz-Gauss transformation [28] and shows further distinct peaks with respect to the bottom spectrum. The latter shows no peak at shifts of about 67 and 72.5 ppm but these clearly appear in the upper spectrum. Although it is difficult to say exactly which kinds of aluminate species correspond to these signals, on the basis of shielding arguments they are tentatively assigned to Al atoms in anions involving cyclic trimers. However, the apparent resolution of these bands is a direct consequence of using the Lorentz-Gauss transformation, [28] since such peaks have not been observed in aluminosilicate spectra of these compositions, which were not resolution-enhanced.[29]

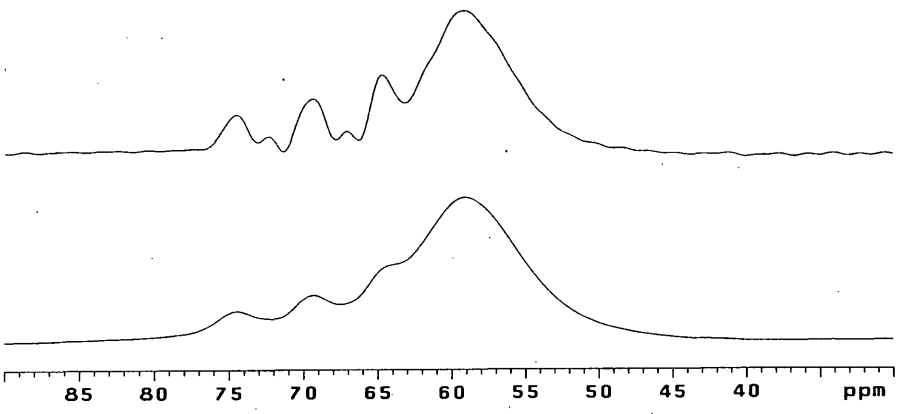

Figure 4.3. High-resolution ^{27}Al NMR spectra at 156.3 MHz of TMAOH aluminosilicate solution of the composition one molar TMAOH, 0.875 molar SiO_2, and Si/Al ratio = 5 at 0 °C. The spectra were taken two weeks after mixing. Spectrum conditions: Spectral width 29996 Hz. Acquisition time 0.02 s. Recycle delay 0.100 s. Pulse angle 158.8° (34 μs). Number of transients 2048.

4.2.2. The effect of aluminium concentration on ^{27}Al NMR spectra with different Al and/or Si concentration at [Si/Al] ratios 0.33-7.5.

In section 4.2.1 it was concluded that the mean degree of polymerisation of aluminate anions present in TMAOH silicate solutions increases with decreasing [Si]/[Al] mole ratio in the range 5-50 (for changing Al concentration in solutions of constant Si/TMAOH mole ratio). In the following, some attempts are reported for finding the solution conditions which maximise the number of signals observed (i.e. which give the optimum resolution of the ^{27}Al spectra). The ^{27}Al NMR spectra have been obtained of aluminosilicate solutions with Si/Al molar ratios in the range 0.33-7.5 but varying Si concentration (dilute solutions specially using constant/and or differing Al concentrations). For this purpose, thirty samples (six sets of Al concentrations, i.e. [Al]=[x=0.014 M, 2x, 4x, 6x, 8x and 10x]), with constant Si/TMAOH= 0.5 were made up. All solutions were prepared at room temperature (ca. 295°K) in water with 13% v/v D_2O. The summarised information about these solutions is listed in table 4.3. The present work demonstrates the application of NMR spectroscopy to defining the effects of silicate to aluminate ratios (with changing Al and/or Si concentration) on the connectivity of aluminium atoms and on the distribution of aluminosilicate species in aluminosilicate solutions pertinent to zeolite synthesis. Most of the evidence offered for the existence of Si-O-Al links in solution has come from ^{27}Al NMR spectroscopy,[21] which to date has given only limited information because of quadrupolar line broadening, i.e. from subtle effects (such as shifting or broadening) on ^{27}Al NMR lines.

Table 4.3. Data for aluminosilicate solutions.*

Sample No.	Molarity TMAOH	Molarity Si	Molarity Al	[Si]/[Al] Ratio
1	0.028	0.014	0.014	1
2	0.056	0.028	0.014	2
3	0.084	0.056	0.014	4
4	0.105	0.084	0.014	6
5	0.210	0.105	0.014	7.5
6	0.028	0.014	0.028	0.5
7	0.056	0.028	0.028	1
8	0.084	0.056	0.028	2
9	0.105	0.084	0.028	3
10	0.210	0.105	0.028	3.75
11	0.028	0.014	0.056	0.25
12	0.056	0.028	0.056	0.5
13	0.084	0.056	0.056	1
14	0.105	0.084	0.056	1.5
15	0.210	0.105	0.056	1.875
16	0.028	0.014	0.084	0.167
17	0.056	0.028	0.084	0.334
18	0.084	0.056	0.084	0.667
19	0.105	0.084	0.084	1
20	0.210	0.105	0.084	1.25
21	0.028	0.014	0.140	0.10
22	0.056	0.028	0.140	0.20
23	0.084	0.056	0.140	0.40
24	0.105	0.084	0.140	0.60
25	0.210	0.105	0.140	0.75
26	0.028	0.014	0.112	0.125
27	0.056	0.028	0.112	0.25
28	0.084	0.056	0.112	0.5
29	0.105	0.084	0.112	0.75
30	0.210	0.105	0.112	0.938

* Note: Na is present in the same concentration as Al because of the method of preparation (see chapter 2).

Detailed information about the preparation and characterisation of the solutions is given in chapter two. In these TMA aluminosilicate solutions, for the first time, additional separated ^{27}Al NMR lines could be observed in the range between ca. 50-80 ppm. The chemical shifts are given in table 4.4.

The ^{27}Al NMR spectrum of 0.014 M sodium aluminate solution (61.3 wt% of Al_2O_3), figure 4.4, shows a single peak at ca. 80.5 ppm before addition of TMAOH silicate solution. The concentrations of aluminium and sodium are the same as for the aluminosilicate solutions discussed in the following sections. This spectrum indicates that the tetrahedral aluminium site of AlO_4^{5-} resonates at ca. 80.5 ppm. The peak is very sharp, illustrating that the aluminium site in the aluminate anion is highly symmetric.

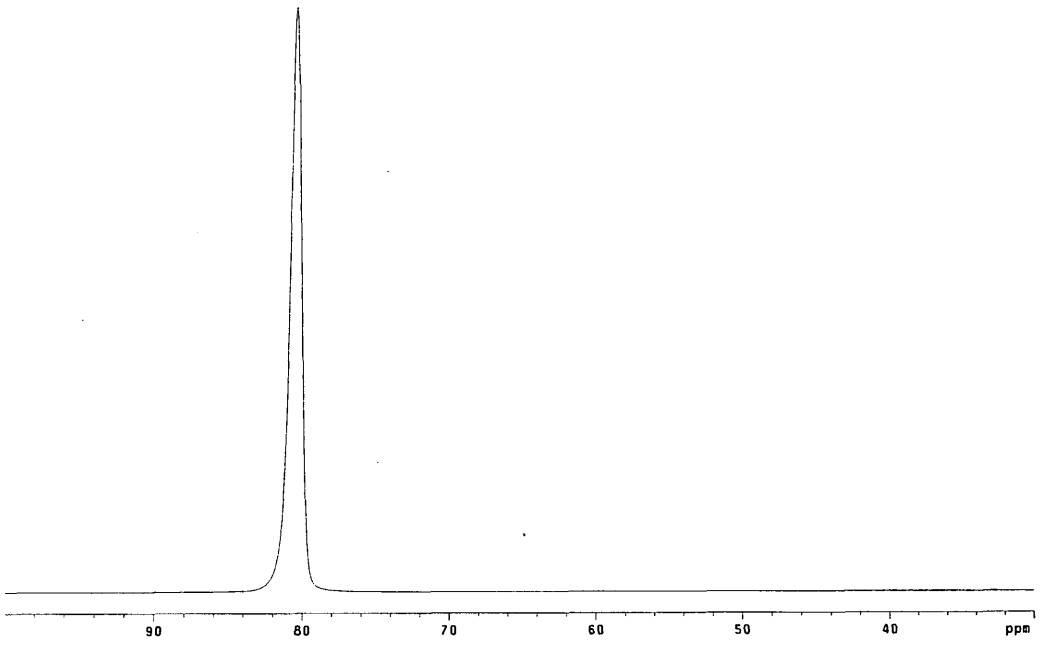

Figure 4.4. ^{27}Al NMR spectrum at 156.3 MHz for a pure aqueous sodium aluminate solution at 25 °C. Spectrum conditions: Spectral width 50000.0 Hz. Acquisition time 0.205 s. Recycle delay 0.100 s. Pulse duration 45.0 μ s. Number of transients 8192

When silicate solution is added, this peak is reduced or disappears completely (depending on composition) and new groups of peaks appear between 80-50 ppm (see typical examples, figures 4.1 and 4.5).

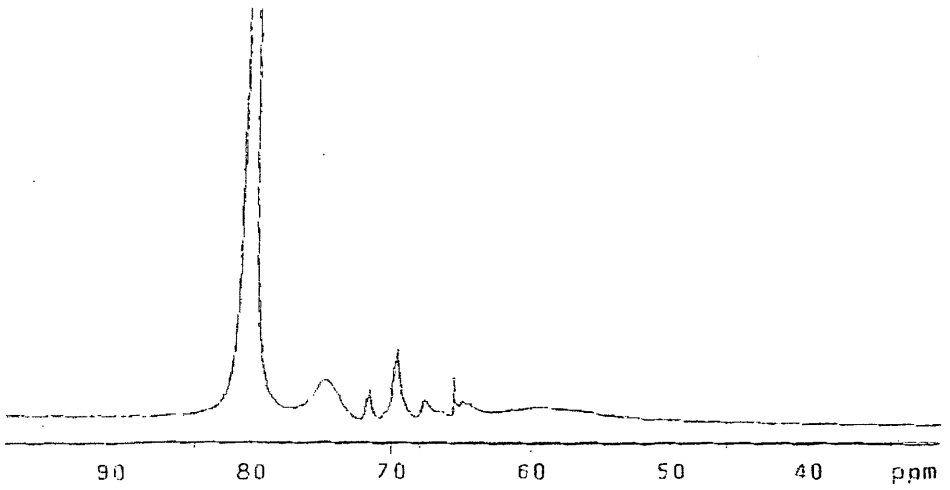

Figure 4.5. High-resolution ^{27}Al NMR spectrum at 156.3 MHz of a TMAOH aluminosilicate solution with the ratio Si/Al = 1 at 25°C (sample No.1). The spectrum was taken two months after mixing. Spectrum conditions: Spectral width 50000.0 Hz. Acquisition time 0.205 s. Recycle delay 0.100 s. Pulse duration 45.0 μs. Number of transients 200000

Figure 4.5 (sample 1) displays the ^{27}Al NMR spectrum for a solution with Si/Al mole ratio of 1 and which is 0.014 molar in SiO_2. The spectrum illustrates that there are many molecular species present, which contain aluminium in tetrahedral environments with a variety of structural differences. It shows different features from the figures in section 4.2.1. For example, it contains a sharp peak at a chemical shift of 65.9 ppm. This signal must arise from a species with a very low electric field gradient (i.e. symmetric environment, at least electronically). In principle this might be $Al(OSiO_3)_4$, but the chemical shift renders this highly unlikely. The following assignment for the ^{27}Al NMR spectrum of figure 4.5 has been suggested in this work (see chapter 5): The bands at ca. 64-68 ppm are assigned to q^3 structural units, with the peak at ca. 65.9 ppm possibly

assigned to the Q^3_8 (1Al) octameric species and the signal at 67.9 possibly assigned to the Q^3_6 (1Al) prismatic species. However, with these assignments, the shift difference of ca. 2 ppm is much less than the value (ca. 10 ppm) observed for ^{29}Si in corresponding silicate solutions.[30] There are very weak bands to the left of the sharp peak at ca. 66-67 which arise from unknown aluminosilicate species. For the spectra of figure 4.5 (sample 1), some suggested assignments are given in table 4.4.

It is clear from the ^{27}Al NMR spectra of the TMAOH aluminosilicate solution shown in figure 4.5 that the peak assigned to q^0 shows the highest intensity, in contrast to the previous studies [31] (see also figure 4.3), which indicates that the relevant aluminosilicate solution is dominated by monomeric aluminate ions. Although the spectrum exhibits at least ten different sites for Al, this does not mean there are only ten kinds of anions. Because of the loss of regular symmetry around the aluminium in aluminosilicate anions and the quadrupolar property of Al nuclei, there is an increased linewidth. The overlaps in the ^{27}Al NMR spectra suggests that the quadrupole coupling constants for the tetrahedral aluminium sites in the aluminosilicate anions are, in general, relatively large. Consequently, to resolve a separate resonance line for each aluminium site seems to be impossible or at least needs special conditions. Some attempts to find better resolution have been carried out. For example, recently further interesting observations as a result of varying the pH [24] (see chapter 5) were obtained.

From figures 4.1, 4.6 (samples 4, 9, 14) and 4.7 (samples 1, 7, 13, 19), it can be concluded that ^{27}Al NMR should be able to provide reliable information on the presence of stable aluminosilicate anions in solution, since characteristic shift effects are to be expected from the formation of SiOAl linkages. It has been shown from ^{27}Al NMR spectra of

aluminosilicates that replacement of Al with Si in the second co-ordination sphere of an Al site causes, in general, a low-frequency shift of about 5 ppm.

Table 4.4. Data from the spectrum of sample 1 (figure 4.5).

Chemical shift/ppm	**Unit**	**Comment**
80.4	q^0	Very intense
75.1	q^1	Broad
71.9	?	Sharp. q^2 in 3-membered rings
69.9	q^2	
67.9	?	Weak. q3 in 3-membered rings e.g. Q^3_6(1Al)
66.6	?	Very weak
65.9	?	Very sharp - must be in symmetrical site (at least electronically). Possibly $Al(OSiO_3)_4$ (but at an odd chemical shift). See chapter 5
65.2	q^3	Weak
64.7	q^3	Weak
59.5	q^4	Very broad

Figure 4.6 (samples 4, 9, 14) corresponds to solutions for which the silicon and TMAOH concentrations are held constant to 0.084 and 0.105 M respectively but the aluminium concentrations are varied so that the Si/Al mole ratio changes from 6 to 1.5 (see table 4.3). The number of signals does not increase with increasing Al concentration, but the intensities of some signals change significantly. In all of them the q^0 and q^1 signals are partially coalesced. When Al is added to TMA silicate solutions to achieve a Si/Al molar ratio of 1 with variation of both Al and Si concentrations (samples 7, 9 and 1, 13), some of the ^{27}Al NMR peaks are broadened (see figures 4.7 and 4.8). The broadening can be attributed, in part, to chemical exchange between aluminosilicate species.

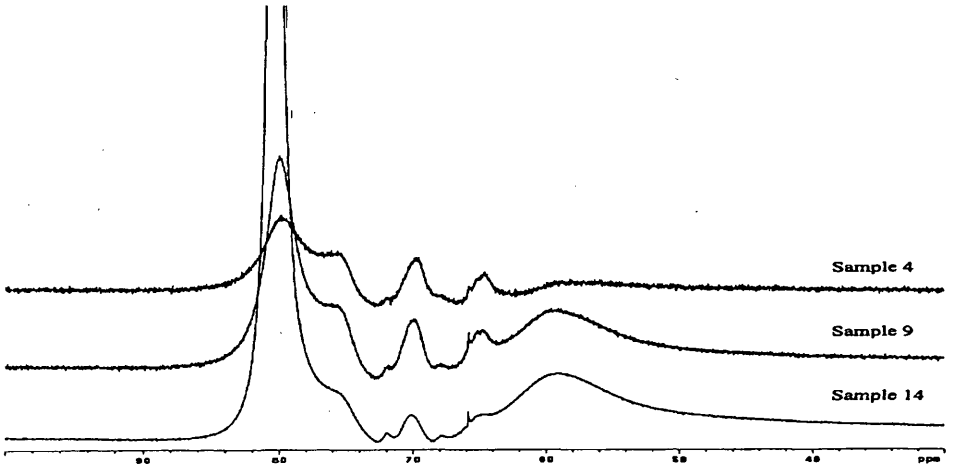

Figure 4.6. Stacked plot of high-resolution ^{27}Al NMR spectra at 156.3 MHz of 0.105 M TMAOH aluminosilicate solutions with constant Si=0.084 M concentration and Si/Al ratios 6, 3, and 1.5 (samples 4, 9, and 14 respectively) at 25°C. The spectra were taken two months after mixing. Spectrum conditions: Spectral width 50000.0 Hz. Acquisition time 0.205 s. Recycle delay 0.100 s. Pulse duration 45.0 μs. Number of transients 8192 for sample 4, 32768 for sample 9, and 73216 for sample 14. BLP 12 points.

As for lowering the exchange rate between q^0 and q^1, the following shows the effect of decreasing the Si and Al concentrations and also of temperature on the Al-27 NMR. Unlike the spectra in figure 4.6, figures 4.7 and 4.8 (samples 1, 7, 13, 19), for which the mole ratio Si/Al is held constant at one but the concentration of Si and Al for each solution decreases by a factor of 1/2 (see table 4.3), show that the q^0 and q^1 signals are completely resolved for samples 1 and 7, especially for the former (sample 1), for which the Al concentration and the mole ratio Si/Al are 0.014 and 1 respectively, giving a chemical shift difference between them of 5.6 ppm. But with increasing Al concentration (spectra of samples 13 and 19 in figures 4.8 and 4.7), significant overlapping can be observed with respect to the spectra of samples 1, 7. It can be concluded that the exchange rate between q^0 with q^1 (and may be with other species) is increased in these situations.

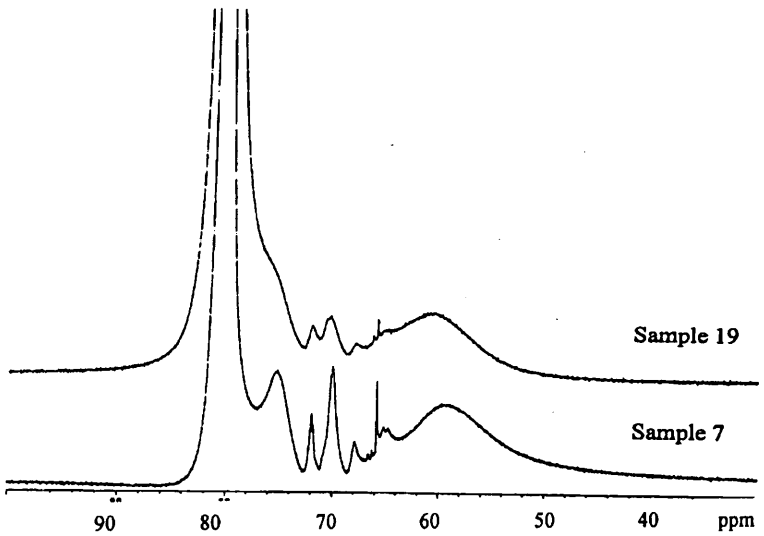

Figure 4.7. Stacked plot of high-resolution ^{27}Al NMR spectra at 156.3 MHz of TMAOH aluminosilicate solutions with the ratio Si/Al = 1 at 25°C and Si=Al concentrations 0.028 M for sample 7 and 0.084 for sample 19. The spectrum was taken two months after mixing. Spectrum conditions: Spectral width 50000.0 Hz. Acquisition time 0.205 s. Recycle delay 0.100 s. Pulse duration 45.0 μ s (192.9 degree). Number of transients 190464 for sample 7 and 169984 for sample 13.

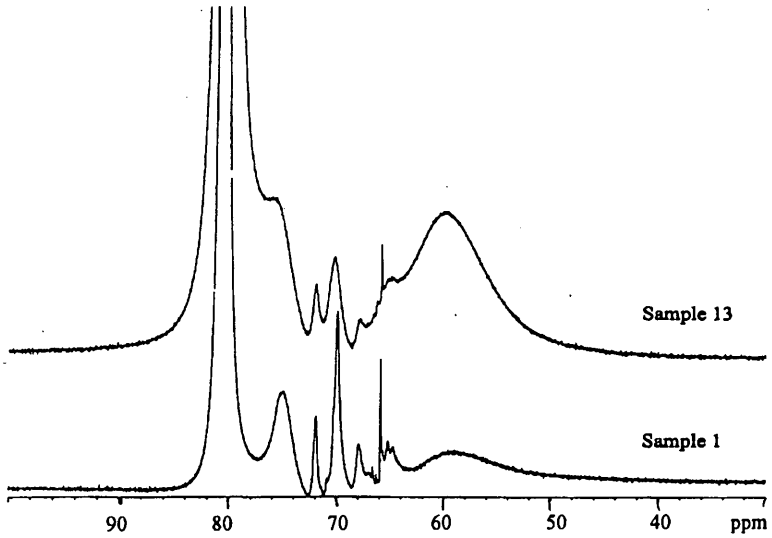

Figure 4.8. Stacked plot of high-resolution ^{27}Al NMR spectra at 156.3 MHz of TMAOH aluminosilicate solutions with the ratio Si/Al = 1 at 25°C and Si=Al concentrations 0.014 M for sample 1 and 0.056 for sample 13. The spectrum was taken two months after mixing. Spectrum conditions: Spectral width 50000.0 Hz. Acquisition time 0.205 s. Recycle delay 0.100 s. Pulse duration 45.0 μ s (192.9 degree). Number of transients 143827 for sample 13 and 200000 for sample 1.

Regarding figures 4.6, 4.7 and 4.8 (samples 1, 7, 13, 19, 4, 9, 14) the very broad band at ca. 60 ppm, must arise from aluminosilicate species of the q^4 type. It may therefore be concluded that the principal aluminosilicate species in solutions of the composition regime considered here form through linkage of Al-O-Si units without breaking Loewenstein's rule. The relative intensity of the q^4 peak varies with the Si/Al molar ratio and the concentration of Si or Al at constant Si/Al ratio 1.

With increasing Al and Si concentrations at constant mole ratio Si/Al=1 as in figures 4.7 and 4.8 (samples 1, 7, 13 and 19) and also with varying Si/Al ratio through changing Al concentrations at the same Si concentration (i.e. 0.084 M), as in figure 4.6 (samples 4, 9, 14,19), the second peak from the high frequency end, assigned to q^1, is apparently shifted to higher frequency (i.e. towards the q^0 position) so that, whereas the q^0 and q^1 signals in the spectrum of figure 4.5 are completely resolved from each other, in figure 4.9 (sample 4) they are almost coalesced. This means the rate of exchange between q^0 and q^1 is increased. On the other hand, the intensity of q^0 increases for the higher concentrations of Al, as can be observed from figure 4.6.

As to the temperature effect (discussed in more detail in the section 4.2.7 below), the exchange rates increase with increasing temperature, as is expected. The spectra shown in figure 4.9 (belonging to sample 4) reveal that significant changes happen between the temperatures of 25 and 0 °C. The spectrum recorded at 0 °C shows completely resolved q^0 and q^1 signals but at 25 °C these are partially coalesced. Also, the q^2 peak shows two signals at zero degrees, which are coalesced at 25 degrees.

Previous reports [25,30] and also section 4.2.1 of the present study have mentioned that no signal is resolved for q^0 for aluminosilicate solutions with low TMAOH: SiO_2 ratios and high SiO_2:Al. However, in all aluminosilicate solutions studied in this section there is a significant and intense peak belonging to q^0, even in low concentrations of aluminium. The strong resonance at ca. 80 ppm shows that a considerable amount of the Al content exists as free $Al(OH)_4^-$ in these solutions. The present data can be compared with those reported by Harris and Samadi-Maybodi [31] for HMBTP silicate solutions.

One point that is interesting in this study (mentioned before), is that there is a very narrow line at a shift of ca. 65.9 ppm. In figure 4.1 and from the other relative literature [25,32] no such sharp single line is visible but in all the figures for the above mentioned concentrations this single line has come into view. In all the samples with Si/Al mole ratio one this signal can be observed more clearly than in the others (see the spectra in figures 4.6, 4.7 and 4.8). It is difficult to say which species could be assigned to this peak, but probably it is highly symmetric and more stable. The assignment is explored in more detail in chapter 5.[24] The chemical shift of this signal does not change in the different solutions.

For better understanding of the effects of Si and Al concentrations on the ^{27}Al NMR spectra, now consider three pairs of spectra for which in each pair the concentration of Al is constant but the mole ratio of Si/Al is varied, whereas the Al concentration changes from one pair to another by a factor of 2, see table 4.5. There are characteristic changes of the spectra (number of signals, chemical shifts, intensities), depending on the composition of the solutions.

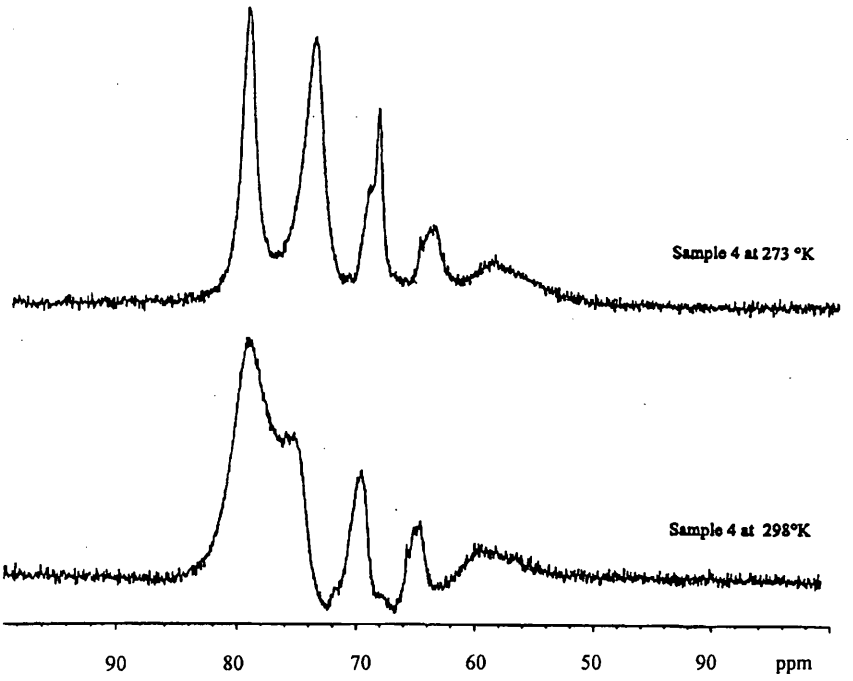

Figure 4.9. Stacked plot of high-resolution 156.3 MHz ^{27}Al NMR spectra at 0°C and 25°C of TMAOH aluminosilicate solutions with the ratio Si/Al = 6 and Si and Al concentrations 0.084 and 0.014 M respectively (sample 4). The spectra were taken two months after mixing. Spectrum conditions: Spectral width 50000.0 Hz. Acquisition time 0.205 s. Recycle delay 0.100 s. Pulse duration 45.0 μs (192.9 degree). Number of transients 8192.

Table 4.5. Characteristics of three pairs of solutions.

Pairs	*Sample No.*	*Molarity Si*	*Molarity Al*	*Si/Al ratio*	*No. of distinct and resolved peaks*
A	14	0.084	4X*	1.5	7
	13	0.056	4X	1	8
B	9	0.084	2X	3	7
	7	0.028	2X	1	10
C	4	0.084	1X	6	7
	1	0.014	1X	1	12

* X=0.014 M

In pair A the mole ratio of Si/Al equals 1 and 1.5, while the Al concentrations are constant at 0.056 M. The spectrum corresponding to sample 13, which has the lower concentration of Si, shows at least one more distinct signal than can be observed for the other one. In the pair C this observation is more significant, so that one of the pair (sample 1) shows at least 12 distinct bands while in the other one there is a maximum of 7 distinct and resolved peaks. Therefore in this range, many more signals are observed for the lowest concentration of Si and Al (i.e. [Si]=0.014 and [Al]=0.014).

From this table it can also be concluded that when the Si concentration is constant (0.084 M) and the Al concentration is changed from X (X=0.014M) to 4X, the number of distinct peaks remains the same, and the spectra only show a little change in the intensities of the signals.

For more evidence of the effect of Al concentration the following further considerations have also been made for ratios Si/Al<4.

4.2.3(a). The effect of Al concentration on ^{27}Al NMR spectra at Si/Al< 4.

Three sets of samples, listed in table 4.6a-c were prepared, in constant Si and TMAOH concentrations but with different Al concentrations in each set.

Figures 4.10, 4.11, 4.12 (Samples 51, 56, 70; 52, 57, 71; and 53, 58, 73 respectively) present ^{27}Al NMR spectra in the absolute intensity mode and with the same vertical scale for each set of solutions. The processing of the spectra was discussed in more detail in chapter 2.

The spectra in figures 4.10-12, as in the former section, illustrate that there is a variety of molecular species present, which contain aluminium in

tetrahedral environments. The figures are characterised by at least four distinct bands. The bands appearing at ca. 80, 74-76, 68-74, and 64-68 ppm are assigned to q^0, q^1, q^2, and q^3 respectively. The number of signals does not increase with increasing Al concentration, but the intensities of some signals like q^3 decrease significantly.

Table 4.6a. Data for aluminosilicate solutions set 1.

Sample No.	Molarity TMAOH	Molarity Si	Molarity Al ≡ atom	[Si]/[Al] ratio	[Si]/[TMAOH]	PH
51=1	0.028	0.014	0.014	1	0.5	12.47
56=6	0.028	0.014	0.028	1/2	0.5	12.66
70=16	0.028	0.014	0.084	1/6	0.5	12.65

Table 4.6b. Data for aluminosilicate solutions set 2.

Sample No.	Molarity TMAOH	Molarity Si	Molarity Al ≡ atom	[Si]/[Al] ratio	[Si]/[TMAOH]	PH
52=2	0.056	0.028	0.014	2	0.5	12.72
57=7	0.056	0.028	0.028	1	0.5	12.86
71=17	0.056	0.028	0.084	1/3	0.5	12.86

Table 4.6c. Data for aluminosilicate solutions set 3.

Sample No.	Molarity TMAOH	Molarity Si	Molarity Al ≡ atom	[Si]/[Al] ratio	[Si]/[TMAOH]	PH
53=3	0.112	0.056	0.014	4	0.5	12.97
58=8	0.112	0.56	0.028	2	0.5	13.02
73=18	0.112	0.056	0.084	2/3	0.5	13.02

As discussed above, for high concentrations of Si in aluminosilicate solutions, as the mole percent of Al increases, the signal-to-noise ratio improves, but the features of the spectra do not change substantially. This means that the distribution of Al in aluminosilicate solutions is not a strong function of the Si/Al mole ratio. In low concentrations of Si (< 0.1M), conversely, as the spectra in figures 4.10-12 show, as the mole percent of Al increases, the intensity of some species like q^0 and q^1 increases but some of them, like q^3, do not improve and nearly disappear, so that the appearance of

the spectra changes. Therefore, the distribution of Al connectivity is influenced by the concentration of dissolved Al. Such a result obviously could be obtained from figure 4.13, which was discussed in section 4.2.3b. This result is not consistent with previous reports [21,25].

It is pertinent to mention that the positions of some bands seem to change as the Si/Al mole ratio decreases, i.e. with increasing aluminate concentration. This phenomenon might be due to an increasing proportion of the AlO_4^{5-}, q^0, anion in the solution, which is in some cases in intermediate or rapid exchange with q^1, causing the averaged peak position to move to higher frequency.

However, there are some matters that should be explained here: the spectra at the lowest concentration of Si, i.e. [Si]=0.014, show no signal for the q^4 site (i.e. at 54 - 63 ppm), see spectra in figure 4.10, though, as discussed earlier, procedures to eliminate the background resonance complicate such statements. However, in the spectra of figure 4.12 for samples 53, 58, and 73, with increasing Si concentration with respect to the previous sets (figures 4.10 and 4.11), a broad peak at this position appears and the broadening becomes much more evident when the Si concentration increases to 0.875 M (see spectra of figure 4.6 (samples 4, 9, 14,19)). Also, this band becomes broader and more intense when the concentration of Al is increased (see figures 4.12 and 4.6).

More explanations can be made about the spectra of figure 4.12 (samples 53, 58, 73), with the Si concentration constant at 0.056 M but Al concentration varied from 0.014 M to 0.084 M. The q^0 and q^1 signals are partially separated for sample 53, at chemical shifts 79.99 and 75.67 ppm respectively. However, when the Al concentration increases, the q^1 peak becomes almost coalesced with q^0, i.e. these two species show intermediate

exchange in the spectra for sample 58, and fast exchange for sample 73 in figure 4.12. In high concentrations of Al, two effects could be involved: a) More free aluminate can be in the solution, for the q^0 signal increases in the figures 4.10, 4.11 and 4.12 (samples 51, 56, 70; 52, 57, 71 and 53, 58, 73).

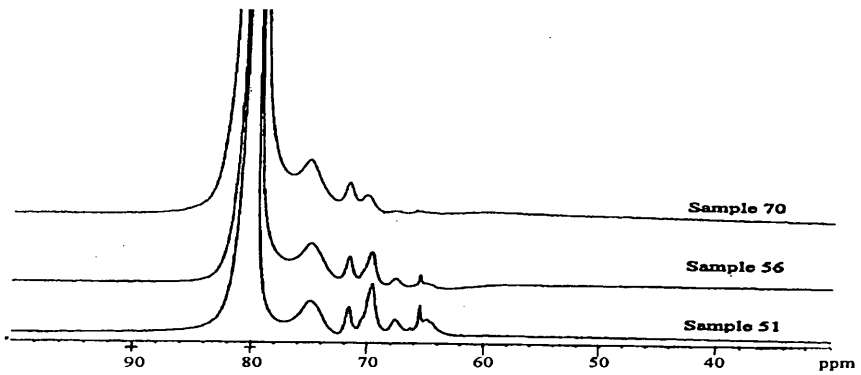

Figure 4.10. Stacked plot of high-resolution ^{27}Al NMR spectra at 130.23 MHz and ambient temperature of tetramethylammonium aluminosilicate solutions (samples 51, 56, 70) with the compositions listed in tables 4.6a. The spectra were taken one month after preparation. Spectrum conditions: Spectral width 25000.0 Hz. Acquisition time 0.081s. Recycle delay 0.200 s. Pulse angle 29.9 degrees. Number of repetitions 8000. All three spectra were obtained using the same processing procedure: setting backward linear prediction to number 12, vertical scale =10000, line broadening =10 and with absolute intensity mode.

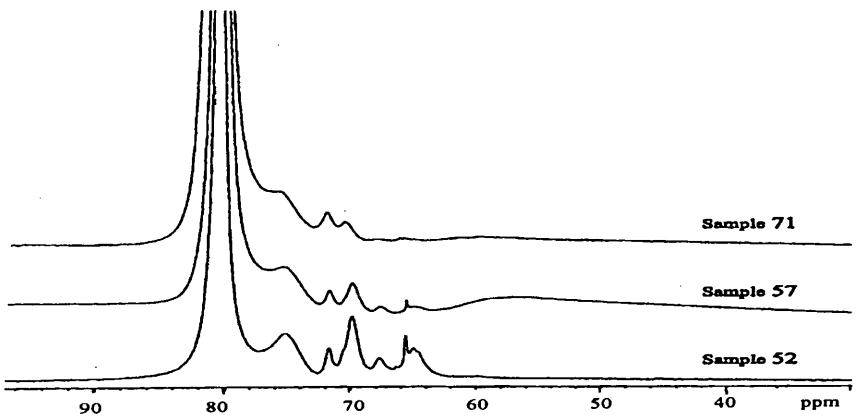

Figure 4.11. Stacked plot of high-resolution ^{27}Al NMR spectra at 130.23 MHz and ambient temperature of tetramethylammonium aluminosilicate solutions (samples 52, 57, 71) with the compositions listed in table 4.6b. The spectra were taken one month after preparation. Spectrum conditions: Spectral width 25000.0 Hz. Acquisition time 0.081s. Recycle delay 0.200 s. Pulse angle 29.9 degrees. Number of repetitions 8000, All three spectra were obtained using the same processing procedures: setting backward linear prediction to number 12, vertical scale=10000, line broadening=10, and with absolute intensity mode.

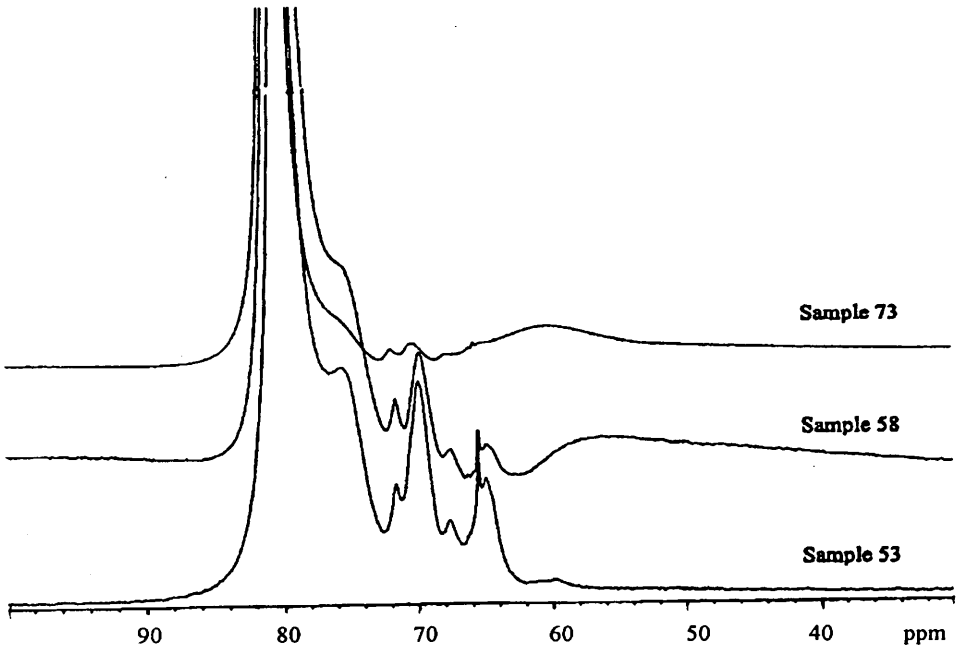

Figure 4.12. Stacked plot of high-resolution ^{27}Al NMR spectra at 130.23 MHz and ambient temperature of tetramethylammonium aluminosilicate solutions (samples 53, 58, 73) with the compositions listed in table 4.6c. The spectra were taken one month after preparation. Spectrum conditions: Spectral width 25000.0 Hz. Acquisition time 0.081s. Recycle delay 0.200 s. Pulse angle 29.9 degrees. Number of repetitions 16000. All three spectra were obtained using the same processing procedures: setting backward linear prediction to number 12, vertical scale 10000, line broadening 10, and with absolute intensity mode.

b) Polymerisation or gelation processes would be expected when the aluminate concentration is increased in the solutions (this phenomenon will be discussed in more detail in chapter 7). One expected reaction is replacement of Al with Si (i.e. intermolecular) and the other is oligomerisation, leading to macromolecules and ultimately to gel formation in very high concentrations.

4.2.3(b). The effect of the aluminium concentration on the ^{27}Al NMR spectra, as in part 4.2.3(a) but at zero degrees:

Because there may be effects of exchange in the spectra obtained at room temperature, some samples have had their spectra recorded at 0°C. Figure 4.13 (samples 10, 20; 8, 18; 6, 16 and 2, 12) presents in four pairs the ^{27}Al NMR spectra of those aluminosilicate solutions for which the silicate concentrations for each pair are constant but the Al concentrations change. Data for the compositions of these solutions are presented in table 4.7.

The spectra in figure 4.13 illustrate the same result as for section 4.2.3a, discussed in more detail there. The main differences observed are: the figures are characterised by at least five distinct bands instead of four. The overlap in the ^{27}Al NMR spectra suggests to us that the quadrupole coupling constants for the tetrahedral aluminium sites in the aluminosilicate anions are, in general, large. Consequently, to resolve a separate resonance line for each aluminium site even at zero degree in this concentration of components seems to be impossible.

The bands appearing at the shift ranges 78-88, 73-78, 68-73, 62-68 and 54-62 ppm are assigned to q^0, q^1, q^2, q^3 and q^4 respectively as discussed in earlier sections. It is clear from the spectra (except for sample 10 in figure 4.13), the peak assigned to q^0 has the highest intensity, which shows that the aluminosilicate solutions are dominated by q^0, i.e. by monomeric aluminate ions. In solutions with the high pH and low Si concentration this can be expected.

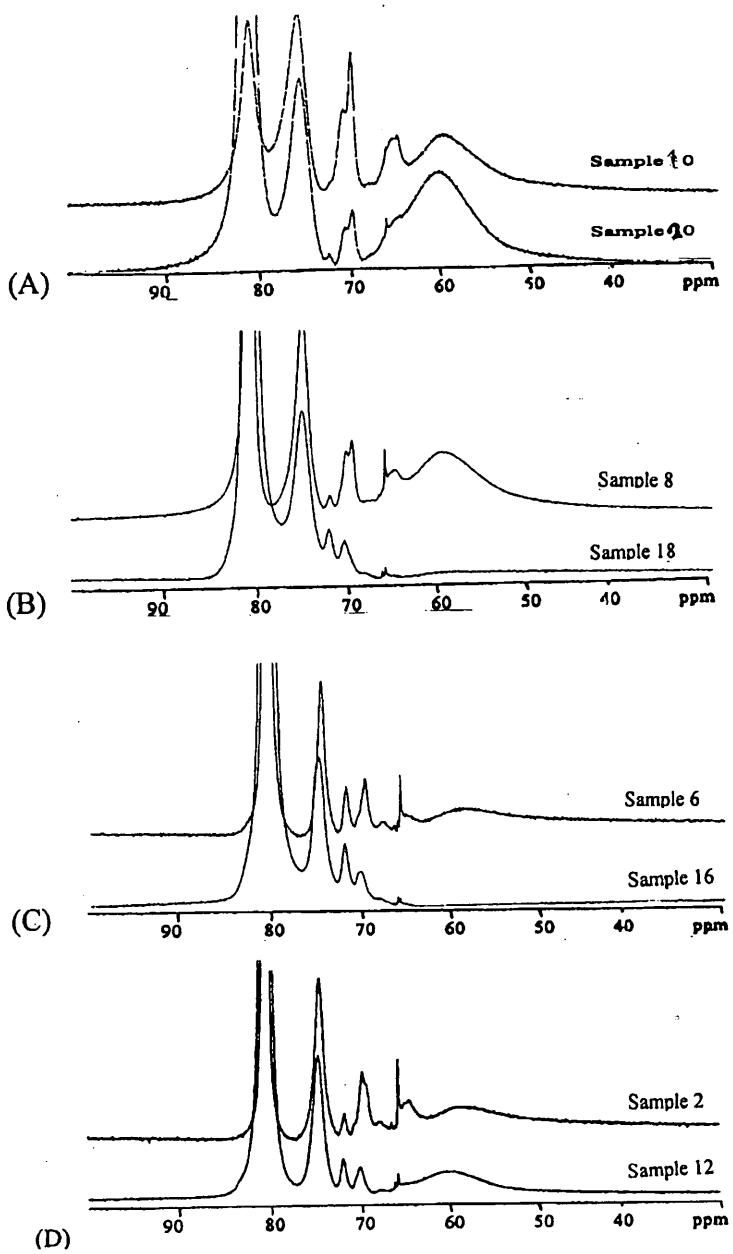

Figure 4.13. Four pairs of high-resolution ^{27}Al NMR spectra obtained at 156.3 MHz and zero degrees for tetramethylammonium aluminosilicate solutions with the compositions listed in table 4.7 (samples 10, 20; 8, 18; 6, 16 and 2,12). The spectra were taken nine months after preparation. Spectrum conditions: Spectral width 50000 Hz. Acquisition time 0.205 s. Recycle delay: 0.100 s. Pulse angle 90 degrees. The number of repetitions for sample 2, 10, 6 and 20 equal 45000, whereas for sample 18, 8, 16, 12 it equals ca. 150000.

Table 4.7. Data for four pairs of aluminosilicate solutions.

Pairs	Sample No.	Molarity TMAOH	Molarity Si	Molarity Al ≡ Na atom	[Si]/[Al] ratio	[Si]/[TMAOH] ratio
A	20	0.21	0.105	0.084	1.25	0.50
	10	0.21	0.105	0.028	3.75	0.50
B	18	0.112	0.056	0.084	0.666	0.50
	8	0.112	0.056	0.028	2	0.50
C	16	0.028	0.014	0.084	0.166	0.50
	6	0.028	0.014	0.028	0.50	0.50
D	12	0.056	0.028	0.056	0.50	0.50
	2	0.056	0.028	0.014	2	0.50

It is also apparent from figure 4.13 that as the mole percent of Al increases, the signal-to-noise ratios improve, and the features of the spectra are changed. Most differences can be observed in the q^3 and q^4 regions. It is pertinent to notice that, as the Si/Al mole ratio decreases with increasing aluminate concentration, the intensity of the band at highest frequency seems to increase and conversely the others decrease. Special cases are the q^3 and q^4 species: this phenomenon might be due to an increasing proportion of the AlO_4^{5-}, q^0, anion in the solution becoming substituted in Q^1, Q^2, Q^3 and Q^4 silicon sites and then forced to equilibrate to the q^4 species. This process is discussed in more detail in section 4.2.4.

4.2.4. Discussion of reactions in aluminosilicate solutions

In the following discussion some ways are speculatively suggested [25] whereby aluminate anions may react with silicate species:

i) Addition: the aluminate ion can be added to any silicate ion to produce an aluminosilicate species with one aluminium q^0 site (eq. 4.1).

$$q^0 + Q^n \rightarrow q^1Q^{n+1} \qquad (n< 4) \qquad (4.1)$$

ii) Substitution: one silicon may replace aluminium, which can lead in principle to q^n with any value of n (eq. 3.2).

$$q^0 + Q^n\text{-}(Q)_n \rightarrow q^n\text{-}(Q)_n + Q^0 \qquad (4.2)$$

e.g.:

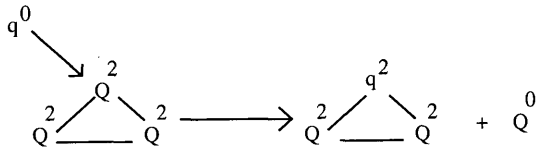

In the above reaction the transition states are ignored

iii) Chelation: This would imply ring or cage formation (eq. 4.3, 4.4 and 4.5).

e.g.:

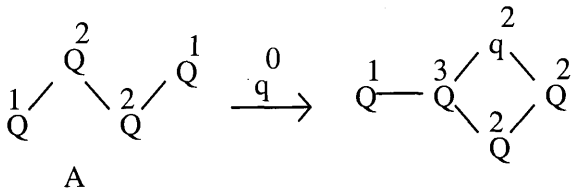

A (4.3)

or

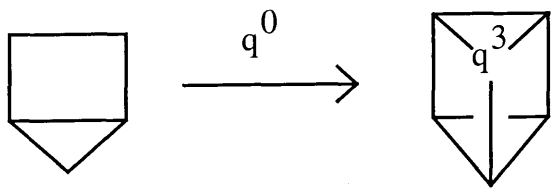

B (4.4)

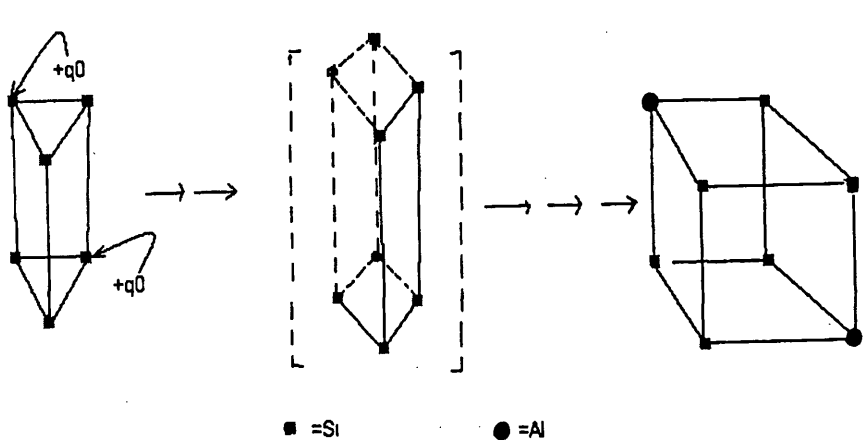

(4.5)

Direct substitution seems unlikely (except, perhaps, replacement of Q^1 by q^1), but chelation would be expected to lead to relatively stable products since it is known that Si-O-Al bonds are relatively difficult to break.[32] Because cage-like silicate species are favoured in TMAOH and HMBTP silicate solutions,[31, 33] it can be expected that analogous species also dominate in the corresponding aluminosilicate solutions. Reactions such as given by equations 4.3, 4.4 and 4.5 would appear to be particularly favourable and may account for the rapid appearance of q^2 and q^3 groups immediately after mixing. Moreover, the formation of tetrameric silicon species favours the cubic octamer. However, the concentrations of species such as A and B in TMAOH silicate solutions are low, so after some initial formation of q^2 and q^3 by this route, further development requires re-equilibration among silicate species to form more A and B, which might be slow. After the initial formation of aluminosilicate ions, these can presumably further equilibrate (though without necessarily breaking the Al-O-Si bridge).

The probability of the reaction of an aluminate ion with an individual silicate species depends upon the size and the charge of the latter. Clearly

the silicate anions contain different amounts of negative charge (depending on the degree of ionisation and therefore on pK_a and pH). The larger ions carry more negative charge. A monomeric (Q^0) ion could theoretically carry a charge up to -4. Dimeric ions and other Q^1 units can carry a maximum of three negative charges per silicon, but Q^2 and Q^3 silicon can carry at most two and one negative charges respectively. As a result, the larger the silicate species, the smaller its average negative charge per silicon, and the easier it will be for it to be approached by a negatively charged q^0 group.

The following reaction (figure 4.14) can be suggested at high concentrations of Al, with the q^0 species forced to substitute into the cage-like species (i.e. $Q^3{}_8$, $Q^3{}_6$) through the Loewenstein Rule and agreement with the Hoebbel observation,[26] to form, for instance, $Q^1{}_1Q^3{}_7q^4{}_1$ or $Q^1{}_4Q^3{}_4q^4{}_4$ (a similar silicate species to the latter was reported by Harris at al.[34]) :

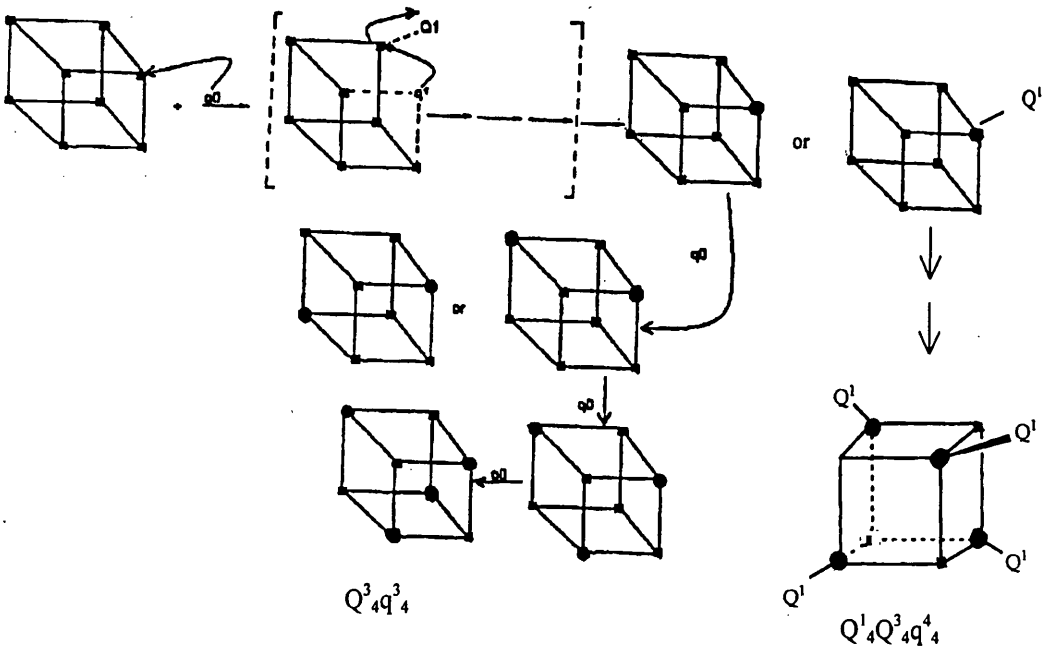

Figure 4.14. Schematic representation of the formation of $Q^3{}_8$(1Al), $Q^3{}_8$(2Al) $Q^3{}_8$(3Al) and $Q^3{}_8$(4Al). Circles represent aluminium atoms and squares indicate silicon atoms.

The actual substitution process may not be reflected by this simplified representation, though, because many different intermediates may be formed during the reaction. The intermediate structures depend on the reaction conditions, the Al concentration, and also the alkalinity of the solution.

Increasing these kinds of species will result in the q^4 signals increasing, because, as is observed in the time-evolution experiments (figure 4.22 through index 1 to 60) the process of formation of q^4 can take place slowly. Therefore, an intermolecular interaction between the above species could be suggested, so that by increasing the amount of these species the formation of q^4 also increass. Such formation of q^4 sites is speculative. Aluminosilicate ions can react, without breaking Si-O-Si bonds, in a manner consistent with the observation of Hoebbel et al.[26] on the formation of double-four-ring aluminosilicates in TMA aluminosilicate solution. They suggested q^4 formation through linkage of Al-O-Si units (without breaking Loewenstein's rule), shown as follows:

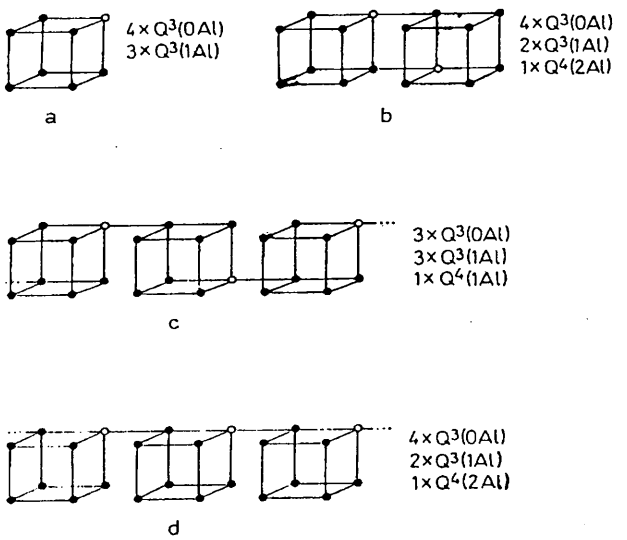

Figure 4.15. Schematic representation of the formation of q^4 sites. Open circles represent aluminium atoms and filled circles indicate silicon atoms.

It should be noted that q^4 sites in zeolites are the positions active for catalysis since they are of Brönsted acid nature [21,31], i.e.

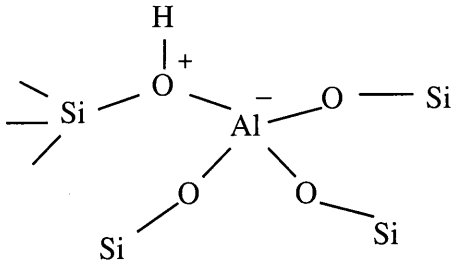

However, in dilute solution the q^0 species is dominant, see figures 4.10-12 (samples 51, 56, 70; 52, 57,71; and 53,58,73) whereas in concentrated solutions, as already shown, cage-like species such as $Q^3_6(1Al)$ or $Q^3_8(1Al)$ might be dominant due to the stability of the corresponding silicate anions in TMAOH silicate solutions.

4.2.5a. The effect of the Si concentration on the ^{27}Al NMR spectra.

In order to understand the effects of Si concentration, consider two sets of spectra, for which in each set the concentration of Al is constant but the mole ratio of Si/Al is varied, whereas the Al concentration changes from one set to another by a factor of 2, see table 4.8. Consideration of the characteristic changes of the spectra (number of signals, chemical shifts, intensities) depends on the composition of the silicate solutions (silica concentration, TMAOH to Si ratio) and the correlation with changes in the silicate anion distribution.

In sections 4.2.3a and b it was concluded that the mean degree of polymerisation of the aluminate anions present in TMAOH silicate solutions increases with decreasing [Si]/[Al] mole ratio in the range 1-4, arising from changing Al concentration for solutions of constant Si/TMAOH mole ratio 0.5. In the present section, ^{27}Al NMR spectra of aluminosilicate solutions for

Si/Al ratios in the range 0.33-7.5 with varying Si concentration are again discussed. These two parts of the present work demonstrate the application of NMR spectroscopy for defining the effects of silicate to aluminate ratios (with constant Al and changing Si concentration) on the connectivity of aluminium atoms and on the distribution of aluminosilicate species in aluminosilicate solutions pertinent to zeolite synthesis. In this part of the work, ten samples with different concentrations of Si, but with the Si/TMAOH mole ratio constant at 0.5 in two sets of Al concentrations, i.e. [Al] = 0.014 M, and 0.028 M, were prepared. All solutions were prepared at room temperature in water with 13% v/v D_2O. The summarised information about these solutions is listed in table 4.8.

Table 4.8. Data for aluminosilicate solutions.

Sample No.	Molarity TMAOH	Molarity Si	Molarity Al ≡ atom	[Si]/[Al] ratio	[Si]/[TMAOH]	pH
51=1	0.028	0.014	0.014	1	0.5	12.47
52=2	0.056	0.028	0.014	2	0.5	12.72
53=3	0.112	0.056	0.014	4	0.5	12.97
54=4	0.168	0.084	0.014	6	0.5	13.1
55=5	0.210	0.105	0.014	7.5	0.5	13.2
56=6	0.028	0.014	0.028	0.5	0.5	12.66
57=7	0.056	0.028	0.028	1	0.5	12.86
58=8	0.112	0.56	0.028	2	0.5	13.02
59=9	0.168	0.084	0.028	3	0.5	13.16
60=10	0.210	0.105	0.028	3.75	0.5	13.23

Detailed information about the preparation and characterisation of the solutions is given in chapter 2. In these TMA aluminosilicate solutions, for the first time, additional separated ^{27}Al NMR lines could be observed in the chemical shift range between ca. 50-80 ppm. Some of them were assigned in the above sections.

Figure 4.16 displays the ^{27}Al NMR spectra for sample 51-55. The spectra were recorded at 21.5°C. It is clear from these spectra that the peak

assigned to q^0 (as for the other dilute solutions) shows the highest intensity, that is, the aluminosilicate solutions are dominated by monomeric aluminate ions.

TMA aluminosilicate solutions are characterised by an equilibrium distribution of coexisting aluminosilicate species with increasing degrees of polymerisation ranging from monomer silicate to 'colloidal' particles. With increasing concentration of silica, the equilibrium is shifted to more highly polymerised species, and vice versa (see the spectra in figures 4.16 and 4.17, for samples 51-55 and 56-60). ^{27}Al NMR has positively proved the existence of a range of stable aluminosilicate anions in aqueous solutions. The results summarised above demonstrate that ^{27}Al NMR can provide valuable information on the structure and distribution of anions in aluminosilicate solutions and on the reactions and transformations of the anionic species caused by various chemical and physical treatments of the solutions. Information of this type is of considerable interest, especially for a deeper understanding of the process of zeolite formation from mixtures of silicate and aluminate solutions.

In dilute solutions (below 0.1 M silicate), a considerable amount of aluminium remains in solution as $[Al(OH)_4]^-$; in other words, not much reaction between silicate and aluminate species takes place under these conditions. In spite of this, there are several aluminosilicate species observed in the ^{27}Al NMR spectra. These species are concluded to contain q^0, q^1, q^2, q^3 and q^4 groups. However, as discussed in section 4.2.1 in the concentrated silicate solutions (more than ca. 0.8 M) the q^0 signal completely disappears, q^4 appears as the dominant species, and some of the other species are not revealed. Therefore, detailed information on the structure and the

quantitative distribution of the various building groups and aluminosilicate species present in the solutions may be obtained from the ^{27}Al NMR spectra.

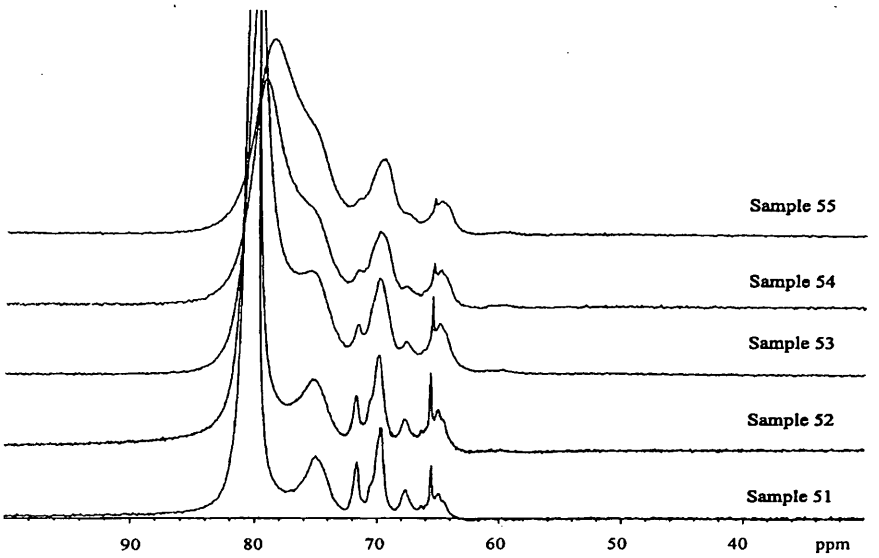

Figure 4.16. Stacked plot of high-resolution ^{27}Al NMR spectra at 130.2 MHz at ambient temperature (ca. 22°C) of tetramethylammonium aluminosilicate solutions (samples 51-55) with the compositions listed in table 4.8. The spectra were taken one month after preparation. Spectrum conditions: Spectral width 25000.0 Hz. Acquisition time 0.081 s. Recycle delay 0.200 s. Pulse angle 29.9 degrees. Number of repetitions 8000 for samples 51, 52, 54 and 16000 for samples 53, 55. All spectra were obtained with the same processing , i.e. setting backward linear prediction number 10, line broadening 10 and with absolute intensity mode and the same vertical scale.

In the spectrum of sample 51 (figure 4.16), the q^0 and q^1 signals are completely separated and show slow exchange. However, with increasing Si concentration the q^1 band is broadened and shifted to higher frequency so that in the spectra of samples 54 and 55 of figures 4.16 it is coalesced with that of q^0 and shows fast exchange. The q^0 signal decreases in intensity and shifts to lower frequency by ca. 2 ppm (see the spectra in figure 4.16). It can be concluded from this phenomenon that the rate of the exchange process between q^0 and q^1 is increased from sample 51 to samples 54 and 55, so that in the last experiment (spectrum of sample 55) just one signal can be

observed for q^0 and q^1, with a shoulder at the right hand side. Also the bands located at chemical shifts 71.7, 69.6, and 67.6 ppm overlap when the Si concentration is increased, so that in the top spectrum (sample 55), only approximately one band with some shoulders can be seen in this region.

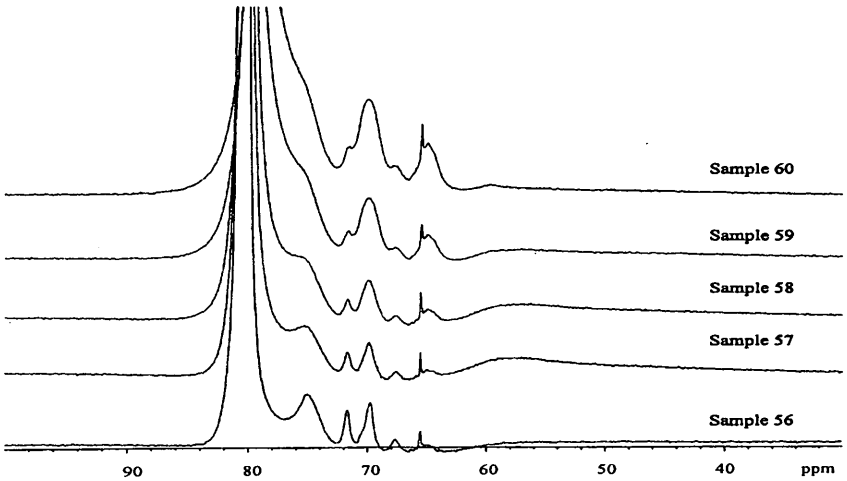

Figure 4.17. Stacked plot of high-resolution ^{27}Al NMR spectra at 130.2 MHz at ambient temperature (ca. 22°C) of tetramethylammonium aluminosilicate solutions (samples 56-60) with the compositions listed in tables 4.8. The spectra were taken one month after preparation. Spectrum conditions: Spectral width 25000.0 Hz. Acquisition time 0.081 s. Recycle delay 0.200 s. Pulse angle 29.9 degrees. Number of repetitions 16000. All spectra were obtained with the same processing, i.e. like setting backward linear prediction number 10, line broadening 10 and with absolute intensity mode and the same vertical scale.

4.2.5b. The effect of silicon concentration on the ^{27}Al NMR spectra for the aluminosilicate solutions at zero degrees:

Because the exchange of polymerisation might be affected in the spectra obtained at room temperature, this part of experiment has been done at 0°C. For this section three groups of aluminosilicate solutions, of which the composition data are listed in table 4.9, were prepared.

Table 4.9. Data for the groups of A, B, and C of aluminosilicate solutions.

Group	Sample No.	Molarity TMAOH	Molarity Si	Molarity Al ≡ Na atom	[Si]/[Al] ratio	[Si]/[TMAOH]
A	16	0.028	0.014	0.084	0.166	0.50
	18	0.112	0.056	0.084	0.666	0.50
	20	0.21	0.105	0.084	1.25	0.50
B	6	0.028	0.014	0.028	0.50	0.50
	8	0.112	0.056	0.028	2	0.50
	10	0.21	0.105	0.028	3.75	0.50
C	2	0.056	0.028	0.014	2	0.50
	4	0.168	0.084	0.014	6	0.50

The spectra of figure 4.17 (samples 16, 18 and 20), relating to the solutions of group A, show a big difference when the Si concentration is increased from 0.014 to 0.105 M at constant Al concentration of 0.084 M. The aluminosilicate species become more condensed, especially involving q^4 sites, which dominate in the last spectrum in contrast to the first one. In fact, in the spectra of sample 20 (figure 4.18) a large hump can be observed, which illustrates polymerised aluminosilicate species.

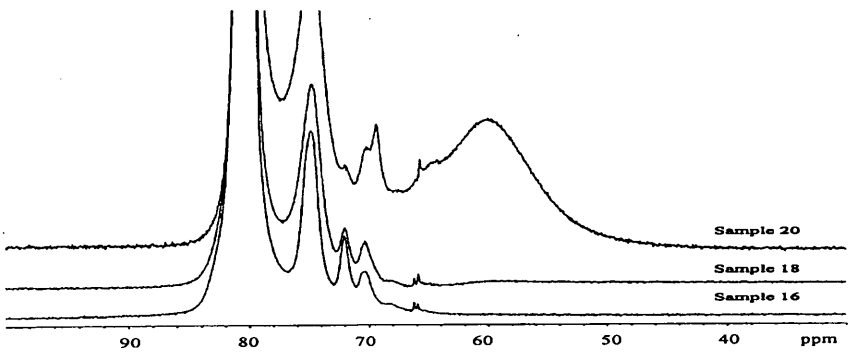

Figure 4.18. Stacked plot of high-resolution ^{27}Al NMR spectra at 156.3 MHz and zero degrees of tetramethylammonium aluminosilicate solutions (samples 16, 18 and 20) with the compositions listed in tables 4.9. The spectra were taken nine months after preparation. Spectrum conditions: Spectral width 50000.0 Hz. Acquisition time 0.205 s. Recycle delay 0.100 s. Pulse angle 192.9 degrees. Number of repetitions 45000 for sample 20, and 150000 for samples 18 and 16. All three spectra were obtained by the same processing procedure such as setting backward linear prediction number 15, line broadening not used but gaussian 0.003 used, and with absolute intensity mode and the same vertical scale.

Another point of interest in this spectrum concerns two peaks located at 66.2 and 65.9 ppm, for which the relative intensities change in the spectra from samples 16 to 20 in figure 4.18 i.e. gradually the peak located at 66.2 ppm decreases and eventually disappears in the last one. However, the other one remains at approximately the same intensity and is still a fairly narrow peak, easily observable. The peaks located in the range 68-73 ppm also alter, illustrating that some new species were formed. For example, in the spectrum of sample 16 the band centred on ca. 72.1 ppm appears strongly. Obviously, the distribution of the species in the aluminosilicate solutions strongly depends on the corresponding silicate species.

A similar result to that for group A can be concluded by looking at the features of the three spectra for samples 6, 8 and 10 (figure 4.19) belonging to group B, in which the Al concentration is held constant at 0.028 M, but the Si concentration is changed as for group A. Firstly, the band centred at ca. 60 ppm belonging to q^4 sites increases substantially in intensity, because the corresponding cage-like silicate species increase with increasing Si concentration. At the lowest concentration of Si (see the spectrum of sample 6 in figure 4.19), for the bands located at 64 - 67 ppm that are assigned to q^3 species, three distinct signals (one is very sharp and relatively intense and two are very small), can be observed. However, by increasing the silicate concentration, the corresponding signals appear as one band at the highest concentration of Si, see the spectrum of sample 10 in figure 4.19. The next point to make for these spectra concerns the two bands located at chemical shifts 68 and 71.9 ppm, which decrease with increasing Si concentration, so that in the spectrum of sample 10 in figure 4.19 these two peaks have disappeared. It may be suggested that these two bands probably belong to q^2 cyclic trimeric or cyclic tetrameric and probably q^3 cyclic trimeric species

respectively. This assignment may be confirmed with the parallels between ^{27}Al and ^{29}Si shifts in corresponding aluminosilicate and silicate species.[24] However, the energy of formation "three-membered rings" is significantly smaller for ^{27}Al than ^{29}Si. Therefore it may be thought that there is some pressure for ring opening of small cyclic species like the cyclic trimer, so that they are not very stable and in high concentration these species polymerise to other higher molecular-mass species.

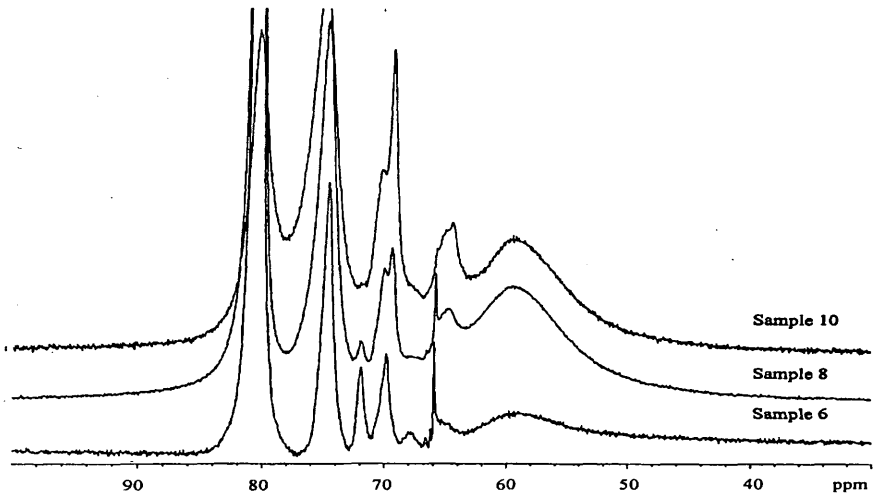

Figure 4.19. Stacked plot of high-resolution ^{27}Al NMR spectra at 156.3 MHz and zero degrees of tetramethylammonium aluminosilicate solutions (samples 6, 8 and 10) with the compositions listed in tables 4.9. The spectra were taken nine months after preparation. Spectrum conditions: Spectral width 50000 Hz. Acquisition time 0.205 s. Recycle delay 0.100 s. Pulse angle 192.9 degrees. Number of repetitions 50000 for sample 6, 150000 for sample 8 and 40256 for sample 10. All three spectra were obtained by the same processing procedure, such as setting backward linear prediction number 15, line broadening not used but gaussian 0.003, and with absolute intensity mode and the same vertical scale.

The band assigned to q^1 species also increases with increasing Si concentration, while conversely the q^0 band decreases. This can be expected, because in low concentration of Si, Q^0 is higher than the other species and vice versa. It should be expected that the reaction between q^0 and Q^0 is more difficult than those between q^0 and other species for charge-density reasons.

Thus, the reaction of $Al(OH)_4^-$, q^0, with different silicate species can occur at different rates. Moreover, re-equilibration among the silicate ions also shows a range of rates, depending on the species concerned.

Also, by considering the features of the spectra for samples 2 and 4 (figure 4.20) belonging to group C, similar results to those for groups A and B can be concluded. This is because, by increasing the Si concentration, the variety of some silicate species and therefore aluminosilicates is increased. Thus, in the range 62-72 ppm in the spectrum of sample 4 (figure 4.20) just two broad bands with some shoulders can be seen instead of the 6 signals for sample 2.

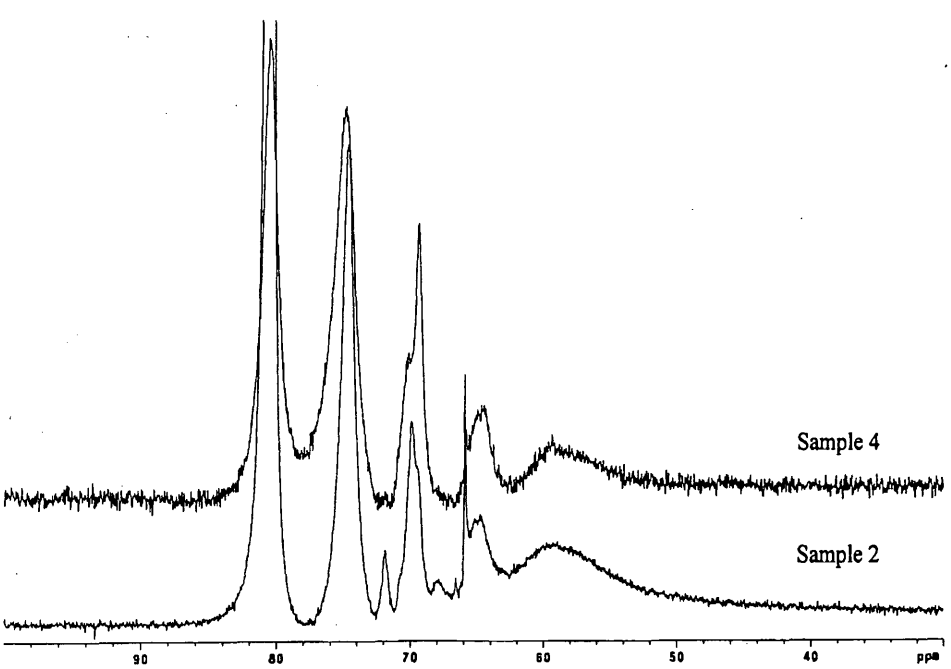

Figure 4.20. Stacked plot of high-resolution ^{27}Al NMR spectra at 156.3 MHz and zero degrees of tetramethylammonium aluminosilicate solutions (samples 2 and 4) with the compositions listed in tables 4.9. The spectra were taken nine months after preparation. Spectrum conditions: Spectral width 25000.0 Hz. Acquisition time 0.081s. Recycle delay 0.200 s. Pulse angle 29.9 degrees. Number of repetitions 45000 for sample 2 and 8192 for sample 4. The two spectra were obtained by the same processing procedure such as setting backward linear prediction number 15, line broadening not used but gaussian 0.003, and with absolute intensity mode and the same vertical scale.

4.2.6. Investigation of the siloxanisation process of the aluminate ion using the evolution with time of high-field aluminium-27 NMR spectra

The aim in this section is to provide some insight into the effects that aluminate/silicate replacement processes have on the appearance of ^{27}Al spectra, and to show how these effects may be exploited in assigning structures and determining reaction mechanisms. The aluminosilicate solution was made by adding TMAOH silicate solution to the freshly prepared sodium aluminate solution to achieve a Si/Al ratio of 4. To study the evolution of the spectra with time, two different protocols were used at a temperature of 21.5°C:

i) Recording ^{27}Al NMR spectrum soon after mixing the solutions (ca. 2 minutes).

ii) The spectra were recorded every 5 minutes for 5 hours with no interval between the spectra, and then continued for five hours accumulation (i.e. the first spectrum was obtained soon after mixing and the next one recorded, for 5 minutes each, without any interval of time between the spectra for the first 5 hours and then subsequently for five hours accumulation).

The ^{27}Al NMR spectrum immediately following mixing of sodium aluminate and TMAOH silicate solutions at 21.5°C is shown for sample 76 in figure 4.21. The peak at ca. δ_{Al} = 80 ppm may be assigned primarily to free aluminate, the value for aqueous sodium aluminate being 80.4 ppm (figure 4.4). However, peaks at 75.2, 69.9, ca. 65 ppm and a shoulder on the right-hand side of the last peak represent q^1, q^2, q^3 and q^4 environments respectively, which are clearly present very quickly after mixing.

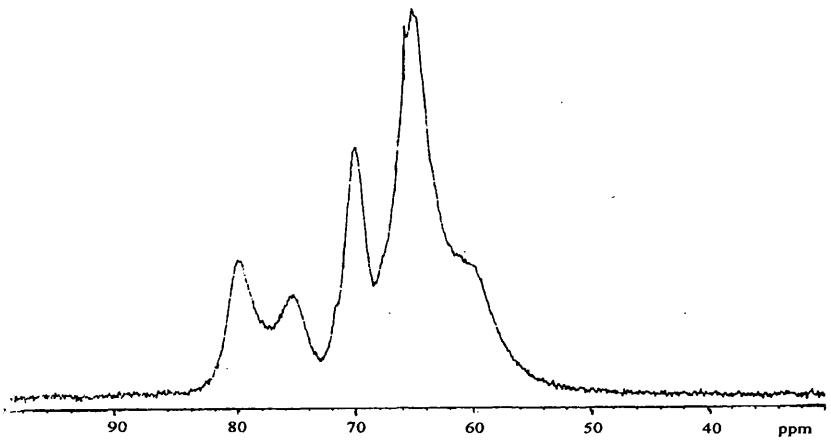

Figure 4.21. 130.23 MHz ^{27}Al spectrum of a tetramethylammonium aluminosilicate solution of composition 0.1 molar SiO_2 and Si/Al = 4 molar ratio (sample No. 76) taken at ambient temperature (ca. 22°C) soon after mixing the TMAOH silicate and aluminate solutions (ca. 2 minutes). Spectrometer conditions: Recycle delay 0.2 s. Acquisition time 0.081 s. Number of transients: ca. 900. Spectral width 25000 Hz. Pulse angle 29.9 degrees.

Figure 4.22 shows vertically and horizontally stacked plots for evolution of the aluminium-27 NMR spectra following the mixing of aluminate and silicate solutions (fresh solution with the same concentration as sample 76). The top or the end trace of figure 4.22 (index 60) displays the last of the spectra carried out in the time frame specified, while the bottom or the first one exhibits the first spectrum and the others show every fifth spectrum from indexes one to sixty. Each spectrum in this figure was accumulated for ca. five minutes (900 transients). At the end of this progressing time the sample was again measured, and subsequently for a total accumulation time of five hours (62180 transients) - see the spectra of fig. 4.23. The spectra were obtained in absolute intensity mode and all were recorded with the same format as for index one. Therefore, the peaks that are highest for the different times can be compared quantitatively. All spectra were carried out with backward linear prediction (or with background subtraction).

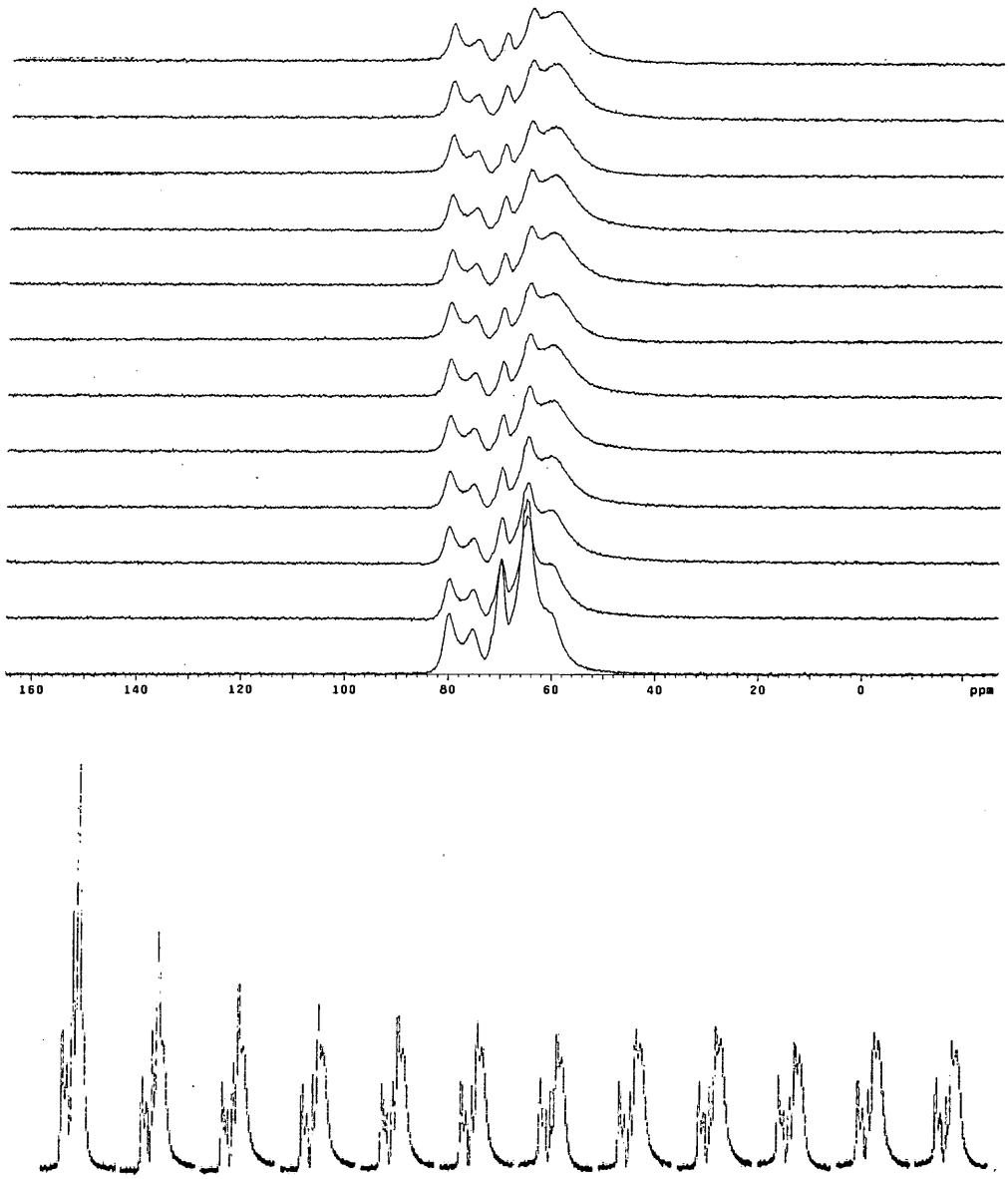

Figure 4.22. Stacked plot of 12 spectra from index one to 60 (every fifth spectrum) illustrating the time-dependence of the reaction between aluminate and silicate anions. The evolution with time of the 130.3 MHz ^{27}Al spectrum of an aluminosilicate solution prepared by rapid mixing of fresh sodium aluminate and aged TMAOH silicate solution, taken at ambient temperature and with a final composition 0.1 molar SiO_2 and Si/ Al = 4. Immediately following mixing, a sample of the solution was placed in a NMR spectrometer and the ^{27}Al spectrum measured as a function of time (i.e. the spectra were recorded every 5 minutes for each index with no interval between the spectra) at ambient temperature (see text). Spectrum conditions were as follows: Recycle delay 0.2 s. Acquisition time 0.081 s. Number of transients 900. Spectral width 25000.0 Hz. Pulse angle 29.9 degrees.

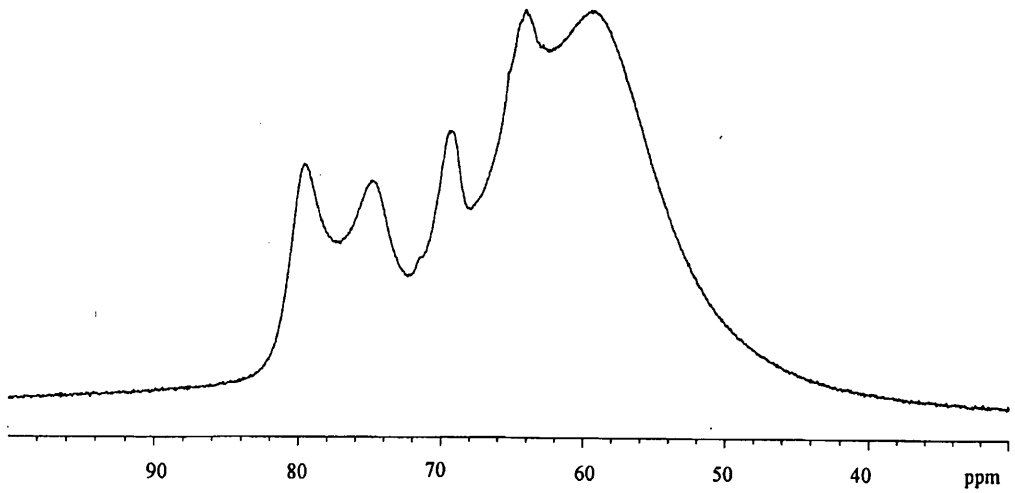

Figure 4.23 130.23 MHz ^{27}Al spectrum of a tetramethylammonium aluminosilicate solution of composition 0.1 molar SiO_2 and TMAOH and Si/Al = 4 molar ratio (sample No. 76) taken at ambient temperature ca. 22°C. Accumulation began 5 hours after mixing the TMAOH silicate and aluminate solutions with a total of 5 hours accumulation. Spectrometer conditions are as follows: Recycle delay 0.2 s. Acquisition time 0.081 s. Number of transients ca. 62180. Spectral width 25000 Hz. Pulse angle 29.9 degrees.

The spectra obtained during the evolution time imply that several things happen when the silicate and aluminate solutions are mixed. This evidence visualises the phenomena that occur soon after the mixing of solutions and proceed up to about 10 hours after mixing, which may be categorised as follows:

i) The intensity in the shoulder located at a shift of ca. 60 ppm increases, whilst the band at ca. 65 ppm decreases in intensity. This process is very slow and is not complete even 5 hours after mixing. The relative concentrations of aluminosilicate species present as q^1, q^2, q^3 and q^4 of structural units, which have been estimated from integrated intensities of the corresponding signals of deconvoluted spectra, are listed in table 4.10. It is pertinent to notice that figure 4.24 and the data in this table show that the intensity of q^4 (the band at lowest frequency) seems to increase as the mixing

time increases. However, the bands are not completely resolved.

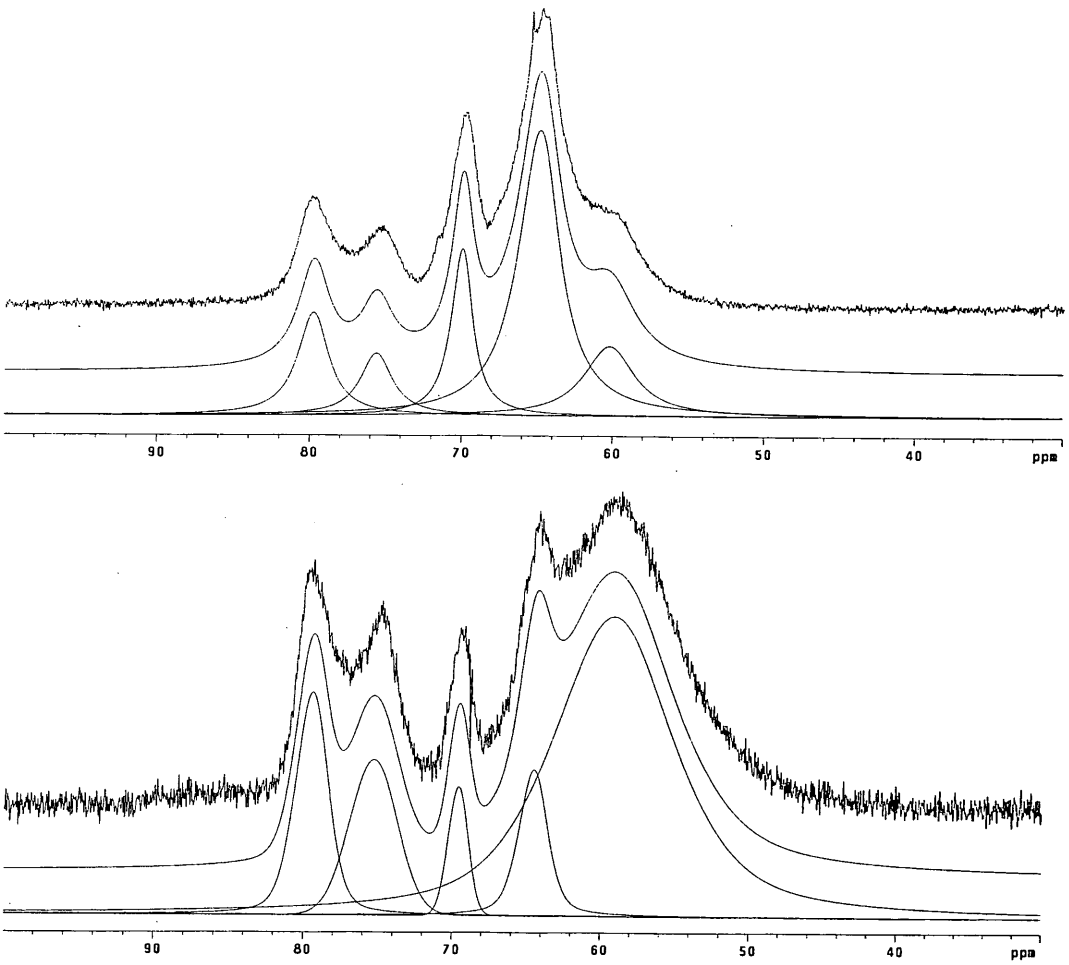

Figure 4.24. Simulation of the first and sixtieth index of figure 4.22. The top is the actual spectrum, the centre is the full fit, and the bottom is the individual component plot.

Table 4.10. Estimated mole % of aluminosilicate species structural units (q^n).

Accumulation time	**No. index**	**q^0**	**q^1%**	**q^2%**	**q^3%**	**q^4%**
Soon after mixing	1	13.2	8.4	14.8	48.8	14.8
After 5 hours	60	11.8	10.6	3.8	7.2	66.6

ii) Clearly, the distribution of Al changes progressively from small oligomeric aluminosilicate species towards the condensed ones, i.e. involving q^4, as time progresses.

By considering the development of the features of the aluminium-27 NMR spectra resulting from the evolution with time, one can imagine that the condensation of aluminosilicates does not necessarily occur step by step. In other words, forming different oligomers occurs at the same time. However, the q^2, q^3 and q^4 equilibrium needs time for completion. Indeed, this process can be expected, since, when the aluminate ions are introduced to the silicate solution, they are presented to a number of pre-existing silicate species,[35-38] for instance, monomer (Q^0), dimer (Q^1_2), cyclic trimer (Q^2_3), linear trimer ($Q^1Q^2Q^1$), prismatic hexamer (Q^3_6) and cubic octamer (Q^3_8). The silicate solution used for this particular experiment was made one week before it was utilised, and, since it was kept in an oven at 60°C, it is supposed that it had already reached equilibrium. Subsequently it is likely that the aluminate ions can react with a number of silicate species at the same time, though the mode of reaction is a matter of speculation. This suggests that aluminate anions react with silicate anions in different ways depending on the individual silicate species involved.

One should remember that, under full ionisation, the silicate species contain different negative charges as well as different molecular sizes. Consequently, the repulsion forces between aluminate anions and different silicate anions should not be the same. A schematic diagram for the reaction of aluminate ions with silicate ions is as follows:

It is supposed that the aluminate ions (q^0) can react with the various silicate sites (Q^n) simultaneously, and produce different aluminosilicate sites (q^n).

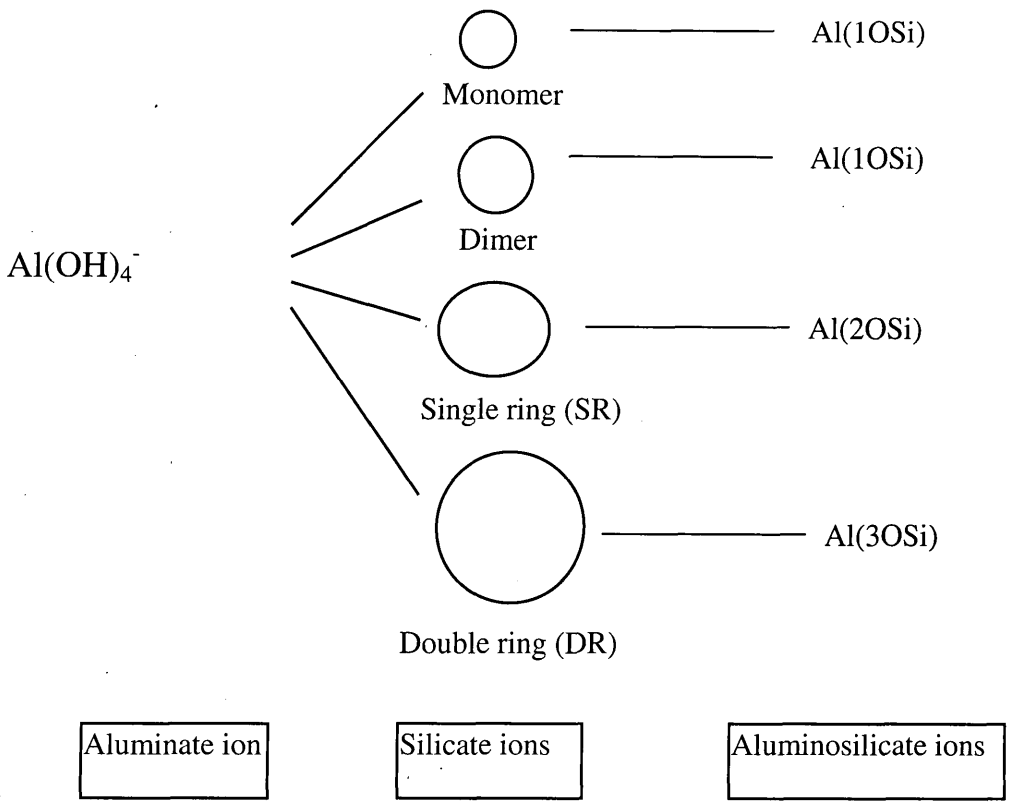

A question arising from the aluminium-27 NMR spectra obtained as a function of time after mixing silicate and aluminate solutions is why the aluminate ions should react to some extent to give large silicate species immediately after mixing (observation of peaks for q^2, q^3 and probably q^4 immediately after mixing), whereas other processes occur much more slowly. The answer is, obviously, reaction of $Al(OH)_4^-$, q^0, with different silicate species can occur at different rates, which is discussed in more detail in section 4.2.4.

4.2.7. Dilution effects and Thermodynamic Equilibrium or Approach to Thermodynamic Equilibrium of the Aluminosilicate Anions in Aqueous Tetramethylammonium Aluminosilicate Solutions:

Aqueous alkaline silicate solutions are known to contain a variety of low molecular weight silicate anions in dynamic equilibrium.[39,40] In early studies it was widely believed that concentrated solutions required many days for their constituents to reach thermodynamic equilibrium following a perturbation, such as dilution or a change of pH.[41] Lagerstrom [42] in 1959 demonstrated that this notion is only correct for solutions that were in, or had passed through, an 'instability range', characterised by an alkali to silica ratio low enough to allow colloidal silica to exist. Equilibrium is attained 'very rapidly' for solutions whose composition places them outside this range. Several workers [43] have since confirmed his findings. Dent-Glasser and Lachowski,[44] using trimethylsilylation followed by chromatographic separation, showed that sodium silicate solutions had returned to equilibrium within five minutes of being diluted, or undergoing a change in pH. Furthermore, Harris *et al.*[37] have used ^{29}Si NMR spectroscopy to demonstrate that a very concentrated (7M) sodium silicate solution reaches equilibrium within the time (1h) taken to record its spectrum and, moreover, that the effects of heating a silicate solution are entirely reversible, again within the time required to record the spectrum. However, by using tetramethylammonium silicate solutions, Knight [45] showed it required many days to re-establish thermodynamic equilibrium following a perturbation, as monitored by ^{29}Si NMR Spectroscopy. This subject has been considered using ^{27}Al NMR, in two parts, A and B, involving two solutions with Si/Al mole ratios one and three respectively.

A). The dilution effect and dynamic equilibrium were considered for the aluminosilicate solution with concentrations of Si, Al, and TMAOH equal to 0.014, 0.028 and 0.014 M respectively (sample 33-A). After measuring this solution with ^{27}Al NMR at ambient temperature (ca. 295 °K), it was diluted 2 and 4 times with distilled water and measured again soon after dilution, see figures 4.25-7 (samples 33-a, 33-b and 33-c). The features of the corresponding spectra changed considerably from figures 4.25 to 4.27. These spectra illustrate that different aluminosilicate species exist in the aluminosilicate solutions.

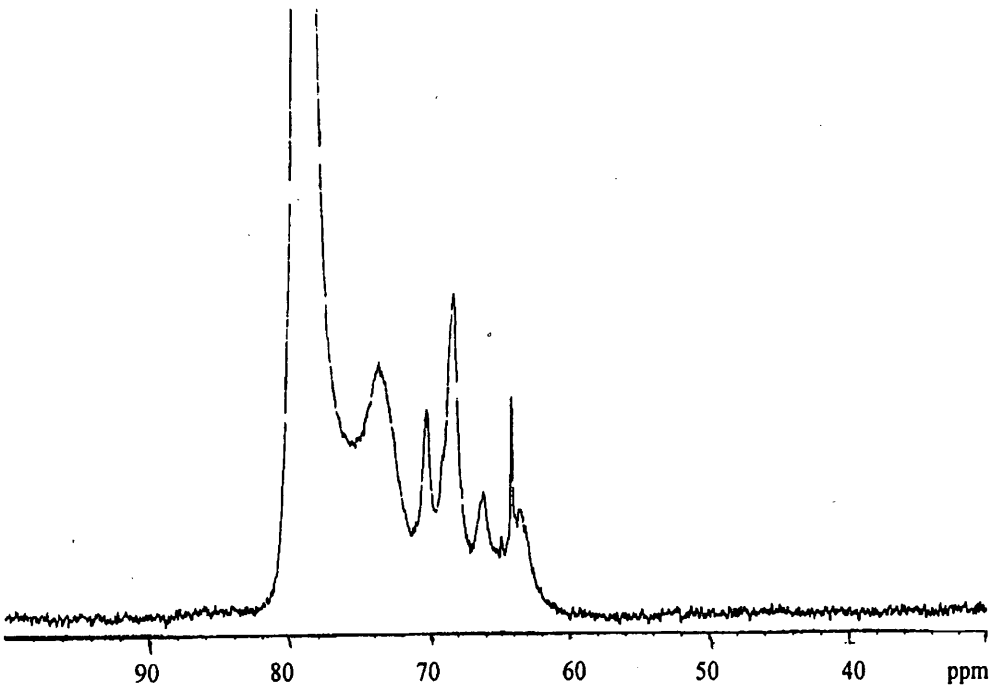

Figure 4.25. High-resolution ^{27}Al NMR spectrum at 130.23 MHz and ambient temperature (22 °C) of a tetramethylammonium aluminosilicate solution with the concentrations Si, Al and TMAOH equal to 0.014, 0.014 and 0.028 molar respectively i.e. [Si/Al] = 1 (sample 33-a). The spectrum was taken one week after preparation. Spectrum conditions: Recycle delay 0.100 s. Acquisition time 0.1 s. Spectral width 51981.8 Hz. Pulse duration 22.0 μs. Number of repetitions 1000

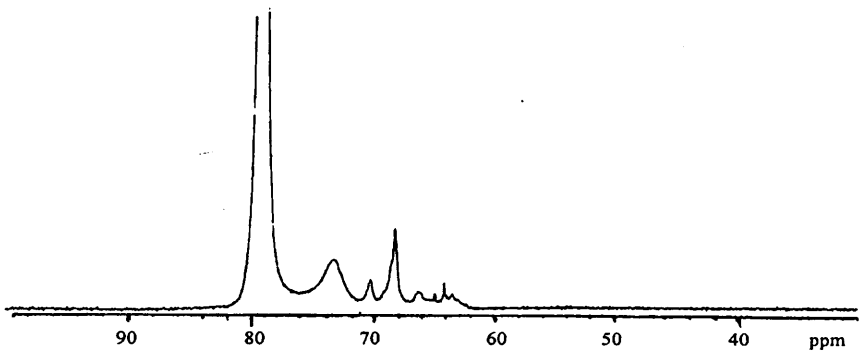

Figure 4.26. High-resolution ^{27}Al NMR spectrum at 130.23 MHz and ambient temperature of a tetramethylammonium aluminosilicate solution with the concentration of Si, Al and TMAOH equal to 0.007, 0.007 and 0.014 molar respectively i.e. [Si/Al] = 1 (sample 33-b). The spectrum was taken soon after preparation (i.e. after diluting sample No. 33-a). Spectrum conditions: Recycle delay 0.100 s. Acquisition time 0.1 s. Spectral width 51981.8 Hz. Pulse duration 22.0 μs. Number of repetitions 12864.

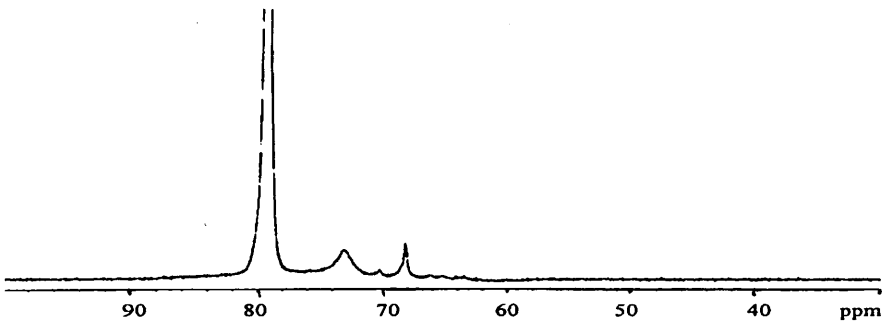

Figure 4.27. High-resolution ^{27}Al NMR spectrum at 130.23 MHz and ambient temperature of a tetramethylammonium aluminosilicate solution with the concentration mposition Si, Al and TMAOH equal to 0.0035, 0.0035 and 0.007 molar respectively i.e. [Si/Al] = 1 (sample 33-c). The spectrum index one was taken soon after preparation (i.e. after dilution of sample 33-b). Spectrum conditions: Recycle delay 0.100 s. Acquisition time 0.1 s. Spectral width: 51981.8 Hz. Pulse duration 22.0 μs. Number of repetitions 17252

To study the evolution of the spectra with time, two different protocols were used at a temperature ca. 22 °C: 1) Recording the ^{27}Al NMR spectrum soon after dilution for the solutions 33-b and 33-c. 2) For the sample 33-c the spectra were recorded successively for ca. 15 hours, see figure 4.28 which shows vertically and horizontally stacked plots of evolution of the ^{27}Al NMR spectra following the dilution. Thus the first spectrum was obtained soon after dilution and the following ones recorded for half an hour

accumulation each with a half-hour interval between the spectra. The figure shows 1-15 for every second spectrum.

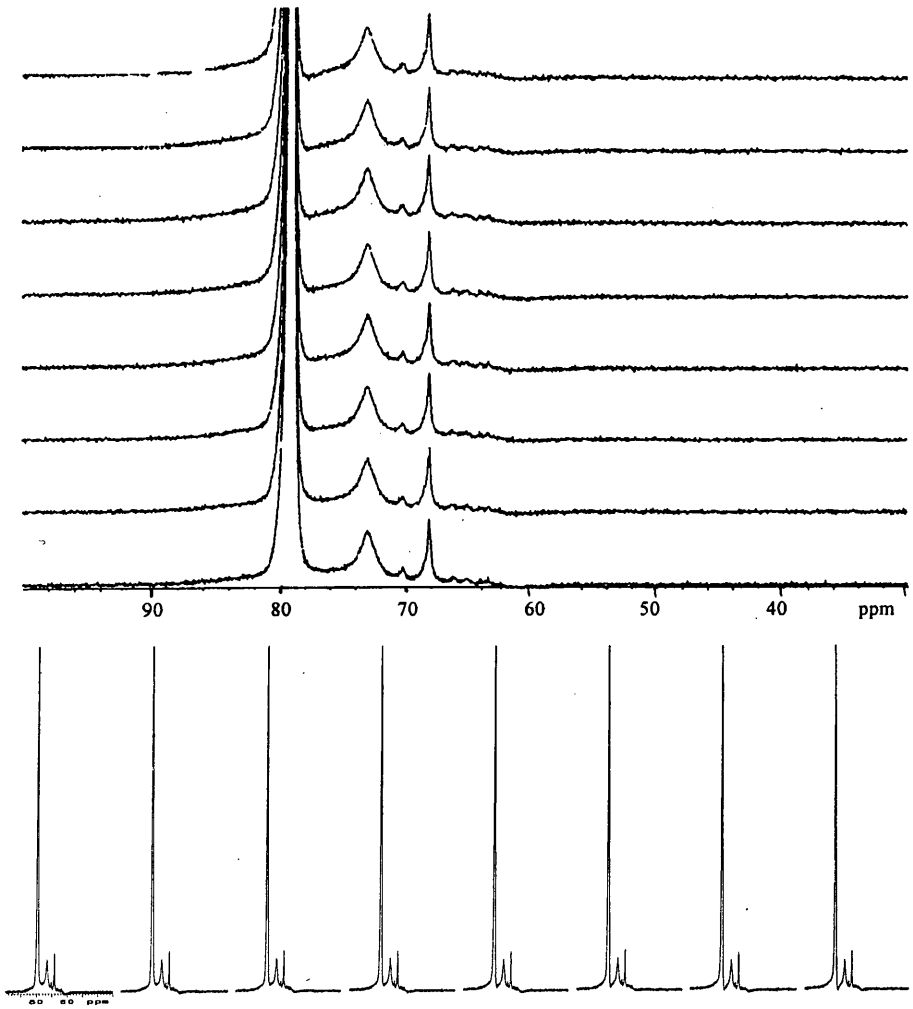

Figure 4.28. Stacked plot to illustrate the time-dependence of the reaction between aluminate and silicate anions. The evolution with time of the 130.3 MHz ^{27}Al spectrum of an aluminosilicate solution prepared by dilution of sample 33-b, taken at ambient temperature and with a final composition 0.0035 molar SiO_2 and 0.007 molar TMAOH and [Si/Al]=1. Immediately following dilution, a sample of the solution was placed in a NMR spectrometer and the ^{27}Al spectrum measured as a function of time at ambient temperature. The bottom trace or the first trace (index 1) was measured soon after mixing, i.e. about 5 minutes after preparation and the top one or the end one (index 15) was measured after 840 minutes. Every second spectrum is displayed. Spectra were taken under the same conditions separated by half an hour time interval. Spectrum conditions, were as follows: Recycle delay 0.1 s. Acquisition time 0.1 s. Number of transients 17252. Spectral width 51981.8 Hz. Pulse angle 29.9 degrees.

Samples of the same compositions as 33-b and 33-c were also measured four days after preparation (see spectra figures 4.29a and b). It is pertinent to notice that the spectra for dilute solutions measured four days after preparation show no change with respect to the spectra that were measured soon after dilution, except in the chemical shift positions of signals which might arise from a reference error. It can be concluded that dilute aqueous solutions of aluminosilicates equilibrate rapidly to a mixture of anionic species. Therefore, the solutions reached equilibrium after about five minutes. However, the situation is complicated because of the sensitivity of the equilibria to concentration, pH and temperature.

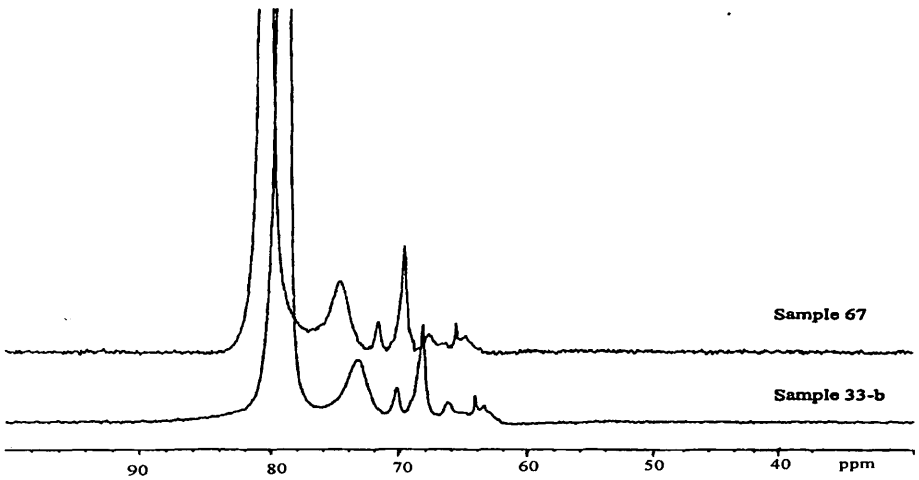

Figure 4.29a. Stacked plot of high-resolution ^{27}Al NMR spectra at 130.2 MHz at ambient temperature (ca. 22°C) for tetramethylammonium aluminosilicate solutions samples (33-b and 67) with the concentrations of Si, Al and TMAOH equal to 0.007, 0.007 and 0.014 M. The spectra were taken a) soon after the preparation of sample 33-b, and b) four days after the preparation of sample 67. Spectrum conditions: Spectral width 25000.0 Hz. Acquisition time 0.081 s. Recycle delay 0.200 s. Pulse angle 29.9 degrees. Number of repetitions 8000 for sample 67 and 12864 for sample 33-b. Spectra were obtained using the same processing procedure, such as setting backward linear prediction number 12, line broadening 5, and with absolute intensity mode and the same vertical scale.

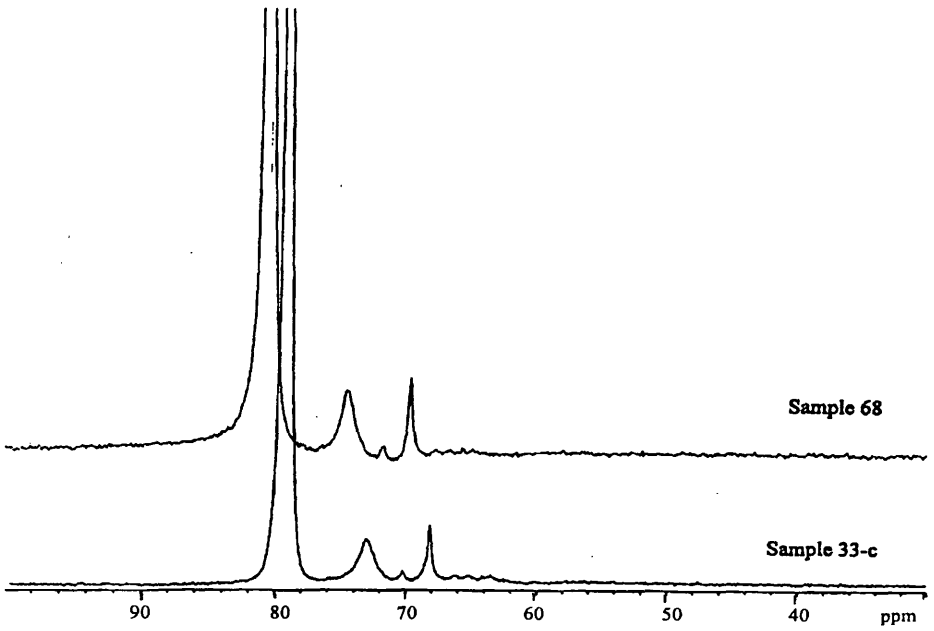

Figure 4.29b. Stacked plot of high-resolution ^{27}Al NMR spectra at 130.2 MHz at ambient temperature (ca. 22°C) of tetramethylammonium aluminosilicate solutions samples 33-c and 68 with the concentrations Si, Al and TMAOH equal to 0.0035, 0.0035 and 0.007 M. The spectra were taken a) soon after preparation (sample 33-c) and b) four days after preparation (sample 67). Spectrum conditions: Spectral width 25000.0 Hz. Acquisition time 0.081 s. Recycle delay 0.200 s. Pulse angle 29.9 degrees. Number of repetitions 8000 for sample 68 and 17252 for sample 33-c. Spectra were obtained using the same processing procedure, such as setting backward linear prediction number 12, line broadening 5, and with absolute intensity mode and the same vertical scale.

The above conclusion implies that little happens when dilute aluminosilicate solutions are aged. This is contrary to the observation of time evolution for spectra of more concentrated solutions discussed in section 4.2.6 (figure 4.22) for sample 76. However, by looking in more detail at the spectra we can observe some changes with dilution in bands located in the low-frequency region. For instance, in the shift range 62 to 68 ppm in figure 4.25 (sample 33-a) at least four bands can be seen, but the spectrum of sample 33-b in figure 4.26 shows these signals at low intensity and in the last one i.e. figure 4.27 (sample 33-c) all these peaks almost disappeared.

The signals assigned to q^0 and q^1 in the spectrum shown in figure 4.25 (sample 33-a, highest concentration) are significantly broadened by exchange (especially q^1), though they are not coalesced, but in spectrum figure 4.27 (sample 33-c) these two signals seem to be sharp and completely separated. Thus in low concentration the exchange rate between these two signals is slower than for higher concentration, presumably because of the lowering of the pH. By looking in more detail at the spectra, one can also observe some changes in the bands located at about 70 and 68 ppm. The broadening of these two peaks changes slightly (though the chemical shift does not change) so that the overlapping of the bands diminishes with dilution.

B). The dilution effect one month after preparation for aluminosilicate solutions with concentrations of Si between 0.042 to 0.42 M, and constånt Si/Al and Si/TMAOH ratios equal to 3 and 2 respectively (samples 61-66), was also considered. The compositions are listed in table 4.11 and the corresponding spectra are shown in figure 4.30 (samples 61-65).

Table 4.11. Data for aluminosilicate solutions with the Si/Al=3.

Sample No.	Molarity TMAOH	Molarity Si	Molarity Al ≡ Na atom	[Si]/[Al] ratio	[Si]/[TMAOH]
61	0.084	0.042	0.014	3	0.5
62	0.168	0.084	0.028	3	0.5
63	0.336	0.168	0.056	3	0.5
64	0.504	0.252	0.084	3	0.5
65	0.672	0.336	0.112	3	0.5
66	0.840	0.42	0.140	3	0.5

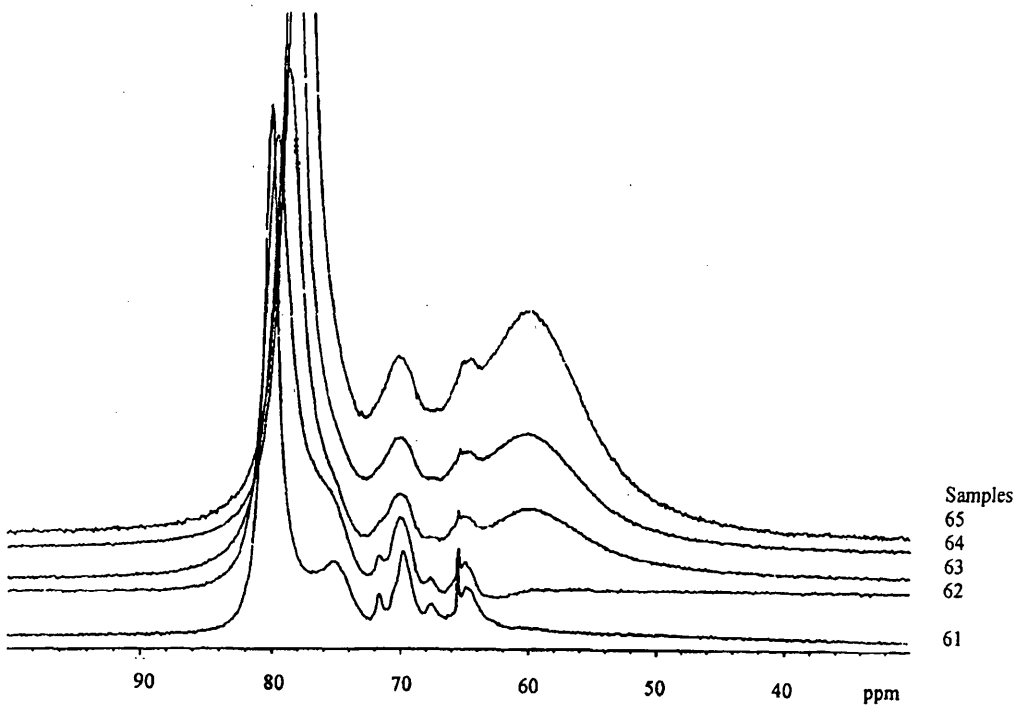

Figure 4.30. Stacked plot of high-resolution ^{27}Al NMR spectra at 130.23 MHz and ambient temperature ca. 295 °C of tetramethylammonium aluminosilicate solutions (samples 61-65) with the compositions listed in table 4.11. The spectra were taken one month after preparation. Spectrum conditions: Spectral width 25000 Hz. Acquisition time 0.081 s. Recycle delay 0.2 s. Pulse angle 29.9 degrees. Number of repetitions 8000. All spectra were obtained with the same processing procedures such as setting backward linear prediction number 10, line broadening 10, and with absolute intensity mode and the same vertical scale.

In the spectrum of figure 4.31 from the most concentrated solution, i.e. sample 66, one can observe only 4 distinct peaks, assigned to q^0-q^1, q^2, q^3 and q^4, located at ca. 77.9, 70.2, 64.4 and 60.6 ppm respectively. By dilution of this sample, some characteristic changes occur, which can be seen in the features of the other spectra. The band at highest frequency is located at 77.9 ppm in figure 4.31, which is not the correct position for q^0 or q^1 so that it can be said that the q^0 and q^1 peaks are fully coalesced. This is confirmed with the spectra that were obtained from dilution of this sample. A shoulder appears at the right hand side of the highest-frequency peak, and finally a

separate q^1 band may be seen; i.e. the spectrum from the most dilute solution shows two resolved peaks located at 80.1 and 75.3 ppm, assigned to q^0 and q^1 species respectively (see figure 4.30). It can be concluded that the exchange rate between the q^0 and q^1 species for the most concentrated solution, sample 66, is high, so that a single coalesced peak is observed located at 77.9 ppm (between the shift ranges of q^0 and q^1). In more dilute solutions the exchange rate between q^0 and q^1 decreases and NMR can detect the two signals separately. Also the spectra of sample 61 in figure 4.30 shows two bands located at chemical shifts 71.6 and 69.8 ppm for the most dilute solution. However, with increasing concentration the corresponding species exchange rapidly, so that in the spectra of sample 63-66 (figures 4.30 and 4.31), one can observe just one band at a shift of ca. 70.2 ppm. Similarly the bands located in the shift range of 64 to 68 ppm coalesce with increasing concentration so that, finally, only one band centred at ca. 65 ppm can be seen. However, these results might be viscosity-affected rather than a result of exchange.

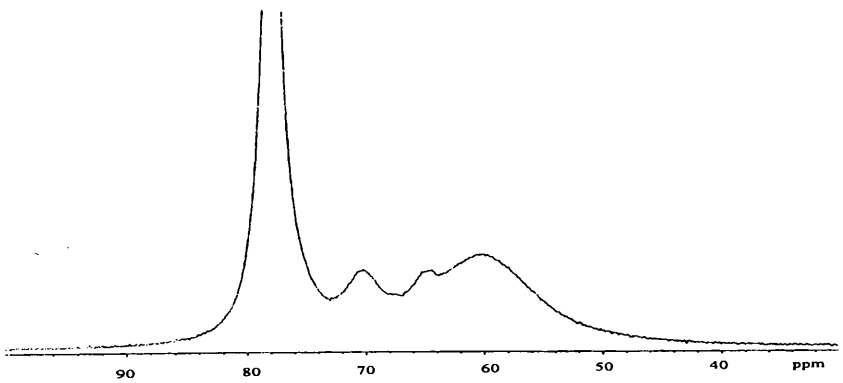

Figure 4.31. High-resolution ^{27}Al NMR spectrum at 130.23 MHz and ambient temperature of a tetramethylammonium aluminosilicate solution with the concentrations Si, Al and TMAOH equal to 0.42, 0.14 and 0.84 molar respectively, i.e. [Si/Al] = 3 (sample 66). The spectrum was taken one month after preparation. Spectrum conditions: Recycle delay 0.200 s. Acquisition time 0.081 s. Spectral width 25000 Hz. Pulse angle 29.9 degrees. Number of repetitions 8000. BLP=10 and lb=10

The other point worth noticing is that the band located at the lowest frequency (i.e. about 61 ppm), assigned to q^4, gradually decreased in intensity with dilution and finally disappeared in the last spectrum, i.e. that for the most dilute sample 61 (figure 4.30). This is expected because in highly concentrated solutions oligomerisation of species can readily occur. In other words dilution of the solution leads to deoligomerisation.

4.2.8. Study of aluminum-27 NMR spectroscopy at variable temperature

There are many chemical processes that occur at rates that are comparable with the appropriate chemical shift differences. This can lead to exchange broadening, which, depending on the circumstances, may be a difficulty to be tolerated or may be highly informative. The condition for slow exchange on the NMR timescale between two species is, in effect, that the exchange rate must be slower than the difference in NMR absorption frequency between the two sites. If the difference in frequencies expressed in hertz is $\Delta\nu$, then the transition from slow to fast exchange takes place when

$$k_{ex} = \pi\Delta\nu\sqrt{2} = 2.22\Delta\nu \qquad (4.6)$$

For chemical exchange processes occurring at rates comparable with the appropriate chemical shift differences, the spectrum at low temperature will be at the slow-exchange limit, and at high temperature it will be in the fast-exchange limit. The temperature at which the lines just merge is the coalescence temperature, T_c. The following section explores in detail the interesting question of the behaviour of the exchange processes among the aluminosilicate species at variable temperature.

Figure 4.32 illustrates ^{27}Al NMR spectra taken at progressively higher temperatures for TMAOH aluminosilicate solutions with SiO_2/Al_2O_3 molar

ratio 5, prepared from TMAOH silicate solution with Si/TMAOH=0.875 and sodium aluminate. These solutions were made two weeks before recording the spectra (to complete the reaction of the aluminate and silicate and subsequently to achieve an equilibrium state). Spectra were recorded over the range 0 to 70 °C, at specific temperatures 0, 20, 25, 50, 60 and 70 °C (uncalibrated). For each temperature, a sufficient time was allowed to elapse for a new equilibrium state to be reached. It is well known that, if a solution containing quadrupolar nuclei (i.e. aluminium-27) is heated then the rate of quadrupole relaxation is decreased and consequently broad resonances will tend to sharpen. In spite of that, no significantly better resolution was obtained by increasing the temperature, probably because the rates of exchange increase with increasing temperature.

The spectra in figure 4.32 reveal that significant changes happened for the ^{27}Al NMR spectra recorded in the range of 0 to 70 °C. The spectrum recorded at 0 °C shows at least 4 bands (i.e. ca. 75.5, 69.5, 64.5, and 58.5 ppm) but when the temperature is raised some bands coalesce due to exchange between some species. Raising the temperature caused more rapid exchange among the aluminosilicate species, so that at the highest temperature, i. e. 70 °C (bottom spectrum) the bands in the range of 66 - 77 ppm are nearly coalesced. This trend can be attributed to an exchange of Al between environments in which Al is bonded to one and two OSi groups. In other words the spectrum recorded at 70 °C shows a nearly exchange-coalesced peak due to the q^1 and q^2 anions, i.e. the corresponding aluminosilicate species undergo rapid chemical exchange. As the temperature increases from 0 °C, the q^3 peak shifts to high frequency slightly, probably as a result of incipient exchange.

It should be noted that the peaks belonging to the q^3 and q^4 ions are relatively well-resolved at all accessible temperatures. Accordingly, it can be concluded that q^3, which for example can be ascribed to the cubic octamer with one or two aluminium sites, i.e. $Q^3_8(1Al)$ or $Q^3_8(2Al)$, is relatively stable on the NMR timescale even at high temperature.

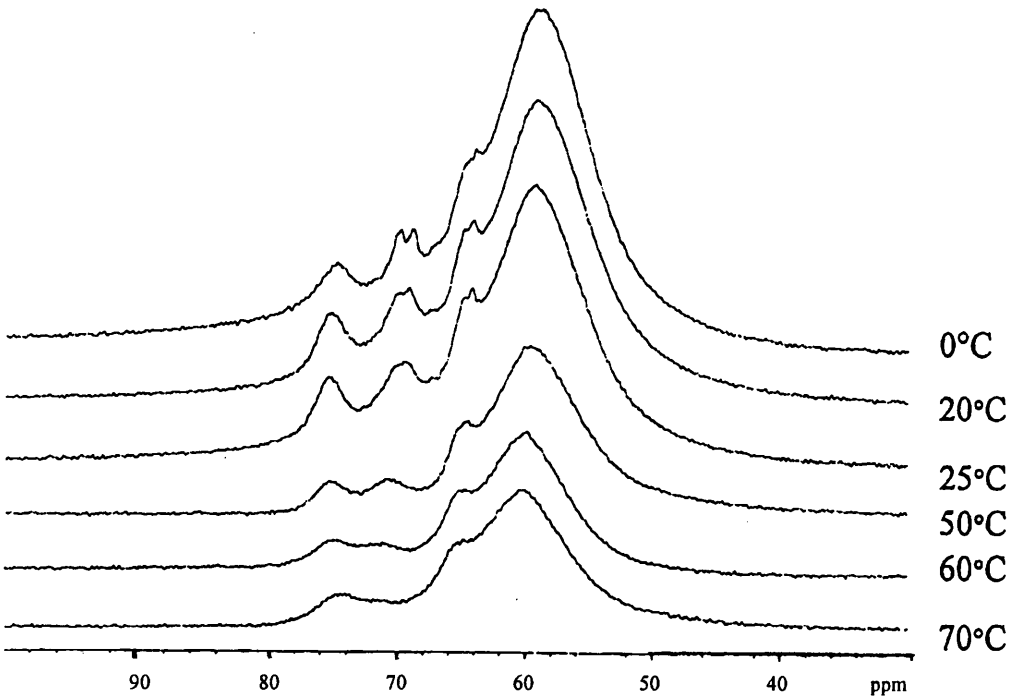

Figure 4.32. High-resolution ^{27}Al NMR spectra at 156.3 MHz of TMAOH aluminosilicate solution of the composition one molar TMAOH, 0.875 molar SiO_2, and Si/Al ratio = 5 at 0 °C. The spectra were taken two weeks after mixing. Spectrum conditions: Spectral width 29996 Hz. Acquisition time 0.02 s. Recycle delay 0.100 s. Pulse angle 158.8° (34 μs). Number of transients 2048.

4.3. Conclusions

High-resolution solution-state ^{27}Al NMR has given considerable insight into the structure and distribution of aluminate anions present in aqueous silicate solutions. The different types of q^n units present in an aluminosilicate solution can be assigned from the corresponding shift ranges, and their relative distributions can be quantitatively determined from

the signal intensities. The ^{27}Al chemical shift of a given q^n aluminium is further affected by the type of the next-nearest and possibly second nearest q^n units connected to it, and also by chain length, cyclisation and steric effects. Detailed information on several specific topics has been obtained from the ^{27}Al NMR studies of aluminosilicate solutions, which may be summarised as follows. TMA aluminosilicate solutions are characterised by an equilibrium distribution of coexisting aluminosilicate species with increasing degrees of polymerisation ranging from monomer silicate to 'colloidal' particles. With increasing TMAOH/Si and/or increasing concentration of silica, the equilibrium is shifted to more highly polymerised species, and vice versa. The existence of stable aluminosilicate anions in aqueous solutions has been positively proved by ^{27}Al NMR. The results summarised above demonstrate that ^{27}Al NMR can provide valuable information on the structure and distribution of anions in aluminosilicate solutions and on the reactions and transformations of the anionic species caused by various chemical and physical treatments of the solutions. Information of this type is of considerable interest, especially for a deeper understanding of the process of zeolite formation from mixtures of silicate and aluminate solutions. Increasing activity in this field is therefore to be expected in the near future.

The formation of aluminosilicate anions is evident in the NMR spectra of the solutions, by the appearance of distinct signals in the range 50-80 ppm. From this study one can also conclude that the distribution of species in aluminosilicate solutions depends on the Si concentration as well as the Si to Al mole ratio in dilute TMAOH silicate solutions. In dilute solutions (below ca. 0.1 M) a considerable amount of aluminium as $[Al(OH)_4]^-$ remains in solution, in other words not much reaction between silicate and

aluminate species takes place under these conditions. In spite of this, there are several aluminosilicate species, which could be observed in ^{27}Al NMR spectra. These species are concluded to contain groups q^0, q^1, q^2, q^3 and q^4. However, the q^0 species is dominant. Therefore, when dilute Si concentration TMAOH silicate solutions are mixed with aluminate solutions, remarkable variations in the ^{27}Al NMR spectra are observed, indicating structural reorganisation of the initial aluminate species and the formation of aluminosilicate anions. However, in the condensed Si solutions (more than ca. 0.8 M) the q^0 signal completely disappears, and q^4 appears as the dominant species, whereas some of the other species were not revealed. Variation of Al concentration does not give rise to significant differences in the spectra for two sets of Si solutions (i.e. diluted or condensed); in both it merely changed the intensities of signals.

These studies clearly demonstrate that ^{27}Al NMR can contribute greatly to the knowledge of the complex nature of aqueous aluminosilicate solutions owing to two fundamental features of the spectra: (i) characteristic and mostly well-separated signals for the AlO_4 groups in different structural surroundings may be observed (i.e. the exchange rate between the species is slow on the NMR time scale), and (ii) from the signal intensities the relative concentrations of the different structural entities can be estimated. Therefore, detailed information on the structure and the quantitative distribution of the various building groups and aluminosilicate species present in the solutions may be obtained.

The observed spectra at different temperatures illustrate that at higher temperatures rapid exchange occurs among some of the species.

4.4. References

1. R.M. Barrer, The Hydrothermal Chemistry of Zeolites, Academic Press, London (1982).
2. R.M. Barrer, *Chem. Brit.* 380 (1966).
3. F. Roozeboom, H. E. Robson, and S. S. Chan, *Zeolites* **3**, 321 (1983).
4. R. M. Barrer, and W. J. Sieber, *Chem. Soc., Dalton Trans*, 1020 (1977).
5. E. G. Derouane, S. Dettermmerie, Z. Gabelica, and N. Blom, *Appl. Catal.* **1**, 201 (1981).
6. R. K. Harris and C. T. G. Knight, *J. Chem. Soc., Faraday Trans.* 2, **79**, 1539 (1983).
7. J. L. Guth, P. Caullet, and R. Wey, *Bull. Soc. Chim. Fr.* 1758 (1974).
8. J. L. Guth, P. Caullet, and R. Wey, *Bull. Soc. Chim. Fr.* 2362 (1974).
9. J. L. Guth, P. Caullet, P. Jacques, and R. Wey, *Bull. Soc. Chim. Fr.* **1**, 121 (1980).
10. S. Ueda, N. Kageyama, and M. Koizumi, *Proc. 6th Int. Zeolite Con. Reno, Nevada, Butterworths,* 905 (1984).
11. P. Wengin, S. Ueda, and M. Kozumi, *Proc. 7th Int. Zeolite Conf., Tokyo, Kodansha, Elsevier,* 177 (1986).
12. S. Kasahara, K. Itabashi, and K. Igawa, *Proc. 7th Int. Zeolite Conf., Tokyo, Kodansha, Elsevier,* 185 (1986).
13. A. V. McCormick, A. T. Bell, and C. J Radke, *Proc. 7th Int. Zeolite Conf., Tokyo, Kodansha, Elsevier,* 247 (1986).
14. D. Muller, D. Hoebbel, and W.Gessner, *Chem. Phys. Letts.*, **84**, 25 (1984).
15. D. Hoebbel, G. Garzo, K. Ujszazi, G. Engelhardt, B. Fahlke, and A. Vargha, *Z. Anorg. Allg. Chem.*, **484**, 7 (1982).

16. G. Engelhardt, D. Hoebble, M. Tarmak, A. Samoson, and E. Lippmaa, *Z. Anorg. Allg. Chem.*, **484**, 22 (1982).

17. R. K. Harris, A. Samadi-Maybodi, and W. Smith, *Zeolite* **19**, 147 (1997).

18. R. K. Harris, J. Parkinson, A. Samadi-Maybodi, and W. Smith, *J. Chem. Soc.,Chem. Comm.* 593 (1996).

19. D. Muller, W. Gessner, A. Samoson, E. Lippmaa, and G. Scheler, *J. Chem. Soc., Dalton Trans.* 1277 (1986).

20. L. S. Dent-Glasser, and G. Harvey, *Proceeding of the sixth International Zeolite Conference,*; Eds. D. Olson, A. Bision, Butterworths: London, 925 (1984).

21. S. D. Kinrade, and T. W. Swaddle, *J. Inorg. Chem.* **27**, 4253-4259 (1988)

22. R. F. Mortlock, A. T. Bell and C. J. Radke, *J. Phys. Chem.* **95**, 7847 (1991)

23. R. F. Mortlock, A. T. Bell and C. J. Radke, *J. Phys. Chem.* **95**, 372 (1991)

24. A. Samadi-Maybodi, S. N. Azizi, H. Naderi-Manesh, H. Bijanzadeh, I. H. McKeag and R. K. Harris, *J. Chem. Soc., Dalton Trans.*, 633-638 (2001) and references therein.

25. Ph.D. Thesis of A. Samadi-Maybodi, "*NMR studies of silicate and aluminosilicate solution as precursors for zeolites*", University of Durham (1996)

26. D. Hoebbel, G. Garzo, K. Ujszaszi, G. Engelhardt, B. Fahlke, B. and A. Vargha, Z.*Anorg. Allg. Chem.*, **484**, 7 (1982).

27. L. F. Gladden, T. A. Carpenter, J. Klinowski and R. S. Elliott, *J. Magn. Reson., 66, 93 (1986)*.

28. D. Muller, W. Gessner, A. Samoson, E. Lippmaa, and G. Scheler, *J. Chem. Soc. , Dalton Trans.*, *1277* (1986)

29. A. G. Ferige, and J. C. Lindon, *J. Magn. Reson.* **31**, *337* (1978).

30. S. D. Kinrade, and T. W. Swaddle, *J. Inorg. Chem.* **28**, 1952 (1989).

31. A. Samadi-Maybodi. R. K. Harris and W.Smith, *Zeolites* 19, 147 (1997).

32. G. Engelhardt, and D. Michel, "*High-resolution solid-state NMR of silicates and zeolites*", Wiley , New York, (1987).

33. S. D. Kinrade, C. T. Knight, D. L. Pole and R.T. Syvitski, *Inorg. Chem.* **37**, 4272 (1998).

34. R. K. Harris, A. Samadi-Maybodi and J. Parkinson, *J. Chem. Soc., Dalton Trans.* 2533 (1997)

35. R. K. Harris, C. T. G. Knight, and W.E. Hull, *J. Am. Chem. Soc.* **103**, 1577 (1981).

36. R.K. Harris, and R.H. Newman, *J. Chem. Soc., Faraday Trans.* **73**, 1204 (1977).

37. R. K. Harris, J. Jones, C. T. G. Knight, and R. H. Newman, *J. Mol. Liq.* **29**, 63 (1984).

38. C. T. G. Knight, R. J. Kirkpatrick, and E. Oldfield, *J. Am. Chem. Soc.* **109**, 1632 (1987).

39. R. K. Iler, The Chemistry of Silica,' Wiley, New York, (1979).

40. 'Soluble Silicates,' ed. J. S. Falcone, *American Chemistry Society* Symposium Series, vol. 194. (1982).

41. J. G. Vail, 'Soluble Silicates,' Reinhold, New York, vol. 1, p. 98. (1952)

42. G. Lagerstrom, *Acta Chem. Scand.*, **13**, 722 (1959).

43. N. Ingri, *Acta Chem. Scand.* **13**, 758 (1959); T. L. O'Connor, *J. Phys. Chem.,* 65, 1 (1961); J. F. Haze, *J. Colloid. Sci.*, **17**, 162 (1962); A. J. Walker and N. Whitehead, *J. Appl. Chem.*, **16**, 230 (1966); W. Stumm, H. Huper, and R. L. Champlin, *Environ. Sci. Technol.*, **1**, 221 (1967).

44. L. S. Dent-Glasser and E. E. Lachowski, *J. Chem. Soc., Dalton Trans.,* 393 (1980)

45. C. T. G. Knight, R. J. Kirkpatrick, and E. Oldfield. *J. Chem . Soc., Chem. Comm.,* (1986).

Chapter Five

Aluminium-27 NMR spectra of aluminosilicate solutions as a function of pH, with linewidth and T_1 measurements.

5.1. Introduction

The objective of the work of the present chapter was to exploit the relative stability of aluminosilicate species to exchange in order to ascertain if more detailed structural information could be obtained. As part of this work a careful study of the effect of lowering the pH was carried out. This resulted in the appearance of the highly-resolved spectra which are the subject of this chapter. In order to further understand the nature of the solutions, spin-lattice relaxation times, linewidths and relative intensities of the highly resolved ^{27}Al spectrum for a pH ~10.35 solution have been measured.

For practical expediency, as discussed earlier, the solutions investigated contain both sodium and tetramethylammonium counter-ions, since the method of preparation was to mix aqueous tetraalkylammonium silicate solutions with aqueous sodium aluminate solutions.

Thus, the first highly-resolved ^{27}Al NMR spectra of alkaline aluminosilicate solutions are presented and discussed. The linewidths and numbers of resolved lines are shown to depend critically on several factors, especially the pH and Si:Al ratio. At least thirteen separate peaks or bands are observed at pH ~10.35 and Si:Al = 1. A substantial range of anionic species, comparable to those found for alkaline silicate solutions, is thus shown to exist in dynamic equilibrium. Tentative assignments of some bands are presented, based on ^{27}Al and ^{29}Si shift comparability, ^{27}Al linewidths and ^{27}Al spin-lattice relaxation measurements. Relative intensities of the various ^{27}Al signals are given for the pH ~10.35 solution.

5.2. Theoretical aspects of the effect of pH on the equilibrium distribution of silicate and aluminosilicate species.

Previous work and the present study show that the distribution of silicate and aluminosilicate anions in TAA and alkali metal silicate and aluminosilicate solutions is a function of Si and Al concentrations, pH, temperature and cation type. For a given cation, the degree of oligomerisation increases with increasing silicate and aluminate to cation ratios and with temperature. This trend has been observed in all of the previous studies of alkali metal and TAA aluminosilicate solutions. The pH effect and the influence of silicate cation ratio can be readily explained by considering the effects of hydroxyl ion concentration on the equilibrium distribution of silicate and aluminosilicate species. For example, the formation of dimer silicate anions from monomeric anions (and similarly for aluminosilicate formation) can be represented by the three equilibria below and can be interpreted in the manner described by Bell and co-workers:[1]

$$M^- + H_2O \longleftrightarrow M + OH^- \quad (1)$$

$$M + M^- \longleftrightarrow D^- + H_2O \quad (2)$$

$$D^- + H_2O \longleftrightarrow D + OH^- \quad (3)$$

Here M^- and D^- refer to the anionic silicate monomer and dimer, whilst M and D indicate the neutral silicate monomer and dimer, respectively. It is apparent that dimer formation or aluminosilicate formation will increase as the pH decreases. Notice that the results of the preceding examples are in agreement with predictions based on Le Chatelier's* principle, increasing the concentrations of reactants and decreasing the

*. Le Chatelier's principle states that a system in equilibrium reacts to a stress in a way that counteracts the stress and establishes a new equilibrium state.

concentrations of products (here OH^-) with addition of HCl, would be expected to increase the deriving force of the reaction to the right. Also, because of repulsion effects, it will be easier for M or D than negatively charged M^- and D^- ions to approach negatively charged groups. Therefore, aluminosilicate formation will increase through the following equations as the pH decreases

$$Q^0+q^0 \Leftrightarrow q^1\text{-}Q^1 \qquad (4)$$

$$Q^1{}_2+q^0 \Leftrightarrow Q^1\text{-}Q^2\text{-}q^1 \text{ or } (Q^2\text{-}Q^2\text{-}q^2)_\Delta \qquad (5)$$

Reactions similar to those shown above can be written to represent higher levels of oligomerisation in silicate or aluminosilicate formation. From these it can be generalised that the degree of oligomerisation or polymerisation of silicate or aluminosilicate species increases with decreasing pH. This phenomenon is examined in the present work using lowering of the pH by addition of HCl or by decreasing the TMAOH concentration in certain aluminosilicate solutions.

5.3. Experimental

Samples were prepared as generally discussed in chapter 2. The initial TMA silicate solution prepared in this way contained 0.7 molar SiO_2 and 1.4 molar amine hydroxide. The molarities of SiO_2, AlO_2^- and Na^+ in the aluminosilicate solutions are equal, with TMA^+ at twice this concentration.

Solutions with lowered pH were prepared by adding concentrated HCl solution dropwise down to pH = 11.8, then with addition of 1M HCl solution to reach lower pH values. The quantities used were such that there is only a small change in the concentrations of Si, Al, TMA and Na (estimated to be a decrease of ca. 1% between pH 12.78 and pH 10.35). Measurement of pH was carried out using a PHM92 LAB PHMETER (Radiometer,

Copenhagen) and a PHC 2015 combined pH electrode, suitable for monitoring pH in the range 0 to 14. The pH values reported are those measured within 5 minutes of sample preparation. At pH < ca. 10.5, when significant coagulation may be occurring as a function of time,[2-5] with turbidity and even precipitation being seen, the pH will clearly change as the samples age. At very low pH (< 4), the solutions again become clear to the eye, although the silica content is in excess of the solubility.[6]

The ^{27}Al NMR spectra at variable pH were obtained using the Varian Inova 500 spectrometer at 130.23 MHz and ca. 22°C. Proton decoupling was employed, though this was not strictly necessary. Typically, 90° pulses of duration 10.7 μs were used, with acquisition times of 180 ms and recycle delays of 20 ms for the variable pH experiments. The probe used for these experiments involved components containing aluminium, so that, as discussed earlier, a broad background signal centred at δ_{Al} ~60 ppm (the same region as the q^4 peak) could be observed. Backward linear prediction for the first 12 points of the FID was used. Whereas this gave spectra of good apparent quality, making many aspects of interpretation easier, it did result in uncertainties regarding the extent of the true q^4 signal from the aluminosilicate solution. Moreover, phasing the spectra was not easy because the background signal invariably had a different phase from those of the peaks arising from the solution. There are further complications affecting the q^4 region because of the presence in the sample (in increasing quantities as the pH is lowered to neutral values, but to unknown extents) of condensed particles, in extreme cases giving rise to gels or even precipitates (see chapter 7). Such particles presumably give very broad signals, which are difficult or impossible to detect in high-resolution spectra, giving rise to the

phenomenon of "invisible aluminium".[7] The signals actually observed at pH values in the range 9-5 represent only a very small fraction of the aluminium content of the samples.

To find the spin-lattice relaxation times of species in aluminosilicate solutions, a TMAOH aluminosilicate solution with the composition TMAOH and Si=Al=Na equal to 0.056 and 0.028 M respectively was prepared as described in chapter 2. Sensitivity enhancement was used for the T_1 measurements, which employed the optimum resolution of ^{27}Al signals for aluminosilicate species (e.g. by avoiding exchange effects). The pH was optimised at pH ca. 10.35 with HCl (figure 5.2).

Spin-lattice relaxation times for the pH 10.35 solution were measured by the inversion-recovery method, using a total of 11 delays for relaxation. However, because the q^0 peak dominates the spectrum (and has the longest relaxation time), it was not feasible to use the full number of points for most peaks. Moreover, peak overlap and S/N considerations, together with the requirement to compensate for the probe background, make determination of T_1 problematic. Four approaches were used: (a) baseline estimation by eye, followed by peak height measurements,* (b) baseline estimation by eye, followed by measurement of both peak height and peak width, the product being used as a crude measure of total intensity,* (c) measurement of τ_{null} and evaluation of T_1 from the equation $\tau_{null}=T_1 ln2$ *or* $T_1=1.44\ \tau_{null}$, and (d) use of the standard software associated with the spectrometer. The values of T_1 reported here are best estimates from a combination of the four methods.

The deconvolution of a spectrum for pH = 10.35 acquired over a long period (ca. 15 hours and plotted with no line broadening) was undertaken in

* Plotting $ln[H_0-H_t]$ and $ln[I_0-I_t]$ against the recovery interval, the *slope* of the lines giving T_1

four sections (76.7–72.7, 72.8–68.5 and 68.8–62.0, plus the q^0 peak separately), with normalisation of intensities to a common scale. Deconvolution proceeded by initial choice of observed frequencies for 3, 4 and 5 peaks in the three complex sections respectively.

It did not prove feasible to record ^{29}Si spectra, at natural isotopic abundance, of the solutions because of the low concentrations and the low natural abundance of ^{29}Si. However, a few spectra were obtained with samples enriched in ^{29}Si, the Varian Inova 500 spectrometer again being used (at a ^{29}Si frequency of 99.29 MHz). These samples were prepared using silica enriched to 99.35%, obtained from Cambridge Isotope Laboratories, Inc.

5.4. Results and discussion

5.4.1. Introduction

A typical ^{27}Al spectrum of an as-prepared solution with Si:Al ratio of 1 is shown in Figure 5.1(a). The solution contains total Si and Al concentrations equal to 0.028 M, with a TMAOH concentration of 0.056 M. The Na content equals that of Al. The pH was measured as 12.78. The spectrum is not dissimilar to that illustrated in Figure 2 of reference 8, except that it has been cosmetically improved (e.g. by backward linear prediction). Several features are immediately apparent:

1. The majority of the Al gives rise to the peak at a chemical shift δ_{Al} = 80.3 ppm, which may be confidently assigned to the isolated aluminate species $[Al(OH)_4]^-$ or one of its more highly ionised forms, i.e. to q^0.
2. The peak at δ_{Al} = 75.4 ppm, assigned to "end-groups" (q^1), is relatively broad, which may be attributed to incipient exchange with

q^0 (see ref. 8). The exchange effect has been confirmed by a spectrum run at lowered temperature (ca. 0°C), which showed no such broadening.

3. There are a number of peaks at lower frequency, which cannot be simply related to q^2, q^3 and q^4 in the manner assumed for solutions with higher Si:Al ratios.[8] Signals at δ_{Al} = 71.7 and 67.7 ppm occur between the values expected for q^1 and q^2 and q^2 and q^3 respectively.
4. Moreover, there is a surprisingly sharp signal at δ_{Al} = 65.6 ppm. In fact this can be seen in figure 2 of ref. 8, but was not commented on at the time.

5.4.2. pH variation

Figure 5.1(b-e) shows what happens to the spectra as the pH is lowered. The first effect is that the q^0 and q^1 peaks become sharper, and the latter splits into two and then into three. This change may be attributed to the slowing of chemical exchange in the system, thus further confirming the origin of some line broadening at pH 12.78, as well as a redistribution among the species present.

At the same time further peaks appear in the lower frequency range, perhaps partly because of the slowing of exchange, but also arising from variations in the range and intensity of species present. The optimum resolution and number of peaks are observed at a pH of approximately 10.3. In fact, in addition to the intense q^0 peak and a broad signal at δ_{Al} = ca. 60 ppm (attributed to various q^4 environments, possibly including some coagulated material, but difficult to distinguish from the probe background), at least 12 peaks can be clearly seen. For the purposes of discussion, the peak numbers shown on Figure 5.2 for a pH = 10.35 solution will be used.

This is the first time such high-resolution ^{27}Al spectra have been obtained for aluminosilicate solutions. The three q^1 peaks change their relative intensities as the pH is lowered further. Moreover the total intensity in the spectrum decreases markedly as the pH is lowered below 9.5. It is obvious that the spectrum is not properly reflecting the presence of larger oligomers, condensed species and even insoluble material. At pH ~8.6 only three relatively sharp signals can be seen (in the q^0, q^1 and q^2 regions), plus a broad intense band centred at δ_{Al} = ca. 64 ppm. Presumably this is because the majority of the aluminium is in relatively large particles - the sample is very turbid. In view of this fact and because of the backward linear prediction which was applied, quantitative conclusions regarding q^4 species cannot be made for any of the spectra. As the pH is lowered still further, the three sharp peaks decrease in intensity. The q^2 peak is not observed below pH ~8.4 and the other two signals are lost below pH ~7.4, only the broad band at δ_{Al} ~57 ppm remaining. Aluminosilicate hydrosol precipitates give rise[4] to a broad ^{27}Al band under magic-angle spinning conditions at slightly lower chemical shifts (δ_{Al} = 53.0 ppm), but the additional shielding may arise from second-order quadrupolar effects. Of course, the existence of q^4 sites implies the presence of cations (or hydrogen) in the structure. At pH ~5 a signal appears at δ_{Al} ~1 ppm, which sharpens and strengthens as the pH is lowered further. This may be confidently assigned to the $[Al(H_2O)_6]^{3+}$ species, resulting from the amphoteric nature of aluminium oxide. At this pH silica is almost insoluble (~150 ppm), and it may be assumed that the medium contains relatively large particles of silica, though the medium is clear to the eye. In actual fact even in the alkaline range, as the pH is reduced from 12.78 the solutions remain clear to the eye only down to pH =

ca. 10.4, whereas light-scattering measurements indicate some condensation. The sample chosen for further detailed study, at pH = 10.35, was on the verge of showing turbidity.

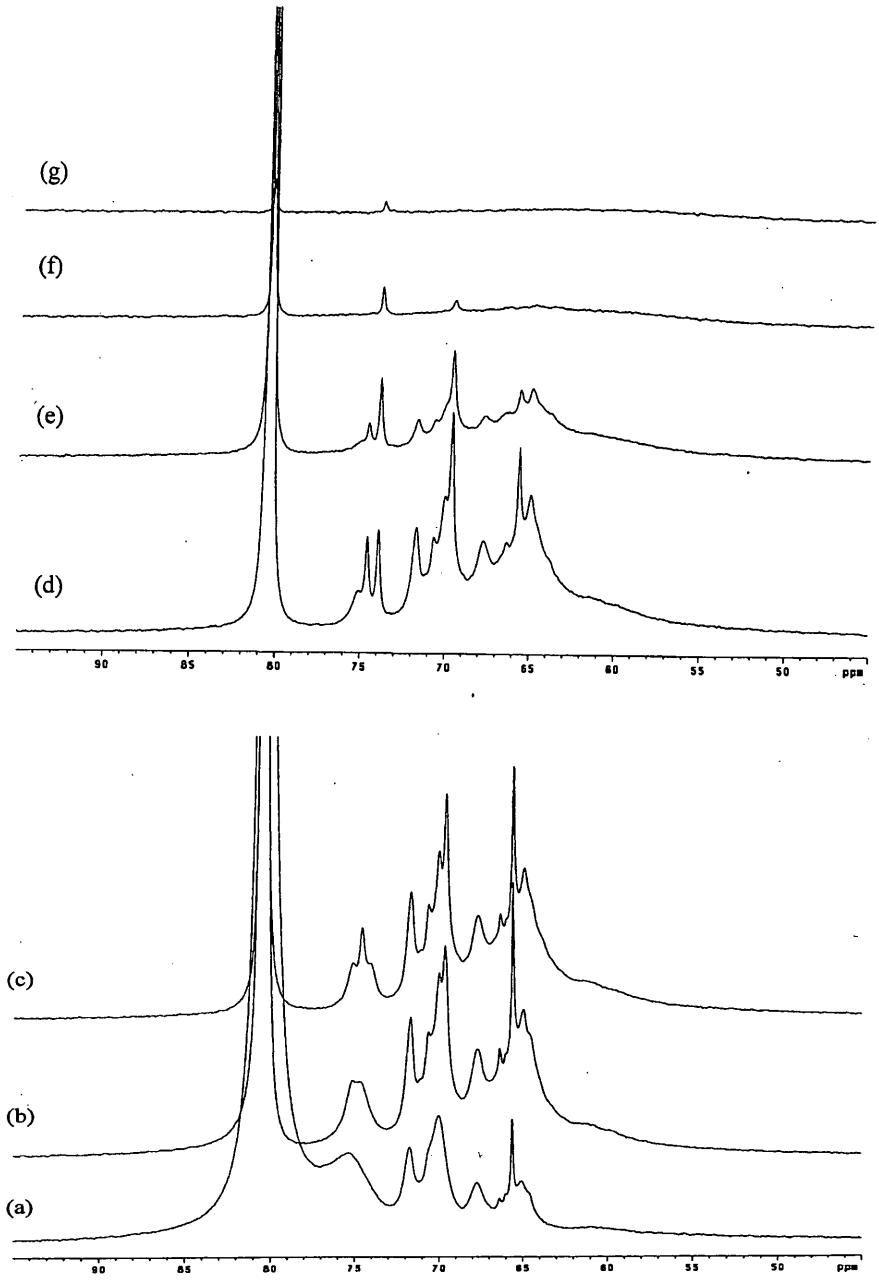

Figure 5.1. Aluminium-27 NMR spectra at 130.23 MHz and ambient probe temperature of an aluminosilicate solution (see the text) as a function of pH: (a) pH = 12.78, (b) 11.80, (c) 10.88, (d) 9.9, (e) 9.5, (f) 8.9, (g) 8.15.

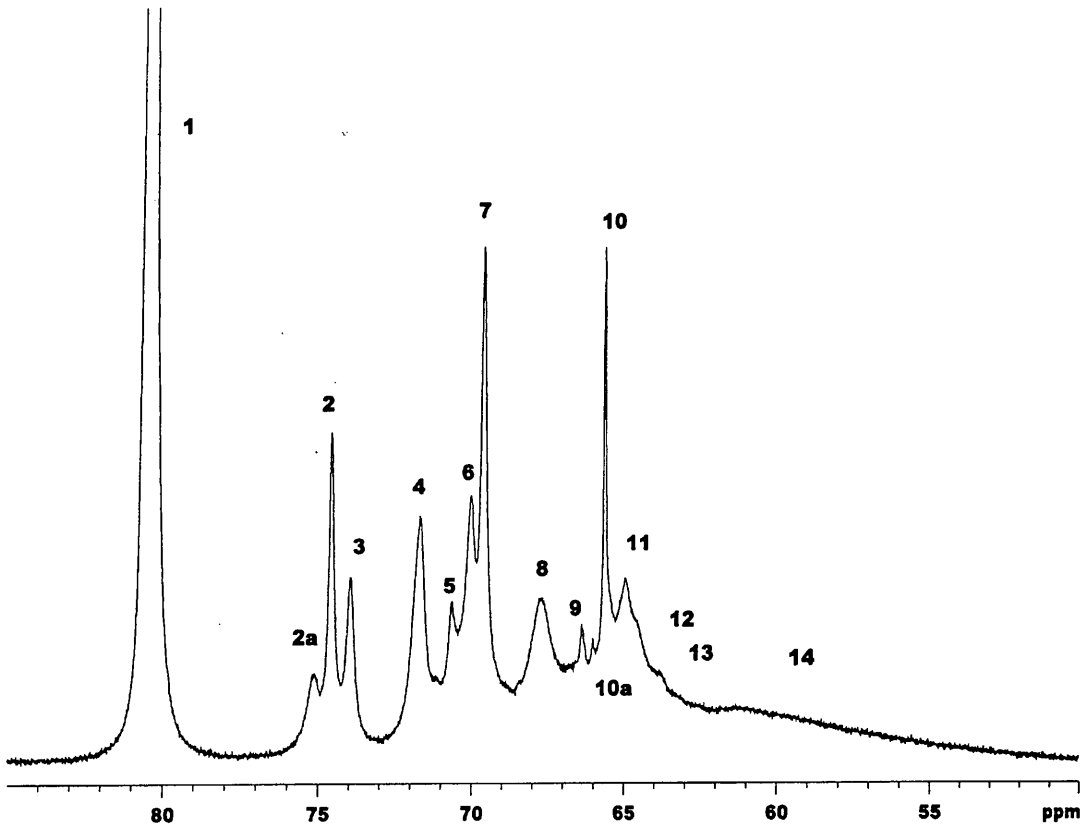

Figure 5.2. Aluminium-27 NMR spectra of an aluminosilicate solution (as in Figure 5.1) at pH = 10.35, accumulated over 14.8 hours. The peak numbers used in the text are marked.

5.4.3. Assignments

Assignment of the peaks in the spectra is difficult, in spite of the high natural abundance of ^{27}Al, since no coupling information is available. Hydroxyl protons on aluminosilicate species are in rapid exchange with water and it is not feasible to observe splittings arising from ^{29}Si, ^{27}Al coupling, both because of the low natural abundance of ^{29}Si and (more particularly, since ^{29}Si could be isotopically enriched) because the ^{27}Al linewidths would obscure the relatively small splittings expected. During this work ^{29}Si spectra for aluminosilicate solutions have been examined, but even for higher concentrations and Si:Al ratios it is not feasible to observe

peaks which could be confidently assigned to aluminosilicate species - presumably because these are in relatively low concentration and the resonances would be broadened by the influence of neighbouring ^{27}Al. For the present solution conditions no ^{29}Si signals could be detected for samples with ^{29}Si in natural abundance (see also refs. 9 and 10). However, a ^{29}Si spectrum was obtained for a 0.028 M silicate solution with Si:TMAOH = 1:2 and isotopic enrichment of ^{29}Si to 99.35%. The pH was ca. 12.8. Three sharp peaks corresponding[11] to species Q^0, Q_2^1 (the "dimer") and Q_3^2 (the "cyclic trimer") were observed, with decreasing intensity in that order, confirming earlier work. The Q_3^2 signal disappeared when the pH was lowered to ~10.4. When sodium aluminate was added, the Q^0 and Q_2^1 signals broadened substantially ($\Delta\nu_{1/2}$ for Q^0 becoming ca. 0.8 ppm), so that the S/N after 10 hr accumulation was only ca. 2:1 for the latter. No new signals were seen. Finally, ^{27}Al, ^{27}Al coupling is unlikely to be observable, both because of the linewidths in the spectra and because the coupling constants are probably small. It is expected that Loewenstein's rule will be obeyed, so that no Al-O-Al bridges will be present. Certainly, pure aqueous sodium aluminate solutions show ^{27}Al spectra which indicate that nothing other than simple mononuclear anions $(Al(OH)_4^-$ or its deprotonated forms at high pH and $[Al(H_2O)_6]^{3+}$ at low pH) is present at any pH. However, the existence of species with Al-O-Al bridges cannot be ruled out. Under certain conditions polymeric aluminate species exist as gels, but the broad ^{27}Al signal in the region for tetraco-ordinate environments is[12,13] at δ_{Al} = ca. 71 ppm (a substantially higher chemical shift than that of our "q^4" band), although the sharp central tetrahedral signal for the Keggin ion is[12] at δ_{Al} = 62.6 ppm.

Some hints for assignments can come by analogy with ^{29}Si spectra of aqueous alkaline silicate solutions, which have been studied under a variety of conditions (including ^{29}Si enrichment). Indeed, this link has already been assumed in the literature, starting with the original article by Mueller et al.[14] who designated broad bands as arising from q^0, q^1, q^2, q^3 and q^4 environments. In the case of ^{29}Si spectra, signals at unusual positions, between either the ranges for Q^1 and Q^2 signals or the regions for Q^2 and Q^3 may arise from two causes:[11] (a) the existence of "three-membered" $(SiO)_3$ rings, a decrease in the SiOSi or OSiO bond angles producing a well-attested shift to high frequency, or (b) the presence of unusual specific cage structures, also giving rise to deshielding, but to a smaller extent than (a). Whereas the positions of peaks 4 (δ_{Al} = 71.7 ppm) and 8 (δ_{Al} = 67.7 ppm) in our ^{27}Al spectra would appear to be more in tune with (b) than (a), the intensities seem rather high for this origin, and we believe, for other reasons as well (see below) that these signals arise from q^2 and q^3 sites in species with "three-membered" rings.

The three signals in the q^1 range are almost certainly due to individual species. The relative intensities of the peaks at 74.6 and 74.0 ppm change with pH, the former being the larger at pH $\geq$ 10.1 but the latter being the more important below this range. At pH < 9.0 only the line at 74.0 ppm can be observed. One of these peaks presumably arises from q^1Q^1 (II), and the most likely assignment (by comparison with the corresponding ^{29}Si case) is that it is the one remaining at relatively low pH, i.e. δ_{Al} = 74.0 ppm. The other probably arises from the linear trimer $q^1Q^2Q^1$ (III). As some confirmation of this possible assignment it may be noted that in ^{29}Si spectra for the corresponding purely silicate species the Q^1 peak for the linear trimer

occurs [11] 0.44 ppm to high frequency of that for the dimer in aqueous KOH solution. However, it is not clear why linear trimeric aluminosilicate ions should be more abundant than dimers at pH ~11. An alternative assignment for the peak at δ_{Al} = 74.6 ppm is to the substituted cyclic trimer IV, since the corresponding pure silicate species in aqueous KOH solution resonates 0.55 ppm to high frequency [11] of the dimer, and this species might also account for the signals at δ_{Al} = 71.7 and 67.7 ppm, which diminish along with the δ_{Al} = 74.6 ppm peak as the pH decreases. However, a high abundance for such a species is unexpected, and it seems more likely that it gives rise to the weak signal at δ_{Al} = 75.1 ppm at pH = 10.35. One puzzle remains from this discussion, namely the assignment of the q^2 signal at δ_{Al} = 69.6 ppm at pH ~9.0, which might be thought to be from the linear trimer but for the fact that the corresponding q^1 signal is scarcely present at so low a pH. Of course, it is possible (though unlikely) that the intrinsic probability of replacing Si by Al is greater for Q^2 than for Q^1 in the linear trimer in spite of the statistical factor of 2:1 in favour of Q^1 replacement.

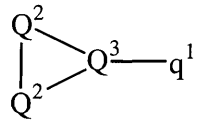

IV

5.4.4. Linewidths

Some peaks are significantly sharper than others, which presumably indicate either that the broader signals are composites or that the electric field gradient at aluminium is significantly smaller for some environments (giving rise to the sharp peaks) than for others. Particularly mobile species may also have higher transverse relaxation times and therefore give sharper

peaks. At the higher values of pH it is difficult to disentangle true peak widths from the effects of chemical exchange, but the signal at 65.6 ppm always remains relatively sharp. This matter is explored in more detail below. Because both of its position and of the known stabilising effect of tetraalkylammonium ions on cage silicate species,[15] it is tempting to assign this signal to the substituted cubic octamer (V). Moreover, the corresponding purely silicate species has[16] a relatively long T_1 (^{29}Si), which might correlate with the narrow ^{27}Al linewidth for the 65.6 ppm peak. A similar species involving germanium has been reported,[17] and even cubic octamers doubly substituted by germanium.[18] Indeed, Engelhardt and co-workers have obtained both trimethylsilylation[19] and ^{29}Si NMR[20] evidence for the existence of V and of cubic octamers multiply-substituted by Al in crystalline tetramethylammonium aluminosilicates. They conclude that Loewenstein's rule is generally obeyed, and they speculated about linkages involving Si-O-Al bridges between the cubic octamers to create polymeric structures. However, any assignment of the relatively sharp peak 7 (δ_{Al} = 69.6 ppm) to the prismatic hexamer would be contradictory to the suggestion above that peaks 4 and 8 arise from three-membered rings.

A high-quality spectrum of a pH = 10.35 solution (figure 5.3), obtained by accumulation over 14.8 hours and plotted with no line broadening, was fitted by deconvolution to 13 lines. Figures 5.4 and 5.5 were obtained by expansion of the q^1, q^2 and q^3 regions of figure 5.3. The quality of the fitting in these regions is shown in Figures 5.3, 5.4 and 5.5. Figure 5.5 is included to show the difference spectra (experimental – simulated). The intensities, normalized to that of the q^0 peak, the linewidths at half-height ($\Delta\nu_{1/2}$) and the implied value of the transverse relaxation times

($T_2 = 1/\pi\Delta\nu_{1/2}$) are given in table 5.1. The background signal complicated this procedure, resulting in an obviously incorrect result for peak number 11.

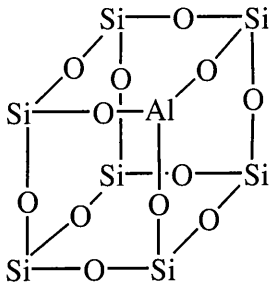

V

(exocyclic O^- or OH omitted)

Indeed, the accuracy of the procedure is best at the high-frequency end of the spectrum. Integration of the spectrum is problematic in the low-frequency region, but better above δ_{Al} = 73 ppm, showing that the total intensity of the three q^1 peaks is 6.6% of that of q^0, whilst deconvolution gives a value of 6.3%. The two independent measurements are thus in good agreement (especially since the background contributes a small amount to the q^1 intensities). The difference between the experimental spectrum and the one simulated by deconvolution shows clearly that peak 4 is asymmetric (see figure 5.5), and therefore consists of signals from at least two environments. Moreover, deconvolution reveals that there are additional (but unquantifiable) signals at least at the following positions: 71.2, 68.4, 64.5 and 63.7 ppm. We have designated the last two as peaks 12 and 13.

Table 5.1. Aluminium-27 NMR data for the aluminosilicate solution at pH = 10.35 and ambient probe temperature.

Peak No.	δ_{Al}/ppm	$\Delta\delta_{Al}$/ppm[a]	Intensity/%[b]	$\Delta\nu_{1/2}$/Hz	T_2/ms	T_1/ms[c]
1	80.4	0.0	100.0	7	46	52
2a	75.1	–5.2	1.5	64	5	d
2	74.6	–5.8	2.6	25	13	22
3	74.0	–6.5	2.2	39	8	23
4	71.7	–8.7	4.2	56	6	8
5	70.6	–9.8	1.3	45	7	11
6	70.0	–10.4	2.9	47	7	9
7	69.6	–10.8	4.0	26	12	13
8	67.7	–12.9	3.5	97	3	2
9	66.4	–14.0	0.7	42	7	24
10a	66.0	–14.4	0.1	11	29	d
10	65.6	–14.8	1.5	11	29	36
11	65.0	–15.6	d	d	d	7
14[e]	ca. 60	ca. –20	d	d	d	d

[a] Separation from the q^0 peak.

[b] By deconvolution; relative to the q^0 signal.

[c] A considered average of the three methods mentioned in the experimental section.

[d] Not measured.

[e] Difficult to distinguish from probe background.

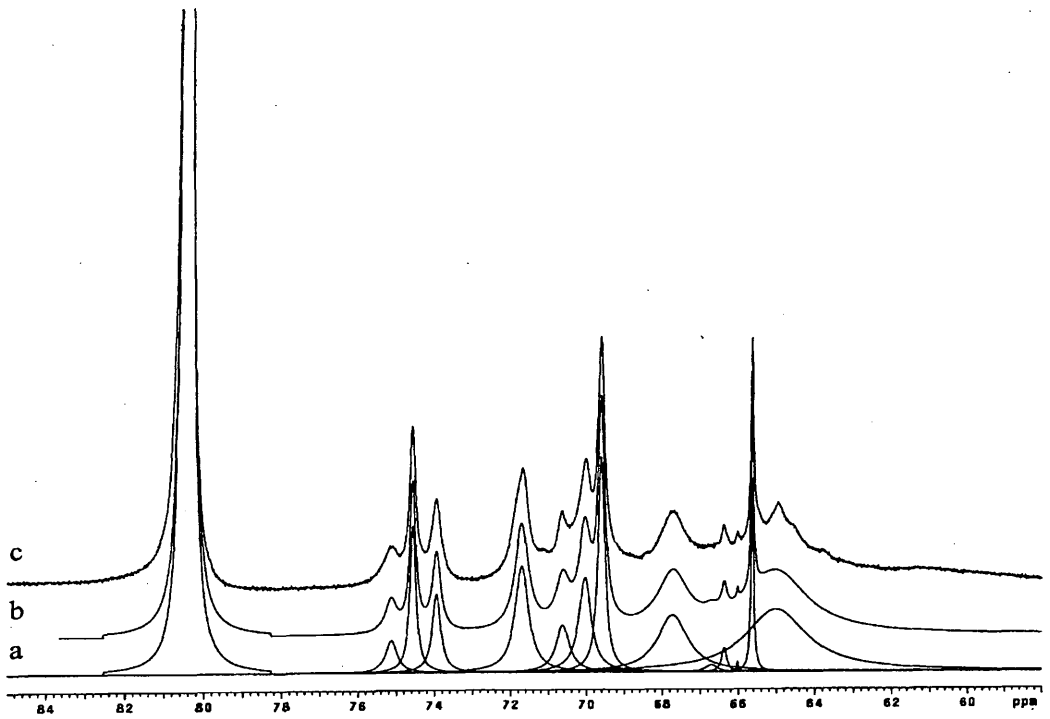

Figure 5.3. Fitting by deconvolution of the peaks observed at pH = 10.35: (a) individual simulated peaks, (b) total simulated spectrum, (c) observed spectrum.

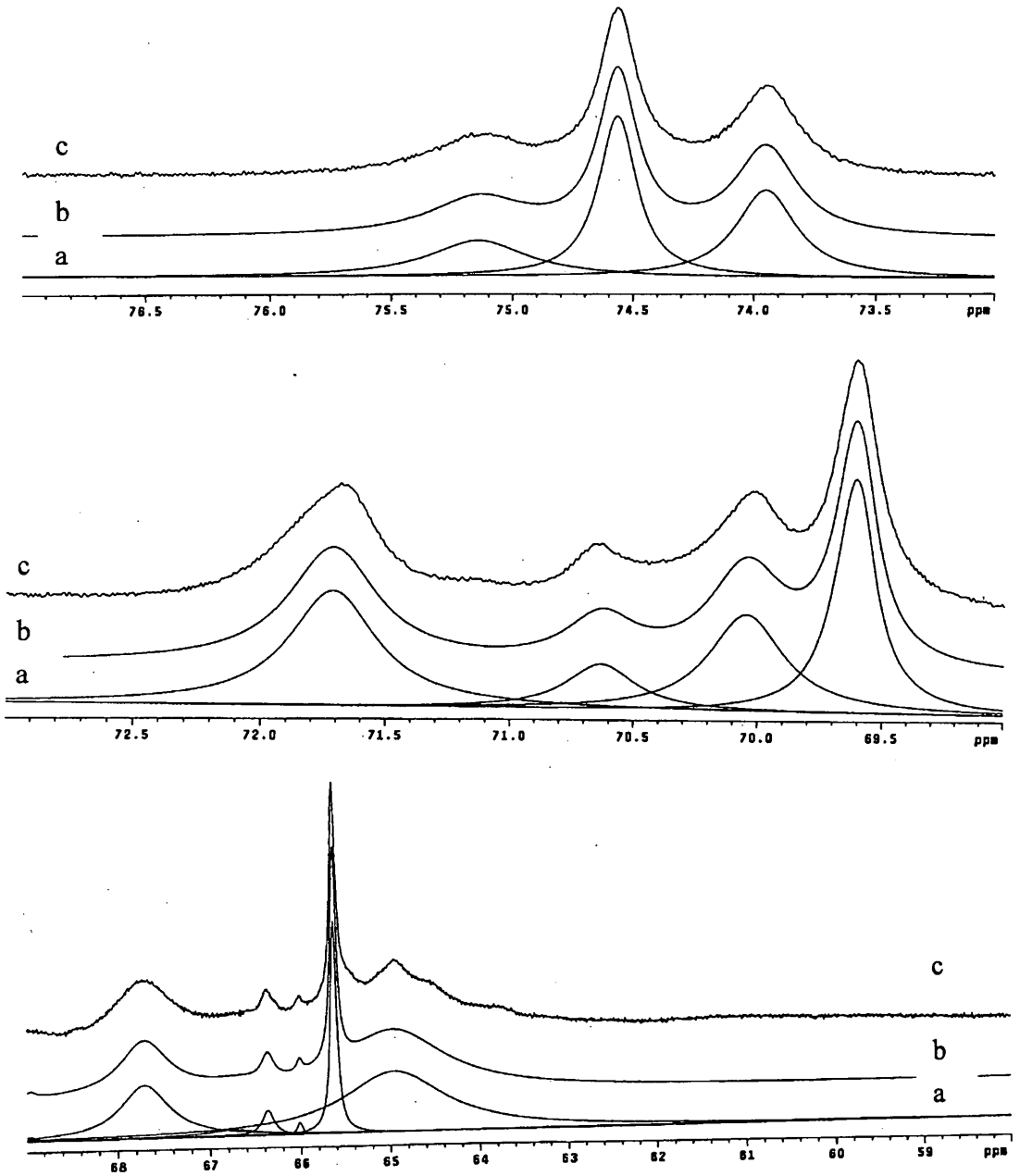

Figure 5.4. The expansion of figure 5.3: top, the three q^1 peaks; middle, the four q^2 lines; bottom, q^3 and q^4 region.

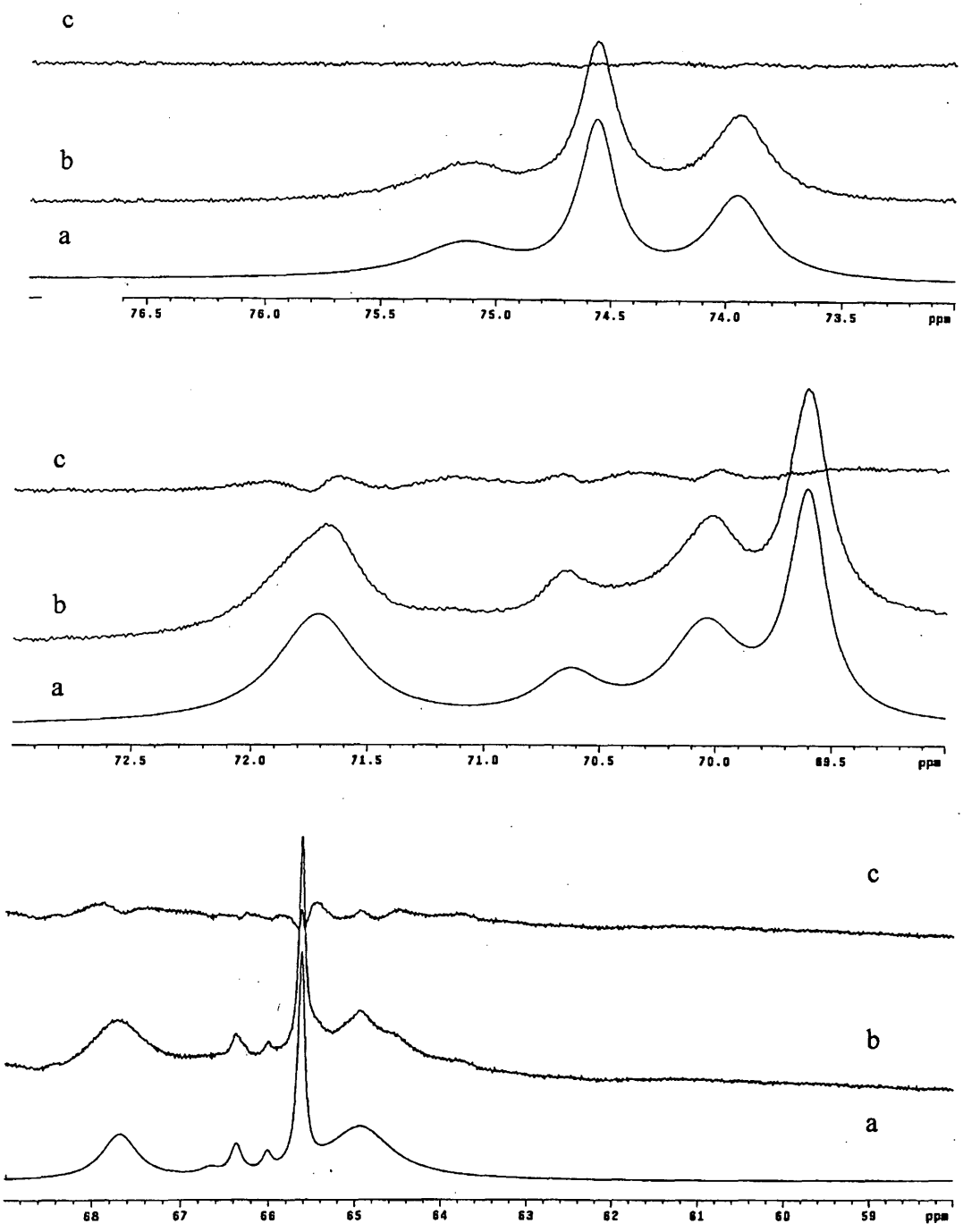

Figure 5.5. Fitting of the (top) q^1, (middle) q^2, and (bottom) q3 and q4 regions by deconvolution: (a) simulated spectrum, (b) experimental spectrum, (c) difference spectrum.

5.4.5. Spin-lattice relaxation times

In order to obtain more information about the species present in aluminosilicate solutions, ^{27}Al spin-lattice relaxation times for the solution at pH = 10.35 were measured, and the results are reported in table 5.1.

Table 5.2 shows data for peak heights, H, linewidths at half-height ($W=\Delta\nu_{1/2}$) (using the estimated local baseline) and intensity calculations, $I=W\times H$ (plus natural logarithms of differences of intensities), for the eleven signals of figure 5.2. Figure 5.6 gives Excel computer program plots of $ln[I_0-I_t]$ against the recovery interval of the eleven signals. The data are derived from table 5.2. The best-fit equation of each plot is shown on the right at the top. Analogous plots were made for $ln(H_0-H_t)$, which are not shown here.

Results obtained from the measurement of spin-lattice relaxation times of this solution illustrate that the different species of the aluminosilicate solution involve different spin-lattice relaxation times. The results indicate that the maximum T_1 (^{27}Al) of species in such aluminosilicate solution is about 52 *ms*, and this is instructive for recording ^{27}Al NMR spectra of TMAOH aluminosilicate solutions quantitatively (i.e. recycle delay $\geq 5 \times T_1$). In order to ensure full recovery of magnetization during the T_1 measurements, recycle delays of 400 ms were selected, with 11 different τ_D values (maximum τ_D 640 *ms*), and 10.7 μs 90° pulse duration (on the basis of the B_1 calibration experiment). To achieve a sufficient signal-to noise ratio, the experiment took more than 24 hours. It should be noted that the relaxation measurements were performed under normal sample conditions and no degassing was done to remove air. The experiment was carried out with a proton decoupling radio-frequency (although this was not necessary) at ambient temperature (22 °C).

Table 5.2. Data for the measured peak heights, H, peak widths $\Delta\nu_{1/2}$ and peak intensities, I, together with calculated natural logarithms of differences I_0-I_t and H_0-H_t (see the text), for the eleven signals in the T_1 measurement. Note that, for each individual peak, the same vertical and horizontal expansions have been used, but these differ from peak to peak. The dashes in this table mean that the peak heights, widths and intensities remain approximately the same (i.e. already fully recovered).

τ_D ms	0.625	1.25	2.5	5	10	20	40	80	160	320	640
H line 1	-97	-94	-89	-81	-78	-42	12	75	11.8x10	12.8x10	12.9x10
W line 1	11	11	12	12	9.5	10	7.7	9.7	9.5	9.5	9.5
I line 1	-107x10	-103x10	-107x10	-972	-741	-420	92.4	728	112x10	122x10	123x10
H line 2	-55	-51	--47	-32	-15	21	49	-	-	-	70
W line 2	25	24	24	24	32	36	29	-	-	-	30
I line 2	-138x10	-122x10	-113x10	-768	-480	765	142x10	-	-	-	210x10
H line 3	-75	-77	-69	-57	-34	0.0	-	-	-	-	46
W line 3	30	30	31	32	32	0.0	-	-	-	-	54
I line 3	-225x10	-231x10	-214x10	-182x10	-109x10	0.0	-	-	-	-	248x10
H line 4	-35	-28	-20	0.0	20	38	-	-	-	-	46
W line 4	58	53	52	0.0	54	54	-	-	-	-	54
I line 4	-209x10	-148x10	-104x10	0.00	108x10	20sx10	-	-	-	-	248x10
H line 5	-11	-11	-9.0	0.0	4.0	-	-	-	-	-	12
W line 5	31	31	26	0.0	18	-	-	-	-	-	32
I line 5	-341	-341	-234	0.00	72.0	-	-	-	-	-	384
H line 6	-20	-19	-13	-5.0	6.5	-	-	-	-	-	22
W line 6	36	41	27	14	32	-	-	-	-	-	33
I line 6	-720	-779	-351	-70.0	208	-	-	-	-	-	726
H line 7	-10x10	-93	-75	-47	11	68	-	-	-	-	12x10
W line 7	29	28	28	28	33	28	-	-	-	-	28
I line 7	-290x10	-260x10	-210x10	-132x10	363	190x10	-	-	-	-	336x10
H line 8	-14	-8.0	0.0	16	-	-	-	-	-	-	19
W line 8	77	80	0.0	85	-	-	-	-	-	-	84
I line 8	-108x10	-640	0.00	136x10	-	-	-	-	-	-	160x10
H line 9	-7.0	-9.0	-8.5	-6.5	0.0	0.0	-	-	-	-	9.0
W line 9	36	36	36	35	0.0	0.0	-	-	-	-	33
I line 9	-252	-324	-306	-228	0.0	0.0	-	-	-	-	397
H line 10	-50	-48	-43	-37	-28	-10	19	44	-	-	58
W line 10	18	20	18	16	15	14	21	18	-	-	17
I line I 0	-900	-960	-774	-592	-420	-140	399	792	-	-	986
H line 11	-20	-20	-14	0.0	-	-	-	-	-	-	28
W line 11	72	64	64	0.0	-	-	-	-	-	-	66
I line 11	-144x10	-128x10	-896	0.00	-	-	-	-	-	-	185x10

go to next page

τ_D ms	0.625	1.25	2.5	5	10	20	40	80	160	320	640
I_0-I_t line 1	230x10	232x10	230x10	226x10	203x10	171x10	114x10	502	110	10.0	0.00
I_0-I_t line 2	348x10	332x10	323x10	287x10	258x10	134x10	680	-	-	-	0.00
I_0-I_t line 3	473x10	479x10	462x10	430x10	357x10	248x10	-	-	-	-	0.00
I_0-I_t line 4	457x10	396x10	352x10	248x10	140x10	430	-	-	-	-	0.00
I_0-I_t line 5	725	725	618	384	310	-	-	-	-	-	0.00
I_0-I_t line 6	145x10	150x10	108x10	796	518	-	-	-	-	-	0.00
I_0-I_t line 7	626x10	596x10	546x10	468x10	300x10	146x10	-	-	-	-	0.00
I_0-I_t line 8	268x10	224x10	160x10	240	-	-	-	-	-	-	0.00
I_0-I_t line 9	549	621	603	525	297	297	-	-	-	-	0.00
I_0-I_t line 10	189x10	195x10	176x10	158x10	141x10	113x10	587	194	-	-	0.00
I_0-I_t line 11	329x10	313x10	275x10	185x10	-	-	-	-	-	-	0.00
ln(I_0-I_t) line 1	7.74	7.75	7.74	7.72	7.61	7.44	7.04	6.22	4.70	230	-
ln(I_0-I_t) line 2	8.15	8.11	8.08	7.96	7.86	7.20	6.52	-	-	-	-
ln(I_0-I_t) line 3	8.46	8.47	8.44	8.37	8.18	7.82	-	-	-	-	-
ln(I_0-I_t) line 4	8.43	8.28	8.17	7.82	7.24	6.6	-	-	-	-	-
ln(I_0-I_t) line 5	6.59	6.59	6.43	5.95	5.74	-	-	-	-	-	-
ln(I_0-I_t) line 6	7.28	7.31	6.98	6.68	6.25	-	-	-	-	-	-
ln(I_0-I_t) line 7	8.74	8.69	8.61	8.45	8.01	7.29	-	-	-	-	-
ln(I_0-I_t) line 8	7.89	7.71	7.38	5.48	-	-	-	-	-	-	-
ln(I_0-I_t) line 9	6.31	6.43	6.40	6.26	5.69	5.69	-	-	-	-	-
ln(I_0-I_t) line 10	7.54	7.57	7.47	7.37	7.25	7.03	6.38	5.27	-	-	-
ln(I_0-I_t) line 11	8.10	8.05	7.92	7.52	-	-	-	-	-	-	-

Figure 5.6. Excel computer program plots of $ln[I_0-I_t]$ against the recovery interval of eleven signals. The data are derived from table 5.2. The equation for each fitted plot is shown on the right at the top.

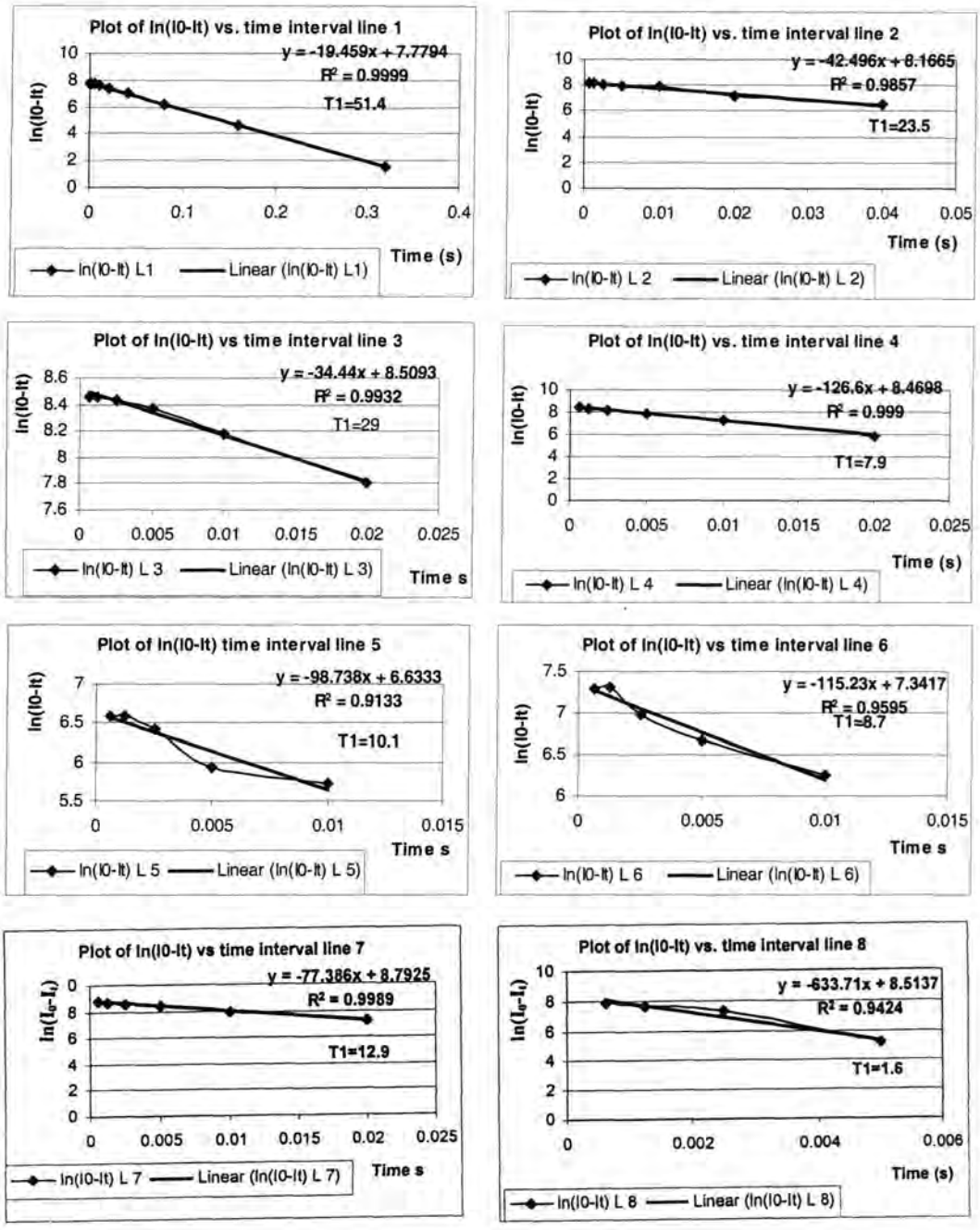

go to next page

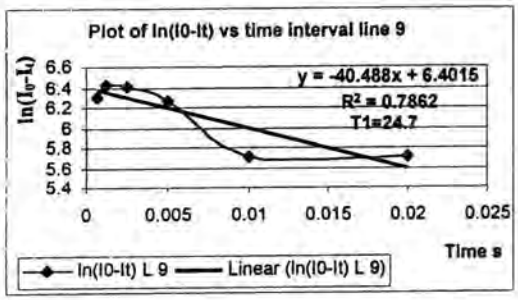

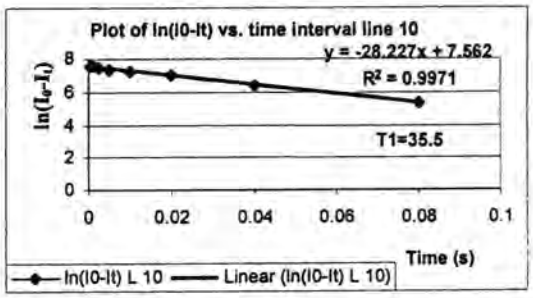

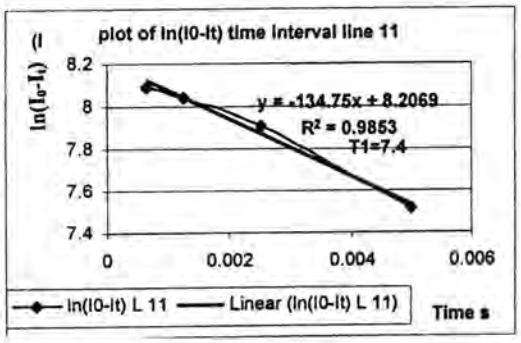

It can be seen that the values vary significantly for the different peaks, suggesting that either electric field gradients or mobility depend strongly on the species and site in question. The results may be compared with data on linewidths, $\Delta\nu_{1/2}$, also reported in table 5.1. In the extreme narrowing approximation, with the quadrupolar interaction providing the dominant relaxation mechanism, values of T_2 ($=1/\pi\Delta\nu_{1/2}$) should equal T_1. The data in table 5.1 show that in general T_1 and T_2 vary in parallel, with T_2 usually a little shorter than T_1. Of course, there are factors, which affect $\Delta\nu_{1/2}$ other than the true T_2, so the latter situation is not unexpected. However, the parallelism of T_1 and T_2 suggests that a dispersion of chemical shifts does not give a strong contribution to line broadening in many, if not most, cases. On the other hand, as noted above, the shape of signal 4 indicates that it consists of at least two peaks, in spite of the fact that the measured values of T_2 and T_1 do not differ very greatly. In fact, the largest deviations between T_1

and T_2 occur for peaks 3 and 9, which is particularly surprising in the former case. Of course peak 1 is assignable to a single type of site (q^0). This peak is by far the most intense and it is isolated from the rest of the spectrum, so the value of T_1, which is significantly higher than for any other signal, is accurate (within a few %). It arises from the smallest species, so the mobility is presumably the greatest of any aluminosilicate anion, which explains why it has the longest T_1. Moreover, when ionisation questions are ignored, q^0 should have a low electric field gradient because of symmetry, thus again leading to a relatively long T_1. It is not obvious why any other Al sites should have low electric field gradients or high mobility. The only species, which might automatically fill these conditions, is $q^4Q^1_4$, but this is not expected to appear in significant amount, since the corresponding $Q_4Q^1_4$ ^{29}Si NMR signals are not normally seen for analogous silicate solutions.[21] The relatively sharp signal 10 at δ_{Al} = 65.6 ppm is therefore difficult to explain except by an "accidentally" small electric field gradient (i.e. electrical symmetry but not true structural symmetry around Al). Our best estimate is that this peak may arise from the cubic octamer, V, as discussed above, the overall shape of this species perhaps giving it an enhanced mobility.

The T_1 values for q^0 display good agreement between the four measurement methods (see experimental section). However for some other signals, because of the above mentioned reasons there is not good agreement between computer-calculated values and those obtained from the slopes of $ln(H_0-H_t)$ or $ln(I_0-I_t)$ *vs. recovery times* (see table 5.3).

Table 5.3. Data for spin-lattice relaxation times of species in TMAOH aluminosilicate solution obtained from different methods.

Peak No.	Estimated species	T_1[a]/ms from H	R^2[b]	T_1[c]/ms from I	R^2	T_1[d]/ms from τ_{null}	T_1[e]/ms from computer
1	q^0	52(10)[f]	0.99	51.4(10)	0.99	51	53.5 (10)
2	q^1	22.1(8)	0.99	23.5(7)	0.98	19	20.5(7)
3	q^1	19.5(6)	0.99	29(6)	0.99	25	25.9(7)
4	q^2_δ	8(6)	0.99	7.9(6)	0.99	9.4	8.8(7)
5	q^2	10.7(6)	0.96	10.1(5)	0.91	11	10.6(10)
6	q^2	9.2(5)	0.99	8.7(5)	0.95	9.4	9.2(7)
7	q^2	13.2(6)	0.99	12.9(6)	0.99	13	12.9(7)
8	q^3_Δ	1.7(4)	0.95	1.6(4)	0.94	2.0	2.9(10)
9	q^3	25.7(7)	0.99	24.7(6)	0.78	21	6.8(10)
10	q^3_β	39(8)	0.99	35.5(8)	0.99	37	28.3(10)
11	q^3	7.7(4)	0.96	7.4(4)	0.98	9.1	6.1(5)

a. Measured T_1 by using peak heights and plotting $ln(H_0-H_t)$ *vs.* recovery intervals, τ_D.

b. Mean squared values from the trend line(fitted line)

c. Measured T_1 by using calculated peak areas i.e. I= W×H and plotting $ln(I_0-I_t)$ *vs.* recovery intervals, τ_D.

d. Measured T_1 by using τ_{null} from the equation $T_1=\tau_{null}/ln2$.

e. Measured T_1 by using the exponential data analysis (computer calculation)

f. The brackets indicate the number of points which was drawn from table 5.2 for plotting of both $ln(H_0-H_t)$ and $ln(I_0-I_t)$ *vs* τ_D.

5.5. Final comments and conclusions

With all these considerations in mind, an attempt has been made here to explore parallels between ^{27}Al and ^{29}Si shifts in corresponding aluminosilicate and silicate species. Table 5.4 shows the data for Si chemical shifts obtained from reference 22 and the Al chemical shifts obtained from figure 5.2. Figure 5.7 shows results. Of course, the ^{27}Al assignments are generally speculative. In some cases (for instance the Q^2 signals linked to ^{27}Al peaks 6 and 7) divisions are arbitrary. However, a general correlation can be observed. This suggests that the weak peaks 5 and 9 may perhaps arise from q^2 and q^3 sites in the unusual cage structures.[11] If the correlation is correct, the effect of incorporation into "three-membered" rings is significantly smaller for ^{27}Al than for ^{29}Si, giving rise to peaks 4 and 8 for

the former. However, Figure 5.7 deviates from our earlier discussion in suggesting the "cubic octamer" ^{27}Al signal corresponds to peak 11 rather than the sharp peak 10. If Loewenstein's rule is violated for any of the species, then further structural assignment possibilities arise.

In this chapter, it has been shown that it is possible to obtain high-resolution ^{27}Al spectra of alkaline aluminosilicate solutions and that they contain at least 13 separate aluminium sites, corresponding to a range of anionic aluminium-containing species. Concentrations, and even relative intensities, vary significantly with the pH. Linewidths and spin-lattice relaxation times have been determined, and they also show a wide variation. Assignments of peaks to chemical structure are highly problematic in most cases, but some informed suggestions are made.

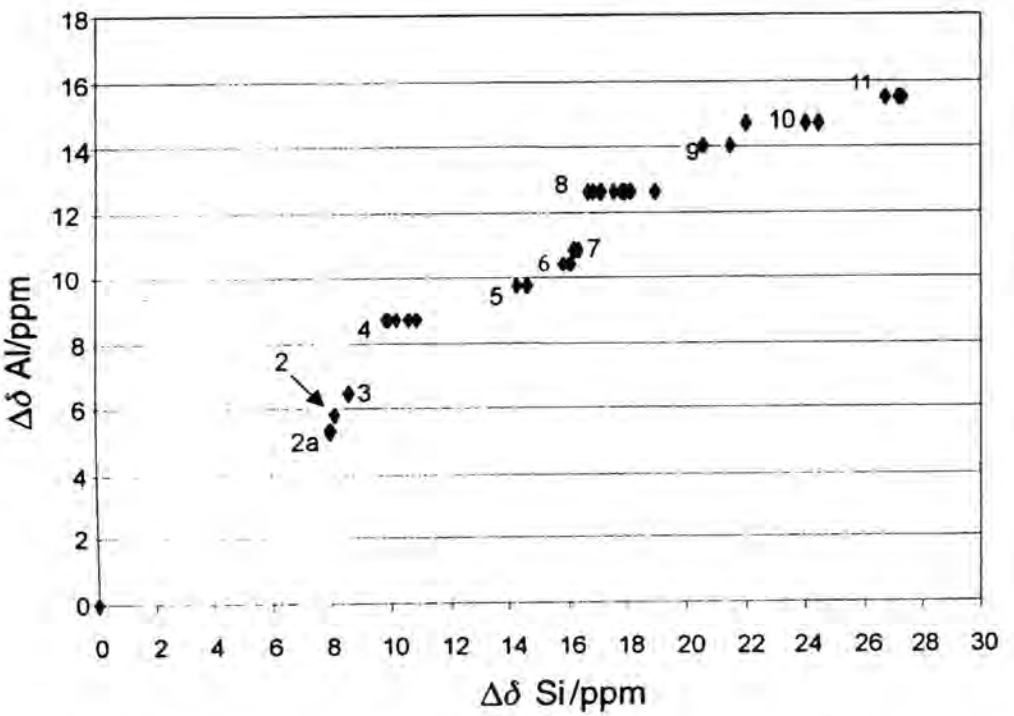

Figure 5.7. Attempted correlation of ^{27}Al chemical shifts for alkaline aluminosilicate solutions with ^{29}Si chemical shifts for alkaline silicate solutions (relative to the signals for q^0 and Q^0 respectively). The ^{27}Al peak numbers, are as given in Figure 5.2 and Table 5.1.

Table 5.4. ^{27}Al and ^{29}Si chemical shifts, δ, of aluminate and silicate anions identified in aluminosilicate and silicate solutions*

δ Al ppm**	Δδ Al ppm	Estimated q^n site	-δ Si ppm	Δδ Si ppm	Q^n site	Silicate species
80.4	0.00	q^0	71.30	0.00	Q^0	Monomer
75.10	5.30	q^1	79.16	7.86	Q^1	Monosubstituted cyclic tetramer
75.10	5.30	q^1	79.22	7.92	Q^1	Monosubstituted cyclic trimer
74.60	5.84	q^1	79.34	8.04	Q^1	Linear trimer
74.00	6.44	q^1	79.81	8.51	Q^1	Dimer
71.70	8.74	q^2	81.08	9.78	Q^2	Monosubstituted cyclic trimer
71.70	8.74	q^2	81.16	9.86	Q^2	Bicyclic pentamer
71.70	8.74	q^2	81.43	10.13	Q^2	Cyclic trimer
71.70	8.74	q^2	81.8	10.50	Q^2	Tricyclic hexamer IIa (cisoid)
71.70	8.74	q^2	82.11	10.81	Q^2	Tricyclic hexamer IIb (transoid)
70.63	9.78	q^2	85.50	14.20	Q^2	Bridged cyclic tetramer
70.63	9.78	q^2	85.87	14.57	Q^2	Doubly bridged cyclic tetramer
70.02	10.41	q^2	87.06	15.76	Q^2	Monosubstituted cyclic tetramer
70.02	10.41	q^2	87.29	15.99	Q^2	Cyclic tetramer
70.02	10.41	q^2	87.38	16.08	Q^2	Monosubstituted cyclic tetramer
69.61	10.80	q^2	87.42	16.12	Q^2	Tricyclic hexamer I
69.61	10.80	q^2	87.47	16.17	Q^2	Linear tetramer
69.61	10.80	q^2	87.58	16.28	Q^2	Bicyclic pentamer
67.78	12.72	q^3	87.94	16.64	Q^3	Tricyclic hexamer
67.78	12.72	q^3	88.10	16.80	Q^3	Tricyclic hexamer IIa (cisoid)
67.78	12.72	q^3	88.38	17.08	Q^3	Prismatic hexamer
67.78	12.72	q^3	88.41	17.11	Q^3	Bicyclic pentamer
67.78	12.72	q^3	88.81	17.51	Q^3	Tricyclic hexamer
67.78	12.72	q^3	89.02	17.72	Q^3	Hexacyclic octamer
67.78	12.72	q^3	89.15	17.85	Q^3	Tricyclic hexamer IIb (transoid)
67.78	12.72	q^3	89.23	17.93	Q^3	Pentacyclic heptamer
67.78	12.72	q^3	89.39	18.09	Q^3	Monosubstituted cyclic trimer
67.78	12.72	q^3	90.23	18.93	Q^3	Pentacyclic heptamer
66.38	14.07	q^3	91.82	20.52	Q^3	Hexacyclic octamer
66.38	14.07	q^3	92.74	21.44	Q^3	Monosubstituted cyclic trimer
66.38	14.07	q^3	93.24	21.94	Q^3	Bridged cyclic tetramer
65.38	14.78	q^3	93.24	21.94	Q^3	Bridged cyclic tetramer
65.38	14.78	q^3	95.29	23.99	Q^3	Monosubstituted cyclic tetramer
65.38	14.78	q^3	96.04	24.47	Q^3	Tricyclic hexamer
64.96	15.45	q^3	98.01	26.71	Q^3	Hexacyclic octamer
64.96	15.45	q^3	98.45	27.15	Q^3	Prismatic decamer
64.96	15.45	q^3	98.61	27.31	Q^3	Cubic octamer

5.6. References

1. W. M. Hendricks, A. T. Bell, and C. J. Radke, *J. Phys. Chem.* **95**, 9513 (1991)
2. G. Harvey and L. S. Dent Glasser in Zeolite Synthesis (Eds. M. L. Occelli and H. E. Robson), *ACS Symp.* **398,** 49 (1988).
3. L. S. Dent Glasser and G. Harvey, *J. Chem. Soc. Chem. Comm.* 1250 (1984).
4. J. J. Fitzgerald, C. Murali, C. O. Nebo and M. C. Fuerstenau, *J. Colloid Interface Sci.* **151,** 299 (1992).
5. B. S. Lartiges, J.Y. Bottero, L. S. Derrendinger, B. Humbert, P. Tekely and H. Suty, *Langmuir* **13,** 147 (1997).
6. R. K. Iler, "*The Chemistry of Silica*", Wiley, New York (1979).
7. A. Samadi-Maybodi S. N. Azizi, H. Naderimanesh, H. Bijanzadeh, I. H. McKeag and R. K. Harris, *J. Chem. Soc., Dalton Trans.*, 633 (2001)
8. R. K. Harris, A. Samadi-Maybodi and W. Smith, *Zeolites* **19** (1997) 147.
9. R. K. Harris, J. Jones, C. T. G. Knight and D. Pawson, *J. Mol. Struct.* **69,** 95 (1980).
10. C. T. G. Knight and S. D. Kinrade, *Anal. Chem.* **71,** 265 (1999).
11. R. K. Harris and C. T. G. Knight, *J.C.S. Faraday Trans.* 2, 1525, (1983); **2,** 1539 (1983).
12. J. W. Akitt and B. E. Mann, *J. Magn. Reson.* **44,** 584 (1981).
13. J. J. Fitzgerald, L. E. Johnson and J. S. Frye, *J. Magn. Reson.* **84,** 121 (1989).
14. D. Mueller, D. Hoebbel and W. Gessner, *Chem. Phys. Lett.* **84** (1981).

15. S. D. Kinrade, C. T. G. Knight, D. L. Pole and R. T. Syvitski, *Inorg. Chem.* **37,** 4272 (1998).

16. C. T. G. Knight and R. K. Harris, *Magn. Reson. Chem.*, **24,** 872 (1986).

17. C. T. G. Knight, R. J. Kirkpatrick and E. Oldfield, *J. Am. Chem. Soc.* **108**, 30 (1986).

18. C. T. G. Knight, R. J. Kirkpatrick and E. Oldfield, *J. Am. Chem. Soc.* **109,** 1632 (1987).

19. D. Hoebbel, G. Garzó, K. Ujszászi, G. Engelhardt, B. Fahlke and A. Vargha, *Z. anorg. allg. Chem.* **484,** 7 (1982).

20. G. Englehardt, D. Hoebbel, M. Tarmak, A. Samoson and E. Lippmaa, *Z. anorg. allg. Chem.* **484,** 22 (1982).

21. R. K. Harris, J. Parkinson and A. Samadi-Maybodi, *J. Chem. Soc. Dalton Trans* 2533 (1997).

22. G. Engelhardt and D. Michel, "*High-resolution solid-state NMR of silicates and zeolites*", Wiley, New York, (1987).

Chapter Six

Aluminium-27 NMR spectra of aluminosilicate solutions as a function of cation type.

6.1. Introduction

The cation of the base is considered to play a structure-directing role in the synthesis of zeolites, an interesting but as yet poorly understood phenomenon. This structure-directing role is commonly discussed in terms of the cation having a template function during the formation of the aluminosilicate framework. However, the importance of the solution chemistry for preparation of a specific zeolite structure that is being formed has long been recognised.[1, 2] Therefore, the question arises whether the organic species already exerts a structure-directing influence in solution via the stabilisation of a particular aluminosilicate species, or even *via* the formation of an aluminosilicate anion which is otherwise not present. Such a pre-selected aluminosilicate in solution may then act as a building unit for the putative zeolite. These considerations have led the Durham NMR group to start a systematic study of the influence of organic and non-organic bases on the occurrence of specific aluminosilicate species in solutions from which zeolites may be formed (though not necessarily under zeolite-forming conditions). Here will be presented results for aluminosilicate solutions based on tetraalkylammonium hydroxides and alkali metal ions.

The effects of tetraalkylammonium (TAA) and alkali metal cations on the equilibrium distribution of aluminosilicate oligomers in aqueous alkaline aluminosilicate solutions have been investigated using the evolution with time of ^{27}Al NMR spectra. The results indicate that there are no differences in the initial equilibria (i.e. immediately following solution mixing) involving the TAA cation and those involving alkali metal cations, provided there is a Na^+ concentration at least equal to the Al concentration. However, intrinsic differences exist in the interactions for linking the oligomers (re-equilibration). In the concentration of components used, the large size of the

TAA cations does not preclude significant ion-pairing; however, hydrophobic solvation, ion-crowding and pH probably play important roles in determining aluminosilicate speciation during re-equilibration, though not at the initial equilibrium.

The striking differences between the effects of inorganic and organic cations on silicate speciation has led to a great deal of confusion in the literature,[3] especially when the organic cations are viewed as merely larger members of a class that begins with the alkali metal cations. To gain a deeper understanding of the different ways in which alkali metal and tetraalkylammonium cations influence silicate and aluminosilicate oligomerisation, it is necessary to understand the intrinsic differences between organic and inorganic cations and the nature of their interactions with the solvent and with other ions.

The purpose of this study is to clarify the role of organic cations in aqueous aluminosilicate solutions and to compare and contrast the behaviour of these cations with alkali metal cations. A time-evolution experiment[4] is used to investigate the differences between alkali metal and TAA aluminosilicate solutions and the influence of cation size on the distribution of aluminosilicate anions.

For practical expediency, the solutions investigated contain both sodium and tetramethylammonium counter-ions, since the method of preparation was to mix aqueous tetraalkylammonium silicate solutions with aqueous sodium aluminate solutions.

6.2. The influence of type and size of cations on the distribution of silicate anions in silicate solutions.

It is obvious that changing the type or varying the concentration of the cation produce differences in pH in a solution. The effect of pH on the equilibrium distribution of silicate and aluminosilicate species was discussed in chapter 5. The influence of cation structure on the distribution of aluminosilicate anions at fixed silicate and aluminate to cation ratios is complex and not well understood.[3] According to Bell and co-workers,[3] consideration of physico-chemical phenomena in ionic solutions suggests that at least three processes may be relevant: a) cation-anion pair formation, b) water structuring, and c) cation crowding. The role that each of these processes might play has been examined in silicate solutions.[3]

a) Formation of cation-anion pairs in concentrated ionic solutions is well known to be a result from coulombic interactions between cations and anions. McCormick et al.[5] have proposed that the formation of such pairs stabilises anions toward hydrolysis, and that larger anions are stabilised relative to smaller ones with increasing size of the cation. The authors state that evidence in support of this conclusion was obtained by cation NMR spectroscopy of alkali metal silicate solutions. Silicate oligomers were found to shield Cs^+ more efficiently than Na^+, and from ^{29}Si NMR spectroscopy it was deduced that the selectivity for large silicate oligomers is higher in the presence of Cs^+ than Na^+. Additional support for the conclusion that large alkali metal cations stabilize large silicate anions preferentially can be drawn from the work of Liebau,[6] who has demonstrated that large, polarisable cations, such as Cs^+, are better able to bind with ring and cage silicates than smaller cations, such as Li^+. For TAA solutions, the silicate oligomers could be expected to be more stable than for alkali metal solutions, since the radii

of all TAA cations are significantly larger than that of Cs^+. In the case of TAA aluminosilicate solutions, the coulombic effect is not an important contribution to the differences between templates. The hydrophobic effect is more relevant for such cases.

b) The second way in which cations might influence the distribution of silicate anions is through their effect on the structuring of water. The interaction of alkali metal cations with water has been modelled by treating the cation as a charged sphere and the water as a series of dipoles.[3] This type of model predicts heats of hydration to within 10% for the series Na^+ to Cs^+ and to within 20% for Li^+. Since the strength of the interaction between water and an alkali metal cation falls off with the square of the distance between their centres, the influence of the cation would not be expected to extend much beyond one or two water molecules and to decrease with increasing cation size. The relative strength of water-cation interactions can be observed by measuring the rotational correlation time, τ^*, of the hydration water molecules.[7] Relative to the bulk value, τ_b, this decreases inversely with cation size for the series Li^+ to Cs^+. Longer correlation times indicate that the water of hydration is more tightly held. For TAA and related anions, one might expect the rotational correlation times to be even shorter than that for Cs^+, since the radii of all of the former are significantly larger than that of the latter. In contrast to the alkali metal cation, according to the work of Bell and co-workers,[3] the rotational correlation time of the hydrating water increases rapidly with increasing cation size. If we take into account hydrated water molecules with cations, then it could be assumed that $Li(H_2O)_n$ are larger than $Cs(H_2O)_n$, and that the role of the alkali metal cations follows the same order as for the TAA cations.

c) The third mechanism by which cations can exert an influence on the distribution of silicate or aluminosilicate anions is through a process that is referred to as ionic crowding. Due to Coulombic forces, the cation in solution tends to distribute so as to produce the maximum cation-cation separation. The free volume per cation can then be defined as the total solution volume per cation minus the volume of the cation. In the absence of strong anion-cation interactions, as is likely to be the case with TAA cations, the anions in solution must have volumes that are equal to or smaller than the free volume associated with each cation. If this condition is not met, local crowding of cations will occur and this will set up an electrostatic field that disperses the cations. On the basis of these considerations, one may postulate that the maximum size that silicate or aluminosilicate anions can achieve in solution is constrained by the free volume per cation. It follows therefore that, for fixed silicate and cation concentrations, cation crowding will work towards decreasing the size of silicate anions as the size of the cation is increased. The free volume per cation varies with cation size, i.e. increases with decreasing cation size and also decreases with cation concentration for solutions with the same type of cation. It is immediately evident that, for cations with radii equivalent to or smaller than TMA^+, the free volume in solution is sufficient to accommodate the q^3_8 aluminosilicate anions and all smaller structures.

All of the alkali metal cations are small enough so that, at a 1M concentration, the free volume per cation is sufficient to accommodate polymerised species and all smaller anions. As a consequence, effects of ionic crowding should not be observable for alkali metal cations. Since these cations do not induce water structuring, the only influence of cation size is on the extent of cation-anion pairing.

All of the TAA cations are sufficiently large that cation-anion pairing should not be extensive. In this case, the effects of cation size should be expressed through changes in the hydrophobicity of the cation and the extent of cation crowding. With increasing cation size, the hydrophobic effect of TAA cations on the structuring of water increases and the free volume per cation decreases. As discussed above, these two effects influence the distribution in opposing ways: for rising cation size the increased hydrophobic effect increases the extent of silicate oligomerisation, while the decrease in cation free volume decreases the extent of oligomerisation.

6.3. Experimental

Several aluminosilicate solutions were prepared by using alkali metal and TAA hydroxide solutions such as NaOH, KOH, TEAOH, TPAOH, TBAOH, HMBTP and $HM(OH)_2$ to provide the cation templates. The aluminosilicate solutions were made by adding the alkali metal or substituted ammonium hydroxide silicate solution to freshly prepared sodium aluminate solution to achieve the ratio Si/Al of 1. The composition data of all the samples are listed in table 6.1.

All samples were measured by using the Varian Inova 500 MHz spectrometer. All spectra were recorded under the same conditions and at ambient temperature (ca. 22 °C). They were processed with backward linear prediction to number 12. The spectra have been recorded as a function of time after preparation. The evolution of the spectra with time after mixing silicate and aluminate solutions has been studied as a function of cation type. All solutions were clear at the time of recording the spectra.

Table 6.1. Data for the aluminosilicate solutions.

Sample No.	Template type	Molarity Template	Molarity Si	Molarity Al≡Na*	Si/Al ratio	Si/Template ratio
278	$HM(OH)_2$	0.028	0.014	0.014	1	1/2
280	HMBTP	0.028	0.014	0.014	1	1/2
275	KOH	0.028	0.014	0.014	1	1/2
274	NaOH	0.028	0.014	0.014	1	1/2
90=1	TMAOH	0.028	0.014	0.014	1	1/2
93	TEAOH	0.028	0.014	0.014	1	1/2
95	TPAOH	0.02	0.01	0.014	0.71	1/2
101	TBAOH	0.028	0.014	0.014	1	1/2
264	NaOH	0.028	0.014	0.028	1/2	1
265	NaOH	0.056	0.028	0.014	2	1/2
272	NaOH	0.007	0.014	0.0035	4	1/2

* In addition to the template concentration given in the second column, there is Na^+ to the same concentration as Al.

6.4. Results

It is pertinent to consider and compare the ^{27}Al NMR spectra of the above alkali metal and TAA aluminosilicate solutions. Figure 6.1 shows ^{27}Al spectra obtained immediately following mixing of sodium aluminate with some the above silicate solutions (sample nos. 278, 280, 275, 274), with total accumulation times of 34 minutes in the absolute intensity mode at ca. 22°C. By comparison of the four spectra, and also the spectra of similar solutions containing TMAOH, TEAOH, TPAOH and TBAOH, it can be seen that there are no substantial differences between the features. The spectra reveal approximately the same distribution of species at the first equilibrium. Such spectra for alkali metal aluminosilicate have not been reported in the previous literature.[8-16]

This proves that there is no significant variation in the distribution of aluminosilicate species soon after preparation by using different cations such as KOH, NaOH, TMAOH, TEAOH, TPAOH and TBAOH, provided there is a concentration of Na^+ at least equal to that of Al. However, some changes are observed, for example the intensity of the sharp peak located at a chemical shift ca. 65.6 ppm varies. Moreover, the rate of formation of oligomers following preparation varies.

The distribution of the species changes with ageing time.[4] Therefore the evolution with time of the spectra for the solutions will be discussed. The assignment of the signals had been discussed in detail in the previous chapters for tetramethylammonium silicate solutions. The spectra of these solutions at the chosen concentrations of the components in index one (that obtained immediately after preparation) exhibit similar features. However, the main differences are in the time evolution spectra.

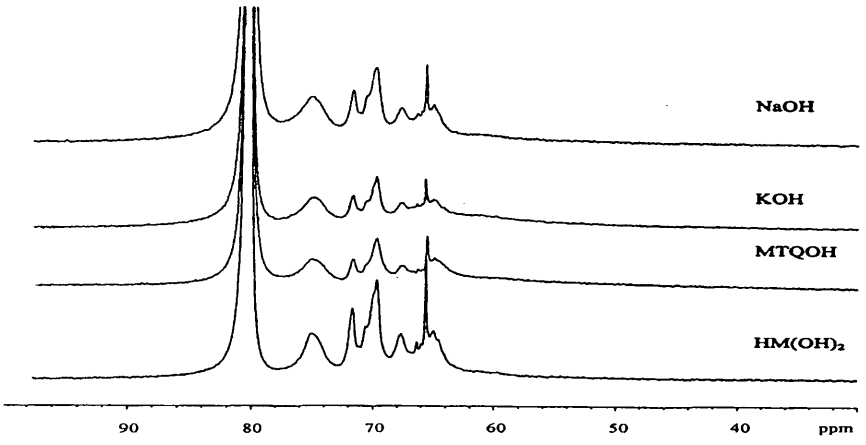

Figure 6.1. High-resolution ^{27}Al NMR spectra at 130.23 MHz and ambient temperature of HMBTP, $HM(OH)_2$, KOH and NaOH aluminosilicate solutions with the compositions Si, Al=Na and template equal to 0.014, 0.014 and 0.028 molar respectively i.e. [Si/Al] = 1 (sample nos. 280, 278, 275 and 274). Spectrum conditions: Spectral width 58394.2 Hz. Acquisition time 0.81 s. Recycle delay 0.020 s. Pulse angle 90 degrees. Number of repetitions 10240

a). Figure 6.2 shows horizontally stacked plots of the aluminium-27 NMR spectra following the mixing of sodium aluminate and aged $HM(OH)_2$ silicate solutions with the composition Si, Al=Na and template equal to 0.014, 0.014 and 0.028 molar respectively, i.e. [Si/Al] = 1 (sample No. 278), to illustrate the time-dependence of the reaction between aluminate and silicate anions. Thirteen spectra have been recorded progressively with time (figure 6.2). The first spectrum was obtained soon after mixing and the other ones recorded for ten minutes each, without any interval of time between the spectra, for 130 minutes. For more evidence, figure 6.3 shows vertically stacked plots of four traces from figure 6.2, i.e. the bottom trace exhibits index one and the others show every fourth spectrum between index one and thirteen. Figure 6.4 shows the spectra that were obtained soon after preparation and one day later, with 34 minutes total accumulation time in absolute intensity mode and with the same vertical scale. All of these results show that there are no significant changes in the features of the spectra.

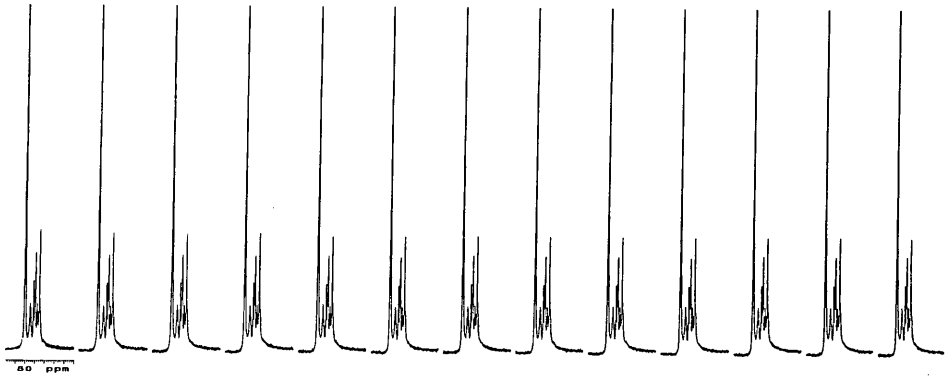

Figure 6.2. The evolution with time of the 130.3 MHz ^{27}Al spectrum of an aluminosilicate solution prepared by rapid mixing of fresh sodium aluminate and aged $HM(OH)_2$ silicate solutions, taken at ambient temperature ca. 22 °C and with the composition Si, Al=Na and template equal to 0.014, 0.014 and 0.028 molar respectively, i.e. [Si/Al]=1 (sample No. 278).

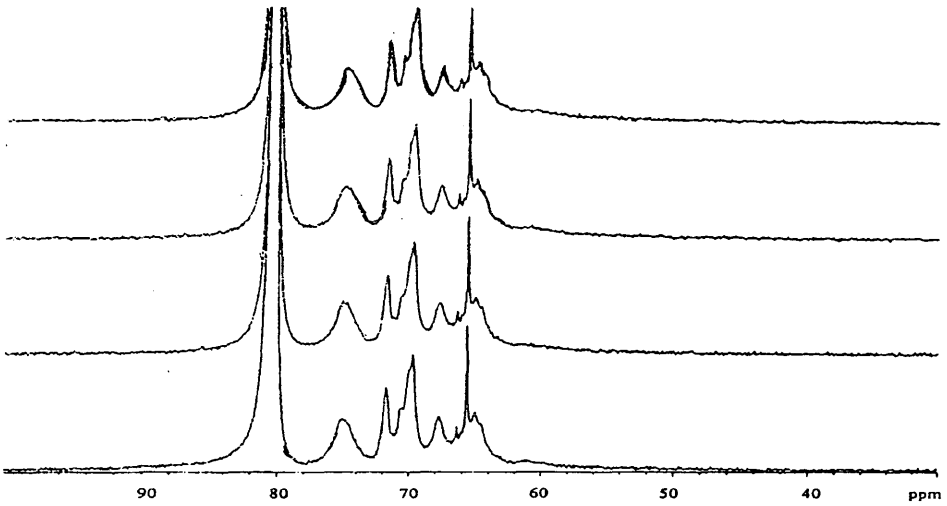

Figure 6.3. The vertically stacked plots of four spectra from figure 6.2. The bottom is index one, and the others are every fourth.

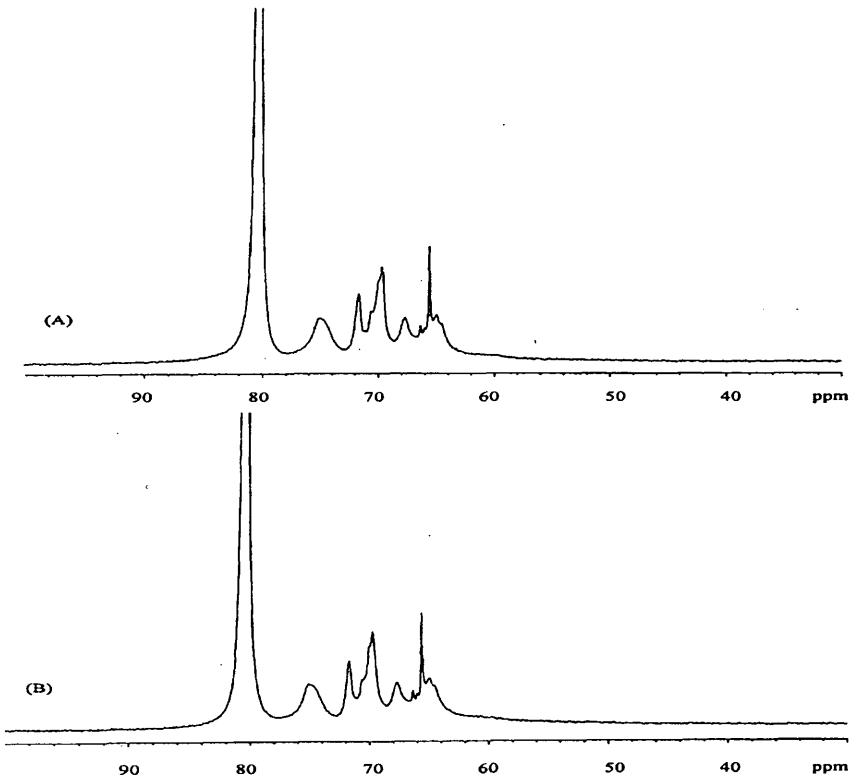

Figures 6.4. This shows spectra obtained A) soon, and B) one day after preparation for sample 278 with 34 minutes total accumulation in absolute intensity mode and with the same vertical scale. Spectrum conditions were as discussed for figure 6.1.

b) In the same way as for $HM(OH)_2$, the spectra of the HMBTP, TMA, TEA, TPA and TBA aluminosilicate solutions were examined and have not shown significant differences between spectra obtained soon after preparation and those from the corresponding aged solutions. For another typical example, see figure 6.5. Therefore, it can be concluded that these solutions quickly equilibrate and later re-equilibration cannot be clearly shown.

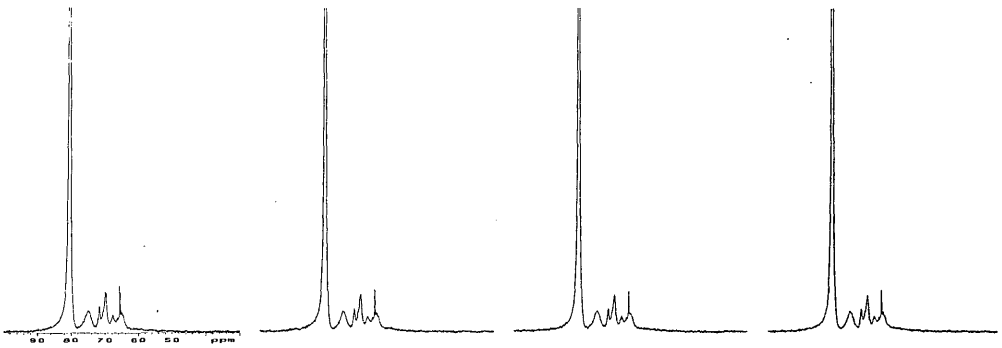

Figure 6.5. This shows horizontally stacked plots from index 1 to 13 (every fourth spectrum) of the HMBTP/NaOH aluminosilicate solution with the same concentrations of Al, Na and Si and also the same spectral conditions as for figure 6.1.

c) Figure 6.6 shows 18 of 25 spectra illustrating the evolution with time of a ^{27}Al NMR spectrum of KOH aluminosilicate solution with the composition listed in table 1 (sample 275), obtained by rapid mixing of fresh sodium aluminate and aged KOH silicate solutions. The spectra were taken under the same conditions as above, with no time interval between them. Each spectrum was obtained from ten minutes accumulation time. The bottom trace is index 1 and the top one is index 18. Of course the time evolution continues to the spectrum index 25. Figure 6.7 shows the spectrum of the above solution obtained 17 hours after preparation with 34 minutes total accumulation. The spectra in figure 6.6 were obtained in absolute

intensity mode. Hence, the peaks that are highest for the different times can be compared quantitatively. In contrast to the results obtained for the aluminosilicate solutions with organic bases, these figures show gradual changes in the spectra, i.e. re-equilibration. The signals in the q^3 and q^2 regions change and appear as broad bands. A broad band in the q^4 region has gradually appeared and grown.

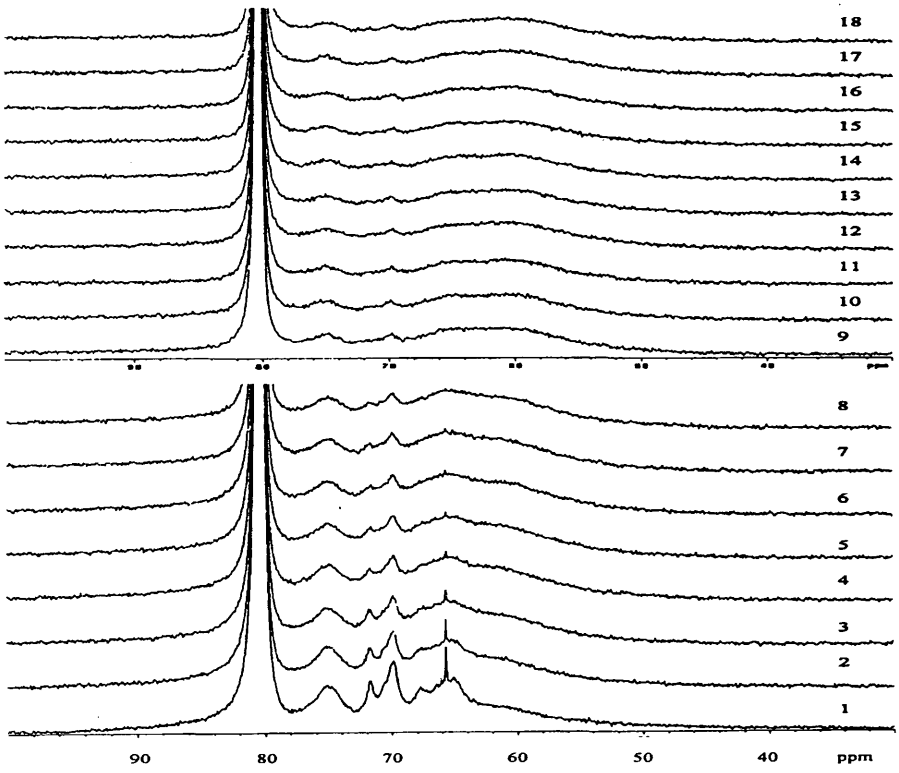

Figure 6.6. Vertically stacked plots of evolution with time of the ^{27}Al NMR spectra of KOH/NaOH aluminosilicate solution with the composition Al=Na, Si and KOH equal to 0.014, 0.014 and 0.028 respectively (sample 275) from index 1 to 18, by rapid mixing of fresh sodium aluminate and aged KOH silicate solution. Spectra were taken under same conditions, separated with no time interval. The bottom trace is index 1, the top one is index 18. The spectrum for index 1 was obtained in absolute intensity mode and the other indexes for each specific time are exclusively in the same format. The spectral conditions are the same as for figure 6.1. Each spectrum was obtained from ten minutes accumulation time with no time interval between them.

From these spectra, it can be concluded that the solution re-equilibrated after about 100 minutes of mixing. After that, the spectra show no change from index 10 to index 25 and to the spectrum in figure 6.7. The above conclusion has proved to be the main difference with the organic bases.

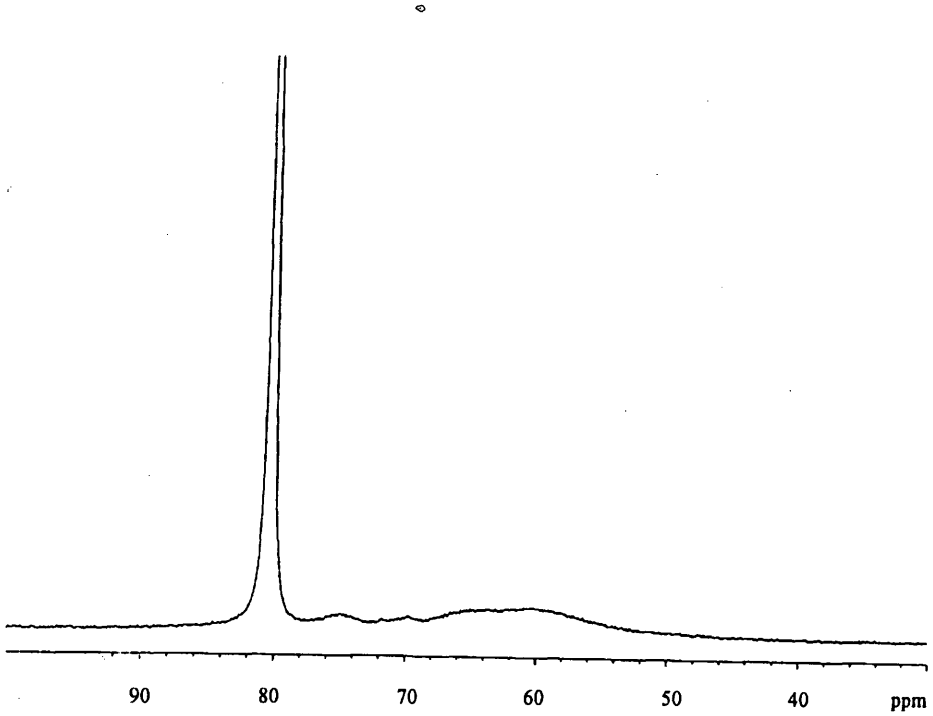

Figure 6.7 The spectrum obtained 17 hours after preparation for sample 275 with 34 minutes total accumulation time and with the spectral conditions discussed for figure 6.1.

d) A similar result was obtained by the method described in comment c but using NaOH aluminosilicate solution (sample 274, see table 1). The main differences are the intensity of the sharp peak at ca. δ=65.6 ppm and the time to re-equilibration. The sharp peak is more intense here in index one and this solution re-equilibrates quicker i.e. it equilibrates at index about 7 instead of index ten for the KOH aluminosilicate solution - see figure 6.8. It can be concluded that linkage of oligomerised species, in this solution is probably faster than for the KOH/NaOH case.

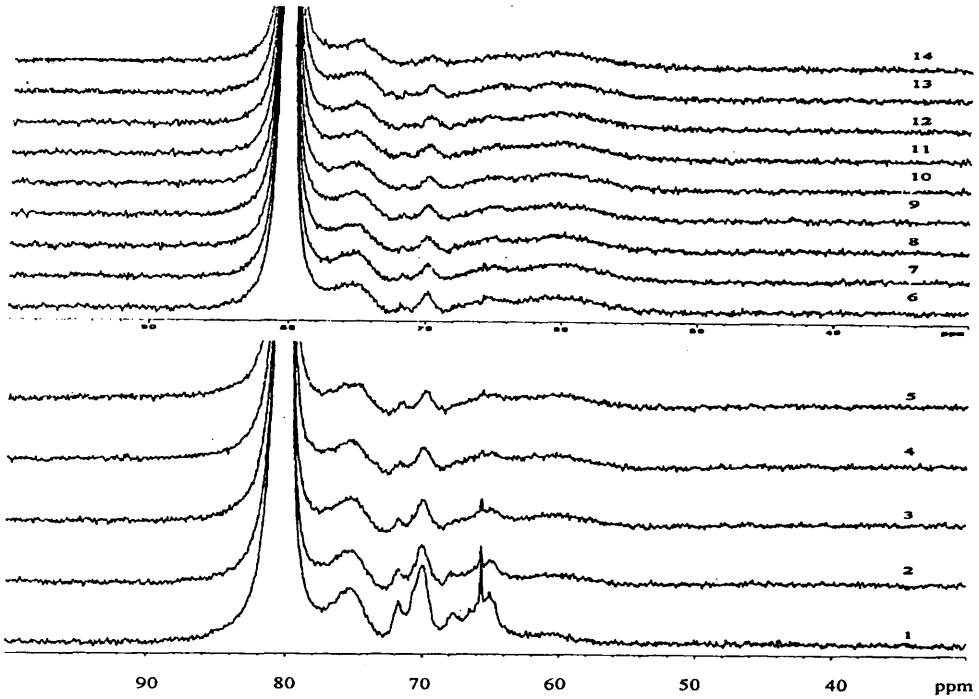

Figure 6.8. Vertically stacked plots of evolution with time for the ^{27}Al NMR spectrum of NaOH aluminosilicate solution with the composition Al, Si and NaOH equal to 0.014, 0.014 and 0.042 (total) respectively (sample 274) from index 1 to 18, following rapid mixing of fresh sodium aluminate and aged NaOH silicate solutions. Spectra were taken under the same conditions, separated with no time interval. The bottom trace is index 1, the top one is index 18. The spectrum for index 1 was obtained in absolute intensity mode and the others are exclusively in the same format. The spectral conditions are the same as given for figure 6.1.

Thus the alkali metal aluminosilicate solutions show some change, especially in the q^3 region, soon after mixing (first equilibration). The number of resolved bands decreases and they broaden or nearly disappear. However, the aluminosilicate species in the TAAOH aluminosilicate solutions do not change during the evolution time, which means they are stable at least at the concentrations used.

e) Sample 264 was prepared with the same composition as sample 274 except for the Al concentration equal to 0.028 M (and therefore the total Na^+

concentration is 0.056 M). It was measured soon after preparation, with an accumulation time of 34 minutes. The spectrum was repeated after another 20 minutes and again 4 hours later (see figure 6.9). The effect of ageing time is very significant.

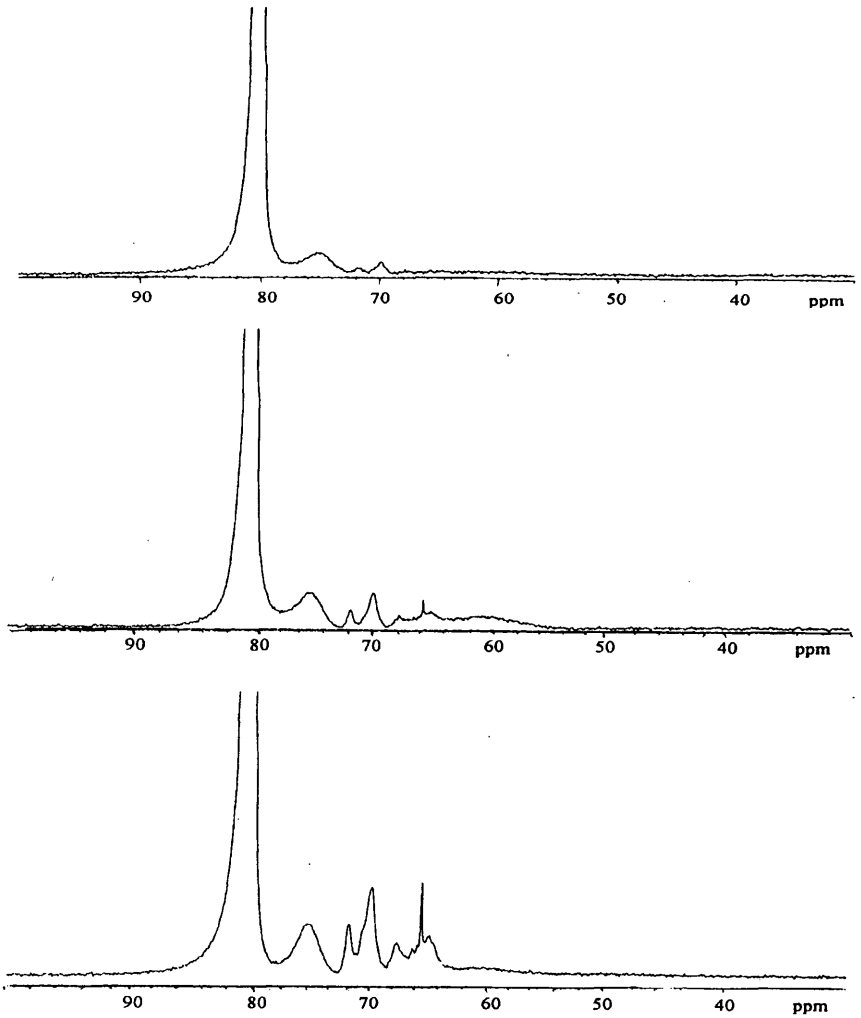

Figure 6.9. High-resolution ^{27}Al NMR spectra at 130.23 MHz and ambient temperature of a NaOH aluminosilicate solution with the composition Si, Al and template equal to 0.014, 0.028 and 0.056 (total) molar respectively, i.e. [Si/Al] = 1/2 (sample No. 264). The spectra were taken (from bottom to top) soon, 20 minutes and 4 hours respectively after preparation, with a total accumulation time of 34 minutes each in absolute intensity mode and with the same vertical scale. The spectrum conditions are the same as for figure 6.1.

f) Sample 265 was prepared with the same Al concentration as sample 274 but with Si and NaOH concentrations equal to 0.028 and 0.070 M (total) respectively. It was measured 30 minutes after preparation with a total of 34 minutes accumulation time (figure 6.10). In the same way as for sample 274, polymerisation shown in the q^3 and q^4 regions is quite significant.

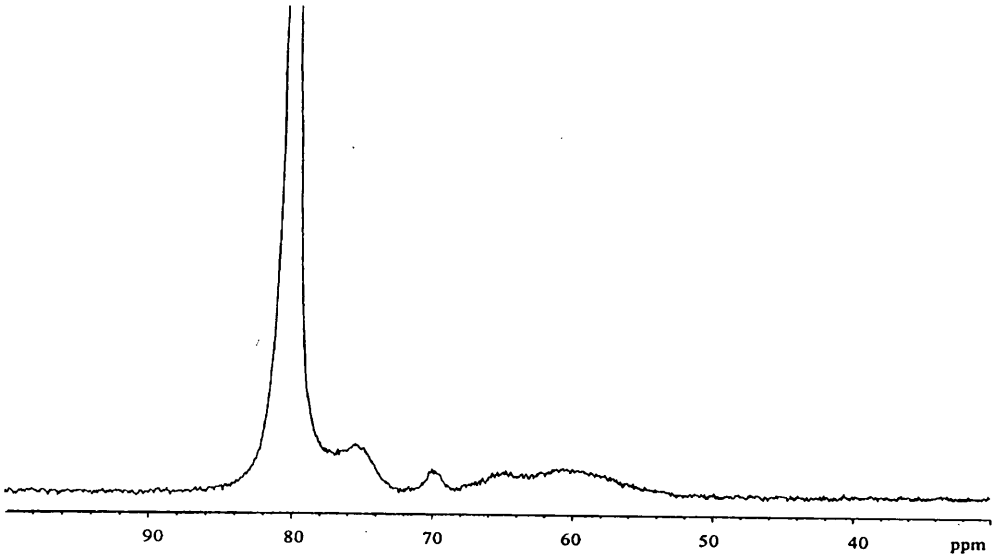

Figure 6.10. High-resolution ^{27}Al NMR spectra at 130.23 MHz and ambient temperature of a NaOH aluminosilicate solution with the composition Si, Al and template equal to 0.028, 0.014 and 0.070 (total) molar respectively, i.e. [Si/Al] = 1 (sample no. 265). The spectrum was taken soon after preparation with a total accumulation time of 34 minutes. The spectrum conditions are the same as for figure 6.1.

g) Finally, a very dilute solution with the composition Si=Al 0.0035 and NaOH=0.0105 (total) M was prepared (sample 272). It was measured approximately twelve hours after preparation with a total accumulation time of 34 minutes (figure 6.11). This spectrum does not show any q^3 or q^4 signals. By comparing with the conclusion for figure 6.8 it is shown that oligomerisation strictly decreases with decreasing Al and Na^+ concentrations (for the given Si concentration). This is presumably mainly a pH effect (see chapter 5),

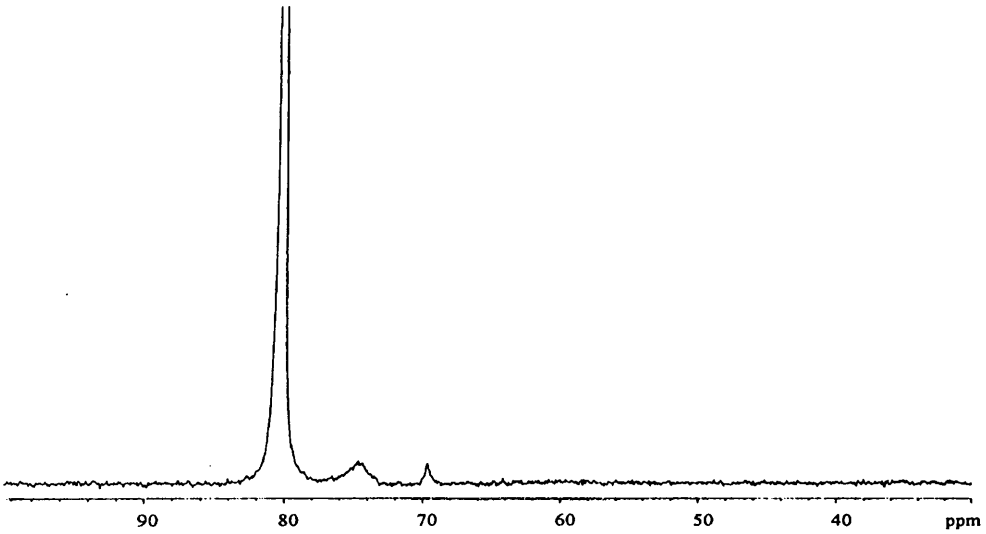

Figure 6.11. High-resolution ^{27}Al NMR spectra at 130.23 MHz and ambient temperature of a NaOH aluminosilicate solution with the composition Si=Al and template equal to 0.0035 and 0.0105 (total) molar respectively, i.e. [Si/Al] = 1 (sample no. 272). The spectrum was taken soon after preparation with a total accumulation time of 34 minutes. The spectrum conditions are the same as for figure 6.1.

6.5. Discussion

There is considerable interest in identifying the structure-directing effects of cations. In this thesis, it is shown that a very effective tool for this purpose in aluminosilicate solutions is ^{27}Al NMR spectroscopy. The results of the present study indicate that the distribution of aluminosilicate anions in aluminosilicate solutions (paralleling silicate anions in silicate solutions) is a function of both cation type and the concentration.

For alkali metal aluminosilicate solutions the first highly resolved spectra (analogous to those for TAA/Na aluminosilicate solutions) have been recorded (see figure 6.1). The linewidth and the number of resolved lines are shown to depend on several factors, such as solution composition, concentrations of components, temperature, pH, aging time and the type of cation. The effects of the last two parameters are examined here. For dilute

TAA/Na aluminosilicate solutions i.e. with the concentration of components lower than ca. 0.014 M, there are no substantial changes in the linewidths or the number of resolved lines, but in more highly concentrated solutions some changes could be seen but not as great as for the alkali metal aluminosilicate solutions (figures 6.2, 6.5, 6.6 and 6.8).

As has been discussed in a previous chapter,[17] one interesting thing about the spectra of all TMA aluminosilicate solutions is the sharp peak at ca. 65.6 ppm which is observed to be very significant. Also, in the present work, the spectra of solutions for the different templates, obtained soon after mixing, have shown this signal to vary significantly (see figure 6.1). In the spectra of TMAOH, $HM(OH)_2$ and NaOH aluminosilicate solution this signal is more intense than when the other cations are present instead. Moreover, in the dilute TAA aluminosilicate solutions the intensity of this signal is nearly constant with ageing, but with the alkali metal cation aluminosilicate solutions it gradually diminishes with time, presumably because of polymerisation. It can be deduced that these changes arise from the role of the template.

This work has implied that nothing happens in the spectra of ^{27}Al NMR when dilute TAA aluminosilicate solutions are aged. This is contrary to the observation of the time evolution for spectra of the alkali metal aluminosilicate solutions (figures 6.6 and 6.8), e.g. for samples 275 & 274, and to the more concentrated solutions, discussed in section 4.2.6 for sample 76 and in the work of Samadi-Maybodi.[15] There are at least four bands in the shift range 62 to 68 ppm on all the spectra in figure 6.1, but in figures 6.6 and 6.8 for the last index all these peaks have almost disappeared or broadened and coalesced into one peak. The spectra in figure 6.1 show there is no substantial difference between the spectra of alkali metal and TAA/Na^+

aluminosilicate solutions through the oligomerisation of species (at least in the initial equilibrium obtained soon after the preparation of the samples). However, after aging the solutions, differences appear for the alkali metal aluminosilicate solutions. It may be concluded that the pre-existing aluminosilicate anions (small oligomers) in this case polymerised (re-equilibration). To justify the differences between alkali metal aluminosilicate solutions and the TAA/Na^+ aluminosilicate solutions in the ^{27}Al NMR spectra one might in general say that relatively large aluminosilicate oligomers are stabilised preferentially by large templates such as TAA (which obviously are larger than Cs^+), and therefore the rate of formation of aluminosilicate polymers (re-equilibration) decreases with the size of the cation. This trend can also be seen in the series of alkali metal aluminosilicate solutions, for which re-equilibration is faster when Na^+ ions are present than for K^+ (see figures 6.6 and 6.8). This effect may demonstrate the anion-cation pairing effect (see comment a in section 6.2).

However, in the case of TAA aluminosilicate solutions the coulombic effect is not so important, and it is proposed that with increasing size hydrophobic solvation effects lead to a greater degree of water structuring rather than ion pairing effects. This promotes the maximum oligomerisation of aluminosilicate anions (not polymerisation) (figures 6.3 and 6.5). Counteracting the water structuring effect is the influence of ion crowding. With increasing cation size, the free volume available per silicate or aluminosilicate ion decreases. The time evolution experiment of TAA aluminosilicate solutions with the concentration 0.014 M illustrates that there are no substantial differences between templates at equilibrium (for instance see the last indexes of figures 6.5 and the spectrum (A) in figure 6.4).

To illustrate the cation crowding effect on the aluminosilicate speciation in TAA solutions, ^{27}Al NMR spectra of some solutions with constant Si, Al and Na concentrations (0.014 M) but differing TMAOH concentration in the range 0.007 to 4 M were obtained on a Bruker 500 MHz spectrometer at Tarbiet Modarres University. The features and the number of the peaks on the spectra show some differences, i.e. the intensity of q^0 increased while the number of signals decreased with increasing TMAOH concentration. This means the number of species in solution decreases with increasing TMAOH concentration. The most important observation is a relative decrease in the intensity of the q^3 signals assigned to the prismatic hexamer, and cubic octamer. However, it seems that the number of resolved signals in the q^3 region is considerably decreased with increasing TMAOH concentration. This occurs possibly because of polymerisation of the aluminosilicate species (re-equilibration), which causes the broadening of bands and/or maybe de-oligomerisation of the species and exchange between them. The last case is probable because it shows an analogous result to the ^{29}Si NMR studies of section 3.10.3. of Samadi-Maybodi's thesis,[15] in which the author deduced that Q^3_6 and Q^3_8 are broken up by increasing the amine concentration, since the Q^0 signal increases. At high concentrations of TMAOH (ca. pH ≅ 14), a narrow peak is observed at ca. 80.4 ppm, which can be assigned to $Al(OH)_4^-$. In highly basic solutions this is dominant. This observation once again strongly supports the role of the structure-directing TMAOH cation, and also the role of the cation crowding effect, demonstrating that in low concentrations of TMAOH the aluminosilicate anions are directed to the cage-like species derived from Q^3_6 and Q^3_8, but

in high concentrations these species are broken up into smaller oligomeric anions. However, it should be noticed that the pH of the silicate solutions decreases with decreasing TMAOH concentration, in this case from ca. pH=14 to ca. 10.5, i.e. the solutions become less basic. This is a critical parameter, since a study of the effect of pH on the distribution of silicate anions shows a similar situation (see chapter 5).

However, the ^{27}Al NMR spectra of Na, K and TAA aluminosilicate solutions in the initial equilibria exhibit, in addition to the $Al(OH)_4^-$ peak at about 80.4 ppm, at least three characteristic bands in the range 60-82 ppm which have been assigned to the various $Al(OSi)_n(O^-)_{4-n}$ building units, i.e. peaks at ca. 75.0, 71.8, 69.8, 67.8, 65.7, 65.1 and ca. 60 ppm may represent q^1, probably $q^2{}_\Delta$, q^2, $q^3{}_\Delta$, q^3, and probably q^4 environments respectively, which are clearly present very quickly after mixing. The assignment of these signals in detail was discussed in chapter 4 and 5.[17] The distribution of aluminosilicate species in alkaline metal aluminosilicate solutions is very similar for the initial equilibrium (figure 6.1) but different in the re-equilibrium from that observed in tetraalkylammonium (TAA) aluminosilicate solutions (see figures 6.2, 6.3, 6.5, 6.6 and 6.8). With aging the solutions, certain line broadenings are observed for alkali metal cation samples, especially in the q^3 and q^4 regions (figure 6.6 and 6.8). Alkali metal aluminosilicates are highly insoluble in neutral water,[10] and precipitates are immediately formed when, e.g., sodium silicate and aluminate solutions are mixed, unless the solutions are very dilute or contain only small proportions of aluminate. The spectra of alkali metal aluminosilicate solutions, unlike the TAA aluminosilicates, contain a broad band ranging from 58-70 ppm at the final equilibrium. Therefore, it may be deduced that the rate to form oligomeric aluminosilicate anions was fast compared to the rate for aqueous

TAA aluminosilicate solutions (figures 6.6, 6.8 and 6.2). Furthermore, increasing cation size (reduced ion pairing) gives the same result, as obtained by Swaddle and co-workers,[10] favouring aluminosilicate formation, and this is precisely as would be expected if, as proposed above, pairing of the smaller oligomers with cations deactivates them towards reaction with further silicate or aluminate units. However, the effect of cation size cannot be explained by the same arguments.

By considering the development of the features of the ^{27}Al NMR spectra resulting from evolution with time, one can conclude that the formation of the q^1, q^2, and q^3 sites is not necessarily step-by-step. In other words, building up the aluminium environment from q^1 to q^3 might occur simultaneously (see figures 6.1 & 6.2). However, the re-equilibration of q^2, q^3 and q^4 in the alkali metal aluminosilicate solutions needs time for completion (see figures 6.6 and 6.8). Such re-equilibration does not seem to occur for the TAA/Na aluminosilicate solutions. These processes can be expected, since, when the aluminate ions are introduced to the silicate solution, they are presented to a number of pre-existing silicate species,[18-21] for instance, monomer (Q^0), dimer (Q^1), cyclic trimer (Q^2_3), linear trimer ($Q^1Q^2Q^1$), prismatic hexamer (Q^3_6) and cubic octamer (Q^3_8). Initial insertion of Al into silicate anions occurs simultaneously, and the rate of equilibrium is very fast (figure 6.1), but re-equilibration of the aluminosilicate species for TAA/Na aluminosilicates is very much slower (usually not detectable on the timescale of the experiments) than when purely alkali metal cations are used.

Therefore it can be concluded that dilute aqueous solutions of aluminosilicates equilibrate rapidly to a mixture of anionic species,

including chains, branched systems and cyclic units (see figure 6.1 which was measured immediately after mixing). The solutions reached the initial equilibrium very rapidly, i.e. after about five minutes. Linking the oligomers to reach re-equilibrium indicates that intrinsic differences exist in the interactions involving TAA cations and those involving alkali metal cations. However, the situation is complicated because of the sensitivity of the equilibria to concentration, pH, template and temperature.

6.6. Conclusion

This work has shown that it is possible to obtain high-resolution ^{27}Al spectra of alkali metallic aluminosilicates. These contain at least 9 aluminium sites, corresponding to a range of anionic aluminium-containing species. In dilute solution for the same silica, aluminate and cation concentrations intrinsic differences for different cations are found only at the re-equilibration stage. The nature of the cations in solution is known to affect the distribution of anionic species and the structure of zeolites which may be formed from such solutions. Alkali metal aluminosilicate solutions exhibit a similar distribution to the TAA/Na case at first equilibrium, but this distribution, in contrast to the TAA/Na solution, is not stable, the species quickly re-equilibrating so that broad signals of q^3 and perhaps q^4 appear. The results indicate that intrinsic differences exist in the interactions involving TAA cations and those involving alkali metal cations. The rate of aluminosilicate anion oligomerization increases with increasing alkali metal cation size at the initial equilibration stage and decreases in the re-equilibration. The effects of cation size are subtle and do not correspond to simple extension of the reasoning for alkali metal cations. However, the interaction between aluminate and silicate ions is greatly influenced by the alkali concentration.

6.7. References

1. B. M. Loc, T. R. Cannan, and C. A. Messina, *Zeolites* **3,** 282, (1983).
2. R. M. Barrer, *'The hydrothermal chemistry of zeolites'*, Academic press London, UK, p. 157 (1982).
3. W. M. Hendricks, A. T. Bell, and C. J. Radke, *J. Phys. Chem.* **95**, 9513 (1991) and references therein.
4. R. K. Harris and A. Samadi-Maybodi, *Zeolites,* 19, 147 (1997).
5. A. V. McCormick, Ph.D. Dissertation, Department of chemical Engineering, University of California, Berkely, CA, (1987).
6. F. Liebau, *The Structural Chemistry of Silicates*; Springer-Verlag: Berlin, (1985).
7. J. D. Worely and I. M. Klotz, *J. Chem. Phys.* **45**, 2868, (1966).
8. G. Engelhardt, *Z. Anorg. Chem.* **22**, 484 (1982).
9. A. V. McCormick, A. T.Bell and C. J. Radke, *Catal Rev. Sci. Eng.*, **31,** 97 (1989).
10. T. W. Swaddle, J. Salerno and P. A. Tregloan, *Chem. Soc. Rev.,* 319 (1994).
11. D. S. Kinrade and T. W. Swaddle, *Inorg. Chem.*, **28**, 1952 (1989).
12. R. F. Mortlock, A. T. Bell and C. J. Radke, *J. Phys. Chem.*, **95**, 7847 (1991).
13. R. F. Mortlock, A. T. Bell, A. K. Chakraborty, and C. J. Radke, *J. Phys. Chem.*, **95,** 4501 (1991).
14. G. Engelhardt and D. Michel, *"High-Resolution Solid-State NMR of Silicates and Zeolites"*, Wiley, New York, (1987).
15. Ph.D. Thesis. A. Samadi-Maybodi, *"NMR studies of silicate and aluminosilicate solution as precursors for zeolites."*, University of Durham (1996).

16. T. Yokoyama, S. Kinoshita, H. Wakita and T. Tarutani, *Bull. Chem. Soc. Jpn.,* **61,** 1002 (1988).

17. A. Samadi-Maybodi S. N. Azizi, H. Naderi-Manesh, H. Bijanzadeh, I. H. McKeag and R. K. Harris, *J. Chem. Soc., Dalton Trans.*, 633 (2001).

18. R. K. Harris, C. T. G. Knight and W. E. Hull, *J. Am. Chem. Soc.,* **103**, 1577 (1981).

19. R. K. Harris and R. H. Newman, *J. Chem. Soc., Faraday Trans.,* **73**, 1204 (1977).

20. R. K. Harris, J. Jones, C. T. G. Knight and R. H. Newman, *J. Mol. Liq.*, **29**, 63 (1984).

21. C. T. G. Knight, R. J. Kirkpatrick and E. Oldfield, *J. Am. Chem. Soc.* **109**, 1632 (1987).

Chapter Seven

NMR studies of aluminosilicate solutions that change to the gel phase

7.1. Introduction

Zeolites crystallise from amorphous alkaline aluminosilicates under the action of heat and pressure. A crystalline zeolite can also be studied by a variety of methods including crystallography and NMR, but the intermediate phase, the gel, has proved very resistant to any type of study. The aim of this work, therefore, was to delay the formation of the gel long enough to investigate the precursor solution (because solutions are generally easier to study than gels), and also to seek evidence for gel formation from solutions, by the use of ^{27}Al NMR liquid-phase spectroscopy. When an alkaline silicate solution and a specific concentration of alkaline aluminate solution are mixed, a white amorphous precipitate or gel normally forms, the amount of gel depending on Al and Si concentrations and the time of formation. It is possible to produce aluminosilicate solutions that remain clear for times varying from five minutes to several days before eventually the particles aggregate into three-dimensional networks and form gels.

7.2. Experiment.

In order to consider the effects of Al and Si concentrations on achieving the gel point, 6 sets of aluminosilicate solutions were prepared so that for each set of 5 samples the Al (equal to Na) concentration was held constant but the Si concentration changed by factors of 2, 4, 6 and 7.5. Also, the Al and Na concentrations changed by a factor 2 from one set to the other. Samples were prepared as discussed in previous chapters and stored in plastic bottles at room temperature (ca. 25 °C). The gel times (determined by observation) and the composition data are listed in tables 7.1-4. At the time of mixing all solutions were clear. The "gel time" is defined as the time from mixing to the point when some colloid particles appeared in the solution, as judged visually.

Table 7.1. Data for aluminosilicate solutions which did not form gel phases after one year.

Sample No.	Molarity TMAOH	Molarity Si	Molarity Al ≡ Na atom	[Si]/[Al] ratio	[Si]/[TMAOH]
1=51	0.028	0.014	0.014	1	0.50
2=52	0.056	0.028	0.014	2	0.50
3=53	0.084	0.056	0.014	4	0.50
4=54	0.105	0.084	0.014	6	0.50
5=55	0.210	0.105	0.014	7.5	0.50
6=56	0.028	0.014	0.028	0.5	0.50
7=57	0.056	0.028	0.028	1	0.50
8=58	0.084	0.056	0.028	2	0.50
9=59	0.105	0.084	0.028	3	0.50
10=60	0.210	0.105	0.028	3.75	0.50
11	0.028	0.014	0.056	0.25	0.50
12	0.056	0.028	0.056	0.5	0.50
13	0.084	0.056	0.056	1	0.50
14	0.105	0.084	0.056	1.5	0.50
15	0.210	0.105	0.056	1.875	0.50
32-2	1	0.875	0.175	5	0.875
32-3	1	0.875	0.000	-	0.875

Table 7.2 Data for aluminosilicate solutions which formed gel phases after ca. one year.

Sample No.	Molarity TMAOH	Molarity Si	Molarity Al ≡ Na atom	[Si]/[Al] ratio	[Si]/[TMAOH]
16	0.028	0.014	0.084	0.167	0.50
17	0.056	0.028	0.084	0.334	0.50
18	0.084	0.056	0.084	0.667	0.50
19	0.105	0.084	0.084	1	0.50
20	0.210	0.105	0.084	1.25	0.50

Table 7.3. Data for aluminosilicate solutions which formed gel phases after about one week.

Sample No.	Molarity TMAOH	Molarity Si	Molarity Al ≡ Na atom	[Si]/[Al] ratio	[Si]/[TMAOH]
26	0.028	0.014	0.112	0.125	0.50
27	0.056	0.028	0.112	0.25	0.50
28	0.084	0.056	0.112	0.5	0.50
29	0.105	0.084	0.112	0.75	0.50
30	0.210	0.105	0.112	0.938	0.50

Table 7.4. Data for aluminosilicate solutions which formed gel phases after less than one day.

Sample No.	Molarity TMAOH	Molarity Si	Molarity Al ≡ Na atom	[Si]/[Al] ratio	[Si]/[TMAOH]	Observed gel time
21	0.028	0.014	0.140	0.10	0.50	After ca. one day
22	0.056	0.028	0.140	0.20	0.50	,,
23	0.084	0.056	0.140	0.40	0.50	,,
24	0.105	0.084	0.140	0.60	0.50	,,
25	0.210	0.105	0.140	0.75	0.50	,,
78	0.21	0.105	0.210	0.50	0.50	After one hour

To observe aluminosilicate species, both silicon-29 and aluminium-27 NMR spectra were obtained using a Varian Inova 500 MHz spectrometer. The ^{27}Al and ^{29}Si chemical shifts are quoted with respect to the signal for 1 M aqueous $AlCl_3$ (implying the $Al(H_2O)_6^{3+}$ ion) and TMS respectively, as usual, and were obtained by the replacement technique, with D_2O field/frequency locking. Because of the Al quadrupole effect, the ^{29}Si signals are not detectable at low concentrations of Si, but the solutions with the highest concentrations (samples 32-2 and 32-3) did allow detection. The Q^0, Q^1 and Q^2 signals are considerably broadened.

The probe used for these experiments involved components containing aluminium, so that a broad background signal centred at δ_{Al} ~60 ppm (the same region as the q^4 peak) could be observed. Several ways of compensating for this signal were tried (see chapter 2). Whereas spectra of good apparent quality were obtained, making many aspects of interpretation easier, it did result in uncertainties regarding the extent of the true q^4 signal from the aluminosilicate solutions. Moreover, phasing the spectra was not easy because the background signal invariably had a different phase from those of the peaks arising from the solution.

7.3. Result and discussion

Figure 7.1 was recorded as soon as possible after preparing the solution of sample No. 78. The solution contains total TMAOH, Al and Na concentrations equivalent to 0.21 M, with a Si concentration of 0.105 M. The spectra of figure 7.2 show horizontally and vertically stacked plots of the first five of 30 spectra of the evolution with time of an aluminosilicate solution prepared by rapid mixing of fresh sodium aluminate and aged tetramethylammonium silicate solutions, with the same concentration as sample 78, taken at ambient temperature (ca. 22 °C). The spectra were recorded by 5 minutes accumulation on each trace under the same conditions, separated by 30-minute intervals for ca. 17 hours; i.e. in figure 7.2 the first spectrum (index 1) was obtained soon after mixing by 5 minutes accumulation time and the last one (index 5) after ca. 140 minutes. In figure 7.3 the first spectrum is for index 1, the middle is for index 15, and the third is for index 30. The q^0 and q^1 signals in figure 7.1 and also in index 1 of figure 7.2 are in fast exchange and are fully coalesced, appearing as just one intense signal. The exchange effect has been confirmed by a spectrum run at lowered temperature (ca. 0°C), which showed no such broadening. The q^0 signal is very intense, so that if it is obtained on scale the other peaks can scarcely be seen. However, it is kept at a constant height for all the traces of figures 7.2 and 7.3. Figure 7.2 shows what happens to the spectra as the solution aged. Obviously changes can be seen from index one to three, but after this all traces remain the same, and this is in agreement with the gel time observed by eye. The peak at about 80 ppm, assigned to coalesced q^0 and q^1 sites, is the most intense throughout, while the peaks corresponding to q^2 and q^3 (and probably q^4) become less intense from index one to three, and after this step remain the same. These spectra illustrate that this solution took

1 hour to gel at 22 °C. In warmer conditions, gelation was rather more rapid. The peaks observed are essentially the same as those of the remaining solution (obtained after filtration of gel); peaks due to the semi-solid gel would be line-broadened and thus unlikely to be detected.

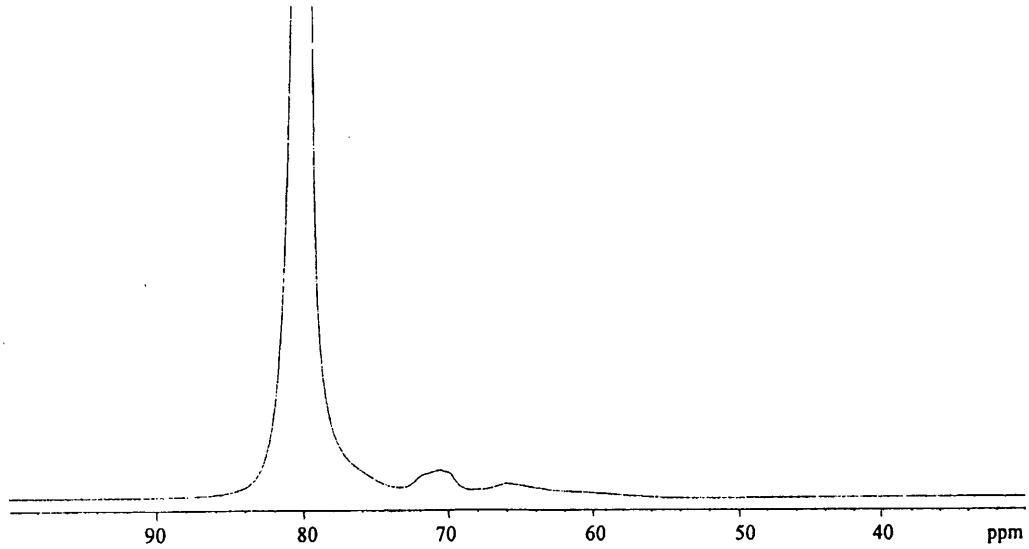

Figure 7.1. 130.23 MHz ^{27}Al spectrum of a tetramethylammonium aluminosilicate solution of composition 0.105 molar SiO_2 and Si/Al = 1/2 molar ratio (sample No. 78) taken at ambient temperature soon after mixing the TMAOH silicate and fresh sodium aluminate solutions. Spectrometer conditions are as follows: Recycle delay 0.2 s. Acquisition time 0.164 s. Number of transients ca. 900. Spectral width: 25000 Hz. Pulse angle 29.9 degrees.

The solution soon after preparation was clear, and over a period of time clouded and gelled. As this happens, peaks assigned to the higher complexes reduce in intensity relative to the q^0 peak. This may indicate that the higher complexes are drawn preferentially into the gel, and are then no longer detectable by NMR. By considering the concentrations of the samples listed in the above tables and some of the spectra which were obtained from these solutions, it could be concluded that the gel time strongly depends on the Al concentration in aluminosilicate solutions, especially in dilute silicate (i.e. [Si]<0.1 M). Thus, by varying the Al concentration from A= 0.014

→B= 0.084 →C= 0.112 →D= 0.140 to E= 0.21 M, the gel times are ca.: A= the solution remained clear for a long period of time, B= one year, C= one week, D= one day and E=one hour.

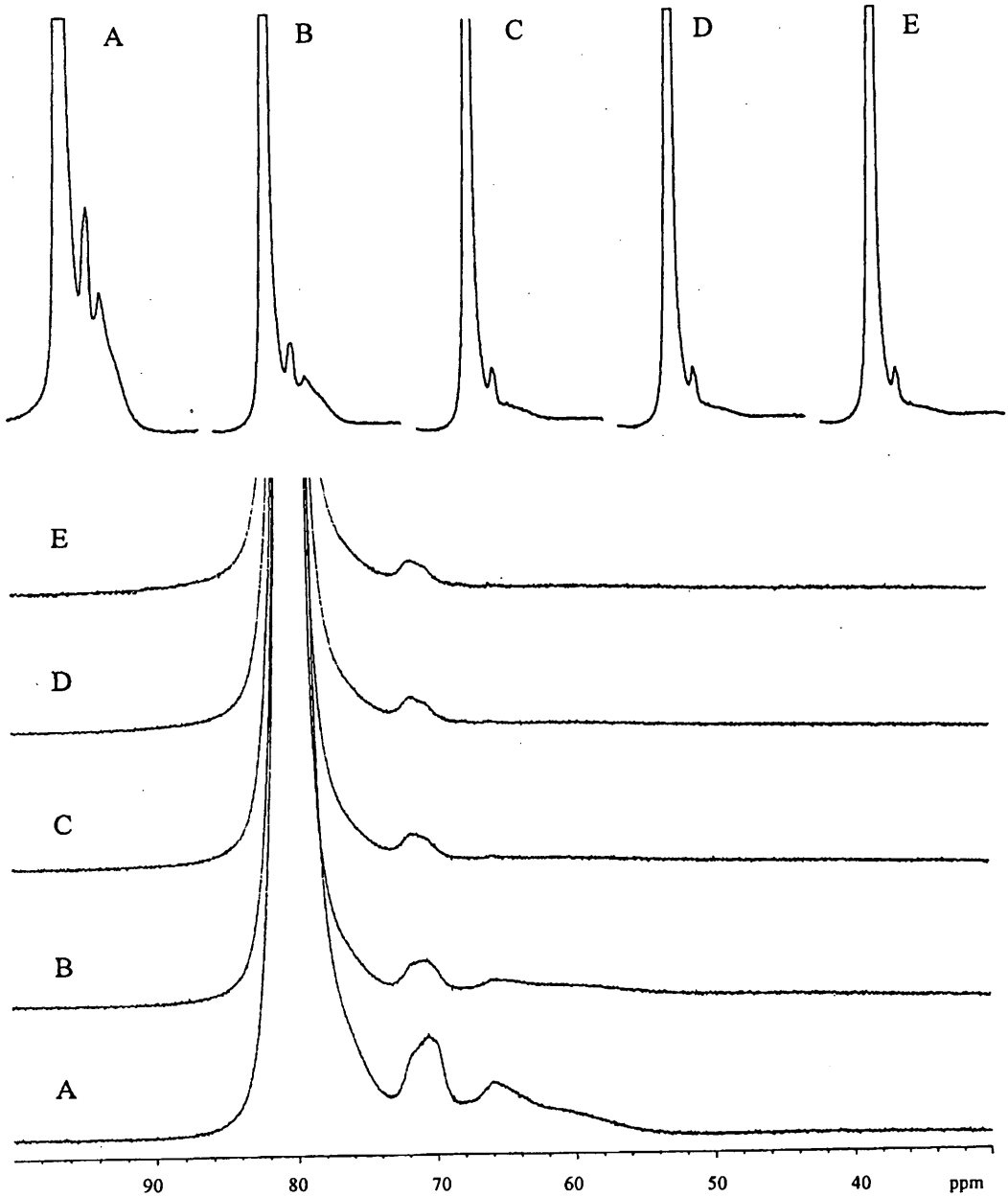

Figure 7.2. Vertically and horizontally stacked plots of evolution with time of the first 5 ^{27}Al NMR spectra for a solution with the composition the same as sample 78 as the time progressed (see text). The spectrum A (which is index 1) was obtained in absolute intensity mode and the other indexes are exclusively in the same format. Spectrum conditions: Spectral width 25000 Hz. Acquisition time 0.164 s. Recycle delay 0.20 s. Number of transitions 900. Pulse angle 29.9 degrees.

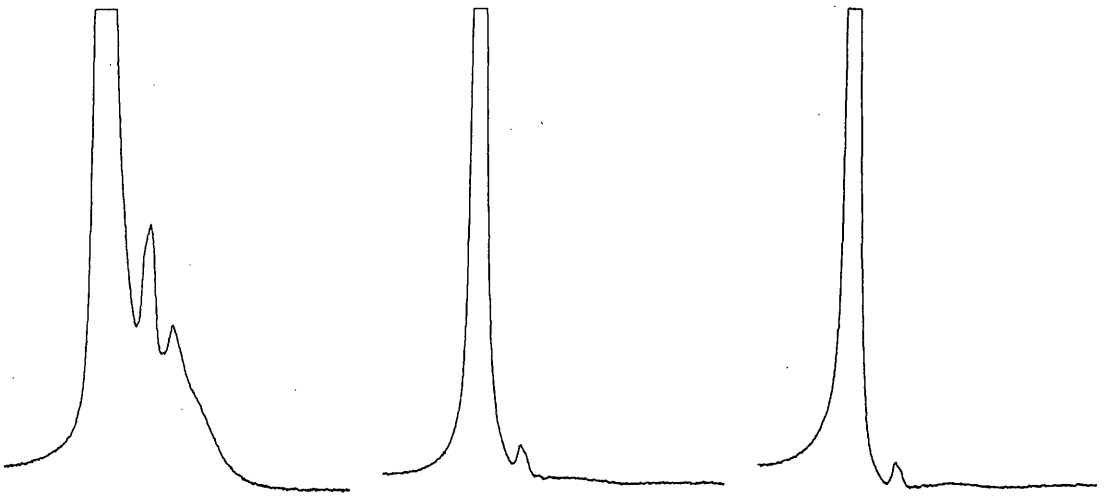

Figure 7.3. Shows three spectra (indexes 1, 15 and 30 from left to right) of the time evolution experiment of sample 78.

Samples No. 26-30 (table 7.3) were measured one and four days after preparation and also samples 27 and 28 one year after preparation (see the stacked plots of figure 7.4 in three columns A, B and C, which were obtained one day, four days and one year after preparation respectively. In these solutions the gel phase appeared (monitored by eye) after ca. one week. Also, when the solution was aged for full equilibration, the amount of gel increased when the Si concentration increased at constant Al concentration. This fact is obviously shown in the spectra; see column A of figure 7.4 (sample nos. 26-30), spectra recorded after one day, and also column B, four days after preparation. In the spectra in column A, the q^4 signal gradually appeared and grew. By looking at the features of the spectra in column B, conversely, the signal located from 54 to 64 ppm that belongs to q^4 species can be seen to decrease in comparison with the same solution in column A. This can be expected, since the greater the amount of colloid the more polymerised species are present and/or coagulation has occurred and therefore NMR can not detect all the ^{27}Al, in part because of the problems caused by the presence of the probe background signal.

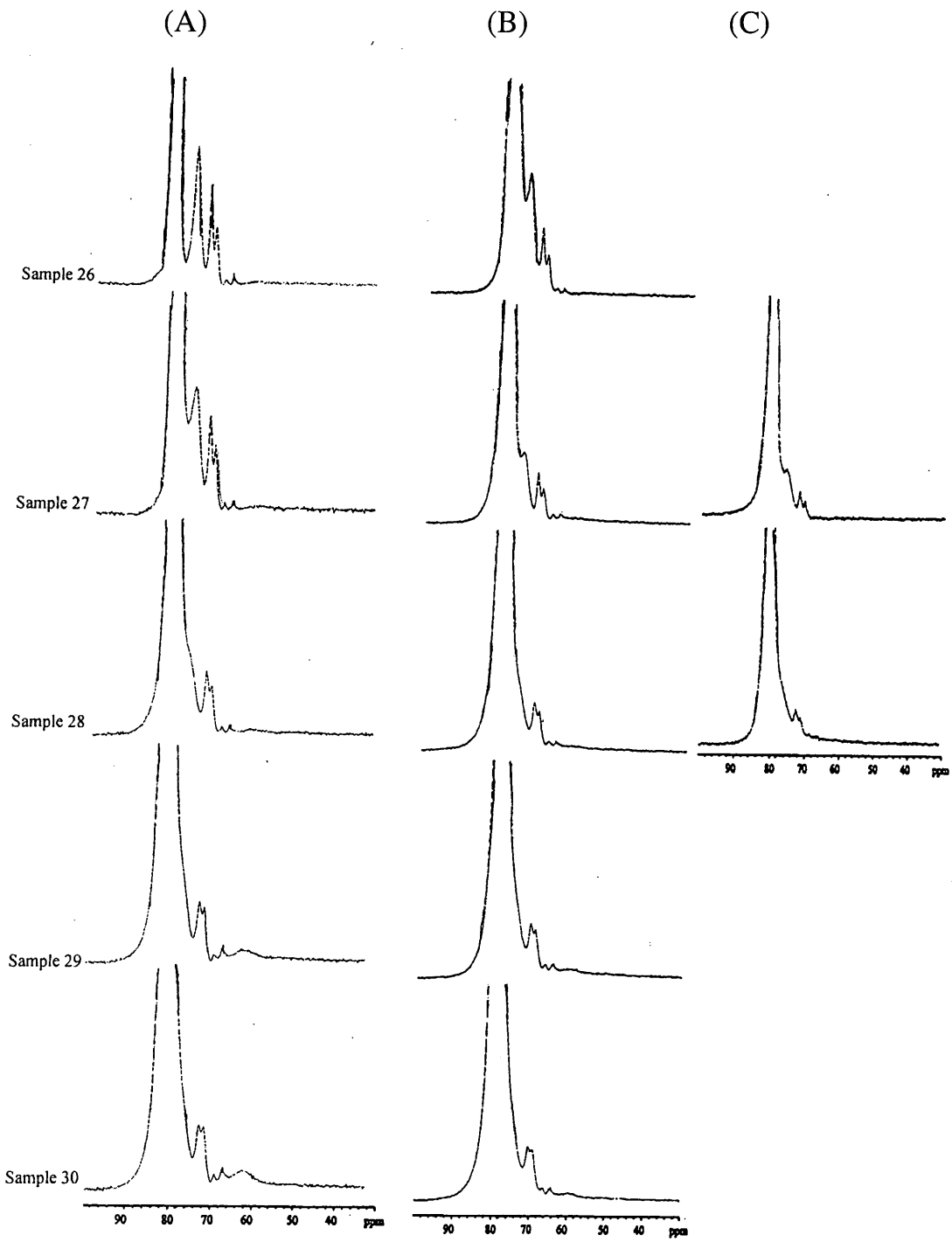

Figure 7.4. Vertically stacked plots of the spectra of samples 26-30 from top to bottom which were obtained (A) one day (B) four days and (C) (for samples 28 and 29 only) one year after preparation. Spectrum conditions: Spectral width 51981.8 Hz. Recycle delay 0.1 s. Acquisition time 0.1 s. Pulse angle 29.9 degrees. Number of repetitions 4000

In aged solutions, when gelation is complete and particles have grown, just q^0 and perhaps q^1 and q^2 signals in very low intensity can be observed, with no q^4 signal detectable (probably because backward linear prediction removes it): See the spectra of column C in figure 7.4, which were obtained one year after preparation for samples 27 and 28, and also figures 7.2 and 7.3. Figure 7.5, obtained for solution samples nos. 21-25 (table 7.4) six months after preparation, are also relevant. The changes occur because NMR can detect very small particles containing q^4 species, but as the particles grow, the q^4 region can no longer be properly detected because the signal is confused with the background. Such a conclusion can be extended to q^3 species, since again corresponding signals, on increasing the amount of colloid, decreased in intensity and eventually could not be detected after BLP, see the spectra in figures 7.4 and 7.5.

In general, the spectra in column A from samples 26 to 30, which keep the Al concentration constant but for which the Si and TMAOH concentration increased by a factor 2, show that the q^0 and q^1 signals for sample 26 are resolved but gradually coalesce with each other. For sample 30 they are fully coalesced and appear as one signal. The same result is seen for the spectra in column B, obtained 4 days after preparation. By looking at the spectra in column A it can be concluded that with increase in the degree of coalescence the intensity of the q^4 signal also increases. This is also in agreement with the visual fact that sample 30 shows the coagulated gel more than sample 26. However, the q^2 signal seems to remain the same in all spectra (at least up to 4 days). Spectra of samples 27 and 28 taken at different times (figure 7.4) show that, before completion of gelation, the two signals for q^0 and q^1 are in partial coalescence, while during the gelling time

the signals appear to fully coalesce and the q^4 signal intensity decreases (which is more obvious for samples 29 and 30). The spectra in column B (sample nos. 26-30) and column C (samples 27 and 28), which were recorded four days and one year after preparation respectively, show approximately no q^4 signal. The above conclusion can be confirmed: when the time for completion of gel formation increases, the features of the spectra, which are obtained, are nearly the same (see the spectra in figure 7.5). Obviously, this gelation process can occur slowly, as it is observed in the time-evolution. It should be pointed out that for the spectra which were recorded after six months, only one signal, in the q^0 position, could be clearly observed, see figure 7.5 (sample nos. 21-30), set at a very high vertical scale so that any other signals can be seen.

The shortest gel times of all are observed when the silicate solution is premixed with excess Al (ca. 0.25 M) for moderately low Si and TMA concentrations. By comparing features of the spectra for samples 1-20, which were discussed in chapter 3, samples 26-30 in columns A and B in figure 7.4 (detected one and four days after preparation respectively) samples 21-25 (figure 7.5) and also sample 78 (figures 7.1-7.3), it can be concluded that the extent of aluminate/silicate association increases in this order. Also, this conclusion is obtained from section 4.2.3a-b. Therefore, the Al concentration seems to be critical for the gel formation time, while the Si concentration is also important for the amount of gel phase. When the former is present in large quantities (more than ca. 0.25 M), gel is formed in less than one hour (almost instantaneous) at room temperature. However, aluminium appears to complex preferentially with any larger silicate species that are present, and these complexes, once formed, polymerise further only slowly. The Al NMR spectra confirm this interpretation. For more detail of

the effect of Al concentration, see section 4.2.3a. Some other factors that influence the gelation of the solutions generally were found to be; cation present, pH and temperature.

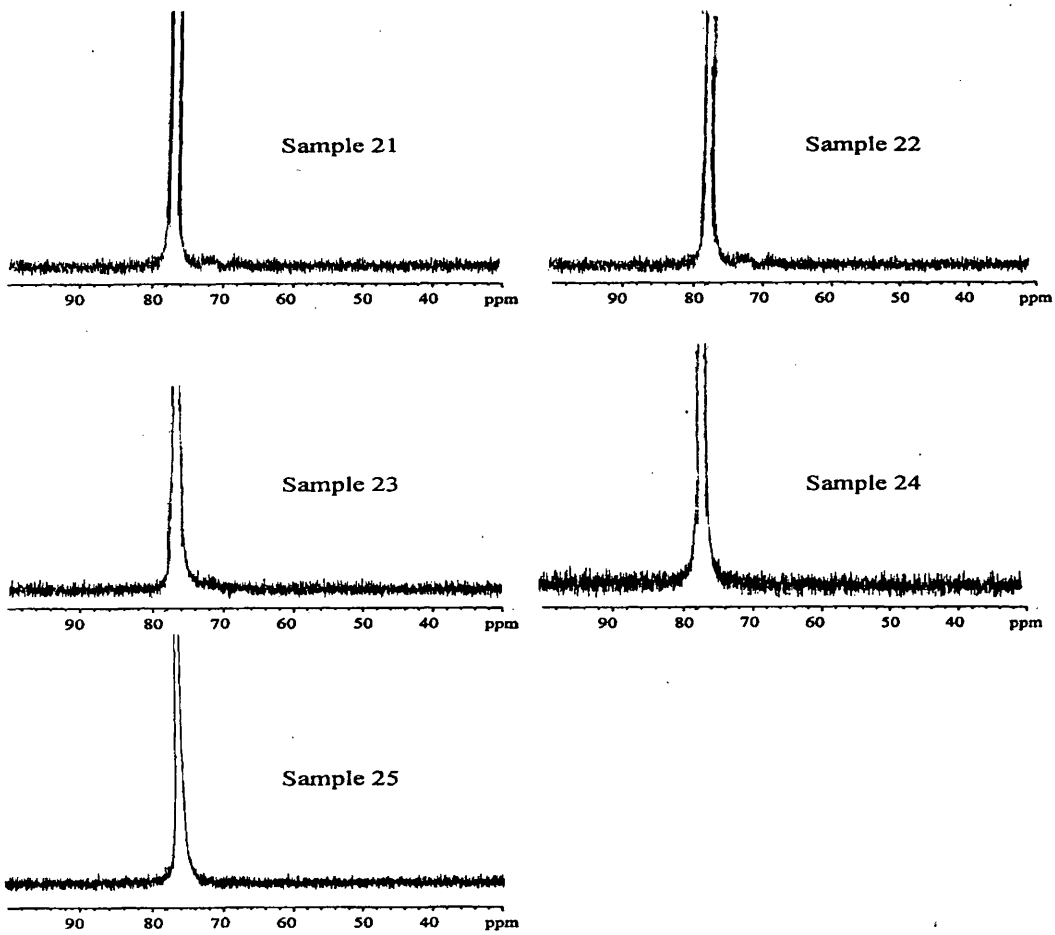

Figure 7.5. High-resolution ^{27}Al NMR spectra at 130.23 MHz and ambient temperature (ca. 22 °C) of tetramethylammonium aluminosilicate solutions (sample nos. 21-25) with the compositions listed in table 7.4. The spectra were taken six months after preparation. Spectrum conditions: Recycle delay 0.150 s. Acquisition time 0.158 s. Spectral width 28591.9 Hz. Pulse duration 40.0 μs. Number of repetitions for samples 21-25: 300000, 300000, 151253, 83008 and 182272 respectively.

Figure 7.6 shows a schematic representation of the formation of the gel phase as a function of Al and Si concentrations and the observed gel

times for tetramethylammonium aluminosilicate solutions. The time, obtained by observation, and the Si and Al concentrations are drawn from tables 7.1-7.4. This scheme obviously shows that, for a solution with an Al concentration lower than ca. 0.084 M at room temperature, the gel phase does not appear, but with increasing Al concentration in a similar Si concentration under the same experimental conditions the gel time scarcely decreased. This also illustrates that the gel time is not dependent on the Si concentration. However, the *amount* of coagulant species in the gel phases of the solutions depends on the Si concentration, but does not appear in this scheme.

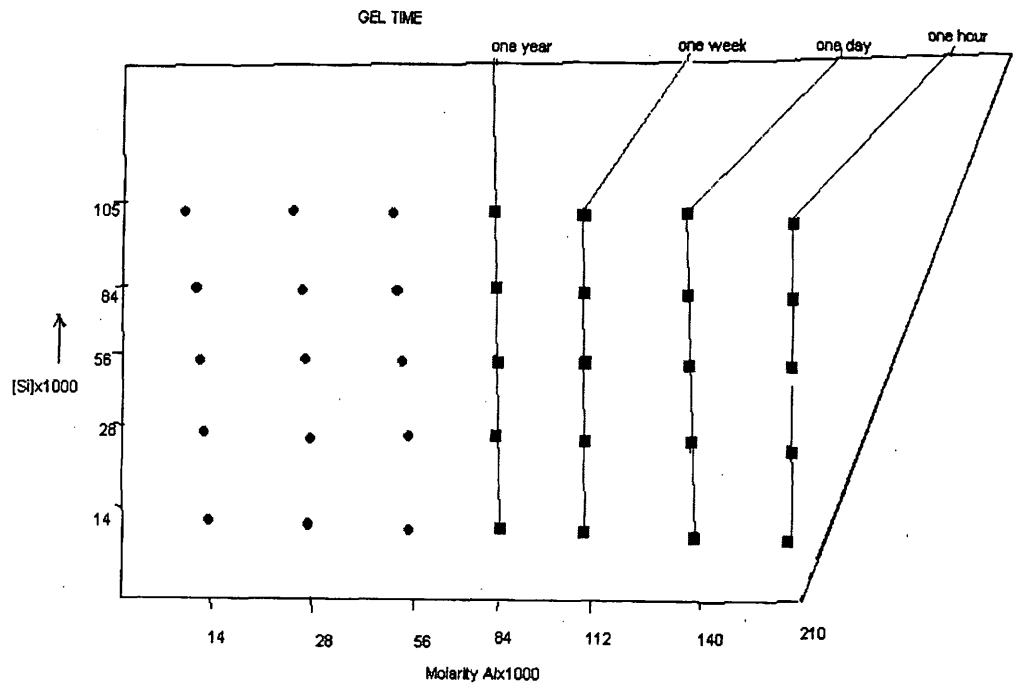

Figure 7.6. Schematic representation of the formation of gel phase for tetramethylammonium aluminosilicate solutions. Circles represent a solution composition from table 7.1 that has not converted to gel one year after preparation at room temperature, and squares indicate a solution composition from tables 7.2-4 that showed gel phase.

Why should aluminium preferentially react with the larger silicate species? The reason may be due to the charge density of the silicate anions. A monomeric (Q^0) ion could theoretically carry a charge of up to –4, although even in very alkaline solutions it will probably be protonated to some extent. Dimers, and other Q^1 units, can carry a maximum of three negative charges per silicon, but Q^2 and Q^3 silicon species can carry at most two and one negative charges respectively. Thus the larger the silicate species, the smaller its average negative charge per silicon, and the easier it will be for it to approach the $Al(OH)_4^-$ group.[1]

Such large species may well wrap themselves around the central aluminium and react further, once bonded to the aluminate group; this is consistent with the observation that the peaks assigned to q^2, Al(2Si), and q^3, Al(3Si), are frequently more intense than the q^1 , Al(1Si), peak (figures 4.21 and 4.22). In this way, the aluminosilicate cages can form Al-O-Si bridges to give more condensed structures without breaking Si-O-Si bonds, consistent with Hoebbel's [2] observations on the formation of double-four-ring aluminosilicates. This is also consistent with the ^{29}Si spectra shown in figure 7.7, obtained for silicate and aluminosilicate solutions (samples 32-3 and 32-2 respectively), since in the region of the Q^3_6 species these signals completely disappeared on addition of sodium aluminate. The total signal in the region of Q^3_8 grows at the expense of the other species. The ^{27}Al NMR spectrum of sample 32-2 also shows a large q^4 peak which confirms this trend (figure 7.8).

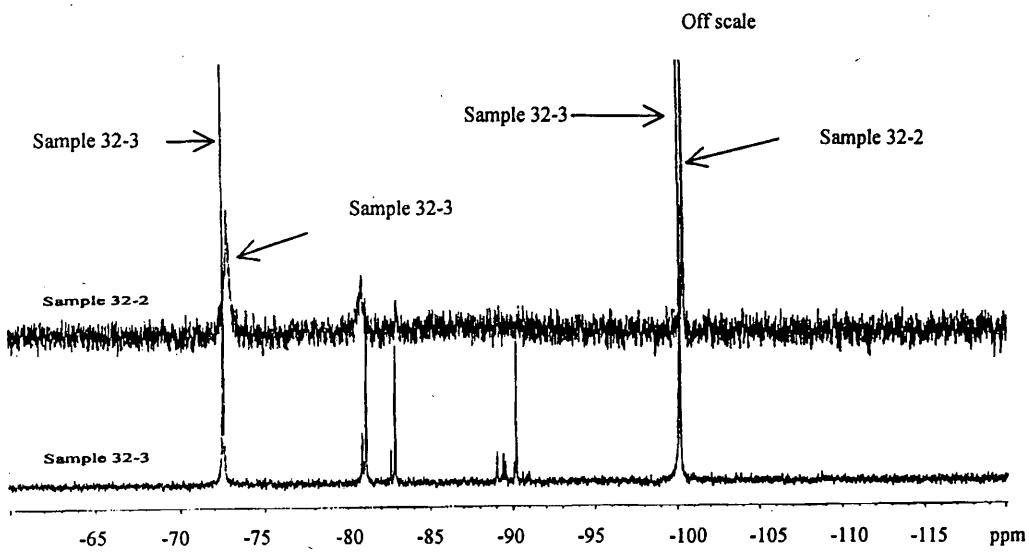

Figure 7.7. High-resolution ^{29}Si NMR spectrum at 99.29 MHz and ambient temperature of a) silicate (sample 32-3) and b) aluminosilicate (sample 32-2) with the compositions listed in table 7.1. The spectrum was taken one week after preparation. Spectrum conditions: Recycle delay 30 s. Acquisition time 1.454 s. Spectral width 22008.3 Hz. Pulse angle 90.0 degrees. Number of repetitions for samples 32-3 and 32-2 are 1664 and 304 respectively. The spectrum of sample 32-2 is vertically expanded.

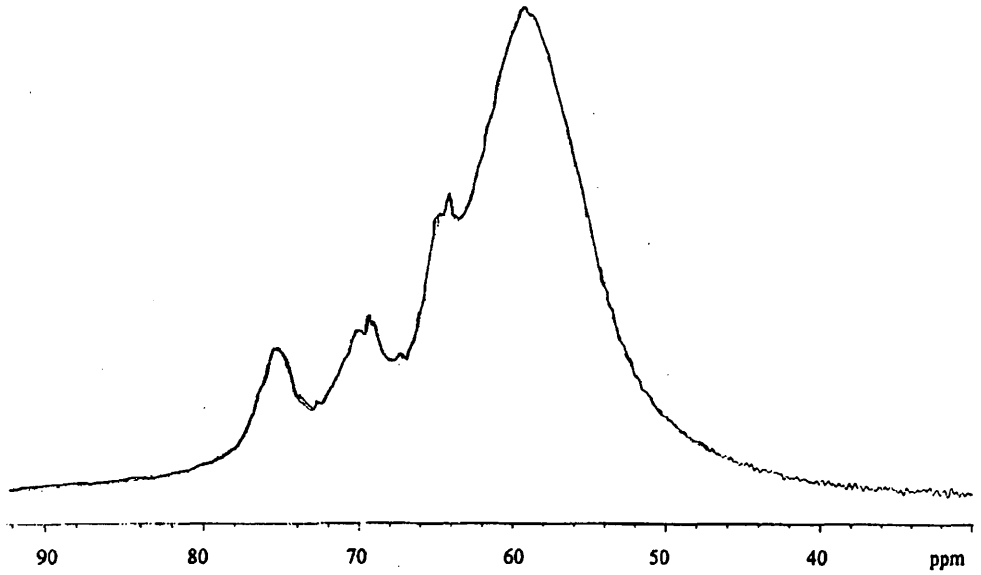

Figure 7.8. High-resolution ^{27}Al NMR spectrum at 156.23 MHz and ambient temperature of sample 32-2 with the composition listed in table 7.1 (the same solution as for figure 7.7). Spectrum conditions: Recycle delay 0.100 s. Acquisition time 0.1 s. Spectral width 51981.8 Hz. Pulse duration 22.0 μs. Number of repetitions 1000.

From the above interpretation of the results, the following schematic conversion of q^3_6 to q^3_8 or Q^3_6 to Q^4_8 (figure 7.9) can be suggested again, as discussed in more detail in section 4.2.4.

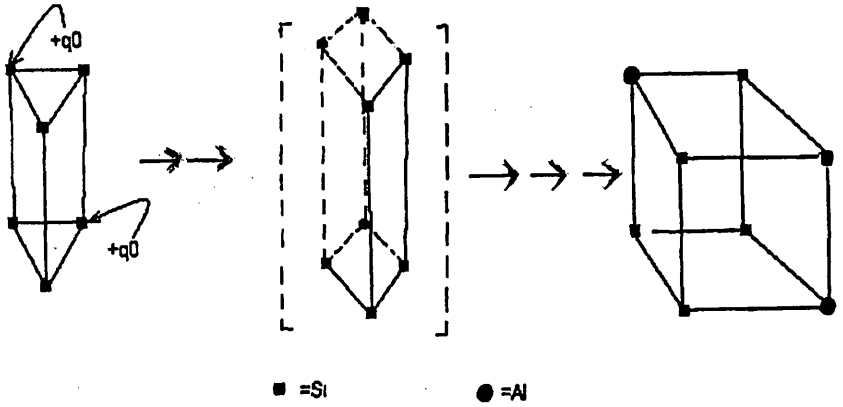

Figure 7.9 Schematic representation of the formation of cubic octamers at the expense of the prismatic hexamer. Circles represent aluminium atoms and squares indicate silicon atoms.

Due to the dilution effect, as discussed in section 4.2.7 in more detail, any later rearrangement in response to dilution or increased alkalinity occurs by breaking Si-O-Si bonds. Note that Al-O-Si bonds do not seem normally to cleave in alkaline solution.[1,3] The high-silica, low-alkali solutions thus have very long gel times because they are unable to rearrange to provide the free aluminate essential for the formation of relevant intermediate. Gelation is then solely dependent on the coagulating ability of the cation. For the coagulating ability - bringing together aluminosilicate complexes and promoting their reaction - as demonstrated in chapter 6, sodium is much better than tetraalkylammonium hydroxide (see also figure 7.7). The aluminosilicate complexes probably substitute for some of the water shell, and are thereby drawn together to form the gel. In this way, the cation determines the insolubility of the aluminosilicate species and therefore the rate of precipitation or gelation. [1] This is consistent with the observation that in zeolite structures the cation is partially co-ordinated to the framework and

never wholly surrounded by water molecules. Moreover, this intimate association of aluminosilicate and cation species may well be the template for the crystallising zeolite. However, in the TMAOH aluminosilicate solutions it can be observed that there are some affecting factors other than the cation for the association of aluminosilicates, which influence the coagulation.

7.4. Conclusion

This work obviously has shown that the gel time strongly depends on the Al concentration and the temperature, while the amount of the gel phase depends on the Si and the alkalinity of the solution. The evolution of the Al spectra with time for solutions with conditions favourable for gelation shows changes as the solution begins to cloud and gel. As this happens, peaks assigned to the higher complexes reduce relative to the q^0 peak, in agreement with the work of Glasser et al. [1] This is surprising but may indicate that the higher complexes are drawn preferentially into the gel, and are then no longer detectable by NMR.

7.5. References.

1. G. Harvey, L. S. D. Glasser, Eds. M. L. Occelli and H. E. Rodson, *ACS Symp.* **398**, Chapter 4, 49 (1989) and references therein.
2. G. Engelhardt, D. Hoebbel, M. Tarmak, A. Samoson, and E. Lippmaa Z. *Anorg. Allg. Chem.*, **484**, 22 (1982).
3. G. Engelhardt, and D. Michel " *High-resolution solid-state NMR of silicates and zeolites",* Wiley , New York, (1987).

Appendix A

Posters presented on the work of this thesis:

1. Aluminium-27 NMR of Aluminosilicate Solutions, *14th International NMR meeting, University of Edinburgh*, 27 June – 2 July 1999.
2. Application of NMR studies on thermodynamic equilibrium of the aluminosilicate anions in aqueous TMA aluminosilicate solutions, *Fifth Iranian Seminar of Inorganic Chemistry*, Isfahan University, 1-2th September 1999.
3. Aluminium-27 NMR spectra of aluminosilicate solutions as a function of cation type, *15th International meeting on NMR spectroscopy,* University of Durham, 8-12 July 2001.
4. The unexpected esterification reaction formed in methanolic tetraalkylammonium silicate solutions, *8th Iranian Seminar of Organic Chemistry, Kashan University*, 16-18th May 2000.
5. Application of electro-spectroscopy method into aluminosilicate solutions, *10th Iranian Seminar of Analytical Chemistry,* Department of Chemistry, University of Sharif, 6-8 February 2001
6. Study of aluminium-27 spin-lattice relaxation times for aluminosilicate solutions, *4th Iranian Seminar of Physical Chemistry*, Kish University, 6-10th May 2001.
7. Study of ^{27}Al NMR spectra of aluminosilicate solutions with different aluminium concentration, *6th Iranian Seminar of Inorganic Chemistry*, Ferdusy Meshhad University, 7-8th November 2001. To be presented.

Publications

1. **Highly resolved ^{27}Al NMR spectra of aluminosilicate solutions**, A. Samadi-Maybodi, S. N. Azizi, H. Naderi-Manesh, H. Bijanzadeh, I. H. McKeag and R. K. Harris, *J. Chem. Soc., Dalton Trans.,* 633 (2001).
2. **Silicon-29 NMR study of the formation of monomethoxysilicic acid in methanolic alkaline silicate solutions**, Samadi-Maybodi, S. N. Azizi, R. K. Harris and A. M. Kenwright, *Magn. Reson. Chem.*, **39**, 443 (2001).
3. **Investigation of aluminium-27 NMR of aluminosilicate solutions as a function of cation type.** A. Samadi-Maybodi, R. K. Harris and S. N. Azizi, *in preparation.*

Appendix B

Research Colloquia, Seminars and Lectures given by Invited Speakers

(* denotes lectures attended)

1997

October 8* Prof. E. Atkins, Department of Physics, University of Bristol.
'Advances in the control of architecture for polyamides: from nylons to genetically engineered silks to monodisperse oligoamides'.

October 15* Dr. R. M. Ormerod, Department of Chemistry, Keele University.
'Studying catalysis in action'.

October 21* Prof. A. F. Johnson, IRC, Leeds.
'Reactive processing of polymers: science and technology'.

October 22* Prof. R. J. Puddephatt, University of Western Ontario.
RSC Endowed Lecture.
'Organoplatinum chemistry and catalysis'.

October 23* Prof. M. R. Bryce, Department of Chemistry, University of Durham.
Inaugural lecture.
'New tetrathiafulvalene derivatives in molecular, supramolecular and macromolecular chemistry: controlling the electronic properties of organic solids'.

October 28* Dr. A. P. de Silva, The Queen's University, Belfast.
'Luminescent signalling systems'.

October 29* Prof. B. Peacock, University of Glasgow.
'Probing chirality with circular dichroism'.

November 5* Dr. Mimi Hii, Oxford University.
'Studies of the Heck reaction'.

November 11*	Prof. V. Gibson, Imperial College, London. 'Metallocene polymerisation'.
November 12*	Dr. J. Frey, Department of Chemistry, Southampton University. 'Spectroscopy of liquid interfaces: from bio-organic chemistry to atmospheric chemistry'.
November 19*	Dr. G. Morris, Department of Chemistry, Manchester University. 'Pulsed field gradient NMR techniques: Good news for the Lazy and DOSY'.
November 20	Dr. L. Spiccia, Monash University, Melbourne, Australia. 'Polynuclear metal complexes'.
November 25*	Dr. R. Withnall, University of Greenwich. 'Illuminated molecules and manuscripts'.
November 26*	Prof. R. W. Richards, University of Durham. Inaugural lecture. 'A random walk in polymer science'.
December 2*	Dr. C. J. Ludman, University of Durham. 'Expolosions'.
December 3*	Prof. A. P. Davis, Department of Chemistry, Trinity College Dublin. 'Steroid-based frameworks for supramolecular chemistry'.
December 10*	Sir Gordon Higginson, former Professor of Engineering in Durham and retired Vice-chancellor of Southampton University. '1981 and all that'.
December 10*	Prof. M. Page, Department of Chemistry, University of Huddersfield. 'The mechanism and inhibition of beta lactamases'.

1998

October 7* Dr. S. Rimmer, Ctr Polymer, University of Lancaster.
'New polymer colloids'.

October 9* Prof. M. F. Hawthorne, Department of Chemistry and Biochemistry, UCLA, USA.
RSC endowed lecture.
Title unknown.

October 21* Prof. P. Unwin, Department of Chemistry, Warwick Univeristy.
'Dynamic electrochemistry: small is beautiful'.

October 23 Prof. J. C. Scaiano, Department of Chemistry, University of Ottawa, Canada.
RSC endowed lecture.
'In search of hypervalent free radicals'.

October 26 Dr. W. Peirs, University of Calgary, Alberta, Canada.
'Reactions of the highly electrophilic boranes $HB(C_6F_5)_2$ and $B(C_6F_5)_3$ with Zirconium and Tantalum based metallocenes'.

October 27 Prof. A. Unsworth, University of Durham.
In association with The North East Polymer Association.
'What's a joint like this doing in a nice girl like you?'

October 28 Prof. J. P. S. Badyal, Department of Chemistry, University of Durham.
Inaugural Lecture.
'Tailoring solid surfaces'.

1999

October 12* Dr. S. Beckett, Nestle.
'Chocolate for the next Millennium'.

October 13*	Prof. G. Fleet, University of Oxford. 'Sugar lactone and amino acids'.
October 19*	Prof. K. Gloe, TU Dresden, Germany. 'Tailor made molecules for the selective binding of metal ions'.
October 20*	Prof. S. Lincoln, University of Adelaide. 'Aspects of complexation and supramolecular chemistry'.
October 25*	Prof. S. Collines, University of Waterloo, Canada. 'Methacrylate polymerisation using Zirconium enolate initiators: polymerisation mechanisms and control of polymer tacticity'.
October 26*	Dr. D. Hughes, AstraZeneca. 'Perspectives in agrochemistry'.
October 27*	Dr. C. Braddock, Imperial College. 'Novel catalysts for atom economic transformations'.
November 3*	Prof. D. W. Smith, University of Waikato, NZ. 'The strengths of C-C and C-H bonds in organic and organometallic molecules: empirical, semi-empirical and ab inito calculations'.
November 10*	Dr. I. Samuel, Department of Physics, University of Durham. 'Improving organic light emitting diodes by molecular, optical and device design'.
November 16*	Prof. A. Holmes. 'Conjugated polymers for the market place'.
November 17*	Dr. J. Rourke, University of Warwick. 'C-H activation induced by water'.
November 18*	Dr. G. Siligardi, Kings College London. 'The use of circular dichroism to detect and characterise biomolecular interactions in solution'.

November 23*	Prof. B. Caddy. 'Trace evidence – a challenge for the forensic scientist'.
November 24*	'Prof. T. Jones, Imperial College. 'Atomic and molecular control of inorganic and organic semiconductor thin films'.
November 30*	Rev. R. Lancaster. 'Principles and practice'.
December 8*	Prof. D. Crout, Department of Chemistry, University of Warwick. 'More than simply sweet: carbohydrates in medicine and biology'.